MECHANISMS UNDERLYING RADIOSENSITIVITY : INVESTIGATIONS IN XPS-5, AN X-RAY SENSITIVE HAMSTER CELL LINE

Peter James Johnston

A Thesis Submitted for the Degree of PhD
at the
University of St Andrews

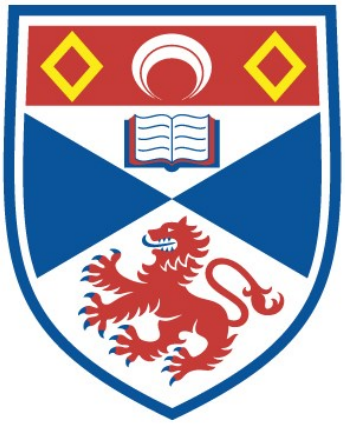

1995

Mechanisms underlying radiosensitivity: Investigations in *xrs-5*, an X-ray sensitive hamster cell line.

Peter James Johnston.

Thesis submitted for the degree of Doctor of Philosophy.

University of St Andrews.

June 1994.

Declaration

I, Peter James Johnston, hereby certify that this thesis has been composed by myself, that it is a record of my own work, and that it has not been accepted in partial or complete fulfilment of any other degree or professional qualification.

21st June 1994

I was admitted to the Faculty of Science of the University of St Andrews under Ordinance General No. 12 on the 1st October 1990 and as a candidate for the degree of Ph.D. on the 1st October 1991.

21st June 1994

I hereby certify that the candidate has fulfilled the conditions of the Resolution and Regulations appropriate to the Degree of Ph.D.

21st June 1994

Copyright

In submitting this thesis to the University of St Andrews I understand that I am giving permission for it to be made available for use in accordance with the regulations of the University Library for the time being in force, subject to any copyright vested in the work not being affected thereby. I also understand that the title and the abstract will be published, and that a copy of the work may be made and supplied to any *bona fide* library or research worker.

Abstract.

The damage caused to cells by ionising radiation is believed to center on damage to the DNA. In particular, the induction of DNA double strand breaks (DSB) have been implicated in biological end-points such as cell killing and the formation of chromosomal aberrations.

The *xrs-5* cell line is a mutant Chinese hamster ovary fibroblast (CHO-K1) mutant which exhibits sensitivity to ionising radiation and a number of other DNA damaging agents. This mutation, postulated to involve the hamster homologue of the human *XRCC5* gene, is believed to be involved in the repair of the DSB. In addition, there are constitutive differences between the wild type and *xrs* cells involving the structure and function of the nucleus and higher order chromatin structures.

The aims of this thesis were to study further the *xrs-5* cell line and its response to DNA damage and to investigate the possible link between chromatin structure and DSB repair.

By the examination of the response of *xrs-5* cells to a number of DNA damaging agents and potential modulators of this response using the cytokinesis block micronucleus assay [Fenech and Morley, 1985] a possible cell cycle defect was identified in addition to elevated levels of chromosomal damage. *Xrs-5* cells appeared to be partially defective in the cell cycle checkpoints involving the passage from G_2 phase to mitosis.

By the use of a modified neutral filter elution procedure variations in the repair of DSB were observed between *xrs-5* and CHO. Conventional neutral filter elution requires harsh lysis conditions to remove higher order chromatin structures which interfere with the elution of DNA containing DSB. By lysing cells with non-ionic detergent in the presence of 2 M NaCl, histone depleted structures which retain the higher order nuclear matrix organisation, including chromatin loops, can be produced. Elution from these structures will only occur if two or more DSB lie within a single looped domain delineated by points of attachment to the nuclear matrix. Repair experiments indicate that in CHO cells repair of DSB in loops containing multiple DSB are repaired with "slow" kinetics ($t_{1/2} \approx 5$ hrs) whilst DSB occurring in loops containing single DSB are repaired with "fast" kinetics ($t_{1/2} \approx 10$ min). *Xrs-5* cells are incapable of repairing these multiply damaged loops. This work indicates that the spatial orientation of DSB in higher order structures of chromatin are a possible factor in the repair of these lesions. By construction of a mathematical model of the process of elution from chromatin loops it was possible to postulate the size of the loops to approximate to 2.5-3 Mbp.

Further evidence of a potential structural defect in the chromatin of *xrs-5* cells was provided by examination of the polypeptide composition and DNA binding activity of nuclear extracts. The affinity of extracted proteins for double-stranded calf-thymus DNA was measured in nuclear extracts of *xrs-5* and CHO cells. There was an alteration in the DNA binding activity of salt extractable proteins from *xrs-5* as measured by a filter binding assay. By the use of SDS-PAGE and the technique of South-Western blotting, it was possible to identify the approximate molecular weights of these DNA binding proteins. Differences were found in DNA binding between proteins from CHO and *xrs-5* extracts of both non-irradiated and irradiated cells. Two proteins with apparent molecular weights of 32.2 and 31.8 kDa exhibited a lower DNA binding activity in *xrs-5* than proteins of similar extracts from CHO. The amount of the 32.2 kDa protein was less in the *xrs-5* extracts than in CHO extracts, as measured by Coomassie blue staining. The two proteins have not yet been identified but comprise a major DNA binding activity in CHO extracts obtained by detergent-free extraction procedures. This work provides circumstantial evidence that suggests these two polypeptides may form part of the histone H1 family.

Acknowledgements

I would like to first thank my supervisor, Peter Bryant, for his help, encouragement and extreme patience over the course of this project.

Many people have provided me with technical help, in particular I would like to thank John Macintyre for all his brilliant assistance in the lab, Dave, Karen and Sean for all their photographic expertise and also Jeff Graves for his patience in explaining statistics to an incompetent.

I am deeply indebted to the following: Kim, Nan and Gary for putting up with my mess and for all their help. To the occupants of the cottage, especially my "Aunties", Tina and Jean for sticky buns and lashings of ginger pop. Mark Armitage, for trying to completely confuse me as we attempted to solve all the problems of the universe in one easy step. Ian, Rupert, Gordon and other "friends of Bert's" for helping me maintain sanity. Allison, for the supply of curry and cas. and for nagging me to get on with this thesis.

Finally, none of this would have been possible without the support and encouragement of my parents.

This thesis is dedicated to my grandmother and to the memory of my grandfather.

Table of Contents.

Chapter 1.

Introduction.

Chapter 2.

Induction of micronuclei in CHO and xrs-5 cells.

Chapter 3.

Relationship of the nuclear matrix to the repair of DNA double strand breaks.

Chapter 4.

DNA binding activities of proteins extracted from xrs-5.

Abbreviations.

3-AB	3-aminobenzamide
ANOVA	analysis of variance
AT	ataxia telangiectasia
AZC	5-azacytidine
BI	binucleate index
BLM	bleomycin sulphate
BSA	bovine serum albumin
CB	cytochalasin-B
CFN	caffeine
CHO	Chinese hamster ovary
CPT	camptothecin
DEB	diepoxybutane
DSB	DNA double strand breaks
DST	distamycin-A
DTT	dithiothreitol
EDTA	ethylenediaminetetraacetic acid
EGTA	ethyleneglycoltetraacetic acid
EMEM	Eagles' minimum essential medium
EMS	ethyl methanesulphonate
EtBrd	ethidium bromide
FA	Fanconi's anaemia
GLM	general linear model
HBSS	Hanks' balanced salt solution
HDR	high dose rate
hprt	hypoxanthine-guanine phosphoribosyltransferase
^{3}H-TdR	methyl-^{3}H-thymidine
INFE	ionic neutral filter elution
IR	ionising radiation
LET	linear energy transfer
LDR	low dose rate
LPC	lysophosphatidylcholine
m-AMSA	4′-(9-acridinylamino)methanesulfon-*m*-aniside
MAR	matrix attachment region
MB	micronuclei per binucleated cell
MD	micronuclei per damaged binucleate cell
MMC	mitomycin C

MMS	methyl methane-sulphonate
MNNG	N-methyl-N'-nitro-n-nitrosoguanidine
MPF	maturation promoting factor
NAD^+	nicotinamide adenine dinucleotide
ND	not determined
NINFE	non-ionic neutral filter elution
NFM	non-fat milk powder
NLS	N-lauryl-sarcosine
OA	okadaic acid
PARP	poly(ADP-ribose)polymerase
PBS	phosphate buffered saline
PCC	premature chromosome condensation
PI	propidium iodide
PKA	protein kinase A
PKC	protein kinase C
PLD	potentially lethal damage
PLDR	potentially lethal damage repair
PMSF	phenyl methyl sulphonyl fluoride
pp	protein phosphatase
PPLACD	proteinase inhibitor cocktail
rag	recombination activation genes
RC	relative sensitivity to chromosomal aberration formation
RE	restriction endonucleases
RMnI	relative micronucleus induction
RS	relative sensitivity to cell killing
SARs	scaffold attachment regions
SCEs	sister chromatid exchanges
SEM	standard error of mean
SLD	sub-lethal damage
SLDR	sub-lethal damage repair
SLO	streptolysin-O
SSB	DNA single strand breaks
STP	staurosporine
TBE	tris-borate-ethylenediaminetetraacetic acid
TEMED	N,N,N,N'-tetramethylethylenediamine
tk	thymidine kinase
topo	topoisomerase
TSDS-PAGE	tricine-SDS polyacrylamide gel electrophoresis
UV	ultra-violet

VM-26	teniposide
VP-16	etopside
XP	xeroderma pigmentosum

Chapter 1.

Introduction.

1.1. Sensitivity of mammalian cells to ionising radiation.

The effects of ionising radiations have long been known to be detrimental to the normal functioning of eukaryotic cells. A variety of biological changes can occur such as cell death, chromosomal aberrations and mutations including transformation and carcinogenesis [Savage 1975; Terzaghi and Little, 1976; Weinstein, 1988; Loeb, 1989]. All these endpoints are relatively well documented, as are the initial reactions ionising radiations have with biological materials [von Sonntag, 1987; Goodhead, 1989; Spotheim-Maurizot et al., 1990].

The response of cells to ionising radiations are dependent in part on certain physical and biological parameters. These include the "quality" of the radiation, linear energy transfer (LET), the dose rate, and the ability of cells to repair damage before any deleterious effect of the lesions produced are manifested by the cell.

The main biological target of ionising radiation has been identified as the nucleus and in particular the genome. Ionising radiation produces a number of lesions within DNA including DNA strand cleavage, base damage and protein-DNA and DNA-DNA cross-linkage. The processes involved in the transition from nascent DNA lesions to the biological endpoints are unclear. This "grey" area would appear to involve several stages including recognition by the cell of the lesion, actions taken by the cell in response to the lesion such as repair, mis-repair, programmed cell death, interruption of normal cellular processes and the subsequent expression of damage. How all these events are linked and how the processes controlling and modifying them operate are still to be elucidated.

Ionising radiations cause damage to biological materials by depositing energy in the form of ionisations of other molecules. These energy depositions can result in either the formation of free radical species which can react further with covalent bonds of biological molecules or in direct damage to DNA. The pattern of energy deposition within biological materials of differing LET affects the form of damage experienced by a cell [reviewed Goodhead et al., 1989; 1994]. High LET particles such as α-and β-particles deliver most of their energy in the form of densely clustered groups of ionisations. These produce similarly clustered lesions in DNA and these areas of intense damage are likely to be irreparable and subsequently lethal [Blöcher, 1988]. Low LET radiations such as X-rays and γ-rays produce tracks in biological materials with more sparsely distributed ionisations, although some clustering of damage does occur particularly at track ends. The lesions produced by these tracks are likely to be simpler in structure and more reparable than high LET damage.

The study of the effects of radiation on cells has been facilitated by the use of mutants sensitive to ionising radiation. These fall into several complementation groups in both rodent

and human cells. The different complementation groups vary in both the form of lesion or lesions to which they are sensitive and the manner in which they express this sensitivity. . Much of the work on higher eukaryotic radiation sensitivity has been performed on rodent cell lines [reviewed in Jeggo, 1990; Collins, 1993]. Some of these exhibit similarities with human radiosensitive conditions such as xeroderma pigmentosum (XP), ataxia telangiectasia (AT) and Fanconi anaemia (FA). Several classifications can be made of these cell lines on the basis of sensitivity to ultra violet (UV), ionising radiation (IR) or cross-linking agents [Collins, 1993]. Cross-sensitivity to UV/IR/cross-linking agents is also observed for several cell lines. The IR sensitive mutants can be further categorised on the basis of their ability to repair DNA strand breaks [Jeggo, 1990].

In each of the above categories several complementation groups have been identified which exhibit different characteristics, both in DNA damage processing and subsequent cellular response to that damage. To date, 10 UV sensitive and 10 potential IR sensitive groups exist [Collins, 1993]. Compared to IR mutants, much progress has been made on the identification and characterisation of the defects responsible for UV sensitivity. Several genes have been cloned and proteins involved in UV sensitivity identified [Lehman et al., 1994 in press]. Several genes are homologous to either human or yeast repair genes.

This thesis is concerned with one of the rodent complementation groups and the mechanisms by which these cells derive their sensitivity to ionising radiation. This group is the *xrs* line which is one of at least four rodent complementation groups which are characterised by defects in the repair of DNA double-strand breaks (DSB) which has been postulated to be the cause of enhanced sensitivity to ionising radiation [Jeggo and Kemp, 1983; Jeggo, 1990; Zdzienicka et al., 1992; Collins, 1993].

1.2. Isolation of the xrs mutants.

The *xrs* mutants were the first mammalian ionising radiation sensitive cell lines isolated which exhibited a defect in the repair of DSB [Jeggo and Kemp, 1983, Kemp et al., 1984]. These cell lines were derived from a heavily mutagenised population of Chinese hamster ovary (CHO-K1) fibroblast cells using the bifunctional alkylating agent ethyl methanesulphonate (EMS). Single cells were grown into colonies and these colonies were screened for sensitivity to X-rays as measured by a clonogenic survival assay. 6 X-ray sensitive cell lines and six partially sensitive cell lines were isolated out of 9000 original colonies.

1.3. Response of xrs cells to DNA damaging agents.

1.3.1. Response of xrs cells to low LET radiation.

1.3.1.1. Clonogenic survival.

The six sensitive cell lines (*xrs -1, 2, 4, 5, 6, 7*) exhibited a reduced survival in response to X-rays [Jeggo and Kemp, 1983]. The mutants differed from CHO-K1 in that they exhibited a reduced or absent shoulder in their survival curves and a steeper linear portion of the curve (Figure 1.1).

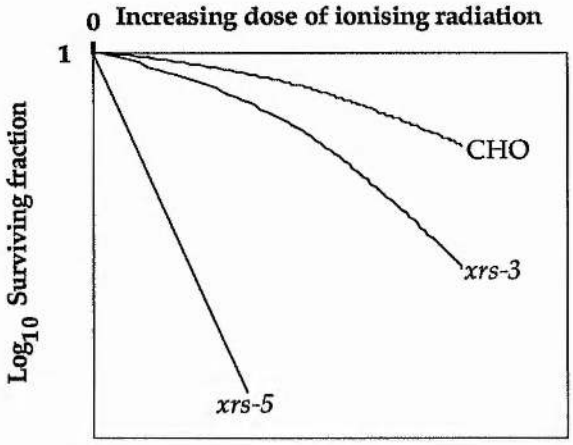

Figure. 1.1. Ionising radiation sensitivity of CHO-K1 and the X-ray sensitive mutant strains; *xrs-5* and *xrs-3*. Graph representing the surviving fractions (log_{10} scale) versus increasing radiation dose for wild-type (CHO), partially sensitive (*xrs*-3) and highly sensitive (*xrs-5*) cell lines. Redrawn (not to scale from Jeggo and Kemp [1983].

The extent of radiation sensitivity varied between cell lines and is indicated by the variations in D_{10} values (dose of X-rays required to reduce survival to 10% of the wild-type) ranging from 0.90 Gy (*xrs-5*) to 2.43 Gy (*xrs*-2) compared to 6.55 Gy for CHO. The six partially sensitive mutants expressed only slight (but significant) sensitivity to X-rays; e. g. *xrs*-3 D_{10} = 4.52 Gy. These D_{10} values give relative sensitivity[1] (RS) values of 7.3, 2.7 and 1.5 for *xrs-5*, *xrs*-2 and *xrs*-3 respectively.

---

[1]The comparisons made between mutant and wild type cells given below all relate to the dose of agent required to give a certain surviving fraction [reviewed in Alper, 1979]. The choice of a specific surviving fraction to use in the assessment of relative sensitivity to an agent varies between authors of the works described. An attempt has been made, where possible, to standardise these parameters and the actual surviving fraction used for estimation is stated. Relative sensitivity (RS) is defined as the ratio of doses required to give the specified surviving fraction (n, given as a percentage of the control) in CHO-K1 versus *xrs* cells.

$$RS = \frac{D_{n(CHO)}}{D_{n(xrs\text{-}5)}} \qquad (1.1)$$

A RS value of 1 means sensitivity to the agent is equal in the two cell lines. RS values do not relate to the actual toxicity of the cells to the agent described.

The sensitivity of cells to ionising radiation varies with their position in the cell cycle. CHO and *xrs* are both maximally resistant to ionising radiation during late S/G_2 phase of the cell cycle and are both most sensitive at G_2/M phase transition, although *xrs* cells remain more sensitive than CHO. The relative sensitivity of*xrs* cells compared to CHO cells is least during G_2. [Jeggo, 1990].

The rate at which ionising radiation is applied to cells can affect the subsequent clonogenic survival of the cells. As the rate at which a dose is given is reduced the proportion of cells surviving increases. This is exhibited as a broadening of the shoulder region of the survival curve. It is believed this may be caused by the repair of lesions prior to the induction of additional lesions [Dewey et al., 1972; reviewed Alper, 1979]. This may be the result of synergistic interactions directly between individual lesions resulting in expression of a lethal form of damage. Alternatively it may be due to the presence of multiple targets within a cell, each of which needs to be damaged to produce a lethal event . The individual lesions which comprise these interactive events can be termed sub-lethal lesions (SLD) and their repair as sub-lethal damage repair (SLDR).

Low dose rate γ-irradiation of CHO cells resulted in an increase in survival compared to high dose rate irradiation over a range of 0.1 mGy to 1 Gy [Thacker and Stretch, 1985]. *Xrs* cells, in contrast, showed virtually no increase in survival with low dose rate irradiation (RS values based on D_{37} were 8.1 and 14.5 for 0.12 and 0.004 Gy min^{-1} respectively [Thacker and Stretch, 1985]).

CHO cells would therefore appear to be competent in SLDR whilst *xrs* cells are either unable to perform SLDR or single lesions are as lethal as multiple lesions.

Potentially lethal damage (PLD) represents another form of damage that is temporally linked to cell killing: If cells are maintained under non-growth conditions post-irradiation; then allowed to resume growth, the surviving fraction is greater than if cells are placed directly under growth conditions. This has been attributed to repair of PLD occurring prior to the cell resuming growth. If the cell resumes growth without repairing all the PLD then fixation of the PLD to lethal damage will occur. It has been suggested that PLD is the result of interacting SLD within chromatin [Dewey et al., 1972].

G_0 CHO cells held for 6 hours post-irradiation before trypsinisation and released into growth conditions exhibited an increase in survival relative to immediately plated cells [Thacker and Stretch, 1985]. In another study survival of CHO cells increased with dose from a 2.6 fold increase at 6 Gy to a 4.9 fold increase at 10 Gy [Nagasawa et al., 1989]. In both of these studies *xrs* cells showed limited or no recovery.

The repair defect in *xrs*-5 may therefore be related to the repair of a lesion or lesions common to both SLDR and PLDR. This damage may be produced by the sparsely ionising component of ionising radiation.

1.3.1.2. Chromosomal aberration formation in cells exposed to low LET radiation.

The death of cells in response to ionising radiation has been correlated with the appearance of chromosomal aberrations [Joshi et al. 1982]. Chromosomal aberrations in animal cells have long been known to result from exposure of cells to ionising radiation. Aberrations occur in many forms involving both individual chromatids and whole chromosomes [reviewed by Scott et al., 1983]. Broadly speaking, aberrations can be classified as to whether they occur as a result of damage to a cell in the G_1 phase of the cell cycle (chromosome aberrations) or in S or G_2 phases of the cycle (chromatid aberrations). Aberrations may involve breakage of one or two chromosomes or chromatids ("breaks") or that illegitimate recombination occurs between different broken chromosomes or chromatids ("exchanges"). Another form of chromosomal rearrangement, not produced particularly efficiently by ionising radiation involves recombination between homologous chromatids during S-phase resulting in sister chromatid exchanges (SCEs) [Perry and Evans, 1975].

When cells are irradiated and chromosomal aberrations recorded in subsequent mitoses a correlation between dose and numbers of aberrations appears. Both CHO and *xrs* cells exhibit a linear dose response with *xrs* cells producing between 4 and 6 times more aberrations than CHO [Kemp and Jeggo, 1986; Darroudi and Natarajan, 1987a; b; 1990; MacLeod and Bryant 1990].

The frequencies of aberrations vary with the time period between irradiation and the point where cells enter mitosis. Approximations of cell cycle phases in which the cells were irradiated can be estimated from the time interval between irradiation and the passage of the cell into mitosis [e.g. Kemp and Jeggo 1986; MacLeod and Bryant, 1990]. This method requires allowances for any radiation induced delay which may occur. The frequency of aberrations expressed at the subsequent metaphase may give an indication of the relative sensitivity of cells at different stages of the cell cycle. Alternatively cells can be synchronised and irradiation carried out on populations of cells of a known phase [e.g. Darroudi and Natarajan, 1987a]. At all fixation times, the relative sensitivities of *xrs* to CHO cells were greater for both chromatid break and exchange type aberrations [Kemp and Jeggo, 1986; Darroudi and Natarajan, 1987a, b, MacLeod and Bryant, 1990]. The frequencies of aberration formation in *xrs*-7 and CHO cells are given in Figure 1.2 The chromatid break-type aberration was the most common type of aberration in both CHO and *xrs*-7 cells.

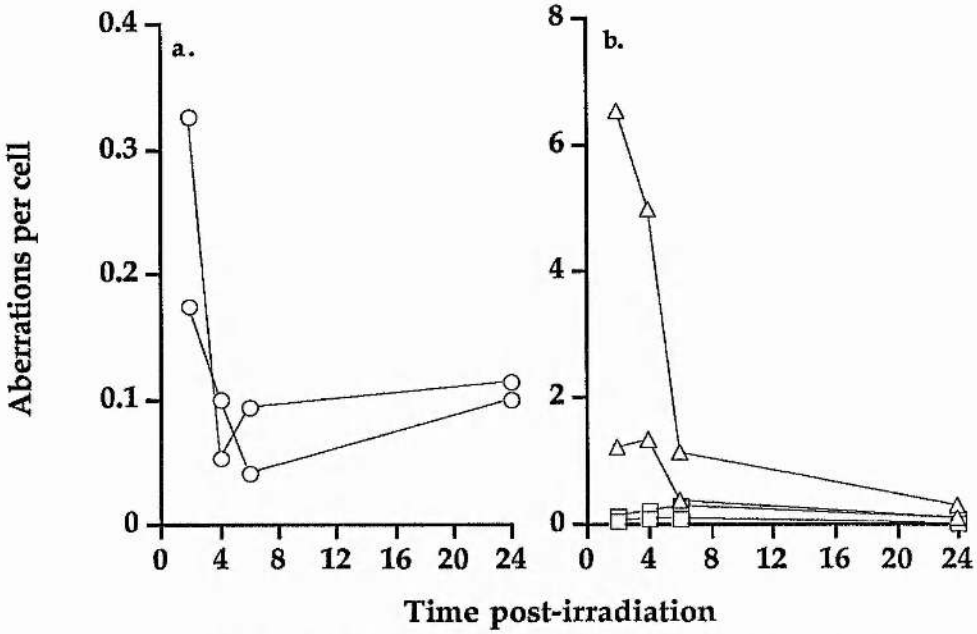

Figure 1.2 Chromosomal aberrations at different fixation times for CHO-K1 and *xrs-7* cells. Cells were irradiated with 0.95 Gy X-rays, fixed at intervals post-irradiation (hrs) and the level of aberrations determined per metaphase cell. □, △, ○, CHO-K1; ■, ▲, ●, *xrs-7*. Left panel; chromosome aberrations (break-type and exchange type pooled). Right panel; chromatid-type aberrations; ▲, △, break-type; ■, □, exchange-type. (Data taken from Kemp and Jeggo, [1986].

Chromosome aberrations also exhibited an increase in frequency in the *xrs* cells although the levels of chromosome aberrations were much lower than for chromatid type lesions. [Kemp and Jeggo, 1986]. Irradiation of synchronised cells in G_1 resulted in only a slight elevation in the frequency of chromatid type aberrations in CHO cells. *Xrs* cells showed a marked elevation in the frequency of all forms of aberration. The relative chromosomal sensitivity [2] (RC) was approximately 3-5 for *xrs-7*, although tri-radial aberrations were 40 fold more frequent for *xrs-7* compared to CHO [Kemp and Jeggo, 1986; Darroudi and Natarajan, 1987a]. There was also an elevated level of sister chromatid exchanges (SCEs) over background in *xrs-6* cells compared to only a slight increase in SCE frequency in *xrs-5* cells and virtually no increase in CHO [Darroudi and Natarajan, 1987b]. SCE formation could be increased further in *xrs-6* cells by irradiation under hypoxic conditions [Darroudi et al., 1990].

---

[2]The relative chromosomal sensitivity (RC)is a measure of the numbers of chromosomal aberrations produced by the same dose of clastogenic agent in CHO-K1 and *xrs* cells.

$$RC = \frac{\text{aberration frequency}_{(xrs)}}{\text{aberration frequency}_{(CHO)}} \qquad (1.2)$$

The value of RC is not a measure of the ability of an agent to produce aberrations but the relative numbers of aberration produced between *xrs* and CHO cells.

Cells irradiated in the G_2 phase of the cell cycle [MacLeod et al., 1990; MacLeod and Bryant 1990] exhibit what appears to be "repair": When either equal or equiclastogenic (0.375 Gy for *xrs*-5 and 1.5 Gy for CHO) doses of X-rays were given, the kinetics of disappearance of breaks were the same for both cell lines. The disappearance followed a single exponential kinetic with half times of 1.65 hours and 1.5 hours for *xrs* and CHO cells respectively [MacLeod and Bryant, 1990]. At the same time the frequency of exchanges rose rapidly to its maximum level after approximately 2-3 hours and subsequently remained at this frequency. The kinetics of exchange formation were again similar in *xrs* and CHO although the mutant cells produced 1.6 fold fewer exchanges.

It was emphasisied in the above papers that even though kinetics of disappearance of breaks are similar in CHO and *xrs* frequency of aberrations induced by a given dose and at a given time is always greater in *xrs-5* cells than in CHO cells. This is thought to be due to a higher rate of conversion of damage to aberrations in *xrs* cells. It is also possible that *xrs* cells could enter mitosis earlier leading to elevated frequencies of damage. There is however no direct evidence for this.

The G_2 assay permits examination of aberrations after times in excess of 30 minutes [MacLeod and Bryant, 1990]. Measurement of frequencies of aberrations at times less than 30 minutes is not practical since many of the mitoses scored will have already been in mitosis at the time of irradiation. These will not express aberrations.

Darroudi and Natarajan [1989c] and Iliakis and Pantelias [1990] examined the frequencies of aberrations by applying the technique of premature chromosome condensation (PCC) to CHO and *xrs* cells. This technique utilises the observation that fusion of a mitotic cell with a non-mitotic cell induces a mitosis like reaction in the non-mitotic cell with nuclear membrane disruption and chromosome condensation. This occurs regardless of the DNA content of the chromosomes [Johnson and Rao, 1970]. With this technique, the presence of aberration forming lesions in various parts of the cell cycle can be determined at time intervals as low as the time required for condensation (approximately 30 minutes). While still not an immediate quantification of the frequency of aberration forming lesions (as in the G_2 assay) this technique permits an examination of the frequency of aberration forming lesions in various parts of the cell cycle. Thus PCC of G_1 cells gives rise to condensed chromosomes. PCC in G_2 cells gives rise to double chromatids, while PCC of S phase cells results in fragmented chromatin due to DNA undergoing replication with associated alterations in chromatin structure such as formation of the replication fork.

The frequency of aberrations immediately after X-irradiation as measured by PCC in G_1 *xrs-5* and *xrs-6* cells was found to give **RC** values of 2.3 and 1.8. The value of **RC** rose to 3.3 and 2.4

respectively for G_2 cells [Darroudi and Natarajan, 1989c]. G_0 *xrs-5* cells exhibited a 2.6 fold increase [Iliakis and Pantelias, 1990].

When aberrations observed in metaphase cells, irradiated in G_2 and in PCC of G_2 cells were compared, no differences in the numbers of breaks were observed for *xrs* cells [Darroudi and Natarajan,1989c]. PCC of G_2 CHO cells resulted in higher frequencies of breaks as compared to metaphase cells irradiated in G_2. The decline in frequency of aberrations with time produces an **RC** of 7.3 and 4 for *xrs-5* and *xrs-6* respectively. Fusion of mitotic *xrs* cells with X-irradiated interphase CHO cells did not elevate the frequency of breaks in CHO. However when CHO mitotic cells were fused with X-irradiated *xrs* cells a decrease was observed in the frequency of breaks with this complementation of sensitivity equal to 77% and 85% for *xrs-5* and *xrs-6* cells respectively [Darroudi and Natarajan,1989c]. That complementation occurred in the time interval between fusion and chromosome condensation of the interphase cell may indicate that the *xrs* defect is either linked to the process of chromosome condensation generating elevated frequencies of breaks or that repair of the aberration forming lesions occurs very rapidly on fusion.

The rate of disappearance or "repair" of fragments observed in cells can be examined by inducing PCC at time intervals post-irradiation. In mutant and wild type plateau phase (G_0) cells given equi-clastogenic doses of X-rays there was an initial rapid rate of repair present in both CHO and *xrs*-5 (e.g. 15 and 6 Gy respectively) [Iliakis and Pantelias, 1990]. After one hour approximately 35% of the chromosome fragments were repaired in the two cell lines. CHO cells continued to repair, at a slower rate until approximately 85% of fragments were removed by 15 hours. In *xrs* cells no further repair occurred after the initial rapid repair leaving a residual fraction unrepaired that was much higher than in CHO.

Xrs cells would therefore appear to be unable to repair a fraction of chromosome breaks either because of a repair defect or because of fixation of the damage to a form which is non-reparable.

The **RC** values obtained from scoring metaphase cells show a closer correlation to survival assays than those obtained from PCC cells [Iliakis and Pantelias, 1990]. The values obtained by PCC indicate that repair of aberration forming lesions occurs to a greater extent in CHO than *xrs* during the time interval between irradiation and expression of damage at mitosis. There would appear to be a correlation between the numbers of residual PCC breaks left unrepaired and the calculated numbers of lethal lesions experienced by cells, as estimated by survival data, on the assumption that cell death results from 1 un-repaired break, for both the wild-type and mutant cell lines [Iliakis and Pantelias, 1990] indicating that irradiation

produces aberration forming lesions, which if left unrepaired prior to division, become aberrations at mitosis and may kill the cells containing them.

The PCC experiments [Darroudi and Natarajan,1989; Iliakis and Pantelias, 1990] and the G_2 assay [MacLeod and Bryant, 1992] have therefore produced different results. The G_2 assay indicates that *xrs-5* cells convert a higher number of lesions into aberrations while retaining similar kinetics of the rejoining of these lesions. The PCC assay would indicate that the kinetics of repair are also defective in the mutant. However, the two assays are examining two very distinct populations; the G_2 assay measures cells which enter mitosis of their own accord; PCC enforces chromosome condensation, regardless of whether cells would normally have reached mitosis. The doses of radiation used in the G_2 assay are considerably lower than those used in the PCC assay. Therefore the differences in the two techniques may be the cause of differences in repair kinetics.

1.3.2. High LET ionising radiation.

As mentioned above, the passage of high LET radiations such as α-particles leads to a very concentrated deposition of energy within a cell. It has been estimated that while 1 Gy of X-rays is deposited by the passage of on average 1000 tracks through a cell, the same dose will be produced by only 4 α-particle tracks [Goodhead, 1989]. The pattern of energy deposition along these α-particle tracks is therefore far more localised if they cross a cell nucleus. A comparison of the sensitivity of CHO and *xrs* cells to radiations of differing LETs has been performed [Thacker and Stretch, 1985; Shadley et al., 1991].

1.3.2.1. Clonogenic survival

It was found that exposure of CHO cells to ^{238}Pu or ^{212}Bi α-particles produced greater cell killing per unit dose than X and γ-rays. This was expressed as both the loss of the shoulder and increase in the slope of the survival curve. The *xrs* mutants expressed only a slight increase in sensitivity to α-particles compared to X or γ-rays. The D_{37} values for *xrs-5* after X, γ, and ^{238}Pu α irradiation gave **RS** values of 6.4, 6.1 and 3.2 respectively compared to CHO. Comparisons of γ-rays to X-rays were more complex; some cell lines (e.g. CHO, *xrs-5* and *xrs-7*) were more sensitive to X-rays than γ-rays whilst other cell lines (e.g. *xrs-1* and *xrs-6*) were more sensitive to γ- than X-rays [Thacker and Stretch, 1985].

1.3.2.2. Chromosomal aberration formation.

The exposure of cells to α-particles emmitted from the radon daughter species ^{212}Bi [Shadley et al., 1991] gave rise to 2-3 fold more aberrations in G_2 CHO cells than X-rays, mainly due to an increase in the number of deletions. In contrast, *xrs-5* cells exhibited a

reduction in the number of aberrations on α-particle irradiation with approximately 30% fewer deletions per Gy when compared to X-rays. The **RC** values fell from approximately 9 fold to 3 fold for X- and α-particle irradiations respectively. This is similar to the apparent lack of additional cell killing by α-particles. However, the similar aberration induction between X- and α-irradiation in *xrs* has been suggested to be the result of an increased cell cycle delay in *xrs* cells which prevents heavily damaged cells from reaching mitosis within the experimental time period used [Shadley et al., 1991].

Generally, it would appear that a higher level of localised energy deposition relates to enhanced cell killing by ionising radiations. The similarity in the shape of survival curves of CHO cells exposed to α-particles and of *xrs* cells exposed to all forms of radiation indicate lesions produced by sparse ionisations of both high and low LET radiations are lethal in *xrs* cells whereas they can be repaired in CHO cells. Clustered damage resulting from high LET particles would appear to have a similar lethality for both CHO and *xrs* cells.

1.3.3. Cross-sensitivity of xrs cells to other DNA damaging agents.

Ionising radiation produces a broad spectrum of lesions to DNA (summarised in Figure 1.3). A narrower spectrum of DNA lesions can be produced by the selection of agents some of which affect DNA more specifically. This allows identification of the involvement of specific lesions involved in defective pathways of ionising radiation sensitivity. The six sensitive mutants have been examined for cross sensitivity to some of these DNA damaging agents.

The *xrs* mutants exhibit a marked sensitivity to a number of DNA damaging agents other than ionising radiations. This sensitivity is manifested as both a decrease in survival and increase in the frequency of chromosomal aberrations compared to CHO. Figure 1.4 gives an indication of the sensitivity of *xrs* cells to a number of these agents and the types of damage that they produce. This graph is only an approximation since two cell lines are represented; *xrs-5* and *xrs-1*, and the values used to estimate sensitivity are obtained by different techniques. Similarly the aberration frequencies were obtained after treatment of cells at different cell cycle times and by different techniques.

Although the *xrs* cells are significantly sensitive to all of the agents shown in Figure 1.4. (with the exception of the topoisomerase II inhibitor novobiocin [Jeggo et al., 1989] which does not damage DNA) there would appear to be a broad range of sensitivities to the different agents. Agents can be classified on the basis of *xrs* cells expressing "sensitivity" or "hyper-sensitivity". These agents give **RS** values of <2 or >2 respectively. Hydrogen peroxide would appear to exhibit an intermediate sensitivity between these two groups [Vaughan and Gordon, 1992]. The *xrs* mutants, while sensitive to alkylating and cross-linking agents and to UV radiation [Jeggo and Kemp, 1983; Schwartz et al., 1988; Darroudi and

Natarajan, 1989a] these cells are hyper-sensitive to the ionising radiations, the radiomimetic bleomycin and the topoisomerase inhibitors which produce cleavable complexes [Jeggo and Kemp, 1983; Thacker and Stretch, 1985; Darroudi and Natarajan, 1989a; b; Jeggo et al., 1989; Iliakis and Pantelias, 1990; Shadley et al., 1991]. The fact that they can be grouped under either "hyper-sensitive" or "sensitive" headings does not mean that agents are not toxic to cells but refers to the relative toxicity to the two cell types.

The sensitivity as measured by survival data and the relative sensitivity measured by chromosomal aberration formation for a particular agent do not always show a direct correlation. Survival measurements are the result of cells retaining the ability to divide over many generations. This will therefore take into account the relative level of perturbations of the genome, including mutagenesis and loss of genetic material which may not be expressed as recognisable chromosomal aberrations. The numbers of aberrations formed in CHO and *xrs* are temporally regulated. Aberration formation is taken over a relatively short interval and is cell cycle phase dependent. It is possible that genetic instability is induced with aberrations formed in cell cycles subsequent to the one in which the cells were damaged [Kadhim et al., 1992]. The correlation between surviving fractions and relative numbers of aberrations formed, particularly breaks type aberrations becomes closer as the time between irradiation and aberration formation increases.

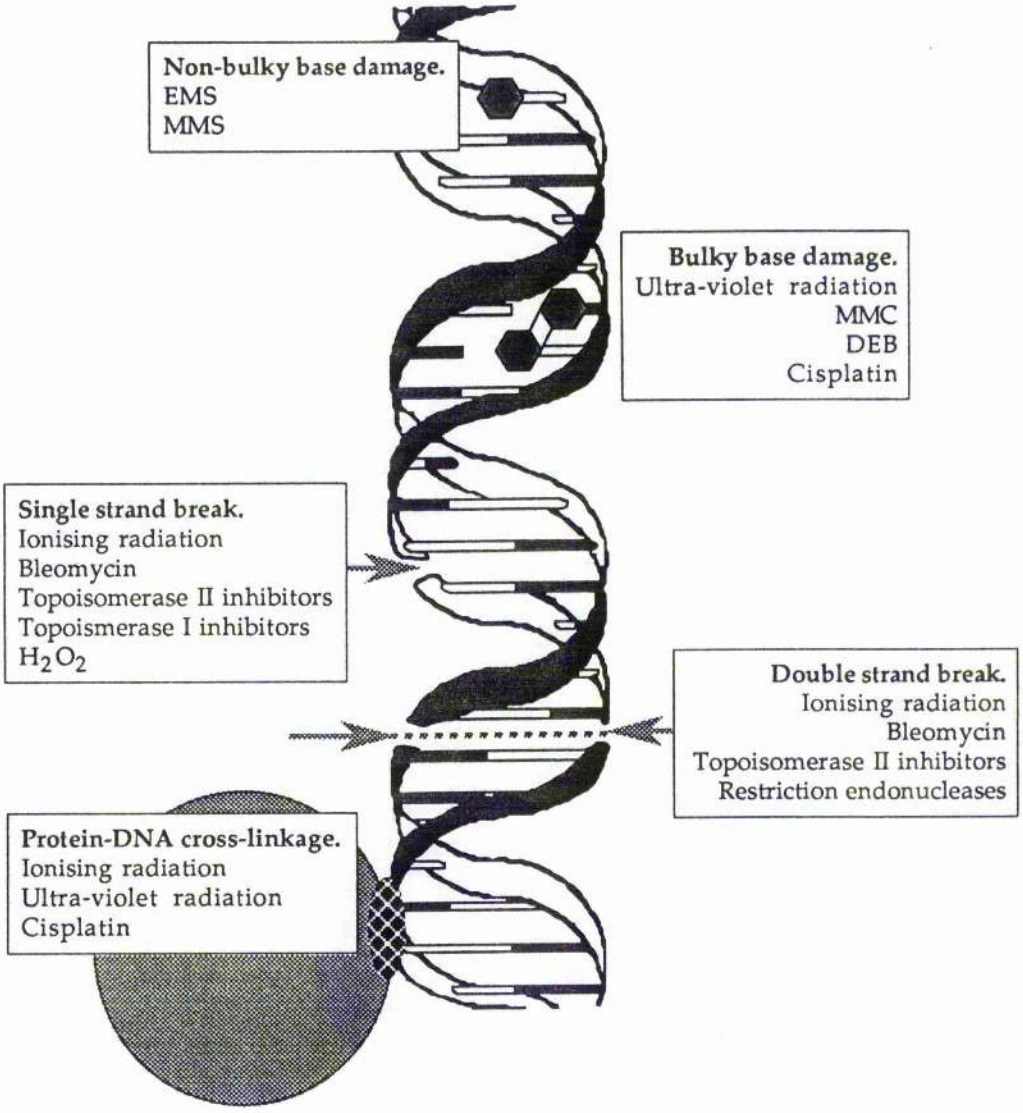

Figure 1.3 Types of DNA damage. Representation of the damage caused to DNA by various clastogenic agents. (Diagram adapted from Ljungman, [1990])

The difference in sensitivity between DNA damaging agents in *xrs* may be related to the methods by which lesions are produced and the types of lesion produced. The hypersensitive group all produce immediate strand cleavage, either by interaction of the agents with DNA or mediated by topoisomerase II. These lesions will occur at all phases of the cell cycle and thus a broad range of aberrations is observed. The sensitive group tend to produce intermediate lesions such as DNA-protein, DNA-DNA crosslinks and base damage. These are lesions which can result in strand cleavage by subsequent enzymatic action. This group can be classified as S-dependent agents since the conversion of nascent DNA damage to aberration forming lesions requires passage through DNA replication [Evans, 1977]. These lesions may either be repaired more proficiently in *xrs* than the lesions produced by the "hypersensitive" group of agents indicating a possible cell cycle dependence of the *xrs* defect. Alternatively repair of these lesions is neither possible in the mutant nor the wild type. High LET radiations and the radio-mimetic BLM form complex lesions which require processing if they are to be repaired. These agents lie towards the "sensitive" group of lesions and either form lesions similar in lethality to the S-dependent agents, or, as has been suggested, form lesions which are non-reparable in both CHO and *xrs* [Blöcher, 1988].

SLDR experiments indicate that interactions between lesions occur which produce an event more deleterious than the sum of two individual events [Fox and Nias, 1970; Dewey et al., 1972; Alper, 1979; Reddy and Lange, 1989]. Also lesions may be repaired if cells are maintained in non-growth conditions as evidenced by PLDR [Frankenberg et al., 1984b]. Both of these forms of repair are defective in *xrs*. From the evidence of SLDR, PLDR and the effects of differing radiations there would therefore appear to be both temporal and spatial components to lesion induction, repair and biological effectiveness. The biological effectiveness of a lesion is determined by the orientation of the lesion with respect to others in both time and space. A simplistic model would involve three groups of lesion: i) Lesions which rarely interact, both by their nature as lesions and their pattern of induction within cells. ii) Lesions which interact if individual lesions are either not repaired prior to the induction of further lesions or there is a local accumulation of damage. iii) Lesions that interact regardless of a temporal component; their interactions the result of the pattern of deposition of the lesions. These can be termed non-interactive lesions, time-dependent interactive lesions and time-independent interactive lesions respectively.

From the results described above *xrs* cells would appear to be defective in the repair of time-dependent interactive lesions which, for example, are produced by sparsely ionising components of radiations. Other lesion types, such as the clustered or complex damage caused by high LET radiations [Goodhead, 1989; 1994] could be categorised as time-independent lesions and are more similar in lethality in the mutant and wild-type. This would appear to

be the same for agents such as the alkylating agents and UV irradiation which might possibly fall into the non-interactive group.

From the evidence of the **RS** and **RC** values described above the more effective agents at producing differential levels of damage subsequent lethality involve the production of DNA strand breaks directly. These were proposed as the lesions that *xrs* cells are defective in the repair of in the original paper of Jeggo and Kemp [1983].

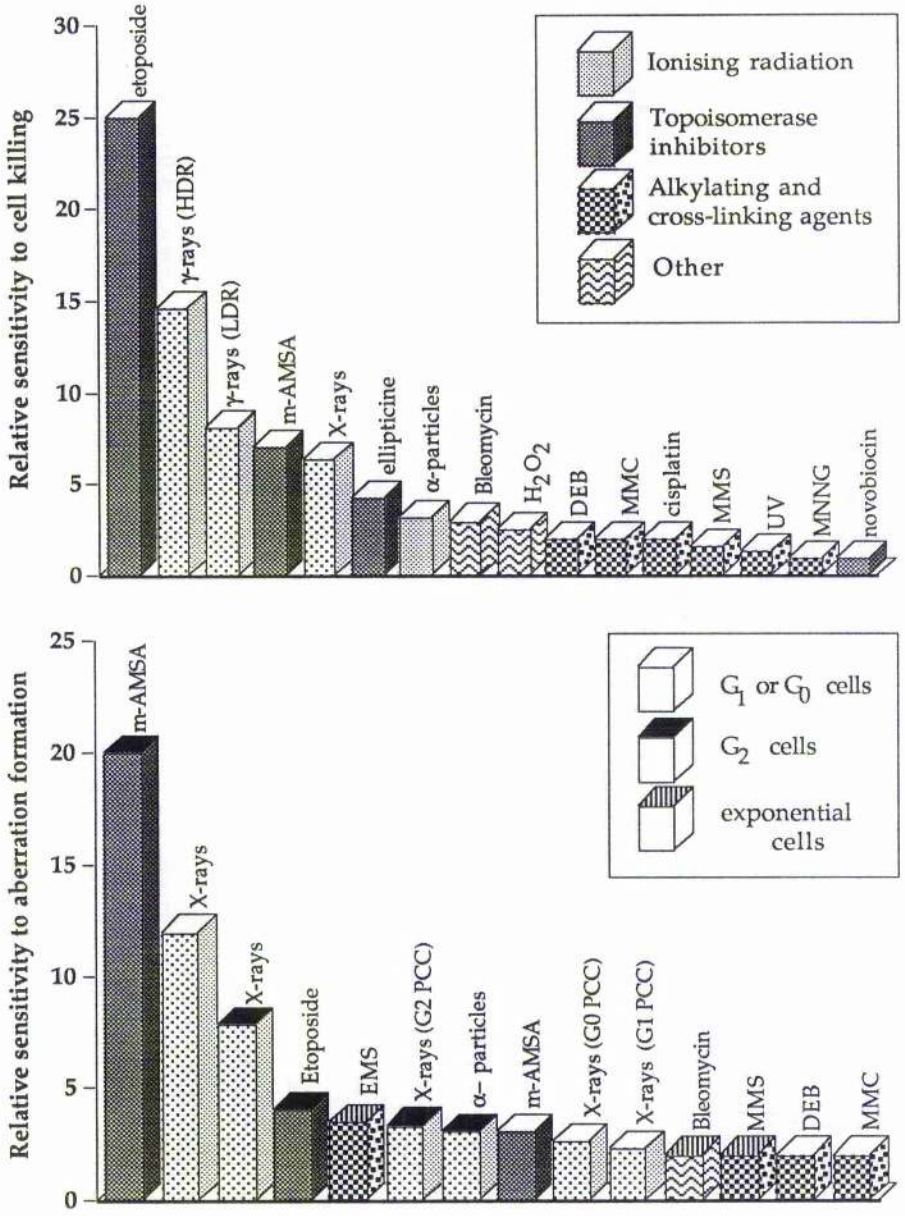

Figure. 1.4 Relative sensitivity of *xrs* cells to DNA damaging agents. Top panel; relative sensitivity to cell killing. Values given are **RS** derived from survival data for *xrs* -5 cells (except VP-16, ellipticine and novobiocin, m-AMSA = *xrs*-1). **RS** values calculated from survival data as in text. Data taken from: Jeggo and Kemp, 1983 (UV, MMS, EMS, MNNG). Thacker and Stretch, 1985 (α-particles, γ-and X-rays). Darroudi and Natarajan, 1989a (bleomycin, MMC, DEB). Jeggo et al., 1989 (VP-16, ellipticine, novobiocin, m-AMSA). Vaughan and Gordon, 1992 (H_2O_2). Schwartz et al., 1988 (cisplatin).
Lower panel; relative sensitivity to aberration formation. Values given are **RC** derived from aberration frequency data for *xrs*-5 cells. Data taken from: Jeggo and Kemp, 1983 (MMS, EMS). Darroudi and Natarajan, 1989a (DEB, MMC, X-rays G_1, G_2 and G_1 and G_2 PCC, VP-16). Iliakis and Pantelias, 1990 (G_0 PCC). Shadley et al., 1991 (α-particles). Front panels of bars indicates type of agent used. Top panel of bars (lower panel only) indicates cell cycle phase of irradiation).

1.4. Induction and repair of DNA strand breaks in xrs cells.

This major group of lesions involves breakage of the DNA molecule. Either direct interaction or radical species can cause cleavage of the phosphodiester backbone of DNA. If only a single cleavage occurs then this is termed a single strand break (SSB). If two or more SSB occur on opposite strands of the helix, in close vicinity to one another, then a double strand break (DSB) is produced. DSB cause an interruption of the integrity of each chromosomal molecule of DNA with the potential of separation of the resulting ends. Breaks may also result from the conversion of base damaged regions (e.g. endonuclease action on apurinic sites). Both types of break result in the release of free energy of supercoiling in circular and looped DNA molecules.

Of the two types of breaks; SSB and DSB; the DSB is thought to be the major deleterious lesion in irradiated yeast and in mammalian cells [Natarajan et al., 1980; Blöcher and Pohlit, 1982; Frankenberg et al., 1984a; Bryant, 1985; Bryant et al., 1987].

The frequency with which strand breaks occur depends on the type of radiation. Approximations of strand break production are 20-40 DSB Gy^{-1} $cell^{-1}$ and 1100 SSB Gy^{-1} $cell^{-1}$ [Blöcher, 1982; van der Schans et al., 1982; Iliakis et al., 1991b].

1.4.1. DNA single strand breaks.

Alkaline sucrose gradient sedimentation, alkaline filter elution filter elution [Kemp et al., 1984] and the technique of DNA unwinding [Costa and Bryant, 1988] have been used to examine the repair of strand breaks in CHO and *xrs* cells. Both the induction and rejoining of SSB were identical in CHO and *xrs* cells. Repair occurred rapidly with 50% of SSB rejoined within 2 minutes [Kemp et al., 1984]. The majority of rejoining occurred at this fast rate within the first 15 minutes followed by a slower rejoining rate. Virtually all breaks were rejoined by 60 minutes post-irradiation [Kemp et al., 1984]. Similar results were obtained with the DNA unwinding technique [Costa and Bryant 1988].

1.4.2. DNA double strand breaks.

Kemp et al [1984] found a deficiency in the rejoining of DSB in all 6 sensitive mutants after γ-irradiation. Rejoining of DSB followed an essentially biphasic pattern in CHO with initial rapid and subsequent slow components of repair. A similar biphasic was demonstrated for DSB repair in other cells [Resnick and Moore, 1979; Weibezahn and Coquerelle, 1981]. A reduction in the overall level of DSB rejoining was observed in *xrs* cells although this initial study did not permit close examination of the two phases of repair.

Subsequent studies showed that the initial fast component of repair occurred at a similar rate and extent in both CHO and *xrs* cells [Iliakis et al., 1992; Dahm-Daphi et al., 1993]. It was the second component to repair that appeared to be defective in *xrs*. This component normally proceeds at a much slower rate than the initial rejoining but in *xrs* the levels of residual damage were virtually unchanged [Costa and Bryant, 1988; Iliakis et al., 1992; Dahm-Daphi et al., 1993]. The fraction of unrepaired damage increased with dose in linear-quadratic fashion until it comprised 50-60% of the total lesions induced [Iliakis et al., 1992]. However, once the fraction damage that remained unrepaired was subtracted from the total lesions a residual repair kinetic could be observed which occurred at the same rate as the residual repair seen in CHO [Dahm-Daphi et al., 1993].

The rejoining of chromatid breaks as measured by the G_2 assay [Bryant and MacLeod, 1990] were observed to be similar in the two cells although the levels of aberrations were 4 fold greater in the mutant. When repair of DSB was examined in synchronised G_2 *xrs-5* cells the second component to repair was apparent [Mateos et al., 1994]. The kinetics of this component to repair was similar to that observed for chromatid break rejoining in G_2.

The repair of strand breaks in the DNA of the *xrs* mutants and the wild-type can therefore be summarised:

i) The induction of SSB and DSB are the same in *xrs* cells as in CHO.

ii) The repair of SSB occurs with biphasic kinetics and is not defective in *xrs*.

iii) The kinetics of both the fast component of repair of DSB and the repair of reparable DSB are the same in the two cell lines.

iv) The fraction of total DSB that remain unrepaired in *xrs* cells is reported to be greater than CHO and it is this that would appear to be the major defect in strand break processing.

v) The repair of DSB in G_2 cells is similar to that of wild-type cells.

DSB could lead to a chromosomal break type aberration if the ends of DNA dissociate from one another and this separation occurred within higher order structures of the chromatin. If the ends of chromatin then became separated sufficiently observation by microscopy might be possible. It is feasible that a DSB could be present within chromatin but the integrity of the chromatin maintained by protein-DNA and protein-protein interactions. However, it is thought likely that for a break type aberration to be witnessed there must be an underlying DSB. Breakage followed by erroneous rejoining might also be involved in the formation of exchange type aberrations.

When the rejoining kinetics of chromatid aberrations are compared with the repair of DSB there would appear to be a correlation between the rate of repair and residual unrepaired fractions of both DSB and chromatid breaks in the mutant and wild-type. The rejoining of PCC fragments [Iliakis and Pantelias, 1990] followed similar kinetics to repair of DSB, namely an initial rapid component similar in both CHO and *xrs* followed by a slow component not seen in the mutant cells [Costa and Bryant, 1988; Iliakis et al., 1992; Dahm-Daphi et al., 1993, Iliakis and Pantelias 1990]. *Xrs* cells may retain a much reduced slow component of repair of both DSB [Dahm-Daphi et al., 1993] and chromatid breaks [MacLeod and Bryant, 1990] although this may be cell cycle dependent response [Mateos et al., 1994]. As mentioned earlier, the residual numbers of chromosome breaks remaining has been correlated with the number of lethal events deposited by radiation per Gy in the mutant and wild type cell lines [Iliakis and Pantelias, 1990].

Therefore, if the repair of DSB, chromosomal aberrations and the survival of cells are all directly related, the ionising radiation sensitivity phenotypes described so far can be attributed to a defect in the repair of a fraction of DSB in *xrs* cells.

There is a problem in correlating DSB repair measurements, chromosomal aberration measurements and survival data. All of these methods utilise both different dose ranges and time-scales over which measurements are made. Although some overlap does occur this may prevent direct correlations between results. Indeed one example of these discrepancies can be observed in interpretation of DSB breaks remaining with dose and the residual fraction of chromatid fragments measured by PCC. It was observed that after a dose of 3 or 6 Gy approximately two thirds of the PCC fragments remained unrejoined in *xrs* after 24 hours [Iliakis and Pantelias, 1990]. In contrast, measurement of residual DSB indicates that the fraction remaining decreases with time with only 25% of breaks remaining in *xrs-5* after a dose of 15 Gy [Iliakis et al., 1992]. It would appear, according to these results that there is a proportion of DSB that do not produce chromosomal breaks. These may be "hidden" by structural components of chromatin where aberrations are concerned or multiple DSB may lead to only a single aberration.

The presence of multiple components to the repair of DSB indicate that either multiple repair mechanisms for the same lesion, multiple forms of lesion with differing "reparability" or a combination of these exist. Based on the above observations the repair of DSB can be divided into three main categories:

i) Rapidly reparable DSB.

ii) Slowly reparable DSB.

iii) Non-reparable DSB.

1.5. *Genetic characteristics of the xrs cells.*

The *xrs* phenotype must have a genetic basis, with a gene product or products inducing the radiation sensitivity observed. There should, thus, be genetic markers which could in theory distinguish between *xrs* and CHO cells. The following Section describes examinations that have been performed on the genetic characteristics of the *xrs* cells.

The *xrs* mutants were originally derived from heavily mutagenised populations of CHO-K1 cells with colonies formed from populations containing 1 EMS induced thioguanine resistance mutant per 10^3 survivors [Jeggo and Kemp, 1983]. The high incidence of *xrs* mutants, with 1.33 per 10^3 colonies examined, may reflect this high mutation load or alternatively it may relate to some inherent instability of the *xrs* gene. Similarly, the high mutation load placed on the cells may have resulted in the presence of additional mutations in the genome of the mutants isolated. These could result in the presence of phenotypes in addition to, but not linked to, the radiation sensitivity phenotype of the *xrs* variants. Caution must therefore be practised when attributing any characteristic of the cell lines to one single *xrs* gene.

1.5.1. *Complementation analysis.*

1.5.1.1. Cellular complementation.

The presence of multiple radiation sensitive mutants may be the result of mutations in a number of enzymes all involved in the same pathway or independent pathways. To ascertain whether this was the case for the *xrs* mutants, complementation analysis was performed [Jeggo, 1985a]. This revealed that the sensitivity observed could be partially complemented by fusion of CHO cells with *xrs* cells. The fusion of differing *xrs* mutants did not produce this increased resistance. This indicates that the *xrs* variants belong to the same complementation group. Complementation by wild-type reveals the recessive nature of the *xrs* mutation. The *xrs* mutants were identified as belonging to a distinct ionising radiation sensitive complementation group to the sensitive cell lines identified at the time and the *xrs* cell lines were subsequently designated ionising radiation sensitive complementation group 5 XRCC5) [Jeggo et al, 1991; Zdzienicka et al., 1992, Jeggo et al., 1992]. The XRCC5 phenotype is one of four rodent DSB repair mutant complementation groups isolated to date [Jeggo; 1990; Collins, 1993]. The partial complementation observed by fusion with wild-type may result from a reduced level of the wild-type gene product relative to the DNA content of the fused cells [Darroudi and Natarajan, 1989c].

Also belonging to XRCC5 complementation group is the cell line XR-V15B [Zdzienicka et al., 1988]. This cell line was isolated from V79 Chinese hamster cells. XR-V15B also exhibits a reduced ability to rejoin DSB [Zdzienicka et al., 1988] with an increase in the levels of DSB

left unrejoined attributable to a reduction in fraction of lesions repaired by the "fast" component and reduced kinetics of the "slow" component of repair [Kysela et al., 1993]. Based on estimates of DSB induction [Iliakis et al., 1991b], there would appear to be a good correlation between the level of unrepaired DSB (2.3 DSB Gy^{-1} for V79B and 0.3 DSB Gy^{-1} for XR-V15B) and the approximate numbers of lethal lesions induced (2.0-2.5 Gy^{-1} for V79B and 0.2 Gy^{-1} for XR-V15B) [Zdzienicka et al., 1988; Kysela et al., 1993].

1.5.1.2. Genetic complementation.

Partial complementation of *xrs* radiation sensitivity can also be produced by the introduction of fragments of human chromosome 2 into cells of the *XRCC5* complementation group by micro-cell mediated chromosome transfer [Jeggo et al., 1992]. This gene has been termed *XRCC5* due to the designation of the *xrs* mutants to mammalian ionising radiation complementation group 5 . *XRCC5* in human cells has been located on the long arm of chromosome 2. Linkage indicates that this gene lies close to the TNP-1 (transitional nuclear protein-1) marker which maps to 2q37. By the laborious task of positional cloning [Jeggo et al., 1992; Hafezparast et al., 1993] and molecular cloning techniques involving human gene libraries of the identified chromosomal regions [Taccioli et al., 1994b in press] the *XRCC5* gene has, during the preparation of this manuscript, been identified as the *Ku 80* gene. The gene product of this gene Ku 80 is, along with Ku 70, one part of a heterodimeric polypeptide which is the DNA-binding subunit of a DNA dependent protein kinase. The Ku heterodimer binds to the ends of DNA and as such may play a part in the repair of DSB.

1.5.2. Mutational and recombinational response of xrs cells.

The formation of DSB has been associated with cell killing [Natarajan et al., 1980; Blöcher and Pohlit, 1982; Frankenberg et al., 1984a; Bryant, 1985; Bryant et al., 1987]. However, DNA damage is also associated with disruptions of the genetic material which do not affect clonogenic survival. Rearrangements of the genetic material can be termed mutations [reviewed in Lewin, 1990]. Mutations can occur in non-functional regions of the genome where their effect will be minimal. Alternatively they can affect the coding sequence of genes directly, resulting in altered gene products, or indirectly via gene control mechanisms such as promoter/represser sequences. Mutations involving the the expression of genes and the sequence of the resulting transcripts may affect the proper functioning of the cell and/or cell death. The processes involved in the formation of mutations are unclear. However, they can result from either the direct effect of damage, e.g. base damage resulting in errors of replication and or transcription, or they may result from repair processes, such as excision of damaged regions followed by incomplete restoration of genetic sequences or translocation of sequences into other regions of the genome.

1.5.2.1. Reversion to wild-type.

The reversion of a mutation occurs when either the mutated sequence of DNA assumes the original sequence or an additional change occurs in the DNA which compensates for the mutation.

An early observation made was the high reversion rate of *xrs* to wild-type after periods of time in culture [Jeggo and Kemp, 1983; Jeggo and Holliday, 1986; Denekamp et al., 1989]. Reversion was dramatically enhanced by treatment with X-rays or bleomycin both in the presence or absence of azacytidine (AZC) [Jeggo and Holliday, 1986; Jaffe et al., 1990]. AZC inhibits methylation of DNA preventing controlled repression of gene function. These revertant populations expressed varying degrees of resistance to DNA damage by X-rays, bleomycin or cisplatin [Jeggo and Holliday, 1986; Jaffe et al., 1990]. This could indicate that either multiple repair mechanisms are defective in *xrs* cells or the original mutation of the *xrs* gene is not a simple "on or off" mutation with the gene existing in varying states of activity.

When survival curves of several of the *xrs* variants were examined over a wide range of X-ray doses there were indications of the *xrs* cell lines composed as a mixture of X-ray sensitive and resistant sub-populations [Denekamp et al., 1989]. Whilst the initial slope of the survival curves proved to be 10-20 fold steeper than CHO-K1 the slopes at high doses were similar. The resistant subpopulations were identified as comprising 0.4-12% of the total population of cells. It was, however, not possible to reproducibly isolate this resistant sub-population. This lack of stabley resistant populations indicated that only a transient reversion of the *xrs* mutation had occurred. These subpopulations were not necessarily the cause of the stable reversions.

The non-stable resistant sub-population, the high incidence of the *xrs* phenotype and stable reversion by AZC led to the hypothesis of functional hemizygosity of CHO-K1 cells with regards the *xrs* gene [Jeggo, 1985a; Jeggo and Holliday, 1986, Denekamp et al., 1989]. It was proposed that epigenetic changes involving methylation of cytosine residues in the DNA of CHO cells caused suppression of one copy of the *xrs* gene [Jeggo and Holliday, 1986]. This silencing can be termed an epimutation [Holliday, 1985] to distinguish it from conventional mutations. The selection of the *xrs* mutant cell lines resulted in a mutation (epimutation or "classical" mutation) silencing the only functional copy of the *xrs* gene. Treatment with AZC activated the silent copy present in both CHO and *xrs* . Subsequent clones continued the pattern of hypomethylation producing a stable revertant cell line [Jeggo and Holliday, 1986].

Transient radio-resistance was postulated to be the result of the silent (normal) copy of the *xrs* gene acquiring a transcriptionally active hemi-methylated state following DNA

replication [Denekamp et al., 1989]. This allows a normal radiation response. As the parental methylation pattern is resumed the transcription of the *xrs* gene is again reduced. From the length of the cell cycle and the proportion of resistant cells estimation of the length of the resistant phase ranges from 4 minutes (*xrs*-5) to 2 hours (*xrs*-7).

EMS has been shown to elevate the level of DNA methylation [Farrance and Ivarie, 1985]. The ethylation of CpG sites within DNA has been shown to stimulate DNA (cytosine-5)-methyltransferase activity possibly by mimicking the post-replicative hemi-methylated form of DNA. This "pseudo-methylation" involving ethylation of a guanine residue on one strand of DNA and methylation on the corresponding cytosine residue could result in a stable epimutation in subsequent daughter strands of DNA.

However, the XR-V15B cell line, which also belongs to the XRCC5 complementation group, is not revertible using AZC [Zdzienicka et al., 1988]. XR-V15B cells do exhibit enhanced resistance to ionising radiation during late G_2/S phase however.

That both xrs cells and XR-V15B cells exhibit G_2/S phase resistance may therefore indicate that processes other than methylation/demethylation events are involved in the cell cycle dependent response of these cells. The mutation in XR-V15B may therefore involve a mutation of the *XRCC5* gene which involves a sequence alteration whilst the mutation in *xrs* cells may involve an epimutation via an altered methylation status of the gene.

1.5.2.2. Mutagenic response of xrs cells to DNA damaging agents.

As described above, reversion of the *xrs* cell lines can be induced by treatment with clastogenic agents. This may involve restoration of the *XRCC5* gene to the wild-type or compensation of the gene defect by an additional mutation elsewhere.

Classically, mutations can involve deletion, insertion and inversion of sequences and also base substitutions resulting in possible coding or gene expression alterations [Lewin, 1990]. Mutations have been linked to the formation of specific DSB by treatment of Chinese hamster V79 and CHO cells with restriction endonucleases [Obe et al., 1986; Singh and Bryant., 1991].

As described in section 1.4.2., *xrs* cells repair only a fraction of the DSB induced in their DNA. Whether the repair defect is also associated with enhanced mutation frequency has been examined by several groups using genes which are non-essential under normal cell culture conditions but which can be selected for by the use of specific growth mediums. *Xrs-5* cells irradiated with X-rays produced a 3-4 fold increase in the formation of mutations per surviving cell compared to CHO cells at the hypoxanthine-guanine phosphoribosyltransferase (*hprt*) and thymidine kinase (*tk*) genes for equivalent doses

[Darroudi and Natarajan, 1989a; Mussa et al., 1990]. Enhanced numbers of mutations were also formed after treatment with equal doses of MMS with a 1.5-2 fold increase in *hprt* mutants [Darroudi and Natarajan, 1989a]. A correlation was found to exist between the mutation frequency and surviving fraction at the doses examined for both CHO and *xrs* cells which has been postulated to be due to the presence of lesions common to both mutagenesis and cell killing [Mussa et al., 1990]. Not all studies showed enhanced mutation frequencies in *xrs* cells. Shadley et al., [1991] found *xrs* cells to be hypomutable at the *hprt* locus after treatment with to X-rays. This hypomutability is also observed when CHO and *xrs* cells are treated with doses of γ-rays which are equitoxic [Zdzienicka et al., 1988]. The XR-V15B cell line has similarly been demonstrated to be hypomutable at the *hprt* locus after γ-ray treatment compared to the V79B parental cell line [Zdzienicka et al., 1988].

Similar rates of mutation at the *hprt* locus were induced by ^{212}Bi α-particles in CHO and *xrs-5* cell lines [Shadley et al., 1991]. These studies were performed using equitoxic doses of α-particles and X-rays. In CHO cells α-particles and X-rays were equally effective at inducing mutations. In contrast, in *xrs-5* cells the mutation rate was higher after α-particle irradiation than after X-irradiation. This was in contrast to clonogenic survival and aberration data which suggested that α-particles were equally lethal and clastogenic as X-rays in *xrs-5*, whilst in CHO, α-particles were 3.5-3.9 fold as effective as X-rays on a per dose basis [Shadley et al., 1991]. It was postulated that although deficiencies in DSB repair affected the survival and aberration frequency of *xrs-5* cells the mutagenic effects were unaffected.

It must be remembered that only the cells which survive treatment with a mutagen can be examined for the expression of mutations. On the assumption that a single unrepaired DSB kills both CHO and *xrs* cells [Resnick and Moore, 1979; Frankenberg et al., 1981; 1984a], only cells capable of repairing all DSB contained within their genome would be able to express mutations. This limits the population studied to ones which either contain low amounts of damage, damage other than DSB or repair proficient sub-populations. The presence of resistant cell sub-populations has been suggested as a cause of the discrepancies observed between studies. Alternatively there is the possibility of mutations comprising of large multi-locus type deletions in the *xrs* cells line which could possibly involve a flanking essential gene resulting in cell killing [Shadley et al., 1991].

Therefore, although some of the evidence is conflicting, it would appear that *xrs* cells do exhibit higher mutation frequencies than CHO cells when treated with ionising radiation, when equal doses are used for both cell types. When equitoxic doses are used *xrs* appear hypomutable. The difference observed in the actual mutation frequency per surviving cell may be due to rejoining, where it occurs, resulting in lethal mutations in *xrs*. These lethal

mutations may be similar to the multilocus deletions induced by α-particle irradiation and may be the result of the delayed DSB repair in *xrs* allowing nuclease activity at the ends or due to aberrant rejoining resulting in the deletion of portions of DNA in an illegitimate recombination reaction.

1.5.2.3. Transfection and homologous recombination of plasmid DNA.

Based on the kinetics of repair in *E. coli* and yeast it has been suggested that the fast component of DSB repair is the result of a simple ligation process whilst the slow component involves recombination [e.g. Weibezahn and Coquerelle, 1981]. The existence of a recombinational repair mechanism has been supported by evidence that two repair processes occur at different stages of the cell cycle, one of which is associated with a recombination process [Resnick, 1976; Resnick and Moore, 1979]. Recombinational intermediates have also been identified [Fonck et al., 1984]. It was postulated that recombinational repair involved the transient exchange of homologous DNA sequences followed by synthesis of DNA, replacing that which had been damaged, followed by disruption of the recombinational complex [Resnick, 1976; Resnick and Moore, 1979]. That the recombination events did not involve the net exchange of genetic material would support this hypothesis [Fonck et al., 1984].

In addition to homologous recombination between DNA molecules which share sequences there is also non-homologous recombination between heterologous sequences. The latter occurs, for example in incorporation of endogenous sequences into genomic DNA e.g. during plasmid transfections which produce stable transfectants. Non-homologous recombination has been shown to be involved in the joining of restriction endonuclease induced staggered ends of DNA which do not share sequence homologies [Pfeiffer et al., 1994]. This process would appear to involve polymerisation, excision and ligation reactions depending on the nature of the ends rejoined.

The possibility of the *xrs* mutants possessing a defect in homologous recombination has been investigated by Moore et al. [1986] and Hamilton and Thacker, [1987] by the use of *in vivo* assays involving the recombination of two non-complementing transfected plasmids in CHO and *xrs* cells. *Xrs*-5 cells showed a reduction in the frequency of transfection (4-fold) and in the level of homologous recombination between the plasmids (6 fold) when compared to CHO-K1. When a double strand break was introduced into one of the plasmids the difference in recombination between the two cell lines was unaffected [Moore et al., 1986]. In the study by Hamilton and Thacker, [1987], no significant differences in the levels of homologous recombination were obtained in the two cell lines once correction for transfection frequency was made. In vitro recombination between the two plasmids mediated by nuclear extracts

was also examined. These experiments showed a slight reduction in recombination frequency by *xrs*-5 nuclear extracts (70% of CHO activity). However this difference was not significant [Moore et al., 1986].

Thus the difference in sensitivity to DSB did not appear to be due to a defect in homologous recombination in *xrs* cells. One result that was observed was the decreased levels of stable transfection of plasmid into *xrs* host DNA in both the above studies. All six *xrs* mutants were subsequently found to be deficient in their ability to integrate foreign DNA into their genome and to produce stable transfectants [Jeggo and Smith-Ravin, 1989; Smith-Ravin and Jeggo, 1989]. This was not due to a decrease in the uptake of DNA by the cells but was attributed to either a defect in the processing of the plasmid DNA to a form that could be integrated or in the mechanism of integration itself. Introduction of single DSB into the plasmid used by restriction endonuclease digestion produced linear molecules which transfected at a frequency proportional to the distance between the DSB and the the selectable marker gene encoded by the plasmid. Linearisation of plasmid with restriction endonucleases produced a slight elevation of transfection frequency in both cell types compared to supercoiled molecules at the distance furthest from this gene. The presence of a DSB within the selectable marker gene resulted in a marked decrease in the transfection frequency in both CHO and *xrs* cells [Smith-Ravin and Jeggo, 1989]. No difference in the level of transfection of linear molecules was observed between CHO or *xrs* cells [Hamilton and Thacker, 1987; Jeggo and Smith-Ravin, 1989; Smith-Ravin and Jeggo, 1989].

γ-Irradiation of plasmid to be transfected resulted in a decrease in the transfection frequency of both CHO and *xrs* cells [Smith-Ravin and Jeggo, 1989]. The reduction in transfection frequency with dose had a biphasic kinetic in both the mutant and wild-type cells. There was an initial rapid reduction in transfection frequency with dose. This corresponded to the relaxation of supercoiled plasmid to the open circular form. This relaxation can be induced by the induction of SSB. However, base damage occurs at a similar rate as SSB induction and so the decrease in transfection could be due to either SSB formation or base damage. The rate of decrease was much more rapid in *xrs* cells than CHO which exhibited a slight shoulder at low doses. This fast component was followed by a slower reduction which corresponded to the formation of DSB and the linearisation of the plasmid from the open-circular form. Although *xrs* cells exhibited a decrease in the frequency of transfection at these high doses compared to CHO the rate of reduction of this DSB component with increasing dose was similar in both CHO and *xrs* [Smith-Ravin and Jeggo, 1989].

These results reveal that *xrs* cells have a defect in the ability to incorporate foreign DNA into their genome. It would appear that this process is not dependent on the presence of DSB but possibly on SSB relaxation of plasmid DNA to the open-circular form. Indeed, the lack of

difference in the kinetics of the reduction of transfection frequency due to DSB formation indicate that repair of DSB as seen in this system is equal in the two cell lines.

The importance of SSBs on the integration of foreign DNA may indicate that *xrs* cells are defective in non-homologous mechanisms which involve integration of DNA containing SSB and/ or base damage. The repair of SSB has been shown to be normal in *xrs* cells [Kemp et al., 1984]. The non-homologous integration step may subsequently be required for the repair of DSB but not SSB.

1.5.2.4. V(D)J recombination in xrs cells.

Extrapolations from results of experiments involving plasmid DNA must be performed with caution. Plasmid DNA does not necessarily attain the same conformation as genomic chromatin. The mechanisms of repair and processing in genomic DNA and integrated or free plasmid DNA may therefore differ significantly.

A system of examining recombination in genomic DNA sequences exists in the formation of immunoglobulin and T-cell receptor variable region domains. This process is termed V(D)J recombination. V(D)J recombination allows the formation of the genetic variation necessary for the production of immune proteins with variable antigen recognition sites. Normally this process occurs in lymphoid tissues only. By transfection and subsequent expression of two genes; recombination activation genes 1 and 2 (*RAG-1* and *RAG-2*); non lymphoid tissues can initiate V(D)J recombination events within their own genomes [Schatz et al.,1990]. This differs from the above experiments involving recombination between exogenous plasmids in that the sequences which are involved in recombination are existing genomic sequences. The *RAG-1* and *RAG-2* sequences activate this process.

These recombination events involve the recognition of specific sites which consists of conserved heptamer-spacer-(oligo-d(A)-oligo-d(T) rich) nonamer sequences (*RS* sequences) that flank germline V, D or J segments. DSB are introduced at specific sites between the elements to be joined and the *RS* sequences. Ligation then occurs between *RS* sequences and between V, D or J segments. This effectively loops out the segment containing the two ligated *RS* sequences. The process of joining of the coding sequences can involve either the addition or loss of nucleotides; increasing the variability of these sequences (Figure 1.5). This would indicate the action of either polymerases and/or exonuclease at the coding segment ends. The ligation of the two *RS* segments is normally performed with a high degree of fidelity.

The X-ray sensitive, DSB repair deficient murine severe combined immunodeficiency (*scid*) cell lines have been shown to be defective in V(D)J recombination [Taccioli et al, 1993; 1994a] and DSB repair [Tanaka et al., 1993]. When plasmids containing *RAG-1* and *RAG-2* were

transfected into CHO and *xrs* cells the mutant cells failed to generate normal V(D)J recombination events in both germline V(D)J sequences and transiently transfected plasmids containing *RS* and coding sequences in various orientations [Pergola et al., 1993; Taccioli, 1993]. While the recognition of the *RS* sequence and formation of the DSBs necessary to initiate the recombination event occurred, subsequent rejoining of the coding regions and the *RS* sequences was impaired with significant reductions in the number of rejoining events. Of the *RS* joins performed, only 14% showed correct rejoining. The remainder exhibited deletions of approximately 20 base pairs from one or both of the *RS* sequences [Pergola et al., 1993; Taccioli, 1993]. This was proposed to be due to nuclease action on the free ends of the DNA produced by the cleavage reaction. This imprecise rejoining was corrected by altering the conditions of transfection namely removing the salmon sperm carrier DNA used in the transfection process. This produced similar recombination frequencies in both wild type and mutant [Pergola et al., 1993]. It was postulated that the presence of salmon sperm DNA caused the titration of a DNA binding protein which protects the free ends of *RS* sequences allowing aberrant exonuclease action [Pergola et al., 1993]. This digestion presumably does not occur in CHO, even in the presence of carrier DNA. The digestion might therefore be the result of the impaired ligation reaction which leaves the ends unrepaired for longer periods of time allowing naturally occuring nuclease activities to act on the DNA.

Comparisons can therefore be drawn between DSB repair, survival, mutagenesis studies and V(D)J recombination events. The decreased numbers of rejoining events observed may be analogous to the decreased level of DSB rejoining as a whole. This then produces the decrease in survival due to elevated levels of unrejoined DSB. The few rejoining events that do occur are performed with a much reduced fidelity. This would be analogous to the higher rate of mutation per survivor in *xrs*.

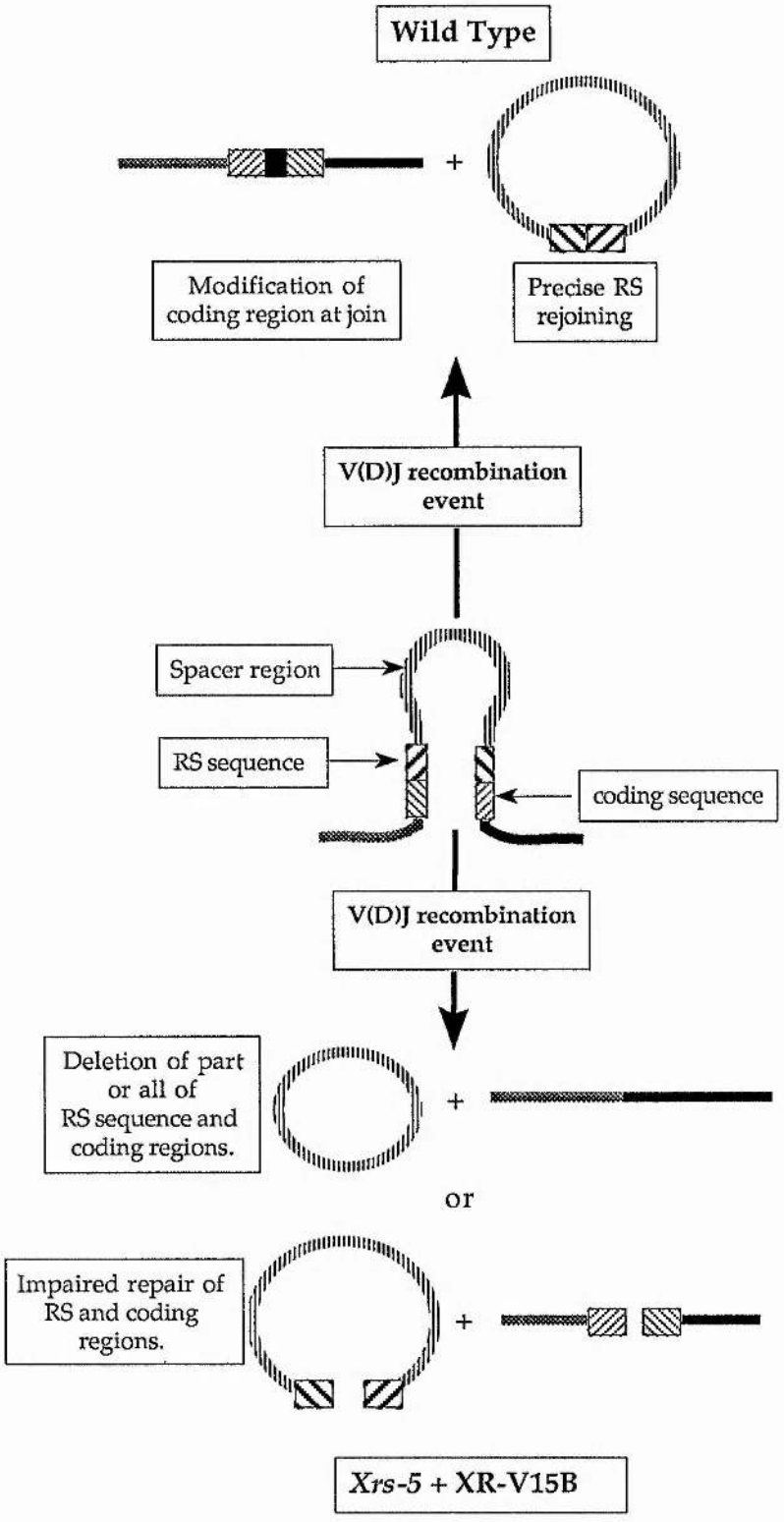

Figure 1.5. Diagram of V(D)J recombination processes in germ-line DNA. See text for explanation.

1.5.3. Gene expression.

By comparing the levels of RNA transcribed in CHO and *xrs* cells several genes have been shown to be repressed in the *xrs* mutants. 11 and 14 species of mRNA were found to be underexpressed in *xrs-5* and *xrs-6* respectively [Zhu et al., 1992]. These included ferritin heavy chain, non-muscle myosin light chain, ribosomal proteins and a novel retroviral sequence (B52). The B52 sequence was the most seriously underexpressed mRNA, with a 26 fold decrease in expression [Zhu et al., 1993]. This sequence proved to have multiple copy numbers in both CHO and *xrs-5* with no gross structural or copy number change observed in *xrs-5*. The reduction in expression has been proposed to be the result of a "trans-acting" repression of the promoter/enhancer region of the B52 sequences. However this trans-acting factor has not yet been identified. γ-Irradiation decreased the expression of only one mRNA species in *xrs-5* while the other 10 mRNA species and all the CHO sequences were unaffected.

The reduction in the levels of these 10-14 mRNA species may be directly related to the ionising radiation sensitivity phenotype produced by the *xrs* gene mutation or be due to unrelated pleiotropic effects. It is feasible that epimutations occurred in all of the genes involved or that the mutation in the *xrs* gene results in silencing of the genes via an *xrs* controlled trans-acting factor. Although methylation may play an important role in the radiation sensitive phenotype of *xrs* cells no evidence of drastically altered levels of methylation of the B52 genome was identified [Zhu et al., 1993].

1.6. Cytological and other characteristics of the xrs phenotype.

The majority of the characteristics of *xrs* cells described so far have been those observed after either damage to DNA or the response of the cells to exogenous genetic material such as occurs during plasmid transfection. The reduced expression of several genes are an example of the *xrs* phenotype having characteristics which are not dependent on either of these two events. *Xrs* cells can therefore be attributed both a constitutive phenotype and a damage responsive phenotype. These two are likely to closely related. This next section reviews some of the constitutive characteristics that have been observed for *xrs* cells.

1.6.1. Nuclear and chromatin structure of xrs cells.

Elements of cellular structure have been observed to differ between *xrs-5* and CHO cells. The metaphase chromosomes of *xrs-5* cells have been observed to be hyper-condensed in appearance [Schwartz et al., 1990; 1993]. By light microscopy *xrs* chromosomes are, on average, 3 fold more condensed, appearing both shorter in length and thicker in width. When examined by transmission electron microscopy the condensation can be attributed to *xrs*

cells maintaining large loops of chromatin extending from the chromosome core. Excluding this material, the cores of the chromosomes are actually thinner than the core of CHO chromosomes. This difference in chromatin loop size did not appear to extend to the structure of interphase nuclei with similar nucleoid sizes for the two cell lines as determined by flow cytometry. Irradiation of nucleoids produces an enlargement due to the relaxation of previously supercoiled DNA looped domains. When CHO and *xrs-5* were irradiated the nucleoid size increase was also similar in the two cell lines [Schwartz et al., 1993]. Neither was there any difference in the relative levels of constitutive supercoiling between the chromatin of the two cell lines. When positive supercoiling was induced by intercalation of ethidium bromide into the DNA *xrs* nucleoids were significantly larger than CHO nucleoids. This indicated some constraint to positive supercoiling in *xrs* cells.

Interphase nuclear structures have also been examined by electron microscopy [Yasui et al., 1991; 1994]. Several morphological changes were observed in the components of the nuclei of CHO and *xrs* cells. Whilst the overall shape and size of the nuclei did not differ significantly, differences were observed in the nuclear envelope of nuclei and the distribution of chromatin within the nucleus. The inner and outer nuclear membranes of *xrs-5* were separated from each other, with inclusions sometimes occurring within this space. This arrangement differs from that of CHO cells were the nuclear membranes maintain a tight association all along their circumference. Enlargement of this perinuclear space is also observed in mitotic prophase [Franke, 1974]. In addition, densely staining structures were apparent at many nuclear pore complexes. Heterochromatin in *xrs* cells was more widely dispersed throughout the nucleus compared to the more discrete organisation of CHO heterochromatin. The nuclear scaffold, polypeptide composition, euchromatin and the nucleoli were indistinguishable from one another in CHO and *xrs* cells [Yasui, 1991; 1994]. Increased digestion of nuclear DNA by nuclease has been given as evidence of reduced attachment of DNA to the nuclear matrix of *xrs-5* cells [Yasui et al., 1994].

Thus the structure of both the metaphase chromosome and the interphase nucleus of *xrs-5* cells contain structural abnormalities. The increase in chromosome compaction may be due to the increase in the size of the loops of chromatin extending from the metaphase scaffold. This may in turn be linked to the altered heterchromatin structure observed in the interphase nuclei.

1.6.2. Topoisomerase II activity.

A major component of the proteinaceous supporting structure of chromatin is topoisomerase II. This forms the second most abundant protein in the mitotic nuclear scaffold [Mirkovitch et al, 1987; 1988]. The functions of topoisomerases includes the removal of topological stresses induced during transcription and replication of DNA. Topoisomerase II produces a covalently

cross-linked protein associated double strand break in DNA permitting the passage of an additional strand through the gap formed. This allows catenation or decatenation of intact circles of DNA. As discussed later; the chromatin of eukaryotic cells is organised into loops attached at the base to a proteinaceous matrix (interphase) or scaffold (mitosis). These loops are the fundamental units of replication and transcription and can be imagined as existing as independent units of DNA subject to torsional stresses independent of other loops [e.g. Cook and Brazell, 1978; McCready et al., 1980; 1982]. Topoisomerase II DNA recognition sites occur within matrix and scaffold attachment regions (MAR and SAR respectively) and so topoisomerase II is likely to be involved in the attachment of loops to the scaffold/matrix [Mirkovitch et al., 1988; Adachi et al., 1989].

Alteration in the structure of the metaphase chromosome and interphase heterochromatin indicate alterations in the structure of chromatin at the loop domain level. A possible candidate for involvement is therefore topoisomerase II.

In vivo measurements of cleavable complex formation in response to topoisomerase II inhibitors have been made. Incubation of cells with etoposide and m-AMSA incubation resulted in equal numbers of cleavable complexes in both CHO and *xrs*-1 [Jeggo et al., 1989]. *Xrs*-2 cells, which do not exhibit sensitivity to etoposide produce fewer cleavable complexes than CHO cells. These measurements were performed by precipitation of protein-DNA complexes which are formed by the covalent bonding of topoisomerase II to DNA at the formation of a cleavable complex.

An alternative method was employed by Warters et al., [1991]. Here alkaline (SSB detection)and neutral (DSB detection) filter elution techniques were performed in the presence or absence of proteinase K. The digestion of protein by the proteinase reveals the strand breaks associated with the cleavable complexes and so the comparison of elution with and without proteolysis gives an estimate of the relative production of cleavable complexes.

When this technique was applied to *xrs-6* cells exposed to m-AMSA there was a consistent reduction (approximately 30%) in the level of cleavable complex formation in mutant cells compared to CHO. From the dose response curves it would appear that while the initial rate is similar in both cell lines (i.e. low doses) the maximum induction of cleavable complexes is greater in CHO (i.e. at high doses). This would indicate that the rate of cleavage is similar per topoisomerase molecule in the two cell lines but the number of breaks produced is lower in *xrs* nuclei and that this may result from a reduction in the numbers of topoisomerase II molecules. As with DSB induced by ionising radiation subsequent repair of these lesions on removal of m-AMSA was seen to be defective in *xrs-6*.

The difference in the numbers of complexes measured between the two methods mentioned above may be due to a number of reasons: i) There may exist functional differences in the responses of the different cell lines used to different topoisomerase inhibitors. ii) The techniques employed to measure cleavable complexes may be affected by factors other than purely the number of strand breaks: It has been demonstrated that chromatin structure can influence filter elution response in a number of cell lines [Warters and Lyons., 1990; Iliakis et al., 1991a; Wlodek and Olive, 1992].

The levels of extractable topoisomerase II and its *in vitro* activity have been examined in order to determine whether there is some fault in the function or differences in levels of the enzyme.

Equal in vitro topoisomerase II activities were found for nuclear protein extracts from CHO, *xrs-1*, *xrs*-2 [Jeggo et al., 1989] and *xrs-6* [Warters et al., 1991] when assays involving the "unknotting" of bacteriophage DNA [Jeggo et al 1989] or decatenation and catenation of kinetoplast and plasmid DNA respectively were used [Warters et al., 1991]. These reactions were performed in the absence of inhibitors.

The formation of cleavable complexes in plasmid DNA by *xrs-1* nuclear extracts in the presence of etoposide was examined by Caldecott et al. [1993]. At low protein concentrations both the rate of complex formation and the etoposide dose response were similar for CHO and *xrs-1* extracts. However at high protein concentrations approximately 50% more cleavable complexes were formed by CHO extracts.

Subsequent resealing of the cleavable complexes under conditions which permit this to occur even in the presence of etoposide indicated that this process occurred in a similar manner in both cell line extracts.

From the above results it can be concluded that the hypersensitivity exhibited to topoisomerase II inhibition by the *xrs* mutants is related more to the repair of DSB induced by topoisomerase II than the levels of DSB induced. Topoisomerase II inhibition produced either equal, or in some cases, fewer cleavable complexes in *xrs* than CHO, in both *in vivo* and *in vitro* examinations. A decrease in the activity of topoisomerase II has previously been shown to produce resistance to the deleterious effects of inhibitors [Glisson et al., 1986; a, b]. The variation in both extractable *in vitro* topoisomerase II activities and reduced activity *in vivo* may indicate that the activity of the topoisomerase is affected by factors other than those controlling topoisomerase activity directly. The difference in the results of cleavage for etoposide and m-AMSA in different cell lines may be cell line dependent or a result of the differing mechanisms of inhibition of topoisomerase II. Etoposide interacts directly with the enzyme while m-AMSA intercalates into DNA and only subsequently inhibits topoisomerase

on the interaction between the enzyme and the region of DNA containing the drug. The reduced level of strand cleavage may therefore indicate a reduced intercalation of drug into DNA. It might also indicate some inherent defect in the numbers of topoisomerase molecules attached to DNA, even if the the numbers of topoisomerase II molecules are similar in the nuclei of the two cell lines. Factors involving chromatin structure and accessibility of topoisomerase to chromatin may therefore play a part. Additional proteins etc. present in both extracts and nuclei of *xrs* may inhibit the action of topoisomerase on DNA in some fashion. These factors may be involved in the differences observed in the actions of DNA-intercalating inhibitors and the direct action of etoposide on cell survival and aberration formation. Again it must be recognised that *in vitro* studies involving non-nuclear DNAs and protein extracts do not necessarily mimic exactly *in vivo* processes.

1.7. Summary of the xrs phenotype and aims of this thesis.

The phenotype of the XRCC5 complementation group to which both *xrs* and XR-V15B cell lines belong to would appear to possess both constitutive and DNA damage responsive elements.

The fundamental characteristic of the cells with respect to their radiation sensitivity is the inability to repair a significant proportion of DNA double strand breaks which can be induced by a variety of agents. This aspect of the cells is thought to lead to subsequent effects such as reduced survival, increased frequencies of aberration formation and, in some cases elevated frequencies of mutations. The precise nature of the DSB which *xrs* are unable to repair is still uncertain, although it would appear that they are produced by the sparsely ionising component of radiations. Interactive lesions are implicated both by SLDR and PLDR experiments and the inability to perform V(D)J recombination which involves the formation of two DSB in close association with one another.

The fact that XR-V15B did not show reversion with AZC but has been shown to exhibit late S/G_2 resistance similar to *xrs* casts doubt on the possibility of an epimutation as responsible for the radiation sensitivity of both of these cells lines. Rather it adds fuel to the possibility of an additional repair mechanism available to the cells post-DNA replication which is not defective in the mutant cells. This may account for both the residual slow component observed in DSB repair and the rejoining of chromatid breaks in G_2 cells. This repair mechanism could be recombinogenic utilising the recently replicated DNA molecules as templates for the repair of a damaged sister molecule.

Xrs cells are also deficient in the incorporation of exogenously introduced DNA although this would appear to be linked to presence of SSB and/or other lesions. This would indicate a defect in a form of a damage recognition mechanism which may not affect repair of lesions

which do not affect the integrity of the DNA duplex such as SSB and base damage but does affect the repair of DSB which disrupt this integrity. That the recent cloning of the *XRCC5* gene [Taccioli et al., 1994, in press] has potentially identified the *Ku 80* gene product as the responsible protein for the *xrs* phenotype would support this possibility since the Ku 80 protein is an DNA end-binding protein.

Constitutive studies on the structure of the nucleus and chromatin of *xrs* cells reveal a defect in higher order chromatin structures which involve the formation of DNA loops. An increase in the mitotic loop size implicates defects in the nuclear scaffold. Topoisomerase II, one of the major polypeptides of this scaffold exhibits a possible reduction in DNA binding sites. This, the extreme sensitivity of *xrs* cells to inhibition of this enzyme and the major role topoisomerase II plays in recombination events implicate it as a possible target for the *xrs* defect. The defect may involve topoisomerase II indirectly since there would appear to be chromatin structural differences such as the retardation of positive supercoiling by ethidium bromide. That these differences exist in non-irradiated cells either indicates pleiotropic effects of a defect in *XRCC5* gene on constitutive nuclear structures or a response to levels of strand breakage which occur as a result of cellular processes.

Thus, in order to determine the nature of the defect in this complementation group further knowledge is required of the precise nature of the DSB that these cells are defective in the repair of, the mechanism by which these DSB are repaired and the role of the recently identified Ku 80 protein in these processes.

Since the nature of the gene defect in *xrs* cells was uncertain at the start of this research several areas of radiosensitivity have been studied. It was decided to examine the cytogenetic response of *xrs-5* to ionising radiation and to other DNA damaging agents by the use of the cytochalasin-B cytokinesis block technique [Fennech and Morley, 1985] and to determine whether the induction of micronuclei could be affected by introduction of agents which could directly and indirectly affect the metabolism of chromatin and the repair of DSB. In addition to examining the levels of micronuclei induced in *xrs-5* cells the cytokinesis block technique permits an evaluation of the effect of agents on cell cycle progression in the mutant cell line compared to CHO.

Secondly, the effect of the spatial orientation of DSB with respect both to other DSB and higher order structures of chromatin was examined and any effect this might have on repair. This was performed by the development of an assay based on the neutral filter elution technique [Bradley and Kohn, 1979] which could identify the position of DSB within higher order structures. This was performed in order to help determine whether structural

abnormalities observed in *xrs* cells could be correlated with the repair defect and sensitivity to ionising radiation or whether they were unrelated events.

Thirdly, the polypeptide composition and DNA binding activities of nuclear proteins was investigated. Originally it was hoped that this would permit a cell free complementation system to be developed using nuclear proteins, similar to previous work performed on xeroderma pigmentosum cells [Wood et al., 1988]. This proved to be unsuccessful. However, in addition characterisation of *in vitro* activities of the nuclear protein was performed including polyacrylamide gel electrophoresis and DNA binding assays involving quantification using a filter binding assay and identification of individual DNA binding proteins using the technique of South-Western blotting [Mazan et al., 1989]. These were carried out in order to examine whether structural abnormalities in the *xrs* cells could be the result of altered levels of DNA binding proteins.

Chapter 2.

Induction of micronuclei in CHO and *xrs-5* cells.

Summary

This chapter details experiments performed on CHO and *xrs-5* cells which examined the production of micronuclei by various DNA damaging agents. Micronuclei can be produced as a result of chromosome damage which gives rise to acentric fragments. The first main results section (2.3.2.) is devoted to examining the formation of micronuclei in CHO and *xrs-5* using the cytokinesis block technique [Fenech and Morley, 1985]. A number of clastogenic agents are used to induce damage including ^{137}Cs γ-rays, the restriction endonuclease *PvuII*, bleomycin and two topoisomerase inhibitors etoposide (topoisomerase II inhibitor) and camptothecin (a topoisomerase I inhibitor). In addition to the frequency of micronuclei within the cellular populations as a whole, an examination is made as to the distribution of this damage within treated populations and the potential use of measurements made during the micronucleus technique to examine cell cycle related effects.

In the second main results section (2.3.3.), a variety of agents are examined for their effect on the expression of micronuclei and other parameters after treatment with clastogens. The agents examined include caffeine, staurosporine and okadaic acid; which affect protein phosphorylation and secondary messenger pathways; distamycin-A a DNA binding agent which can disrupt the DNA binding activities of nuclear proteins and 3-aminobenzamide, an inhibitor of poly(ADP-ribose)ylation of proteins. The effect of nuclear proteins and T4-DNA ligase are also examined.

2.1. *Introduction.*

Micronuclei are formed from fragments or whole chromosomes that remain separate to the main nucleus of cells after nuclear division. They can be induced in response to DNA damage which results in the formation of acentric fragments of chromosomes. These lack the centromere which acts as the site of attachment to the spindle pole via microtubules. The number of micronuclei within a cell can therefore be indicative of the extent of chromosomal damage [Fenech and Morley, 1985; Müller and Streffer, 1991; Matsuoka et al., 1993]. The number of micronuclei is not a precise quantification of chromosome breakage or gap formation since multiple fragments may reside within a single micronucleus. However, there is a relationship between the induction of micronuclei and level of clastogen. The frequency of micronuclei also correlates to reduction in survival in clonogenic assays [Wandl et al., 1989].

As with conventional karyotypic analysis of chromosomal damage expression of micronuclei requires a preceding metaphase division. This separates centromeric from acentromeric fragments on the basis of their ability to move to the spindle poles. Further rounds of replication and division may alter the level of micronuclei by further deletion, replication or redistribution of the fragments. It was therefore identified that in order to maximise the quantitative potential of micronucleus assays a technique was required which could distinguish between cells which divided only once and those which had not undergone division or had passed through several rounds of division. A simple method for performing this was through the blockage of cytokinesis by the addition of cytochalasin-B [Fenech and Morley, 1985]. Cytochalasin-B (CB) is a fungal metabolite which acts through the inhibition of actin polymers; inhibiting the contractile ring which forms between the two daughter nuclei during cytokinesis at the end of metaphase. CB therefore permits replication and nuclear division but prevents the subsequent separation into two daughter cells. Cells are formed with two distinct nuclei (termed binucleate cells). Further rounds of division will produce increasingly multinucleated cells. Micronuclei within binucleate cells will exist within cells which have undergone only one round of division since addition of CB. This technique is a rapid and convenient technique for the measurement of damage to cells by a wide variety of clastogens.

Comparisons between clastogenic agents and between different cell types made using the cytokinesis block micronucleus technique should, however, still be treated with a certain caution. The only end-point which is commonly used is the frequency of micronuclei within a given population of binucleate cells. This value takes no account of: i) the distribution of micronuclei within that population; ii) the number of cells reaching their first division and so included in the assay; iii) the cytotoxicity of CB and the effect this may have on micronucleus induction in conjunction with clastogens [Matsuoka et al., 1993].

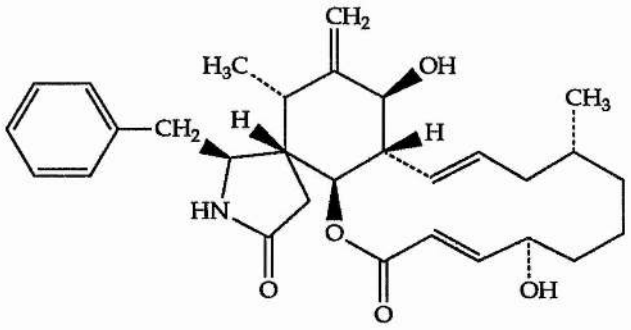

Figure 2.1. Structure of cytochalasin-B.

The first point can be attributed to heterogeneous cell populations. Cells in an exponentially growing population for example, will express different sensitivities to clastogens depending on their position within the cell cycle [Alper, 1979]. This sensitivity may be due to differences in the levels of initial damage induced and subsequent ability to process and repair this damage. Other cells, although damaged may not express this damage as fragments which lead to the formation of micronuclei. For example; cells damaged during mitosis, after chromosome condensation, may not produce micronuclei until they next enter mitosis. Heterogeneous populations may therefore contain cells with levels of damage which does not follow the Poisson distribution which would be expected from a homogeneous population. The practical aspect of this would be apparent differences in the frequency of micronuclei due to alterations in relative levels of the subpopulations and not to actual differences in individual radiosensitivity of cells.

The second point is related to this in that only a specific proportion of cells may reach their first division. This could be due to damage within cells in certain cell cycle phases inducing cell cycle blocks or check-points. The two main cell cycle blocks occur within G_1 and G_2. If damage occurs to cells which lie prior to one of these check-points then these cells may be delayed sufficiently to prevent their division within the time period of the assay. Alternatively, a proportion of damaged cells may be lost from the system entirely via cell death, possibly including apoptotic mechanisms. This fraction of the population could be damage dependent resulting in the loss of heavily damaged cells.

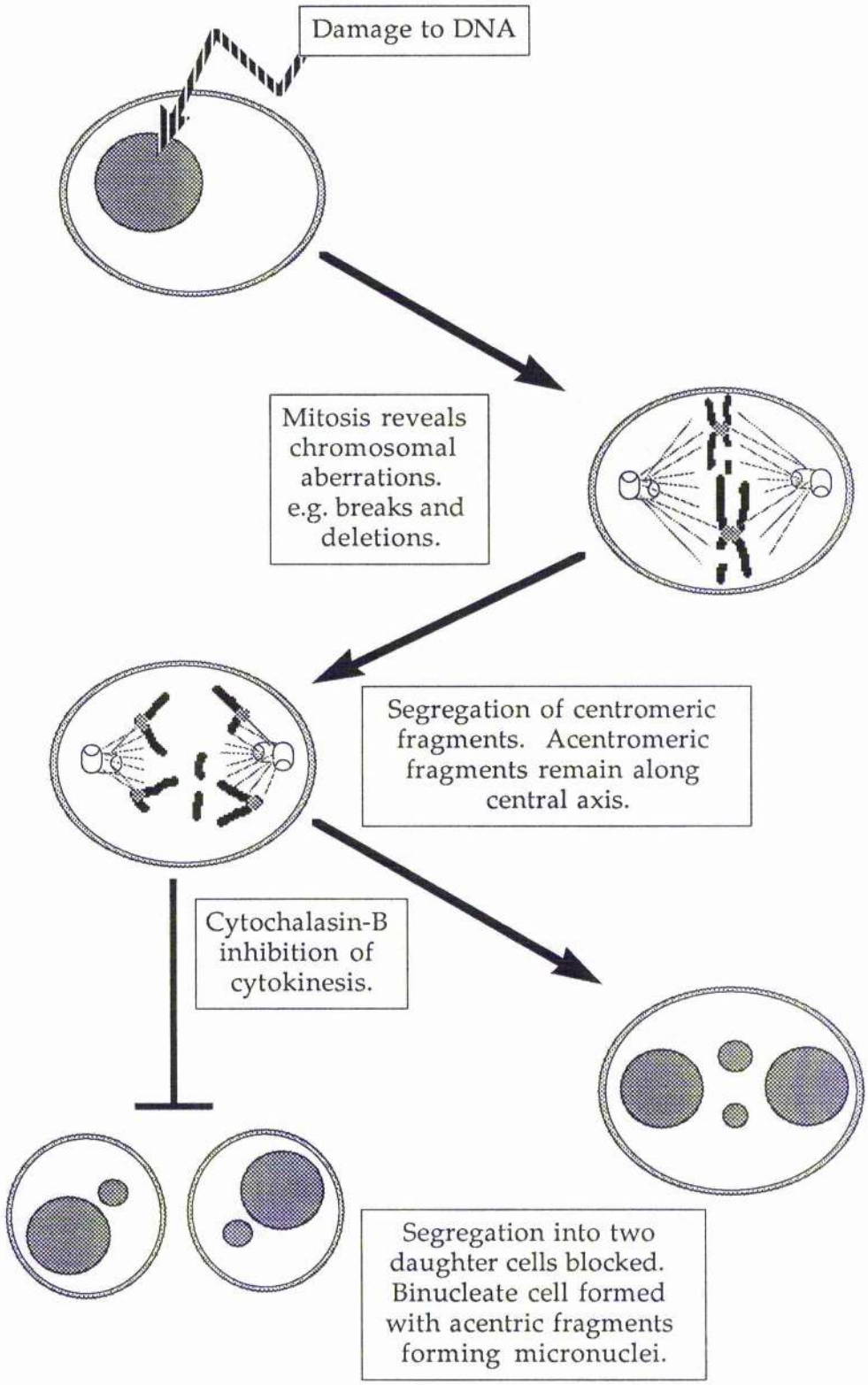

Figure 2.2. Diagram of the cytokinesis block micronucleus technique.

This chapter attempts to address some of these problems using the cytokinesis block technique in ways which retain the ease and rapidity of the method. In an attempt to monitor the importance of the effect of heterogeneous populations and/or cell cell cycle effects on the assay two additional parameters were measured in addition to the frequency of micronuclei. The first was the relative rate of passage of cells through their first division via measurements of the frequency of binucleate cells within the population studied. Although this value should detect alterations in the cell cycle it still does not measure the removal of cells by cell death etc. The second additional parameter measured was the distribution of micronuclei within the population examined. Distribution of micronuclei within populations has been examined [e.g. Catana et al., 1992; Matsuoka et al, 1993]. These techniques involved the scoring of large populations of cells to allow statistical analysis. In the following experiments simplified analysis was performed which gave information on populations containing under-or over dispersion of micronuclei. The collection of data for all three parameters could be made simultaneously by recording the numbers of micronuclei per binucleate cell and the frequency of binucleate cells within the population.

As described in chapter 1, the *xrs* cell lines have been observed to show elevated levels of chromosomal aberrations in response to several clastogenic agents; in particular those which induce DSB. These include ionising radiations, bleomycin, restriction endonucleases topoisomerase II inhibitors and to a lesser extent UV, alkylating agents and hydrogen peroxide [Reviewed in Jeggo, 1990; Collins, 1993]. The first section of this chapter examines the induction of micronuclei by five agents; g-rays, bleomycin, etoposide and the restriction endonuclease *PvuII* which all produce DSB and the topoisomerase I inhibitor camptothecin (CPT) which produces predominantly single strand breaks. These agents all act via different mechanisms and possibly on different subpopulations. By the examination of the additional parameters described above an attempt is made to determine whether the sensitivity of *xrs-5* cells can be attributed to factors other than DSB induction alone.

The repair of DNA damage and subsequent expression of damage as observed by aberration formation or clonogenic survival assays, can be modulated by a number of means. These include modification of the cell cycle and associated check-points, damage recognition systems and DNA repair mechanisms. Five agents were examined in the second section to this chapter, all of which can be related either directly or indirectly to alterations in chromatin structure. This occurs either via interaction/modification of protein-DNA associations or mechanisms involving possible alterations in cell cycle mechanisms such as phosphorylation of proteins. The direct chromatin structure altering agents are 3-aminobenzamide (3-AB) and distamycin-A (DST). 3-AB is an inhibitor of poly (ADP-ribose) polymerase (PARP) and is implicated in strand break recognition and subsequent relaxation of chromatin via

modification of DNA binding proteins [Ahnström and Ljungman, 1988]. DST binds to the minor groove of the DNA double helix, specifically at AT rich sites. It can inhibit the binding of DNA ligases, topoisomerase II and histone H1 and can affect higher order chromatin structure [Beerman et al., 1991; Käs et al., 1993; Montecucco et al ., 1993]. More indirect cellular effects are produced by the other three agents; caffeine (CFN), staurosporine (STP), and okadaic acid (OA). STP and OA acid are inhibitors of protein kinases and protein phosphatases respectively [Tamaoki et al., 1986; Bialojan and Takai, 1988; Haystead et al., 1989]. Phosphorylation of proteins can alter both enzymatic and structural activities of proteins and these events are critical in the cell cycle regulation. CFN has been more indirectly implicated in the cell cycle with effects predominantly catalogued in response to DNA damage although it does possess cytotoxic properties on its own [Rowley and Kort, 1988; Warters et al., 1989; Hirano et al., 1993]. These agents are more fully discussed in the the following sections.

Overall therefore, the purpose of this chapter is two-fold. Firstly to characterise the cytokinesis block assay more fully and secondly to apply the technique to examining the response of *xrs-5* to radiation and various clastogenic agents.

2.2. *Materials and Methods.*

2.2.1. *Cell culture.*

Chinese hamster ovary (CHO-K1 strain) and *xrs-5* cells were routinely maintained as exponentially growing monolayers in tissue culture flasks in EMEMS (=Eagles' minimal essential medium supplemented with Earles' salts (Gibco), 10% (v/v) newborn calf serum (Gibco), 100μM $FeCl_3$ (to saturate transferrin), 50 IU ml^{-1} penicillin (Gibco) and 50 mg ml^{-1} streptomycin (Gibco)). All incubations were performed at 37°C in an atmosphere of 5% CO_2 unless otherwise stated. Cells were passaged or collected for treatment by trypsinisation. Briefly, cell monolayers were rinsed with 0.05% trypsin (Difco Laboratories), 0.7 mM sodium ethylenediaminetetraacetic acid (EDTA) in phosphate buffered saline (PBS; 140 mM NaCl, 2.5 mM KCl, 8.1 mM Na_2HPO_4, 1.5 mM KH_2PO_4). The flasks were incubated at 37°C for 6 minutes and cells resuspended in EMEMS. Determination of cell numbers was performed by Coulter counting.

2.2.2. *Materials.*

All reagents were of analytical or molecular biological grade unless otherwise stated. Solutions for cell culture were prepared under normal sterile conditions. Sterilisations of aqueous solutions were performed using 0.22 μm disposable filter units (Millipore) and/or autoclaving. Bleomycin sulphate (Lundbeck) and streptolysin-O (SLO) (Wellcome Diagnostics) were made up as stock solutions (BLM = 1 mg ml^{-1} in H_2O, SLO was made up as per manufacturers instruction to 1.82-1.90 IU ml^{-1}). The following stock solutions were made up using dimethyl sulphoxide (Sigma) as a solvent (stock concentrations given in parentheses); Cytochalsin-B (Sigma, 3 mg ml^{-1}); distamycin-A (Sigma, 5 mg ml^{-1}); camptothecin (Sigma, 1 mM); 3-aminobenzamide (Sigma, 0.5 M); staurosporine (Sigma, 100 μg ml^{-1}). Etoposide (Bristol-Myers, 1 mM) was received as a gift from Dr K. Caldecott at the National Institute for Medical Research, Mill Hill, London. All stock solutions were stored as aliquots at -20°C. T4 DNA ligase and the restriction endonuclease *PvuII* (Northumbria Biologicals or Gibco BRL) were stored in the storage buffers provided by the suppliers (*PvuII* 50 mM tris-HCl (pH 7.4) 50 mM KCl, 0.1 mM EDTA, 10 mM 2-mercaptoethanol, 0.5 mg ml^{-1} BSA, 50% (v/v) glycerol; T4 DNA ligase, 10 mM tris-HCl (pH 7.5), 50 mM KCl, 1 mM dithiothreitol (DTT), 50% (v/v) glycerol).

2.2.3. *Enzyme purification.*

The restriction endonuclease *PvuII* and T4 DNA ligase were supplied in buffers containing 50% glycerol which required removal prior to treatment of cells to prevent hyper-tonic shock. This was performed using centrifugal ultrafiltration [Bryant and Christie, 1989]. Briefly, the

required quantity of enzyme was added to Amicon-10 filters (10 kDa exclusion limit) along with 40 µl modified Hanks' balanced salt solution (=HBSSB; 140 mM NaCl, 5.4 mM KCl, 0.34 mM Na_2HPO_4, 0.44 mM KH_2PO_4, 6 mM $MgSO_4$, 5.6 mM D-glucose, 4.2 mM $NaHCO_3$, 1% (w/v) bovine serum albumin (BSA)) plus 1 ml HBSS (as above but without BSA). The filters were centrifuged at 5000g for 1 hour at 4°C. An additional 1.5 ml HBSS was added to the filter and the enzymes centrifuged for a further 1.5 hours at 4°C. After this time the purified enzymes would be contained in approximately 40 µl HBSSB. The enzymes could then be diluted to the required concentration and were maintained on ice until required. Generally, purified enzymes were used immediately.

2.2.4. *Micronucleus assay.*

The cytokinesis block micronucleus assay was based on the technique of Fenech and Morley [1985].

2.2.4.1. Gamma irradiation.

For γ-irradiation experiments cells were grown in either multi-well tissue culture plates (2 cm^2 wells) or 25 cm^2 flasks. Cells were plated at a concentration of approximately $2.5x10^4$ cells cm^{-2} at least 16 hours prior to irradiation to ensure attachment. The cells were placed on ice for a minimum of 10 minutes and the medium aspirated. The cells were irradiated on ice using a ^{137}Cs IBL437C γ-irradiator (CIS UK Bio International) at a dose rate of 4.6 Gy min^{-1}. Dosimetry was checked by a ferrous sulphate method [Frankenberg, 1969]. After irradiation, medium containing 3 µg ml^{-1} cytochalasin-B and any other agent under examination was added and the cells incubated at 37°C for 24 hours.

2.2.4.2. Etoposide, camptothecin and chronic bleomycin treatment.

For these agents cells, grown as above on multi-well plates, were exposed to medium containing dilutions of either VP-16, CPT or BLM plus 3 µg ml^{-1} CB for 24 hours at 37°C.

2.2.4.3. Streptolysin-O mediated treatment.

To facilitate the entry of proteins and BLM, cells were porated using streptolysin-O (SLO) based on the technique of Bryant [1992]. Cells were trypsinised and resuspended in EMEMS at $\approx 10^6$ cells ml^{-1}. The cells were washed twice by centrifugation in HBSS and resuspended at $2x10^6$ cell ml^{-1}. 100 µl ($2x10^5$ cells) were aliquoted into plastic eppendorf tubes (Treff). To these 100 µl of HBSS ± 0.090 IU ml^{-1} SLO and 2x the dilution required of the agent under examination added. This gave a final concentration of $1x10^6$ cell ml^{-1} and 0.045 IU ml^{-1} SLO. The cells were incubated for 6 minutes at room temperature before the addition of 1 ml of ice-cold EMEMS. They were then immediately centrifuged (6500 RPM) for 1 min in a microfuge

(MSE Micro-Centaur) and the supernatant aspirated. The cell pellet was carefully resuspended in 1 ml EMEMS + 3 µg/ml cytochalasin B before plating out in multi-well tissue culture plates. In some experiments irradiation or BLM addition was performed on cells 30 min post-poration treatment with nuclear extracts. The cells were subsequently incubated for 24 hours at 37°C.

An alternative method of SLO-mediated poration was used for treatment with bleomycin. Cells, attached as monolayers to multi-well plates were washed twice with HBSS (room temperature). 0.5 ml of HBSS containing various concentrations of SLO ± BLM was added. After 6 min incubation at room temperature. 1 ml of EMEMS was added and this medium aspirated. The cells were washed twice with EMEMS before addition of 1 ml EMEMS plus 3 µg cytochalasin-B. These cells were then incubated at 37°C for 24 hours.

2.2.4.4. Fixation and scoring of micronuclei.

After the incubation period the cells were trypsinised as above and the cells resuspended at approximately $2.5x10^5$ cells ml^{-1} in EMEMS. Approximately $5x10^4$ cells were cytospun (Shandon Cytospin II) onto glass slides and air dried. The cells were fixed for 10 min in methanol and again air dried before staining in 10% filtered aqueous Giemsa solution (BDH) for 20 minutes. Slides (without coverslips) were examined under high magnification (oil immersion x1800) and the number of micronuclei in 100 binucleate cells scored. This data was collected on an individual number of micronuclei per binucleate cell basis to permit later damage distribution studies. In addition, the frequencies of binucleate cells were scored. The criteria for the scoring of micronuclei was as follows; i) samples were scored "blind". ii) Only cells with two distinct nuclei contained within a recognisably independent cell membrane were classified as binucleate. iii) Micronuclei were classified as nuclear material (as judged by staining) existing independently of the nuclei and not in excess of approximately $1/8^{th}$ of the size of an individual nucleus. iv). Cells without a distinct cellular boundary (e.g. lysed cells) were excluded from all counts. Cells apparently undergoing cell death , mitosis or with greater than 2 nuclei were excluded from binucleate scores but included in calculations of binucleate frequency.

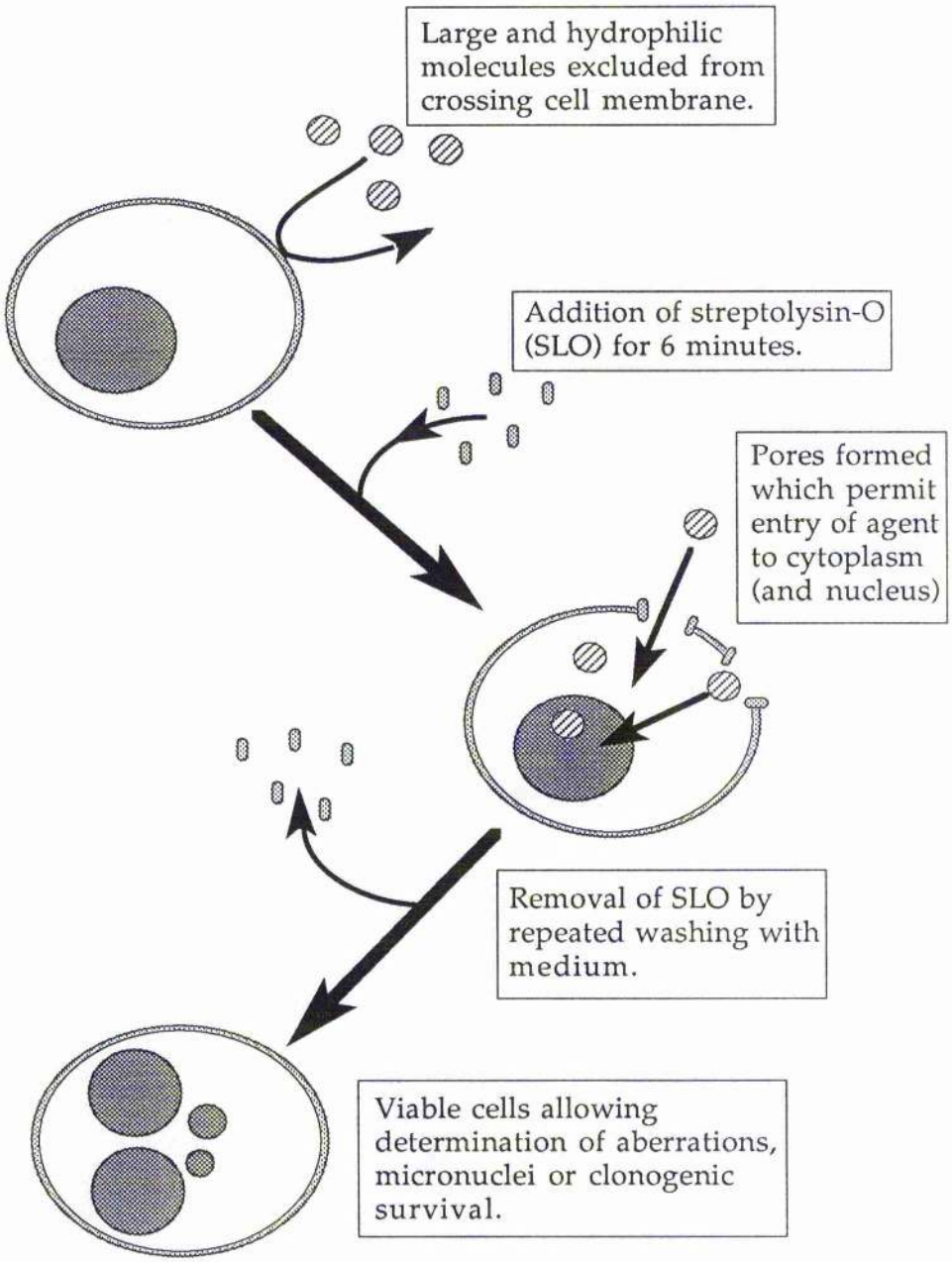

Figure 2.3. Diagram of the poration of cells using streptolysin-O.

2.2.4.5. Treatment of data.

The frequency of micronuclei is expressed in several forms in the following results section. The first is the frequency of micronuclei per binucleate cell (**MB**). This is representative of the damage expressed in the entire population of cells which survive through one mitosis within 24 hours. These values are adjusted for background micronucleus induction by subtraction of the number of micronuclei in untreated controls for each experiment. This gives the value $\mathbf{MB_{adj}}$.

When examining possible modulators of micronucleus induction it was necessary to normalise data in terms of both the clastogen treated controls (i.e. γ-irradiated/BLM treated) and also controls treated with the modulator alone. This gives the term relative micronucleus induction (**RMnI**) and is given by the equation;

$$\mathbf{RMnI} = \frac{\mathbf{MB_{adjsample}}}{\mathbf{MB_{adjcontrol}}} \qquad (2.1)$$

Here $\mathbf{MB_{adjsample}}$ is the adjusted micronucleus frequency for the modulator treated sample and $\mathbf{MB_{adjcontrol}}$ is the adjusted micronucleus frequency of the clastogen treated control.

To estimate the pattern of distribution of damage within the population of binucleate cells assayed the mean number of micronuclei per **damaged** binucleate (**MD**) was measured. This value is a function of the total damage expressed by a population of binucleate cells and the fraction of this population which express one or more micronucleus (f_α);

$$\mathbf{MD} = \frac{\mathbf{MB}}{f_\alpha} \qquad (2.2)$$

If damage is expressed randomly throughout the population then the distribution of micronuclei should be in a Poisson fashion. The value of **MD** can be used to examine whether the distribution follows this Poisson distribution since it is a function of the fraction of cells containing damage. An ideal f_α can be calculated for any given value of **MB** by the following equation

$$f_\alpha = \sum_{n=1} \frac{MB^n e^{-MB}}{n!} \qquad (2.3)[\text{Wardlaw, 1985}]$$

Here n is the number of micronuclei per binucleate

This Equation (2.3) can be simplified by calculating the fraction of cells with no micronuclei (f_β) which is derived as follows

$$f_\beta = \frac{MB^0 e^{-MB}}{0!} \quad (2.4)$$

$$= e^{-MB} \quad (2.5)$$

Since f_α will be given by (1-f_β)the expected mean number of micronuclei per damaged binucleate (MD_{exp}) will be given by ;

$$MD_{exp} = \frac{MB}{1-e^{-MB}} \quad (2.6)$$

To test whether observed values of MD (MD_{obs}) were significantly different from the expected values based on a Poisson distribution a chi-square (χ^2) goodness of fit test was performed on the mean numbers of damaged (A_α) and undamaged binucleates(A_β) versus the expected numbers E_α and E_β respectively alculated using MB and MD_{exp}. The value of χ^2 was calculated by the equation;

$$\chi^2 = \frac{(A_\alpha - E_\alpha)^2}{E_\alpha} + \frac{(A_\beta - E_\beta)^2}{E_\beta} \quad (2.7)[\text{Wardlaw, 1985}]$$

Here A_α, A_β, E_α, E_β are given by

$$A_\alpha = q\left(\frac{MB}{MD}\right) \quad (2.8)$$

$$A_\beta = q - A_\alpha \quad (2.9)$$

$$E_\alpha = q - E_\beta \quad (2.10)$$

$$E_\beta = q(1-f_\beta) \quad (2.11)$$

Here q is the number of cells scored (which in most cases was 100)

For comparing between a range of expected and observed values (e.g. in dose repsonse experiments) the value of χ^2 was calculated as the sum of individual χ^2 values for e.g. each dose. The degrees of freedom equaled the twice the number of doses minus 1. The significance of the χ^2 values was obtained using Minitab statistical software.

The $\chi 2$ test only indicates whether or not significant deviations from Poisson do occur, not the extent or cause of this deviation. This would require a much more detailed analysis using much larger population sizes than those used in this study.

The third parameter examined was the fraction of the total population of cells which were binucleated after 24 hours. This value was termed the binucleate index (BI) and was calculated by the equation;

$$\mathbf{BI} = \frac{\text{number of binucleate cells}}{\text{total number of cells}} \qquad (2.12)$$

This value gives an approximation of the effect of treatment of cells on their apparent ability to pass through one mitosis within 24 hours. This value is only an approximation since it is measured relative to the whole population. It will be affected not only by cell cycle perturbations such as blocks and delays, but also by cell death which will remove cells from the population scored. Since the **BI** is a function of the total number of cells present in the sample scored then a decrease in the value of **BI** will also be observed if there is an increased proportion of cells which pass through more than one division (e.g. tetranucleated cells). It was impractical to exclude tetranucleated cells from the scoring process and therefore the time of 24 hours post-treatment fixation was chosen as a compromise between maximal binucleate numbers and minimal tetranucleate numbers.

In following sections, data is expressed as the means and standard errors of the means (SEM) of these values. Statistical analysis of the data was performed, where possible, on initial transformations of the pooled data from several independent experiments. Analysis between individual data points was performed using the students t-test. In dose response experiments deviation from the control values was examined by one-way analysis of variance (ANOVA) over the entire dose range. For comparisons between multiple data points between cell lines etc. a two-way analysis of variance was performed based on the general linear model (GLM). As described comparisons between observed and expected values were performed using χ^2 goodness of fit analysis.

2.3. *Results.*

2.3.1. *Induction of binucleate cells.*

Figure 2.4 indicates the rate of binucleate cell formation in the presence of 3 μg ml^{-1} cytochalasin B along with the proportions of cells in the various stages of the cell cycle as estimated by flow-cytometry [E. Stoppard; personal communication]. The rate of disappearance of mononucleate cells is exponential in both cell lines. However, instead of all the cells leaving this population there is a significant fraction which remains after 36 hours. This indicates that not all of the cells are dividing, i.e. they are either in G_0 or undergoing a form of cell death. This fraction is mirrored in the maximum levels of binucleate cells although this is also a function of the rate that cells divide for a second time. There is a larger proportion of CHO cells which divide compared to *xrs-5*. For CHO 12.0 (±1.07)% of cells remain undivided after 36 hours compared to 37.5 (± 6.32)% for *xrs-5*. That there is an increased non-dividing population of *xrs-5* cells is supported by the flow-cytometric results which indicate elevated levels of G_0/G_1 cells in the mutant cell line.

The proportion of cells which are non-dividing affect the apparent rates of accumulation of binucleate cells. Figure 2.5 shows the frequencies of mononucleated (Figure 2.5a) and binucleated cells (Figure 2.5b) after corrections were made for the non-dividing fraction of cells. It would appear that both rates were similar in the two cell lines. This would indicate that the cell cycle times for dividing CHO and *xrs-5* are similar although the rate at which the overall mutant populations will grow will be less. Similar corrections were made for the proportions of cells in different phases of the cell cycle (Figure 2.5c) (mitotic proportion calculated from the mean mitotic frequency observed)

Therefore it would appear that in comparisons between the two cell lines these cell cycle differences should be noted, especially in comparisons of binucleate indices.

In the following experiments 24 hours was chosen as the harvest time. This was a compromise between maximal binucleate induction and minimal polynucleate frequency. It was not certain whether DNA damage or the other treatments performed would affect the size of the dividing fraction of cells and therefore the binucleate indices in the following experiments are not corrected for non-dividing populations.

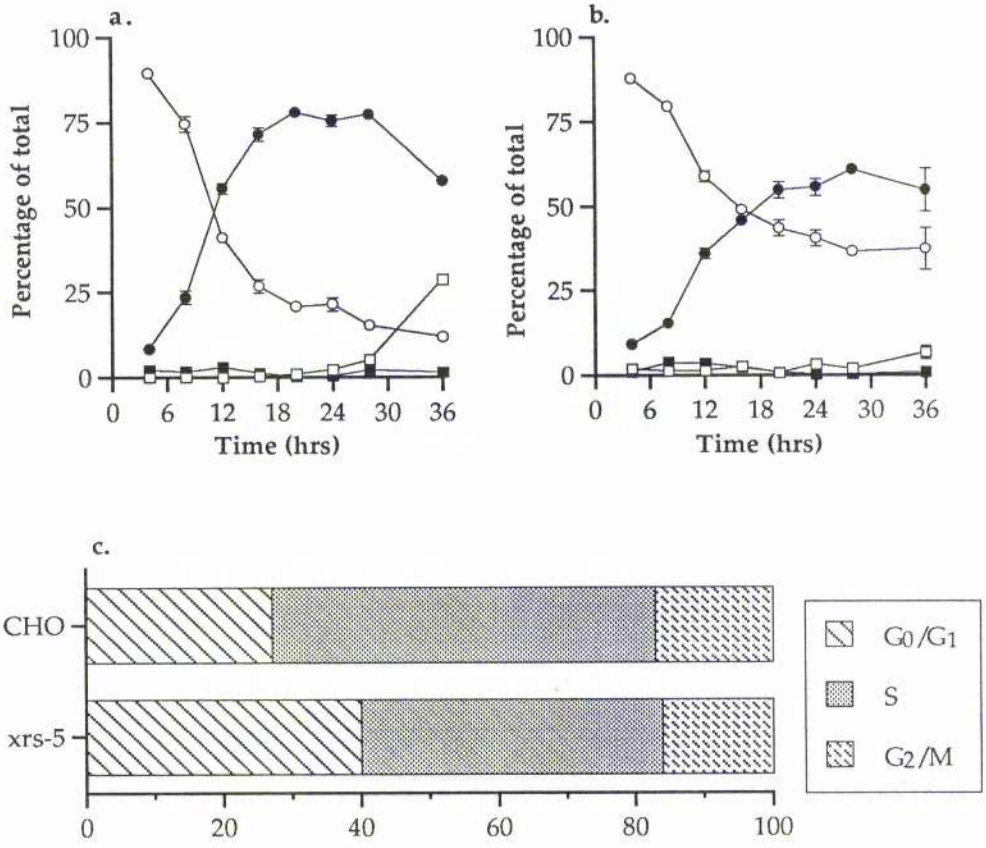

Figure 2.4. Cell cycle kinetics for CHO and *xrs-5* cells. a, b) Effect of 3 μg ml^{-1} cytochalasin-B on the formation of binucleate cells in CHO **(a)** and *xrs-5* **(b)**. Data represents the frequencies of mononucleate (○), binucleate (●), polynucleate (>2 nuclei) (□) and mitotic cells (■) with time. Error bars represent the SEM of 4 independent experiments. Proportion of cells in the various stages of the cell cycle as determined by flow cytometry [E. Stoppard, personal communication].
GLM two-way analysis of variance indicates significant differences in the frequencies of mononucleate ($p \leq 0.001$, $F=9.56$, $df=7$), binucleate ($p \leq 0.001$, $F=12.05$, $df=7$) and polynucleate cells ($p \leq 0.001$, $F=75.78$, $df=7$). c).

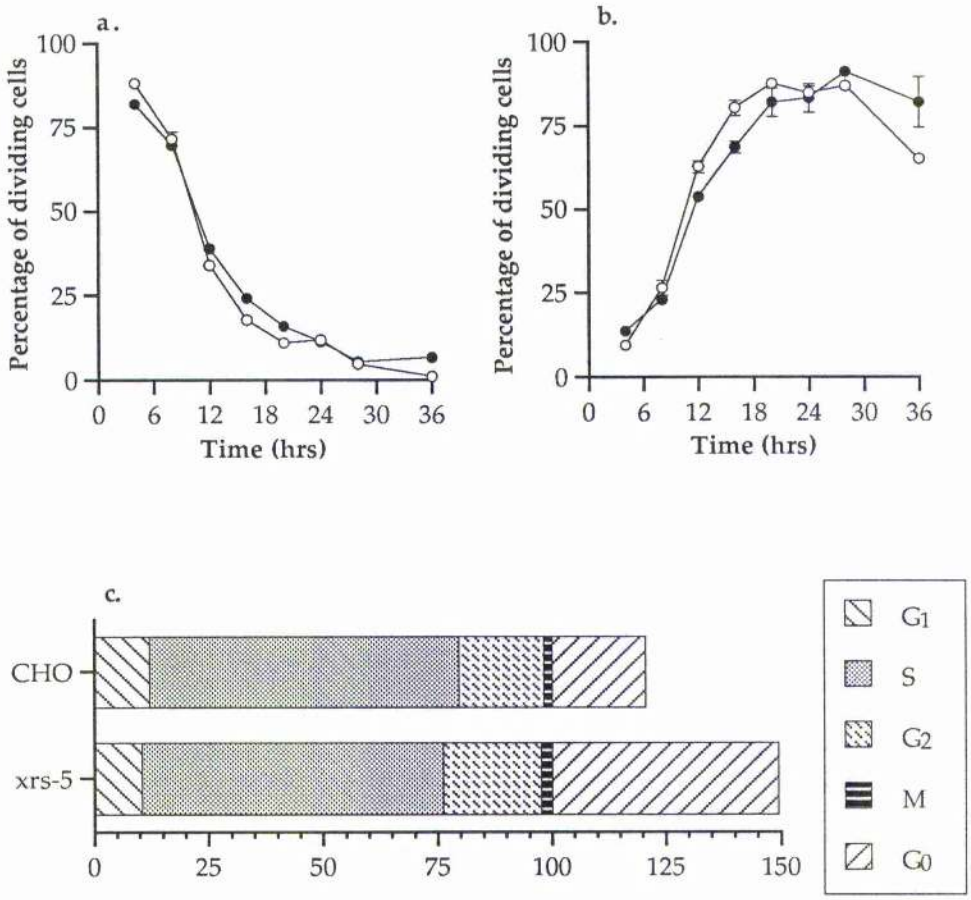

Figure 2.5. Cell cycle kinetics for CHO and *xrs-5* cells after correction for the non-dividing populations of cells. Effect of 3 μg ml^{-1} cytochalasin-B on the disappearance of mononucleate **(a.)** and appearance of binucleate **(b.)** cells in CHO (○) and *xrs-5* (●). Data (as in Figure 2.4 corrected for the non-dividing population of cells to give the percentage of dividing cells with time. c). Proportion of cells in the various stages of the cell cycle as determined by flow cytometry [E. Stoppard, personal communication] and corrected for the non-dividing population of cells (G_0). Values represent the percentage of dividing cells in a particular phase where the sum of G_1, S, G_2 and M phases = 100%.

2.3.2. *Induction of micronuclei by DNA damaging agents.*

2.3.2.2. Response of CHO and xrs-5 to gamma rays.

The frequency of chromosomal aberrations induced by ionising radiation is elevated in *xrs* cells compared to the wild type [Kemp and Jeggo, 1986; Darroudi and Natarajan; 1987a, b; MacLeod and Bryant, 1990]. This sensitivity has been exhibited to be cell cycle dependent [Kemp and Jeggo, 1986]. Generally, *xrs* cells exhibited a 3-5 fold elevation in aberration frequency relative to CHO with the chromatid break type the predominant aberration for both cell lines [Darroudi and Natarajan, 1987a; Kemp and Jeggo, 1986]. The frequency of aberrations in both cell lines decreases in a time dependent manner [Kemp and Jeggo, 1986]. The kinetics of this decrease, attributed to repair of lesions, has been observed to be similar in both G_2 CHO and *xrs-5* cells even though the frequency remains approximately four-fold higher in *xrs-5* [Macleod and Bryant, 1990]. *Xrs-5* cells synchronised to the G_2 phase of the cell cycle exhibited DSB repair which was not observed in G_1 cells [Mateos and Bryant, paper under revision]. This indicates that G_2 cells, although proficient at DSB repair, convert more damage into aberrations. This may occur via a process not linked to DSBs, but linked instead to the fixation of damage during repair processes into a form expressed as aberrations or through *xrs-5* cells entering mitosis more rapidly post-irradiation and thus with more damage.

CHO and *xrs-5* cells were irradiated as monolayers as described in the materials and methods. The frequency of micronuclei per binucleate cell increased in a dose dependent manner for both wild-type and mutant cell lines (Figure 2.6a). Over the dose range examined there was initially a linear response for both cell lines with *xrs-5* having a sensitivity to γ-rays approximately 7 fold that of CHO (based on doses required to produce equal micronucleus frequencies). The CHO dose response remained linear over the range 0-7 Gy. *Xrs-5* exhibited a linear response up to approximately 1 Gy after which the rate of micronucleus induction decreased until at 4 Gy a reduction in micronucleus frequency was observed. The frequency of micronuclei per damaged cell (Figure 2.6b) appeared to correspond with the frequency per binucleate cell although by this parameter *xrs-5* cells were approximately 12 fold as sensitive as CHO. When the two frequency parameters were correlated (Figure 2.6c) there appeared to be a correlation between them which, for CHO matches the expected values based on a Poisson distribution of damage (as indicated by the dotted line). The correlation for *xrs-5* also appeared to follow the expected distribution at low doses (0-1 Gy). However, at higher doses the distribution deviated from the Poisson based model with damage becoming increasingly over-dispersed. Whether this would occur for CHO as well is uncertain due to the low levels of damage induced by the doses used.

Figure 2.6d shows the effect of γ-rays on the frequency of binucleates. There was no significant alteration in the frequency for CHO cells over the dose range examined. *Xrs-5* cells exhibited a lower number of cells passing through one division. This lower number would appear to correlate with the increase in micronucleus frequency. This would imply that it is the level of damage present within a cell that determines the passage of these cells through a cell cycle. It has been reported that *xrs* cells exhibit a prolonged inhibition of DNA synthesis compared to CHO after ionising radiation exposure [Jeggo, 1985b]. This has been attributed to the defect in DSB repair which is present in the mutant cells which prevents levels of damage falling below a threshold required for progression into S phase.

The *xrs-5* binucleate index fell from the control value of 42.6 (±16.2) % to 19.0 (±10.0) % of the population after 2 Gy. Further increases in dose, and frequencies of micronuclei, do not affect this final value. This would indicate that there is possibly a sub-population of cells which are inhibited from passing through the first division within the time-course of the experiment. The dose required to inhibit all of this sub-population, if it exists, would appear to correspond with the deviation of damage distribution from Poisson. That ≈20% of the population are apparently resistant to the cell cycle block would indicate that either the block exists for a limited time regardless of dose or that a certain proportion of the *xrs* population lies at a point in the cell cycle which is after any checkpoint induced by γ-rays. This subpopulation cannot be identified using this technique. Further work would be required to e.g. identify any specific cell cycle phase in which *xrs-5* cells do not experience any delay. From the evidence of Jeggo, [1985b], this may involve cells in either S or G_2 phases of the cell cycle.

At low levels of damage (less than 1 micronucleus per binucleate) it would appear that for both cell lines γ-ray induced micronuclei are randomly distributed throughout the binucleate population. It is only at higher levels of damage (only apparent for *xrs-5* in these experiments) that deviation from the Poisson distribution occurs and that this may be related to a sub-population of cells which exhibits resistance to a possible cell cycle delay/block.

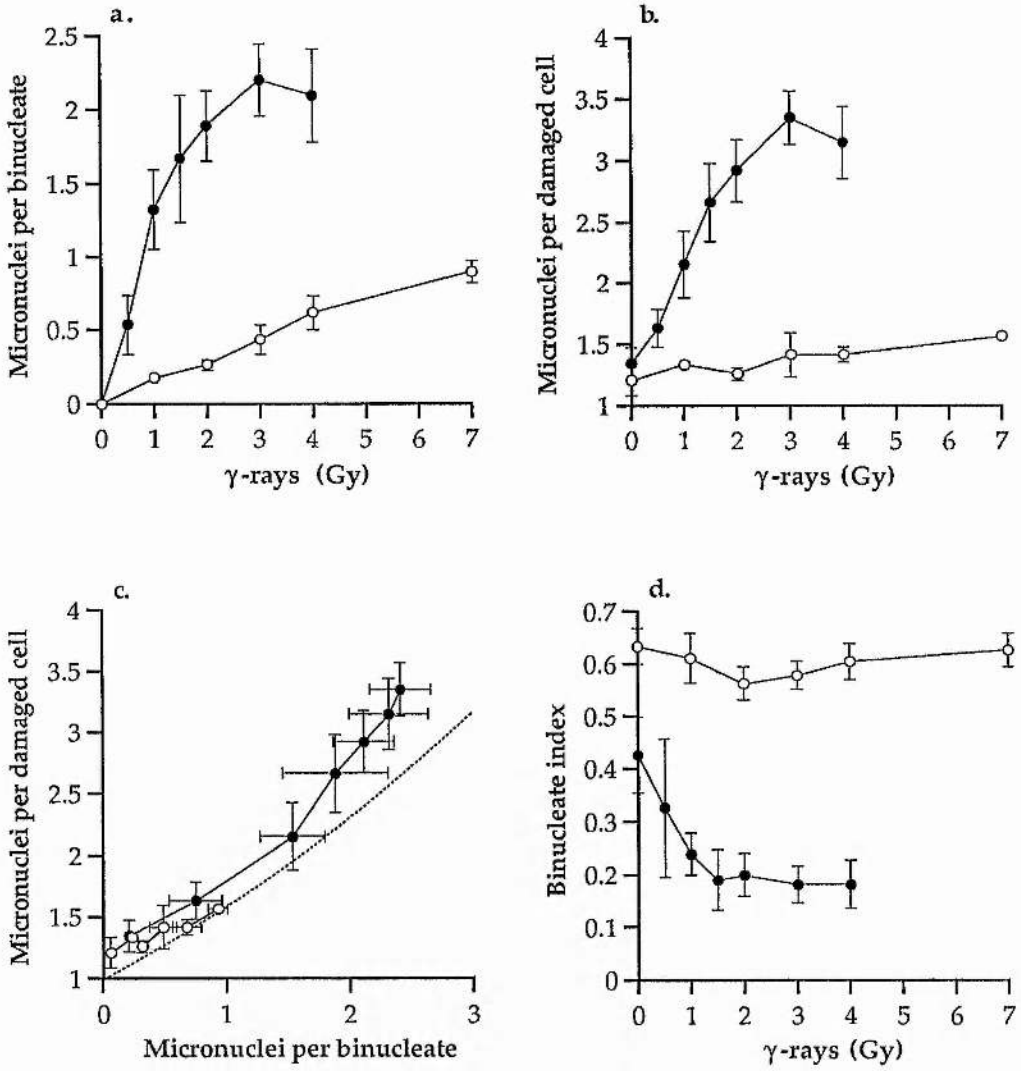

Figure 2.6. Effect of ^{137}Cs γ-rays on CHO (○) and *xrs-5* cells (●).

a) Frequency of micronuclei per binucleate cell (corrected for background). One-way ANOVA indicates significant increases in frequency with dose (CHO, $p<0.001$, $F=21.79$, $df=5$; *xrs-5*; $p<0.001$, $F=11.53$, $df=6$). GLM analysis indicates significant differences between CHO and *xrs-5* response ($p<0.001$, $F=10.60$, $df=4$).

b) Frequency of micronuclei per damaged binucleate cell. One-way ANOVA indicates no significant increase in frequency with dose for CHO ($p= 0.100$, $F=2.07$, $df=5$) and a significant increase in *xrs-5* ($P<0.001$, $F= 10.77$, $df=6$).

c) Correlation of the frequency of micronuclei per damaged binucleate versus the frequency of micronuclei per binucleate cell. Dotted line represents the expected frequency of micronuclei per damaged binucleate as calculated by Equation (2.7). χ^2 analysis indicates no significant deviation from the expected frequencies for CHO ($p=0.834$, $\chi^2=2.108$, $df=5$) and a significant overdispersion in *xrs-5* ($p<0.001$, $\chi^2=118.2$, $df=6$)

d) Binucleate index. One-way ANOVA indicates no significant decrease in CHO ($p=0.627$, $F=0.70$, $df=5$) and a significant decrease in *xrs-5* ($p=0.048$, $F= 2.6$, $df=6$)

Error bars represent the standard error of the mean of a minimum of 3 independent experiments.

2.3.2.2. Response of CHO and xrs-5 to the restriction endonuclease PvuII

Restriction endonucleases are bacterial enzymes which recognise specific DNA sequences and cause cleavage of the phosphodiester backbone at specific sites, often within the recognition sequence. These DSB have well ordered structures with 5'-phosphoryl and 3'-hydroxyl end-groups. Breaks of this nature can be rejoined *in vitro*, with no further modification, by DNA ligases. The precise end structure of the DSB can vary with the two component strand breaks aligned directly opposite one another ("blunt-ended" DSB) or staggered several base pairs apart ("cohesive ended" DSB) on the opposite strands.

Restriction endonucleases (RE), since they are large polypeptides which are not transported across the cell membrane, need to be introduced into the cells by artificial means. Methods used include the use of Sendai virus, electroporation or, more recently, with the aid of the bacterial endotoxin streptolysin-O (SLO) [Bryant, 1984; Bryant and Christie, 1989; Winegar et al., 1989; Costa and Bryant, 1990; Bryant, 1992]. When introduced by these methods DSB formation was observed using neutral filter elution, DNA unwinding and pulsed field electrophoresis [Costa and Bryant, 1990; 1991a, Costa and Thacker, 1993]. Unlike ionising radiation induced DSB, RE induced DSB appeared in a time dependent manner [Costa and Bryant, 1990]. The rate of accumulation was endonuclease type dependent. Certain REs give rapid increases (e.g. *PvuII*) whilst others exhibited a much reduced level of DSB formation (e.g. *BamH1* and *EcoR1*). REs were shown to induce both chromosomal aberrations [Bryant, 1984] and a reduction in surviving fraction [Bryant, 1985]. This has provided evidence for the involvement of DSB in the clastogenic effects of ionising radiation. It was shown that, in general, blunt-ended DSB accumulated more rapidly than cohesive-ended DSB. This was attributed to the repair of cohesive-ended DSB occurring more efficiently than that for blunt-ended DSB. The accumulation of DSB was postulated to be the result of a competition between cleavage and repair [Costa and Bryant, 1990]. That there existed a difference between the response to different types of DSB end-structure would indicate two different repair processes exist. It has been speculated that repair of cohesive-ended DSB may occur as the repair of two independent SSB since the overlap may allow the DNA ends to maintain their alignment relative to one another [Bryant 1984; 1988].

The response of *xrs* cells to restriction endonucleases has also been examined [Bryant et al., 1987; Darroudi and Natarajan, 1989b]. Both of these studies found an elevated level of chromosomal aberrations in *xrs* compared to CHO cells. Treatment with REs which induced cohesive ended DSB also produced elevated levels of aberrations although this level was lower than that observed for blunt-ended DSB inducing endonucleases.

Xrs cells have been observed to be proficient at the repair of SSB [Kemp et al, 1984; Costa and Bryant, 1988] and so the difference that is observed between the two types of RE cannot be attributed wholly to repair of cohesive-ended DSB occurring as two SSB. An alternative suggestion would be that a fraction of cohesive-ended DSB are treated similarly to the blunt-ended DSB in both CHO and *xrs* cells.

The induction of micronuclei by *PvuII* (cutting sequence 5'-CAG$^{\blacktriangledown}$CTG-3')is shown in Figure 2.7a As expected, *xrs*-5 cells exhibit an elevated frequency of micronuclei per binucleate cell. Over the dose range examined the CHO dose response appears curved with a reduced frequency at high doses. The *xrs-5* dose response is linear. From estimates of the initial rates of induction *xrs*-5 would appear to be approximately 1.5-2 fold more sensitive than CHO at 5 U ml^{-1}. However at 40 U ml^{-1} *xrs-5* was approximately 3.5-4 fold more sensitive (sensitivity estimated on the basis of the dose required to give the equivalent frequency of micronuclei in *xrs-5*).

The introduction of restriction enzymes into cells has been reported to produce over-dispersion of damage with a significant sub-population experiencing reduced levels of damage. This could be observed by the formation of "tailed" survival curves [Costa and Thacker, 1993] whereby a proportion of cells exhibit resistance to killing at high doses of RE. The difference in response to REs by *xrs-5* might therefore have been due to an elevated proportion of cells which experience damage. Figure 2.7b shows the mean number of micronuclei per damaged binucleate cell. When sensitivity was compared using this graph *xrs-5* cells appear to be 6-6.5 fold more sensitive at 40 U ml^{-1}. This would indicate elevated levels of over-dispersion in *xrs-5* compared to CHO. When the frequency of micronuclei per damaged binucleate cell was correlated to the frequency of micronuclei per binucleate cell (Figure 2.7c) it was observed that both cell lines deviated significantly from the expected distribution of damage. This would indicate that a significant sub-population received or expressed more damage than other cells. At high levels of damage (per binucleate cell) the over-dispersion would appear to be greater in *xrs-5* than CHO. However, the data is scattered and direct comparisons on this graph are not possible.

Analysis of the binucleate indices after *PvuII* treatment (Figure 2.7d) reveal a significant decrease in the binucleate index with dose in both CHO and *xrs-5* cells. This decrease would appear to be dose dependent and similar in the two cell lines. It would therefore appear that the levels of micronuclei per binucleate cell does not correlate with the reduction in binucleate cell frequency and that this reduction may occur on the basis of the levels of damage induced within the cells as opposed to the levels of damage expressed. This contrasts with γ-irradiation where there did appear to be a correlation between micronuclei frequencies and

reduction in the binucleate index. However, this may be accounted for by greater levels of damage induced in the γ-ray experiments than in the RE experiments.

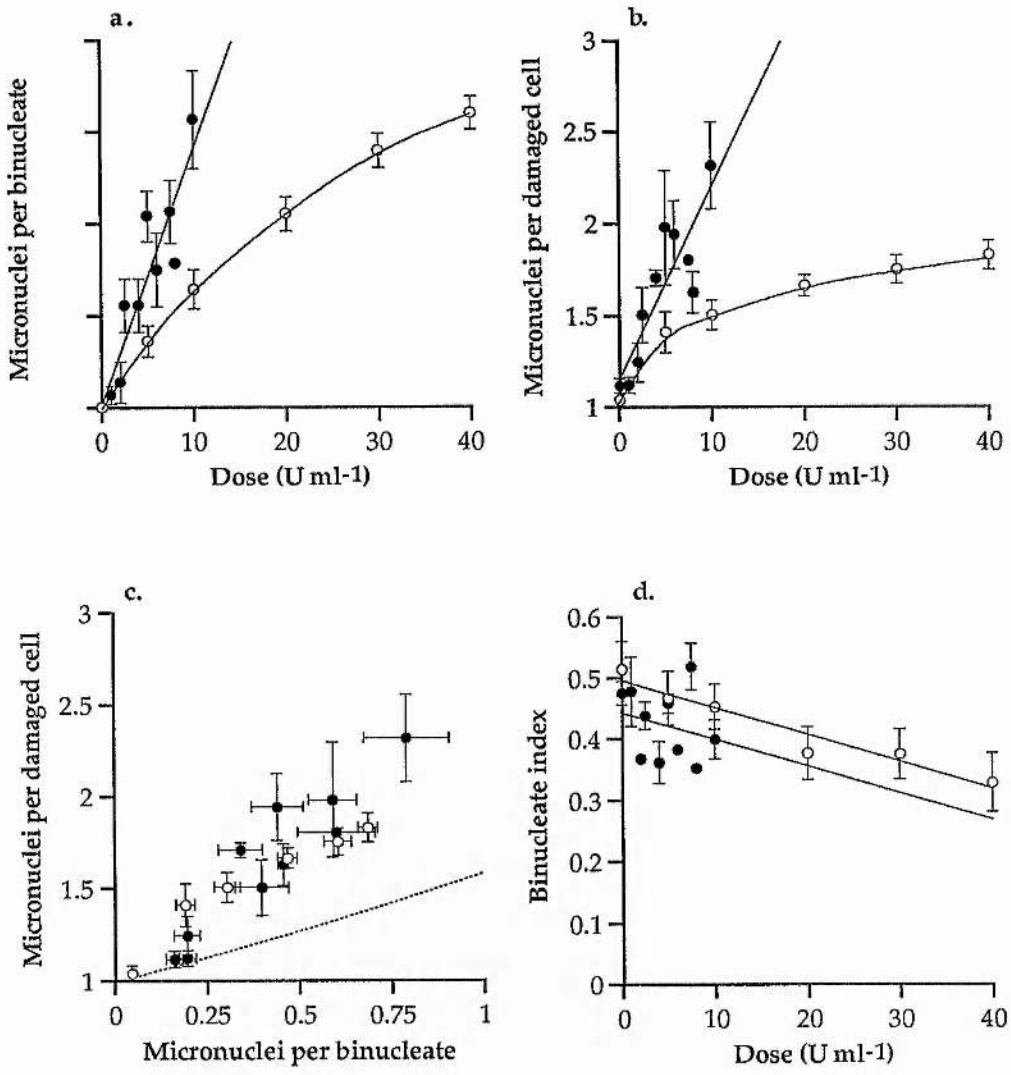

Figure 2.7. Effect of *PvuII* on CHO (○) and *xrs-5* cells (●).

a) Frequency of micronuclei per binucleate cell (corrected for background). One-way ANOVA indicates significant increases in frequency with dose (CHO, $p<0.001$, $F=51.58$, $df=5$; *xrs-5*; $p<0.001$, $F=12.76$, $df=9$).

b) Frequency of micronuclei per damaged binucleate cell. One-way ANOVA indicates significant increases in frequency with dose (CHO, $p<0.001$, $F=13.74$, $df=5$; *xrs-5*; $p<0.001$, $F=7.36$, $df=9$).

c) Correlation of the frequency of micronuclei per damaged binucleate versus the frequency of micronuclei per binucleate cell. Dotted line represents the expected frequency of micronuclei per damaged binucleate as calculated by Equation (2.7). χ^2 analysis indicates significant deviation from the expected frequencies for CHO ($p=0.0024$, $\chi^2=18.59$, $df=5$) and *xrs-5* ($p\leq0.001$, $\chi^2=47.89$, $df=10$)

d) Binucleate index. One-way ANOVA indicates significant decreases with dose (CHO,$p=0.042$, $F=2.65$, $df=5$;*xrs-5* , $p=0.047$, $F= 2.44$, $df=9$)

Error bars represent the standard error of the mean of a minimum of 3 independent experiments.

2.3.2.3. Response of CHO and xrs-5 cells to bleomycin sulphate.

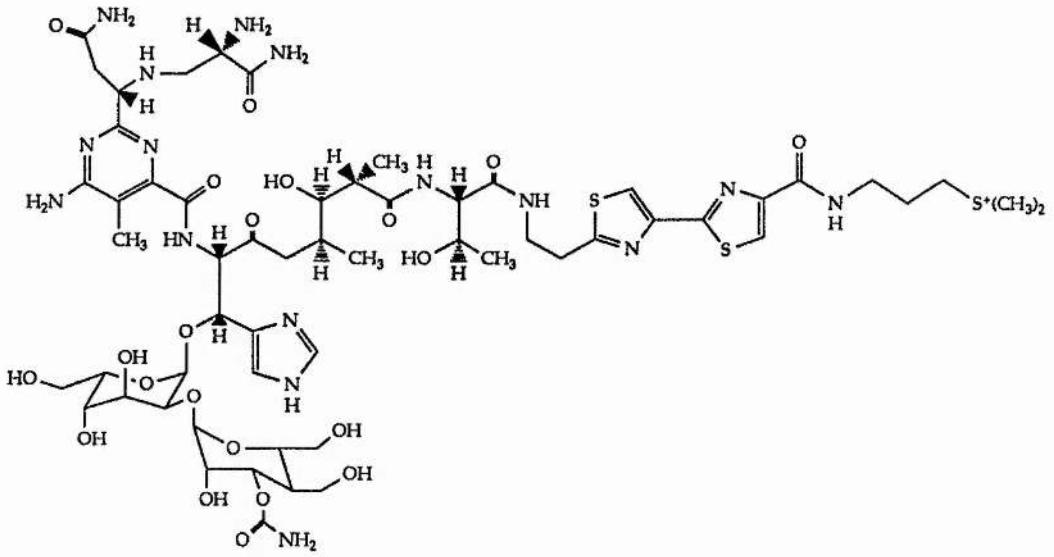

Figure 2.8. Structure of Bleomycin-A_2. [Redrawn from Levy and Hecht, 1988].

Bleomycin sulphate (BLM) is a radiomimetic glycopeptide (molecular weight approximatly 660 Da) (Figure 2.8) with antitumour properties. It is widely used clinically, particularly in the treatment of malignant lymphomas, Hodgkins' disease and squamous cell carcinoma [Hecht, 1986]. The action of BLM is believed to be mediated by the oxidative production of SSB and DSB in the presence of Fe(II) or Cu(II) [Byrnes et al., 1990]. The nature of these breaks are more defined than those observed with ionising radiation. They involve damage primarily to the sugar component of the sugar phosphate backbone of DNA resulting in strand breaks which also involve base loss [von Sonntag, 1987; Povirk and Goldberg, 1987; Hecht, 1986]. BLM leaves 3'-phosphoglycolate and 5'-phosphates as the major species of DSB end structures. These ends cannot be simply ligated but require processing with excision of the 3'-phosphoglycolate moiety; possibly involving an exonuclease associated with DNA polymerase-β [Seki and Oda, 1988], followed by repolymerisation of the lost base. These lesions are also produced by ionising radiations and so the repair of BLM and ionising radiation induced lesions may involve similar processes. BLM also causes aggregation of DNA, preferentially of newly replicated DNA [Woynarowski et al, 1988] and membrane peroxidation [Ciriolo et al., 1989]. BLM induced damage results in chromosome aberrations and growth inhibition [Larramendy et al., 1989]. Generally, the lesions induced by BLM are proposed to be similar in nature and repair pathways to those produced by ionising radiations [Byfield et al., 1976].

All six *xrs* mutants express sensitivity to BLM as measured by clonogenic assays [Jeggo and Kemp, 1983]. However, this cellular sensitivity could not be directly correlated with that

produced by X-rays. Three mutants; *xrs-4*, *xrs-6* and *xrs-7* were relatively more sensitive to BLM than X-rays. Two others; *xrs-1* and *xrs-5* were less sensitive to BLM than X-rays. The sensitivity of *xrs-5* to BLM (2.8 fold as sensitive as CHO) was similar to the least ionising radiation sensitive mutant from this group, *xrs-2*. (2.1 fold as sensitive). This difference in sensitivities between BLM and X-ray response for *xrs-5* was also observed by Darroudi and Natarajan [1989] with *xrs-5* and *xrs-6* having sensitivities to BLM 3 and 13 fold greater than CHO respectively.

BLM also produced elevated frequencies of chromosomal aberrations in *xrs* cells [Darroudi and Natarajan, 1989a]. Treatment of exponentially growing cells produced elevated frequencies of chromatid breaks and exchanges with *xrs-5* expressing a 2 and 2.3 fold elevation and *xrs-6* a 2.3 and 2.9 fold elevation of these aberrations respectively.

Thus, although sensitivity to BLM, as measured by survival, was much greater in *xrs-6* than *xrs-5*, this difference was not observed in the production of chromosomal aberrations. A larger difference between cell lines was observed in the induction of sister-chromatid exchanges (SCEs). When exponentially growing CHO and *xrs-5* cells were treated with BLM, few SCEs were formed compared to background. In comparison, *xrs-6* showed elevated frequencies of SCEs which increased in a dose dependent fashion.

The decrease in survival of *xrs-5* compared to CHO in response to BLM correlated well with the increase in levels of BLM induced aberrations. If a correlation between cell killing and aberration formation is maintained, as with X-rays, *xrs-6* should have expressed a far greater number of aberrations than was actually observed. It is therefore possible that BLM induced a type, or types of lesion in *xrs-6* which were lethal but did not produce chromosomal aberrations such as chromatid breaks and exchanges. This may or may not be related to the observed increase in SCEs.

An important distinction must be made between ionising radiation induced damage and radiomimetics such as BLM. Ionising radiation induced damage should be homogeneous throughout an irradiated cellular population. In addition, the time course over which damage is effected is relatively short. Entry of the hydrophilic BLM into cells is known to be strongly hindered by the cell membrane with only approximately 0.1% of available BLM taken up by HeLa cells and only 20% of this amount entering the nucleus [Roy and Horwitz, 1984]. As a result of this, and in order to induce levels of damage in cells comparable to that produced by ionising radiation, high concentrations of BLM and long exposure times are required. In addition, BLM action is not uniform across a cell population treated [Östling and Johanson, 1987]. The main clinical side effect of BLM treatment is pulmonary fibrosis. Pulmonary fibrosis occurs in a dose dependent manner and is generally the main limiting

factor of the total clinical dose that can be administered to a patient [Sidik and Smerdon., 1990a].

The permeabilisation of the cell membrane by lysophosphatidylcholine (LPC) has been shown to facilitate both increased uptake of BLM (as measured by repair synthesis and DNA cleavage) and an increase in the proportion of cells damaged [Sidik and Smerdon, 1990a; b]. Electroporation has also been shown to enhance the uptake of BLM *in vitro* [Poddevin et al., 1991]. Electric pulses applied directly to tumour sites *in vivo* have successfully increased the antitumour activity of BLM in spontaneous mammary tumours in mice [Belehradek et al., 1991]. Other factors which undoubtedly play a part in the clastogenicity of BLM (and other radiomimetics) are accessibility of the drug to chromatin and its cellular half life. Experiments have shown that cellular DNA specifically binds 1 molecule of BLM per 10^8 base pairs *in vivo* whereas *in vitro*, free DNA binds at an average of 1 molecule of BLM per 3.1 base pairs [Roy and Horwitz, 1984]. Cells are also known to break down BLM using the BLM-inactivating enzyme bleomycin-hydrolase [Umezawa et al., 1974] with varying activities occurring in different cell types [Müller and Zahn, 1977].

The variations in sensitivity to BLM between *xrs* cell lines and between *xrs* and CHO cells may therefore be related not to intrinsic repair defects but to the efficiency of BLM in causing damage and to the size of any sub-populations with susceptibility to damage. The following experiments deal only with treatment of CHO and *xrs-5* cells not other members of the *xrs* complementation group.

It is feasible that the difference in sensitivity to BLM of CHO and *xrs-5* could be related to the permeability of the cell membrane to BLM in the two cell lines. By comparing frequencies of micronuclei induced in permeable and impermeable cells by BLM it was hoped that it could be determined whether permeability was indeed a factor. Initial experiments were performed on CHO cells to study the effects of SLO mediated poration on BLM induction of micronuclei. As described in Section 2.3.2.2. SLO has been used to mediate the entry of large macromolecules into cells. SLO has advantages over both LPC and electroporation in that it produces dose dependent sized pores up to approximately 12 nm in diameter which permit the passage of proteins up to 483 kDa [Buckingham and Duncan, 1983]. Compared to electroporation a higher cell recovery can be obtained after treatment with 0.045 IU ml^{-1} SLO for 5 minutes at room temperature [Bryant, 1992]. Although, as seen following treatment with *PvuII* in the previous section there may be significant differences in the distribution of damage as evidenced by deviation from a Poisson based distribution of micronuclei.

CHO cells (in suspension) were exposed to BLM for either 24 hours in the absence of SLO or for 5 minutes in the presence or absence of 0.045 IU ml^{-1} SLO. Figure (2.9a) shows the frequency of micronuclei per binucleate cell as a function of a logarithmic dose range for each of these

treatments. A dramatic elevation in the micronuclei frequencies was observed in cells treated for 6 minutes in the presence of SLO with approximately 10^3 and 10^6 fold increases in the efficiency of micronucleus induction compared to 24 hour or 5 minute exposures in the absence of SLO respectively.

This elevated sensitivity to BLM correlated with an increase in the frequency of micronuclei per damaged cell in the presence of SLO (Figure 2.9b). However, the peak of the frequency of micronuclei per damaged cell occurred at a greater dose of BLM than the peak of micronuclei per binucleate cell frequency and also remained high even though the damage within the population as a whole decreased. The distribution of the damage expressed therefore increasingly deviated from the Poisson distribution (Figure 2.9c). The deviation was similar to that observed in the absence of SLO. Therefore, although BLM would appear to selectively cause expression of micronuclei in only a proportion of cells, SLO treatment does not appear to alter this selectivity. The selectivity of BLM induced micronuclei would indicate that the difference in levels of damage in SLO treated and untreated cells is not a function of the permeability of the cell membrane. Although SLO does not necessarily porate all cells of a given population to the same extent, it might have been predicted that if a porated subpopulation had existed then SLO would have diminished the relative size of this proportion of the cells. Alternative hypotheses are therefore required for the subpopulations of cells expressing sensitivity to BLM such as variations in BLM-hydrolase.

When binucleate indices of SLO treated and untreated CHO cells were compared (Figure 2.9d) there was an apparent decrease in the frequency of cells completing one mitosis which occurred in proportion to the increase in micronuclei per binucleate. However, a large difference occurred between BLM treatment of CHO cells in the presence or absence of BLM with regards to the minimum binucleate index. The binucleate index of CHO cells treated with BLM for 24 hours in the absence of SLO decreased in a dose dependent manner to only 4.62% (±1.34%) after 100 $\mu g\ ml^{-1}$. BLM treatment in the presence of SLO produced a decrease in binucleate index but this levelled off at approximately 18 % at BLM concentrations of 0.01 $\mu g\ ml^{-1}$ and a slight rise was observed at 1 $\mu g\ ml^{-1}$. The difference between BLM treatment in the presence and absence of SLO may be accounted for by SLO only porating a proportion of cells although, the damage distribution in Figure 2.9c would indicate that this is not necessarily the case. Alternatively the difference might reflect the length of exposure to BLM. The SLO treated cells are exposed to BLM for 5 minutes plus any length of time that is required to inactivate the BLM that enters the cell. Any cell cycle block imposed by the BLM damage in this instance may be overcome with time. The cells exposed continuously to BLM in the absence of SLO will experience a continual level of damage which may prevent recovery from cell cycle blocks.

These initial experiments indicated that treatment with SLO could overcome the cell membrane barrier to BLM permitting treatment, which retained the possible selectivity of BLM for different proportions of the cellular population but which permitted increasingly low doses and shorter exposure times.

A drawback of the SLO treatment described above was the treatment of trypsinised cell suspensions. Although this permitted treatment to be performed on very small numbers of cells in low volumes, it was thought that an improved system would be one where BLM could be introduced to cells attached to tissue culture dishes. Preliminary experiments had been performed using restriction endonucleases as clastogens [E. Stoppard, personal communication] which indicated that higher concentrations of SLO were required to produce similar results to treatment performed on cell suspensions. The following experiments were therefore performed using attached cells and increasing amounts of SLO. Using this system it was possible to examine the relative sensitivity of *xrs-5* cells to BLM in the presence or absence of SLO.

Results from experiments using SLO to facilitate entry of BLM into CHO and *xrs-5* cells are shown in Figure 2.10 SLO treatment on its own, even at high concentrations, produces few micronuclei above background levels (Figure 2.10a). The elevation of BLM induction of micronuclei by SLO was obvious in both CHO and *xrs-5* cells. This response was linearly proportional to dose for *xrs-5*, with a maximum efficiency of micronucleus induction occurring at 0.09 IU ml^{-1}. In contrast, the CHO dose response remained linear up to 0.18 IU ml^{-1} SLO. *Xrs-5* cells exhibited a sensitivity approximately twice that of CHO on the basis of concentration of SLO required to produce equal frequencies of micronuclei in both cell lines. The elevation in micronuclei per damaged cell was similar (Figure 2.10b) and the correlation analysis between the the micronucleus frequency per binucleate and damaged cell (Figure 2.10c) indicated that similar subpopulations of cells were damaged in the two cell lines.

The decrease in binucleate frequency following BLM treatment in the presence of SLO (Figure 2.10d) showed, after allowing for the control binucleate indices, a similar response in the two cell lines. This decrease appeared independent of the level of damage expressed.

Figure 2.11 shows the effect of BLM on CHO and *xrs-5* cells for 24 hours in the absence of SLO. *Xrs-5* expressed a marked sensitivity to BLM with similar frequencies of micronuclei per binucleate cell produced at approximately 50-100 fold lower BLM concentrations than CHO (Fiure 2.11a). The level of sensitivity to BLM is, however, only 2-3 fold greater than CHO if the frequency of micronuclei is measured for a given dose. This is similar to that observed with chromosomal aberration formation [Darroudi and Natarajan, 1989a] where comparisons were made between unit doses. The frequency of micronuclei per damaged cell (Figure 2.11b) again correlates with the frequency per binucleate cell with the exception of a continued increase after maximum frequency per binucleate cell is passed. The damage distribution

correlation between the two cells is also similar; deviating significantly from the Poisson (Figure 2.11c). This may indicate that the sensitivity of *xrs-5* cells is not due to BLM affecting different subpopulations.

Similar to treatment in the presence of SLO the binucleate indices (Figure 2.11d) of CHO and *xrs-5* cells exposed to BLM in the absence of SLO exhibited similar decreases with dose (after allowing for the reduced binucleate indeces observed in controls). This would indicate that although the frequency of micronucleus expression is greater in the mutant, this does not correlate with inhibition of cells from passing the first mitosis.

To confirm that SLO poration was enhancing the levels of damage as opposed to the poration influencing repair of damage, Figure 2.12 shows results of experiments performed on γ-irradiated cells. Here, cells were porated as per the BLM experiments using increasing concentrations of SLO. Immediately after removal of the SLO the cells were irradiated with 1 (CHO) or 7 (*xrs-5*) Gy. The cells were subsequently scored for micronuclei etc. after 24 hours. SLO produced no significant effect on the parameters measured that was not observed by either γ-irradiation or SLO treatment alone. From this it could be concluded that the enhancement of the effectiveness of BLM in inducing micronuclei in CHO and *xrs-5* cells came from elevated amounts of BLM entering the cell and producing a resultant increase in levels of DNA damage. The results with SLO also indicate that the sensitivity of *xrs-5* cells to BLM results from mechanisms other than elevated permeability to BLM.

The elevated frequencies of micronuclei induced by BLM in *xrs-5* cells compared to CHO after both treatment with and without SLO was not accompanied by a corresponding difference in the decrease in the binucleate indeces of the two cell lines. This would imply that cell cycle delay was not correlated with the levels of expressed damage in *xrs-5* and CHO cells.

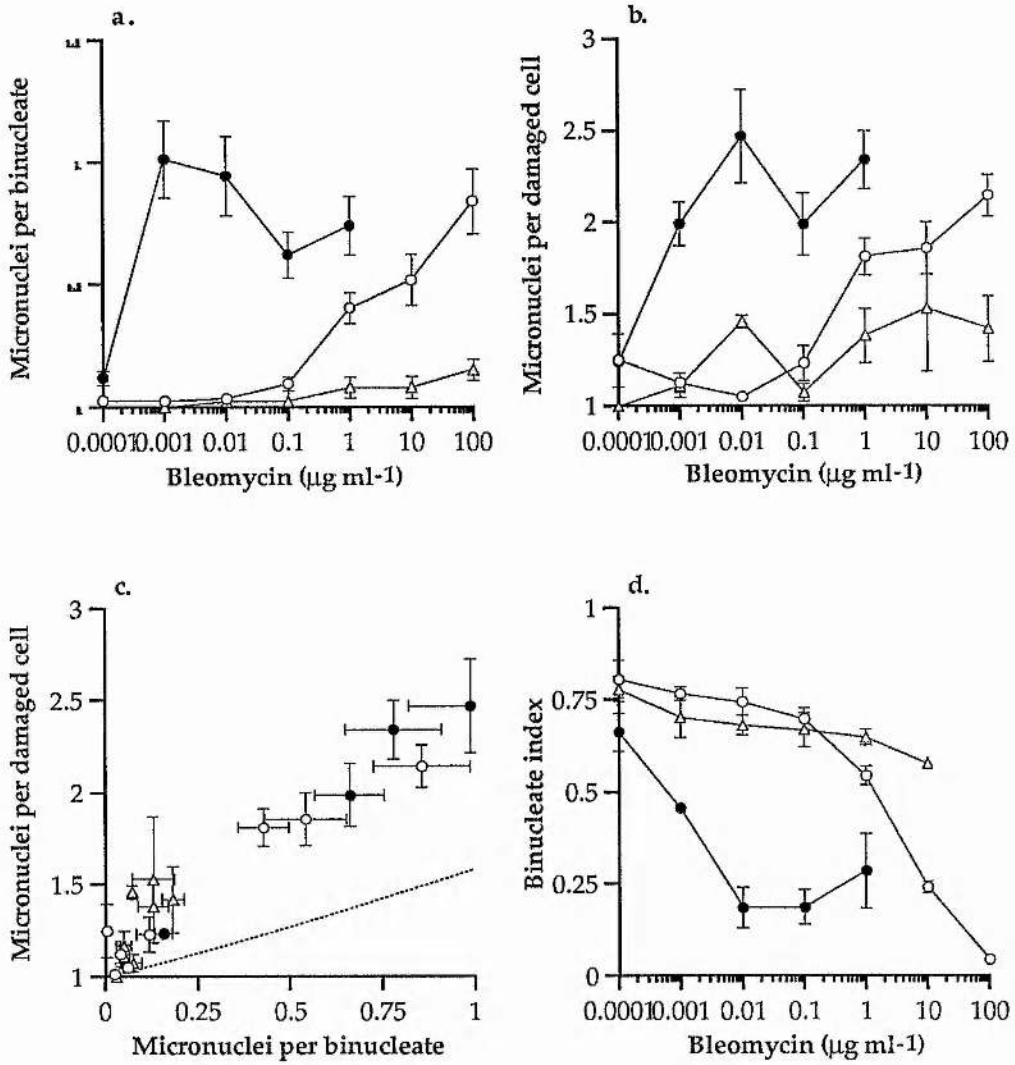

Figure 2.9. Effect of streptolysin-O on the response of CHO cells to bleomycin.
CHO cells were exposed to varying concentrations of BLM in the presence (●) or absence (○, Δ) of 0.045 IU ml^{-1} SLO. Treatment with BLM was for 5 min (●, Δ) or 24 hrs (○)

a) Frequency of micronuclei per binucleate cell (corrected for background). One-way ANOVA indicates significant increases in frequency with dose (5 min -SLO, $p<0.045$, $F=2.54$, $df=7$; 5 min +SLO, $p<0.001$, $F=16.88$, $df=5$; 24hr -SLO, $p<0.001$, $F=23.07$, $df=7$).

b) Frequency of micronuclei per damaged binucleate cell. One-way ANOVA indicates significant increases in frequency with dose (5 min -SLO, $p=0.543$, $F=0.89$, $df=7$; 5 min +SLO, $p\leq0.001$, $F=26.04$, $df=5$; 24hr -SLO, $p<0.001$, $F=22.78$, $df=7$).

c) Correlation of the frequency of micronuclei per damaged binucleate versus the frequency of micronuclei per binucleate cell. Dotted line represents the expected frequency of micronuclei per damaged binucleate as calculated by Equation (2.7). χ^2 analysis indicates significant deviation from the expected frequencies 5 min + SLO ($p\leq0.001$, $\chi^2=56.47$, $df=5$) and 24 hrs - SLO ($p\leq0.001$, $\chi^2=60.02$, $df=7$)

d) Binucleate index. One-way ANOVA indicates significant decreases with dose (5 min - SLO, $p=0.266$, $F=1.5$, $df=7$; 5 min +SLO, $p<0.001$, $F=11.65$, $df=5$; 24hr -SLO, $p<0.001$, $F=55.26$, $df=7$)

Error bars represent the standard error of the mean of a minimum of 3 independent experiments.

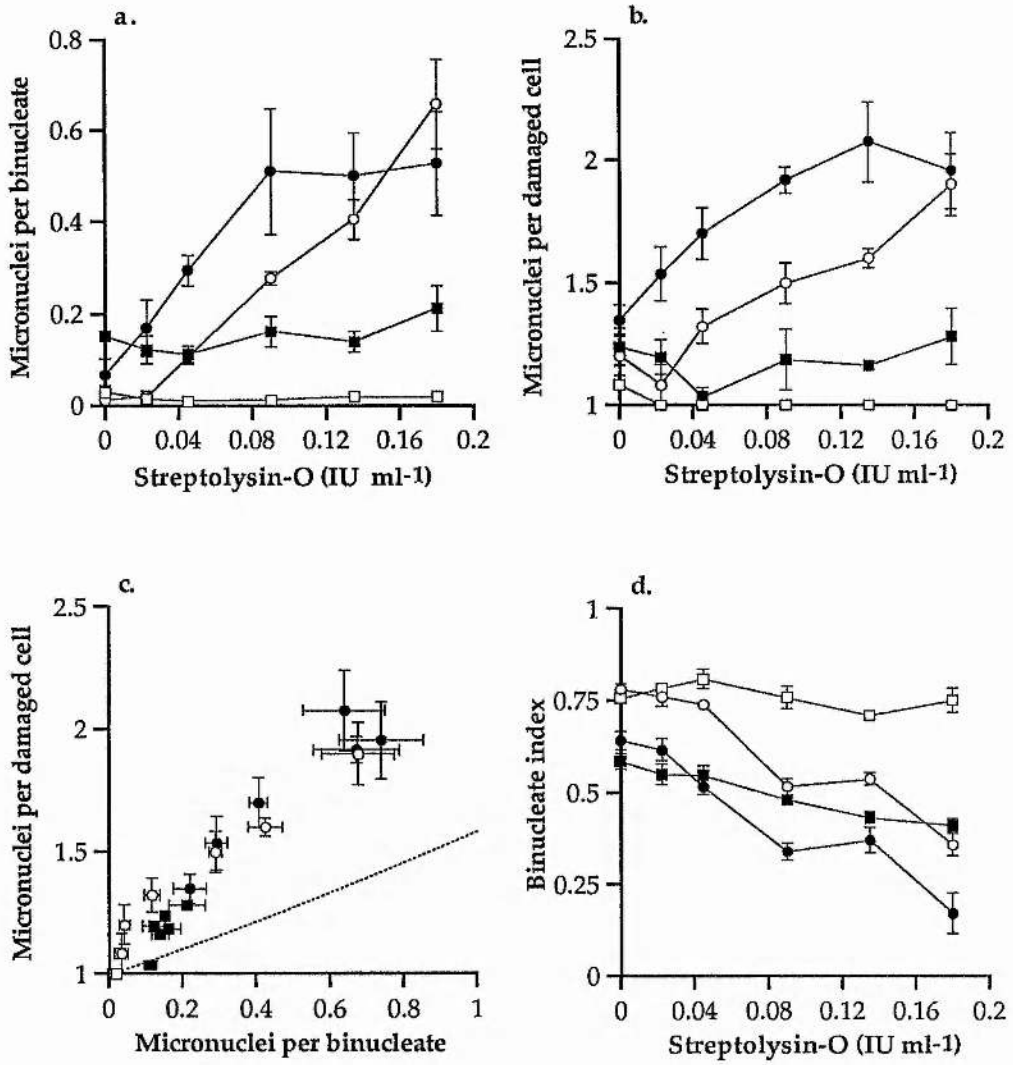

Figure 2.10. Effect of bleomycin on CHO (○, □) and *xrs-5* cells (●, ■) in the presence of varying concentrations of streptolysin-O. Cells were treated with (○, ●) or without (□, ■)10 ng ml^{-1} BLM.

a) Frequency of micronuclei per binucleate cell (corrected for background). One-way ANOVA indicates significant increases in frequency with dose (CHO, $p<0.001$, $F=29.57$, $df=5$; *xrs-5*, $p=0.005$, $F=4.98$, $df=5$).

b) Frequency of micronuclei per damaged binucleate cell. One-way ANOVA indicates significant increases in frequency with dose (CHO, $p<0.001$, $F=12.35$, $df=5$; *xrs-5*, $p=0.002$, $F=5.73$, $df=5$).

c) Correlation of the frequency of micronuclei per damaged binucleate versus the frequency of micronuclei per binucleate cell. Dotted line represents the expected frequency of micronuclei per damaged binucleate as calculated by Equation (2.7). χ^2 analysis indicates significant deviation from the expected frequencies for CHO ($p=0.0336$, $\chi^2=12.082$, $df=5$) and in *xrs-5* ($p\leq0.001$, $\chi^2=33.678$, $df=5$)

d) Binucleate index. One-way ANOVA indicates significant decreases with dose (CHO, $p\leq0.001$, $F=63.72$, $df=5$;*xrs-5*, $p<0.001$, $F= 30.52$, $df=5$)

Error bars represent the standard error of the mean of a minimum of 3 independent experiments.

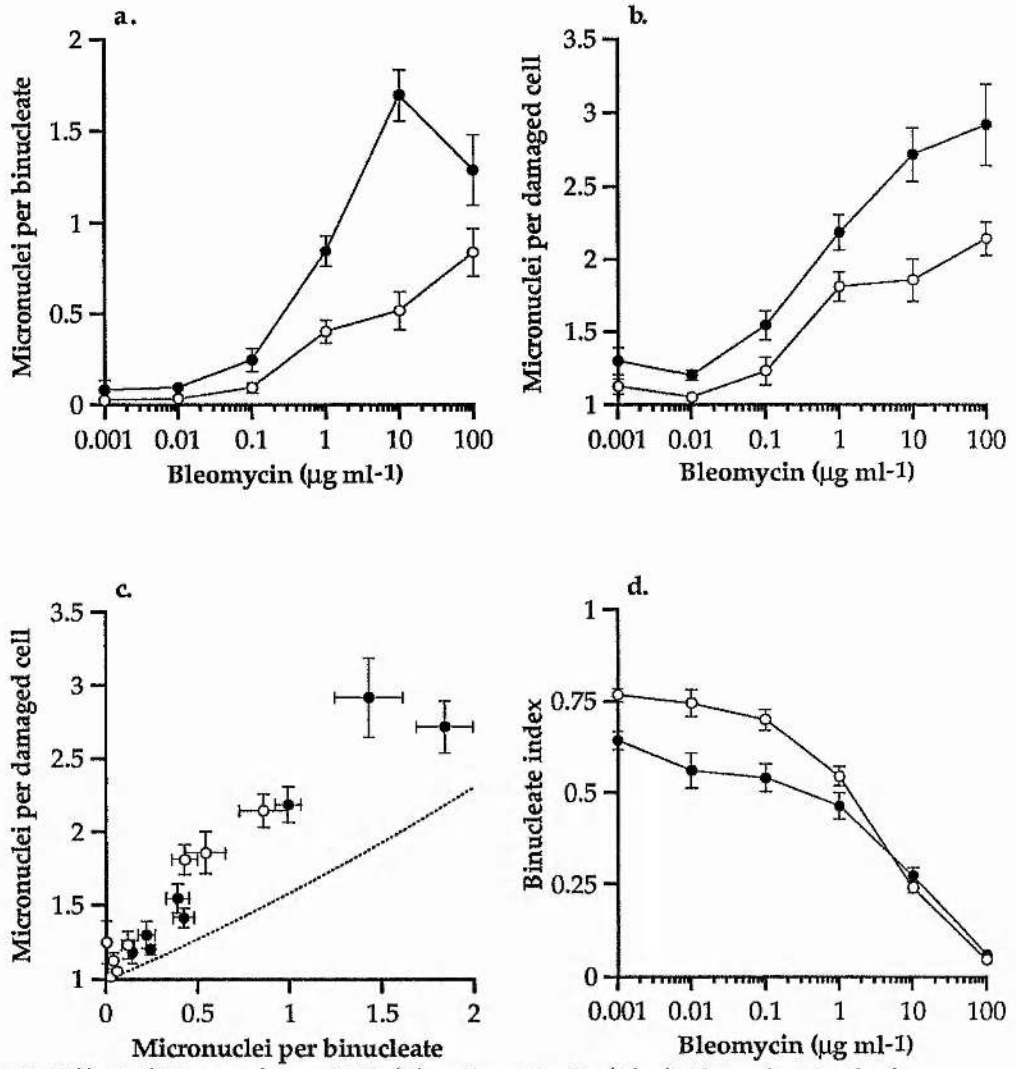

Figure 2.11. Effect of bleomycin on CHO (○) and *xrs-5* cells (●). (24 hour incubation).

a) Frequency of micronuclei per binucleate cell (corrected for background). One-way ANOVA indicates significant increases in frequency with dose (CHO, $p<0.001$, $F=23.07$, $df=7$; *xrs-5*, $p<0.001$, $F=55.78$, $df=6$). GLM analysis indicates a significant difference between the response of CHO and *xrs-5* ($p<0.001$, $F=15.82$, $df=6$)

b) Frequency of micronuclei per damaged binucleate cell. One-way ANOVA indicates significant increases in frequency with dose (CHO, $p<0.001$, $F=22.78$, $df=7$; *xrs-5*, $p<0.001$, $F=29.48$, $df=6$).

c) Correlation of the frequency of micronuclei per damaged binucleate versus the frequency of micronuclei per binucleate cell. Dotted line represents the expected frequency of micronuclei per damaged binucleate as calculated by Equation (2.7). χ^2 analysis indicates no significant deviation from the expected frequencies for CHO ($p\leq0.001$, $\chi^2=60.32$, $df=7$) and no significant overdispersion in *xrs-5* ($p\leq0.001$, $\chi^2=76.31$, $df=6$)

d) Binucleate index. One-way ANOVA indicates significant decreases with dose (CHO, $p<0.001$, $F=55.26$, $df=7$;*xrs-5*, $p<0.001$, $F=27.98$, $df=6$)

Error bars represent the standard error of the mean of a minimum of 3 independent experiments.

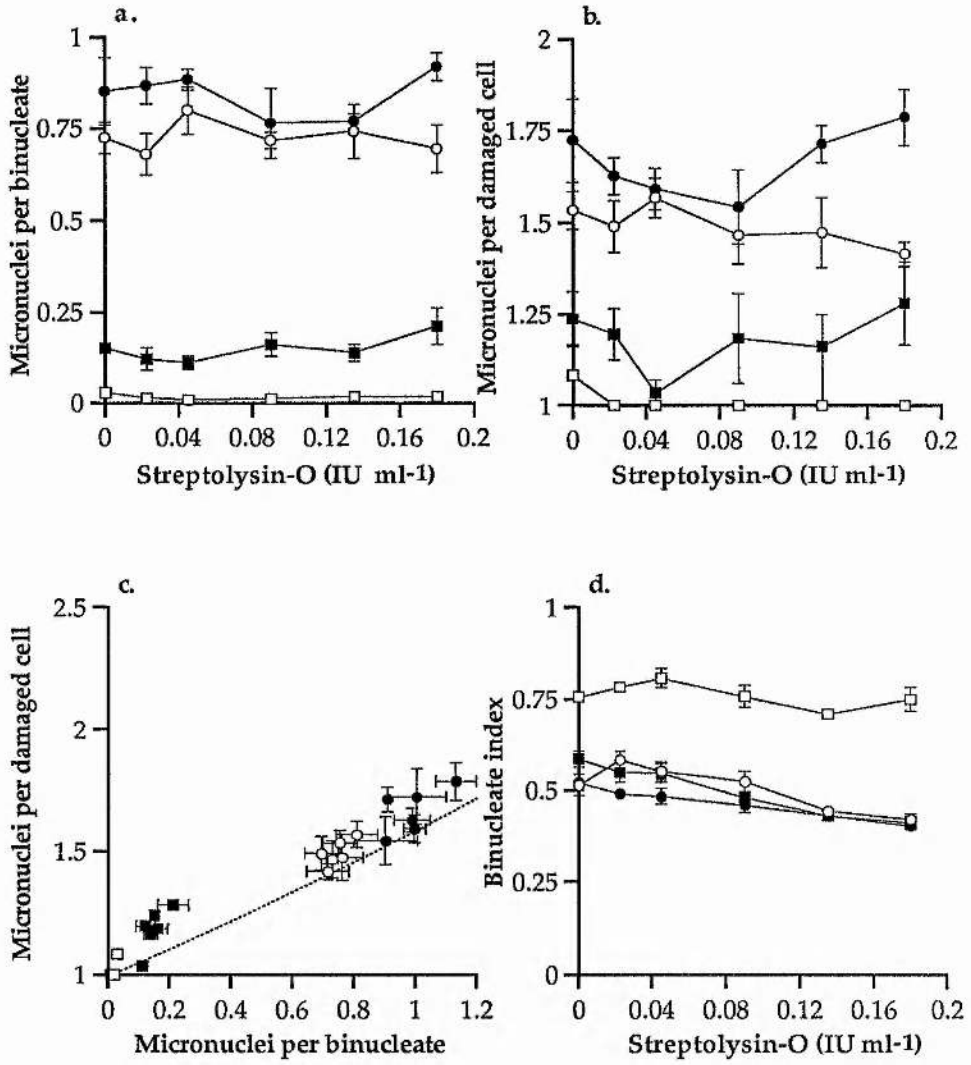

Figure 2.12. Effect of γ-rays on CHO (○) and *xrs-5* cells (●) in the presence of varying concentrations of streptolysin-O. Cells were irradiated with 7 Gy (CHO) or 1 Gy (*xrs-5*) ^{137}Cs γ-rays.

a) Frequency of micronuclei per binucleate cell (corrected for background). One-way ANOVA indicates no significant increases in frequency with dose (CHO, p=0.736, F=0.55, df=5; *xrs-5*, p=0.431, F=1.03, df=5).

b) Frequency of micronuclei per damaged binucleate cell. One-way ANOVA indicates no significant increases in frequency with dose (CHO; p=0.660, F=0.66, df=5; *xrs-5*; p=.277, F= 1.38, df=5).

c) Correlation of the frequency of micronuclei per damaged binucleate versus the frequency of micronuclei per binucleate cell. Dotted line represents the expected frequency of micronuclei per damaged binucleate as calculated by Equation (2.7). χ^2 analysis indicates no significant deviation from the expected frequencies for CHO (p=0.879, χ^2=1.7757, df=5) or *xrs-5* (p=0.489, χ^2=4.4277, df=5)

d) Binucleate index. One-way ANOVA indicates significant decreases with dose (CHO, p≤0.001, F=7.93, df=5;*xrs-5*, p=0.001, F= 6.32, df=5)

Error bars represent the standard error of the mean of a minimum of 3 independent experiments.

2.3.2.4. *Response of CHO and xrs-5 to etoposide.*

Drug induced inhibition of topoisomerase II (topoII) can result in the the formation of protein associated DNA strand breaks termed cleavable complexes [reviewed Liu, 1989]. TopoII exists as a 170-180 kDa homodimer, each monomer of which is capable of inducing a single strand break with covalent bonding to one strand of the helix. This results in a 4 base pair cohesive ended DSB with the two monomers covalently attached to the 5'-phosphoryl end of the strand break and non-covalently to the 3'-hydroxyl [Mattern et al., 1987]. The cleavable complex is in rapid equilibrium with the non-cleavable complex. Interaction of a second intact duplex of DNA with a cleavable complex triggers an ATP dependent strand passing reaction. This permits the relaxation of supercoiled circular molecules or the decatenation/deknotting of DNA molecules. It is the strand passing reaction which results in relaxation of supercoils since the cleavable complex itself does not produce free ends which would be required for passive DNA unwinding. Several inhibitors of topoII exist which alter the cleavage equilibrium towards the cleavable complex [Liu, 1989]. The cleavable complexes which then accumulate can be quantified only after protein denaturation and/or proteolysis of the topoII dimers.

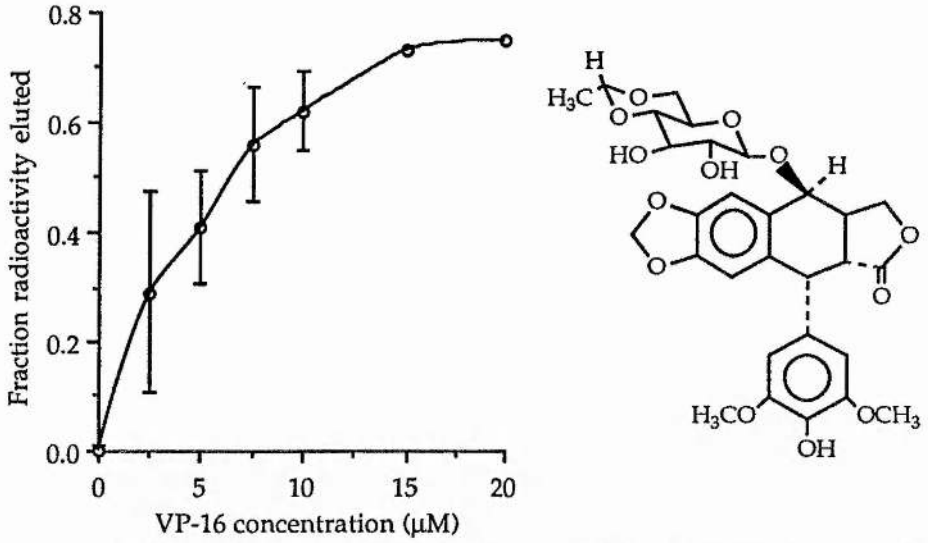

Figure 2.13. DSB induction by and structure of etoposide. Graph represents the relative induction of DSB in CHO cells incubated for one hour at 37°C in the presence of varying concentrations of etoposide (VP-16) as measured by non-denaturing neutral filter elution [redrawn from Johnston and Bryant, 1991]. Error bars represent the SEM from 2-3 independent experiments.

One of these inhibitors is etoposide (4'-demethylepipodophyllotoxin-9-(4,6-O-ethylidine-β-D-glucopyranoside) (abbrev. VP-16). That this agent produces DSB *in vivo* is demonstrated

in Figure 2.13 [redrawn from Johnston and Bryant, 1991]. This shows the relative induction of DSB as measured by non-denaturing filter elution.

Etoposide has been shown to produce higher frequencies of chromosomal aberrations in *xrs-5* cells than in CHO cells [Darroudi and Natarajan, 1989b]. *Xrs-5* and *xrs-6* cells produced approximately 4 and 2 fold more aberrations per unit dose respectively than CHO cells. TopoII is implicated in cellular repair mechanisms [reviewed Downes and Johnson, 1988] and so in addition to inducing DSB the repair of this damage may also be impaired by inhibition of the enzyme. As described in Chapter 1, the activity of topoII in *xrs* cells has been investigated and some reduction in the overall levels of topoII activity as measured by the accumulation of cleavable complexes in the presence of etoposide has been reported [Caldecott et al., 1993]. Other studies revealed no discernible difference in extractable topoII activity in the absence of topoII inhibitors [Jeggo et al., 1989; Warters et al., 1991].

When the induction of micronuclei by etoposide was investigated (Figure 2.14a) it was found that there were non-linear dose response curves for both CHO and *xrs-5*. Micronucleus frequencies increased in both cell lines up to a maximum after which there was an exponential decrease. *Xrs-5* cells produced significantly more micronuclei per binucleate cell than CHO at lower doses with the maximum frequency occurring at 0.625 μM compared to 5 μM for CHO. This gives *xrs-5* a sensitivity to etoposide approximately 8 fold higher than CHO. To measure relative sensitivity of CHO and *xrs-5* cells on the basis of a single dose of etoposide is impractical since the dose response is non-linear. At high doses (e.g. at etoposide concentrations of greater than 2.5 μM) there is little difference in the micronuclei frequencies of the two cell lines).

The maximal micronucleus frequency per damaged cell (Figure 2.14b) lagged behind the maximum per binucleate (1.25 μM and 10 μM for *xrs-5* and CHO respectively). When correlated (Figure 2.14c) there was a significant deviation from the expected Poisson distribution which is similar for both cell lines. Thus, although increased frequencies of micronuclei are observed with *xrs-5* compared with CHO, the distribution of micronuclei within the population of cells is similar and one can therefore deduce that that the populations of cells damaged may also be similar. The inability of *xrs-5* to repair DSBs resulting from cleavable complexes induced by etoposide may be the reason for the elevated micronucleus frequencies.

Etoposide also causes a significant reduction in the binucleate index in both cell lines (Figure 2.14d). In CHO cells the largest reduction occurs after the maximum micronucleus frequency is reached (greater than 2.5 μM). In *xrs-5* cells the reduction occurs at lower doses than in CHO cells and there is a closer correlation between micronucleus frequency increase and binucleate index decrease. This may indicate that in CHO cells the reduction in micronucleus frequency

is due to heavily damaged cells not entering or completing the first mitosis. In *xrs-5* cells the defect in DSB repair may be causing non-recoverable cell cycle delay even at low etoposide doses. A complete block was not observed, however, both cell lines exhibited a reduction in the binucleate index which leveled off to approximately 10 and 5 % for *xrs-5* and CHO respectively, indicating sub-populations of cells which were resistant to the induced block. The proportion of the cells which were resistant to etoposide would appear to have been higher in *xrs-5*.

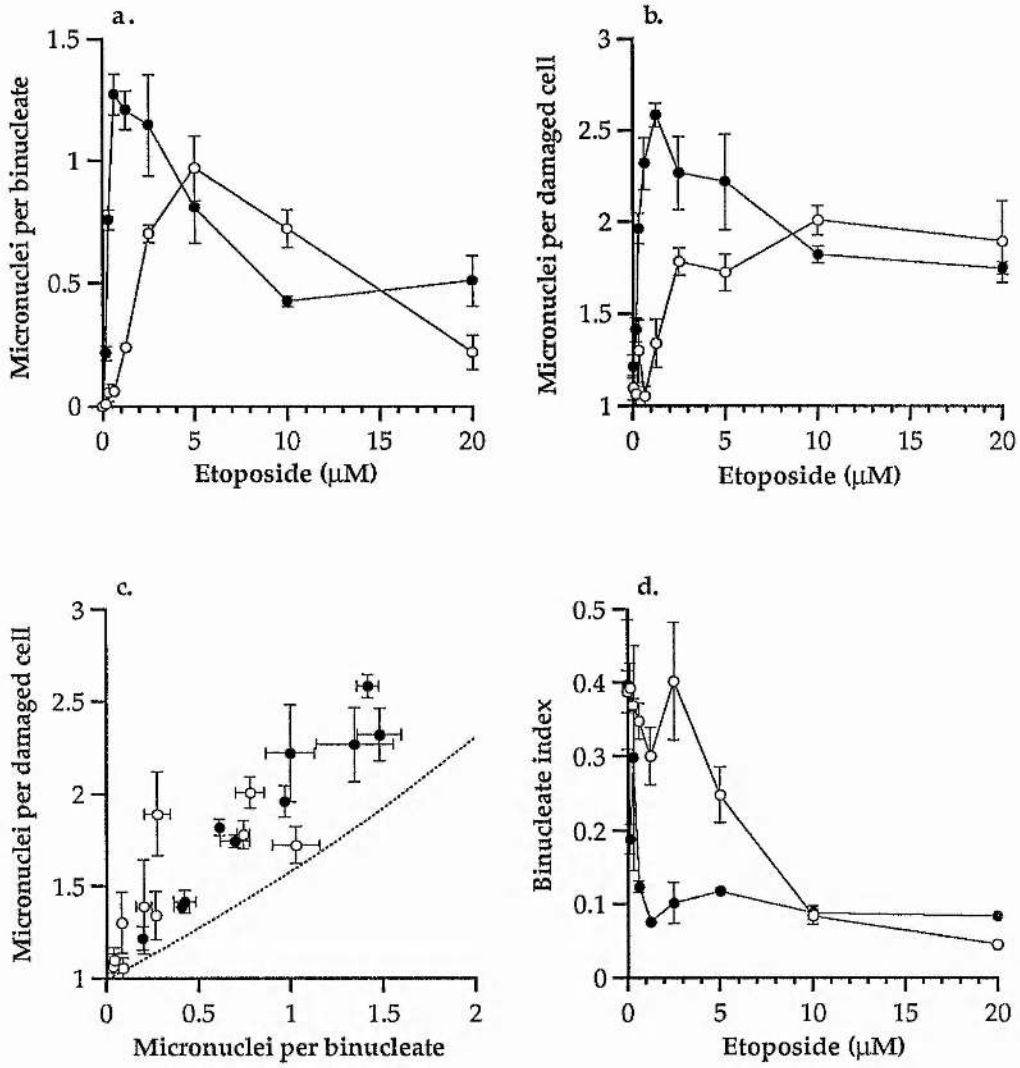

Figure 2.14. Effect of etoposide on CHO (○) and *xrs-5* cells (●).

a) Frequency of micronuclei per binucleate cell (corrected for background). One-way ANOVA indicates significant increases in frequency with dose (CHO, $p<0.001$, $F=51.40$, $df=9$; *xrs-5*, $p<0.001$, $F=13.72$, $df=9$). GLM analysis indicates significant differences between the response of CHO and *xrs-5* cells ($p<0.001$, $F=10.85$, $df=9$).

b) Frequency of micronuclei per damaged binucleate cell. One-way ANOVA indicates significant increases in frequency with dose (CHO, $p<0.001$, $F=8.12$, $df=9$; *xrs-5*, $p<0.001$, $F=10.93$, $df=9$).

c) Correlation of the frequency of micronuclei per damaged binucleate versus the frequency of micronuclei per binucleate cell. Dotted line represents the expected frequency of micronuclei per damaged binucleate as calculated by Equation (2.7). χ^2 analysis indicates significant deviation from the expected frequencies for CHO ($p=0.013$, $\chi^2=21.07$, $df=9$) and in *xrs-5* ($p\leq0.001$, $\chi^2=78.006$, $df=9$)

d) Binucleate index. One-way ANOVA indicates significant decreases with dose (CHO, $p<0.001$, $F=8.24$, $df=9$;*xrs-5*, $p=0.005$, $F=3.56$, $df=9$)

Error bars represent the standard error of the mean of a minimum of 3 independent experiments.

2.3.2.5. Response of CHO and xrs-5 cells to camptothecin.

In addition to topoII, eukaryotic cells posses an additional topology modifying enzyme; topoisomerase I (topoI). This is an abundant and ubiquitous monomeric protein (100 kDa) [Zhang et al., 1988]. It catalyses the relaxation of both positive and negative supercoils in topologically restrained DNA via a reaction which requires no energy co-factor [Stewart and Schütz, 1987]. TopoI produces transient SSB by forming a covalently linked cleavable complex, with topoI bound to the 3'-phosphoryl end of the broken DNA strand via a tyrosyl-phosphate bond. The 5' end of the transient break is not tightly held during the entire breakage-reunion reaction and this permits rotation of the two ends relative to each other resulting in the relaxation of supercoils. Unlike topoII, topoI is unable to perform decatenation or deknotting reactions. The cleavage complex is in rapid equilibrium with a non-cleavable complex and this, in turn, with free topoI. Exposure to a strong protein denaturant, e.g. alkaline conditions or SDS, results in a nascent SSB covalently linked to denatured topoI by the 3'-phosphoryl end [Mattern et al., 1987].

The function of topoI is apparently during transcription of RNA. Cleavage sites occur within a hexadecameric recognition site containing poly-A and poly-T sequences [Busk et al., 1987]. However, the topology of DNA may also influence binding and recognition of DNA cleavage sites [Smith et al., 1989; 1990a; b]. The recognition sequences have been located primarily within transcribed regions of genes [Zhang et al., 1988]. Actual cleavage by topoI occurs predominantly in actively transcribed regions with the SSB occurring within the transcribed strand [Stewart and Schütz, 1987]. TopoI was found to be tightly complexed with RNA polymerase [Smith, 1990a] and is though to be involved in the modulation of torsional waves generated by transcriptional elongation. Although any role in the replication of eukaryotic DNA is uncertain topoI can support the replication of SV40 DNA *in vitro* by acting at the replication fork. However this produces catenated DNA molecules and topoI can be fully substituted for by topoII [Liu, 1989]. The exogenous cleavage of DNA, e.g. by X-irradiation, causes a partial inactivation of topoI, possibly allowing increased time for repair processes to occur prior to DNA transcription [Smith, 1990a; b]. This inactivation of topoI may be via poly(ADP-ribose)ylation in response to DNA strand breaks [Downes and Johnson, 1988; Mattern et al., 1987].

Similar to the inhibition of topoII by etoposide, the equilibrium between topoI cleavable complex and non-cleavable complex can be shifted towards the cleavable-complex by drug inhibition. Camptothecin (CPT) is a reversible inhibitor of this topoI breakage-reunion process [Liu, 1989]. CPT is an alkaloid derived from the asian shrub *Camptotheca acuminata* [Jaxel et al., 1989].

CPT is a potent cytotoxic versus a number of experimental murine neoplasms [Mattern et al., 1987]. It induces sister chromatid exchanges, chromosomal aberrations and the inhibition of DNA and RNA synthesis [Liu 1989]. It acts specifically on topoI, causing rapid topoI mediated DNA cleavage producing protein associated SSB [Mattern et al., 1987]. However, CPT results in the inhibition of relaxation of super-coiled DNA, presumably by the prevention of the strand passing reaction and the normal cycling of the enzyme.

Xrs cells have been demonstrated to be proficient at SSB repair and therefore if SSB are the only lesions caused by CPT then wild-type resistance to CPT might be expected. However, *xrs* cells have been shown to be partially sensitive to hydrogen peroxide, which produces predominantly SSB [Vaughan and Gordon, 1992].

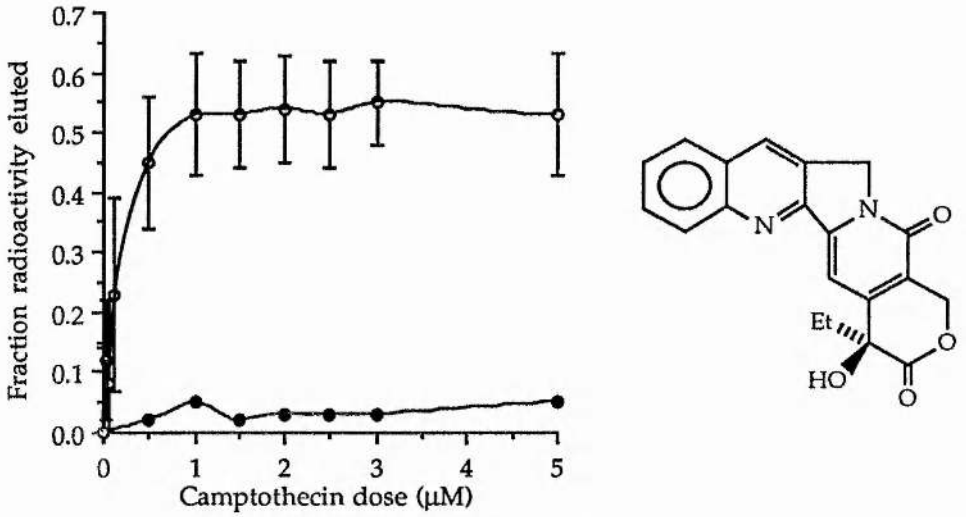

Figure 2.15. Induction of DSB and SSB by and structure of camptothecin. CHO cells were incubated with various concentrations of CPT for one hour at 37°C and elution was performed under non-denaturing (pH 9.6) (●) or denaturing (pH 12.1) (O) and the fraction of DNA remaining on the filter estimated to give approximations of the relative induction of DSB and SSB respectively. Error bars represent the SEM of 2-5 independent experiments. Non-denaturing data taken from a single experiment [graph redrawn from Johnston and Bryant, 1991]. CPT structure redrawn from Jaxel et al., [1989].

DSB/SSB repair proficient radiation sensitive ataxia telangiectasia (AT) cells have been demonstrated to be sensitive to CPT [Falk and Smith, 1992]. This was manifested as a reduction in survival in AT5BIVA cells versus the normal MRC5SVI cells. However, this sensitivity, similar to ionising radiation, could not be attributed to higher levels of DNA damage in the AT cells. CPT was demonstrated to be S-phase specific in its actions in both cell lines and this was thought to result from the interaction of these complexes with replicons resulting in the generation of lethal DSB [Falk and Smith, 1992; Liu, 1989]. DSBs were produced at a ratio of 1 DSB to 150-200 SSB in L1210 cells at concentrations of 100 μM and

these DSB were proposed to be the result of closely associated SSB [Jaxel et al., 1989]. That few DSB are produced in CHO cells is demonstrated in Figure 2.15 where cells treated with CPT were exposed to either denaturing (alkaline conditions)-filter elution or non-denaturing (pH9.6) filter elution to estimate relative levels of SSB and DSB respectively [Redrawn from Johnston and Bryant, 1991]. Although the number of DSB is low in exponentially growing cells, CPT induces DSB specifically in newly replicated DNA [Ryan et al., 1991]. This occurs via an interaction between replication machinery and the drug mediated topoI cleavable complex. These DSB are particularly long lived, remaining detectable 24 hours after induction. It is these DSB that are proposed to be the main cause of CPT cytotoxicity.

24 hours incubation with nM concentrations of CPT produced significant micronuclei frequencies in both CHO and *xrs-5* (Figure 2.16a). Both cell lines exhibited a rapid rise in frequencies with dose with *xrs-5* having a sensitivity approximately twice that of CHO on a dose response basis. Both cell lines reached a maximum micronucleus frequency at approximately 20-40 nM although this maximum micronucleus frequency was greater in *xrs-5* than CHO. As the concentration increased from the maximum micronucleus frequency CHO cells exhibited a marked reduction in micronucleus frequency per binucleate. This decrease was reduced in *xrs-5* cells compared to that observed in CHO cells. Over the dose range examined the dose response of *xrs-5* was significantly different to that of CHO.

To examine whether the difference between cell lines could be attributed to a different distribution of damage in the two cells lines the frequencies of micronuclei per damaged cell were examined (Figure 2.16b). Although the frequencies of micronuclei per damaged cell in *xrs-5* were significantly higher than CHO the shape of the dose response curves were similar. When the values of micronuclei per damaged cell were correlated to the frequencies of micronuclei per binucleate cell (Figure 2.16c) the two cells lines appeared to deviate similarly from the Poisson distribution although when a χ^2 analysis was performed CHO cells did not deviate significantly from the expected values. This would indicate that there may be some cell cycle specificity in *xrs-5* that is not present in CHO cells.

Examination was made of the binucleate indices of the two cell lines with increasing CPT dose (Figure 2.16d). CPT produced a significant reduction in the binucleate indices of both cells lines (the initial rise in CHO cells could be attributed to an elevated level of tetranucleates in the control samples, cell cycle delay reduces the frequency of these and produces an increase in binucleate frequencies). The shape of this dose response curves (excluding the rise in CHO at low doses) appeared similar between the two cell lines. However, at high CPT doses *the xrs-5* binucleate index would appear to be larger than that of CHO. At 80 nM 10% (±0.25%) of CHO cells were binucleated compared to 22.17% (±1.59%) of *xrs-5* cells. This would indicate that although the distribution of damage was similar, the proportion of cells which

exhibited a cell cycle block was significantly higher in CHO than for the mutants. The cell cycle block may be the cause of the reduction in micronucleus frequencies in the two cell lines with heavily damaged cells prevented from completing one mitosis. The extent of this block affects a higher proportion of CHO cells than *xrs-5* therefore the steepness of the reduction in CHO micronucleus frequencies may reflect this. Since CPT has been demonstrated to exhibit cytotoxic effects on cells in S phase [Ryan et al., 1991], the difference in minimum binucleate indices for the two cell lines might represent the proportion of cells which have completed all DNA synthesis prior to passing through their first mitosis i.e. G_2 cells.

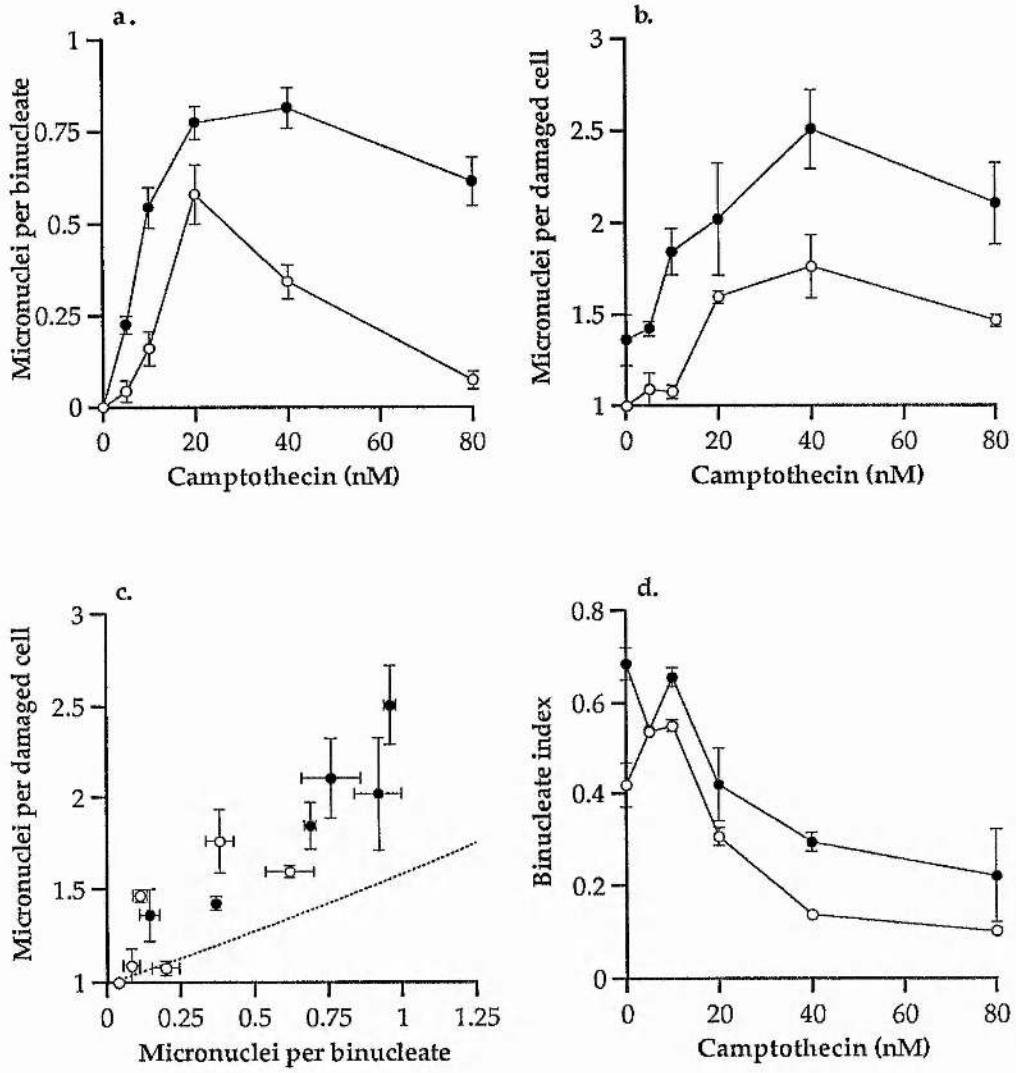

Figure 2.16 Effect of camptothecin on CHO (○) and *xrs-5* cells (●).
a) Frequency of micronuclei per binucleate cell (corrected for background). One-way ANOVA indicates significant increases in frequency with dose (CHO, $p<0.001$, $F=26.64$, $df=5$; *xrs-5*,$p<0.001$, $F=47.87$, $df=5$). GLM analysis of variance indicates significant differences between the response of CHO and *xrs-5* ($p<0.001$, $F=9.25$, $df=5$).
b) Frequency of micronuclei per damaged binucleate cell. One-way ANOVA indicates significant increases in frequency with dose (CHO, $p<0.001$, $F=14.65$, $df=5$; *xrs-5*, $p=0.037$, $F=5.04$, $df=5$).
c) Correlation of the frequency of micronuclei per damaged binucleate versus the frequency of micronuclei per binucleate cell. Dotted line represents the expected frequency of micronuclei per damaged binucleate as calculated by Equation (2.7). χ^2 analysis indicates no significant deviation from the expected frequencies for CHO ($p=0.194$, $\chi^2=7.3176$, $df=5$) and a significant overdispersion in *xrs-5* ($p\leq0.001$, $\chi^2=52.34$, $df=5$)
d) Binucleate index. One-way ANOVA indicates significant decreases with dose (CHO, $p<0.001$, $F=75.36$, $df=5$;*xrs-5*, $p<0.001$, $F= 61.63$, $df=5$).
Error bars represent the standard error of the mean of a minimum of 3 independent experiments.

2.3.3.6. Summary of the induction of micronuclei by clastogenic agents in CHO and xrs-5 cells.

Table 2.1. summarises the data obtained on the induction and distribution of micronuclei in the mutant and wild type cells and the the ability of cells to complete one round of division after treatment with ^{137}Cs γ–rays, *PvuII*, bleomycin, etoposide or camptothecin.

All five clastogens induced micronuclei in CHO and *xrs-5* with the mutant cells expressing a significantly increased sensitivity compared with the wild type. The extent of this sensitivity varied from 2 fold with CPT to 10-100 fold with BLM. However, what did become obvious was that the assessment of relative sensitivity varied depending on the shape of the dose response curves. Linear curves, such as for γ-rays, present no problem since the sensitivity can be measured either on the basis of the dose required to produce equal micronuclei frequencies (equi-clastogenic) or the the frequency of micronuclei for a given dose (equal dose). The non-linear dose responses, most marked with BLM treatment, present difficulties. On a equi-clastogenic basis the sensitivity proved to be in the order of 10-100 fold. On a equal dose basis the sensitivity was only 2-3 fold greater for *xrs-5*. The appearance of maximal frequencies of micronuclei also presents problems since, at high doses, in negative dose response regions, sensitivity can appear negligible.

When maximal frequencies were obtained on a per binucleate cell basis it was apparent that *xrs-5* cells accommodated a higher level of damage than CHO cells. Although the maximum frequencies of micronuclei per damaged cell, where observed, were often found at higher doses compared to the maxima observed for frequencies of micronuclei per binucleate cell, these too exhibited higher values for *xrs-5*. That *xrs-5* cells exhibited increased maxima compared to CHO would indicate that the elevated frequencies of micronuclei in *xrs-5* cells was not necessarily caused solely by differences in the level of damage a cell contained at any period of time but also by the maximum amount of damage that cells could carry through into the first division.

Examination of the distribution of damage also revealed differences between both the mode of damage and between CHO and *xrs-5* cells. *Xrs-5* cells exhibited over-dispersion of damage after all five forms of treatment, although for γ-irradiation this was noticeable only at high doses. Over-dispersion was also observed in CHO cells after trteatment with bleomycin, etoposide and *PvuII* although, the relative level of CHO over-dispersion would appear to be less pronounced than for *xrs-5* cells. This may be the result of lower levels of damage in CHO. Compared to the other treatments γ-rays generally produced a more random spread of damage. The cause of this is likely to be due to several factors; i) irradiation occurs over a short timescale whereas the other four treatments exposure was for much longer periods of time. This may result in extended cell cycle delays at checkpoints, resulting in selective sub-

populations not passing through one division. ii) Initial levels of damage will be more evenly spread across irradiated populations than in other treatments where additional factors such as permeability of both the cell membrane and the nuclear membrane to the agents will restrict levels of damage. The increased numbers of variables involved in the actual induction of damage will produce a less random distribution.

Therefore *xrs-5* cell sensitivity could be observed by measurements of both the frequency of micronuclei per binucleate and per damaged cell. The dose range of frequencies per damaged cell often proved to be wider with maximal frequencies observed at higher doses than the dose range observed for frequencies per binucleate cell.

The use of binucleate indices to assess senstivity to specific agents was not as reliable as the measurement of micronucleus frequencies. The binucleate index dose response curve for *xrs-5* cells was steeper than that observed for CHO cells when treated with γ-rays or etoposide. BLM, CPT or *PvuII* produced similar binucleate index responses in the two cell lines indicating that cell cycle delays measured were produced by either the initial level of damage or by mechanisms unrelated to either the expression or repair of damage. BLM and CPT both act at S phase producing either aggregation or DSB formation within newly synthesised DNA [Woynarowski et al., 1988; Ryan et al., 1991]. If these processes block DNA synthesis and therefore cell cycle progression, then the observed similarities between CHO and *xrs-5* with these two agents might be explained by similar S phase specific damage processing in the two cell lines. The differential reductions observed with γ-rays and etoposide would imply that with these agents cell cycle delay corresponds with the level of damage that is expressed. That delay often coincides with reductions in micronucleus frequency (e.g. etoposide) may indicate that it is heavily damaged cells which are incapable of progressing through cell division and that here the DNA repair defect of *xrs-5* determines not only this level of expressed damage but also the extent of the cell cycle delays. Hence there is a possible correlation between micronucleus frequency and binucleate index.

The examination of binucleate frequencies are further complicated by the presence of plateau regions after doses of several agents which still produced increases in micronucleus frequencies. Here it would appear that sub-populations of the cell lines were resistant to inhibition of cell division. Increases in micronuclei would therefore be wholly contained within this population. The proportions of these sub-populations are also variable between mutant and wild type cells. In the two instances where stable plateaus are obtained with both cell lines (etoposide and CPT) *xrs-5* exhibits a higher proportion of un-blocked cells which in both cases is two-fold that of CHO. These proportions may be significant to the apparent sensitivity of *xrs-5* cells. The larger proportions of *xrs-5* cells capable of still dividing after damage may also mean that higher levels of damage are carried through into

the first division. This is supported by the higher maximum frequencies of micronuclei observed, although this latter effect is also observed with BLM which does not produce a plateau. To obtain precise position within the cell cycle for the check-points responsible for reductions in binucleate indices requires further work. However because of the requirement of division for the micronucleus assay it could be speculated that the plateaus observed are the result of cells which exist after a checkpoint prior to or at some point within G_2.

Therefore, to conclude this section, it is apparent that the use of the cytokinesis block micronucleus assay to estimate the sensitivity of cells to different agents will be dependent not only on the level of damage and/or repair of that damage but also effects on the cell cycle and the relative distribution of that damage. However, by taking a "holistic" approach to the assay by the measurement of a number of parameters it is possible to obtain a more meaningful understanding of the processes involved in cellular sensitivity. If combined with additional measurements of the cell cycle it might prove a very powerful technique.

With regards to the sensitivity of *xrs-5*, the above approach has proved useful in revealing possible cell cycle related differences in the way mutant and wild-type cells respond to and express damage.

Table 2.1. Summary of the induction of micronuclei in CHO and *xrs-5* cells.

		γ-rays	*PvuII*	Bleomycin[1]	Etoposide	Campto-thecin
Micronucleus induction[2]	a) relative sensitivity	a) 7	a) 2-4	a) 10-100	a) 10	a) 2
	b) shape of dose response.	b) CHO= linear *xrs* = non-linear at high doses	b) CHO = non-linear *xrs*= linear	b) Logarithmic (*xrs* decreases at high dose)	b) non-linear (decrease at high doses)	b) non-Linear (decrease at high doses)
	c) CHO maxMn	c) ≥0.90(±0.08)	c) ≥0.64(±0.04)	c) ≥0.84 (±0.13)	c) =0.97 (±0.13)	c) =0.58 (±0.08)
	d) *xrs* max Mn	d) = 2.2 (±.0.24)	d) ≥0.64(±0.11)	d) =1.70 (±0.14)	d) = 1.15(±0.21)	d) =0.82 (±0.06)
Damage distribution[3]	a) Dispersion	a) CHO = random *xrs*= over-dispersed	a) Over-dispersed	a) Over-dispersed	a) Over-dispersed	a) Over-dispersed
	b) CHO maxMD	b) ≥1.57(±0.03)	b) ≥1.83(±0.08)	b) ≥2.14(±0.11)	b) =2.01(±0.08)	b) =1.76(±0.17)
	c) *xrs* max MD	c) = 3.35(±0.22)	c) ≥2.32(±0.24)	c) ≥2.92(±0.27)	c) =2.58(±0.06)	c) =2.50(±0.22)
	$\frac{MD_{obs}}{MD_{exp}}$ d)CHO	d) = 1.019	d) = 1.325	d) = 1.441	d) = 1.079	d) = 1.190
	e)*xrs*	e) = 1.265	e) = 1.602	e) = 1.242	e) = 1.210	e) = 1.612
Binucleate Index[4]	a) correlation to dose or level of expressed damage	a) CHO = no sig. decrease. *xrs* = not proportional to freq. of Mn	a) CHO =proportional to dose *xrs*= proportional to dose	a) CHO proportional to dose *xrs* = proportional to dose (not correlated to freq. of Mn)	a) CHO no correlation *xrs* = proportional to dose	a) Decrease proportional to dose.
	b) CHO min. BI	b) N.D.[5]	b) N.D.	b) ≤ 4.6%	b) = 5 %	b) = 10%
	c) *xrs-5* min. BI	c) 20%	c) N.D.	c) ≤ 6.0 %	c) = 10%	c) = 22%

1) Bleomycin; only 24 hour incubation results shown.
2) Micronucleus induction a) Relative sensitivity = sensitivity of *xrs-5* cells compared to CHO as estimated by doses required to produce equal numbers of micronuclei per binucleate (after correction for background). b) Shape of dose response refers to increase in micronuclei per binucleate after linear increases in dose of agent. c) and d) MaxMn = maximum frequency of micronuclei per binucleate (after correction for background), where ≥ symbol is used refers to the frequency after the maximum dose applied in these experiments.
3) Damage distribution. a) Dispersion = comparison between expected and observed values of the micronuclei per damaged cell as tested by chi-squared analysis. b) and c)maxMD = maximum frequency of micronuclei per damaged cell, where ≥ symbol is used refers to the frequency after the maximum dose applied in these experiments. d) and e) MD_{obs}/MD_{exp} = the ratio of the observed mean frequency of micronuclei per damaged cell at the maximum mean frequency of micronuclei per binucleate versus the expected value.
4) Binucleate index. a) Correlation of reduction in BI to either to the expressed level of damage or to dose (i.e. independent of expressed levels of damage) or no effect of agent on BI. b) and c) minBI = the minimum value of binucleate index attained, where ≤ symbol is used refers to BI after the maximum dose of agent is applied.
5) ND = not determined.

2.3.3. *Effect of various agents on the response of CHO and xrs-5 to DNA damaging agents.*

2.3.3.1. Effect of 3-aminobenzamide on the response of irradiated CHO and xrs-5 cells.

In order for DNA lesions to be effectively repaired it is important that repair enzymes can identify sites of damage and obtain access to the lesions. As discussed later in Chapter 3; chromatin consists of a complex of proteins and DNA and can exist in varying levels of condensation. The presence of DNA binding proteins and/or supercoils may result in lesions which are inaccessible to repair complexes.

The enzyme poly(ADP-ribose)polymerase (PARP) is a zinc finger protein [Mazan et al., 1989]. It catalyses the covalent attachment of ADP-ribose units from the co-enzyme nicotinamide adenine dinucleotide (NAD^+) to various nuclear receptor proteins including the histones and nuclear lamins [Panzeter et al., 1993; Pedraza-Reyes and Alvarez-Gonzalez, 1990] and also to itself. These polymers may exceed 200 individual ADP-ribose units in length. The addition of poly(ADP-ribose) to proteins alters the affinity of the proteins for DNA and can result in dissociation of all or parts of the proteins [Ahnström and Ljungman 1988; Panzeter et al., 1993]. PARP has been localised predominantly to the nuclear matrix [Kaufmann et al., 1991]. The activity of PARP at the nuclear matrix decreases during DNA synthesis and increases during interphase. This was consistent with the reported role of PARP in the modulation of chromatin-nuclear matrix interactions via poly(ADP-ribose) modification of nuclear lamins A and C [Pedraza-Reyes and Alvarez-Gonzalez, 1990] and other proteins such as topoisomerases I and II [Mattern et al., 1987].

PARP has also been identified as binding to DNA in the vicinity of strand breaks. It then catalyses the polymerisation of (ADP-ribose) on both itself and on chromatin proteins, including histone H1, in the near vicinity to the strand break. The build up of the negatively charged (ADP-ribose) polymers results in a disruption of protein-DNA binding activity of the proteins resulting in displacement of H1 and PARP from the DNA [Ahnström and Ljungman, 1988]. This produces an area of localised decondensation and reveals the strand break. Repair enzymes, such as ligase etc. have access to the lesion and repair may be performed.

3-aminobenzamide (3AB) is a competitive inhibitor of PARP which decreases the rate of poly(ADP-ribose) accumulation on proteins. 3AB has been demonstrated to potentiate the effects of H_2O_2, MMS and γ-irradiation by inhibiting the repair of both SSB and DSB [Cantoni et al., 1989; Ahnström and Ljungman, 1988; Smit and Stark, 1994] and also the strand breaking activities of CPT, and teniposide (VM-26) which are topoI and topoII inhibitors respectively [Mattern et al., 1987]. While it inhibits the repair of methylating and

alkylating agents such as MMS, it has limited effects on the repair of bulky lesions such as pyrimidine dimers produced by UV. The strand break rejoining which 3AB inhibits can be either formed as a direct consequence of damage or through excision repair processes which result in strand breaks [Ahnström and Ljungman, 1988].

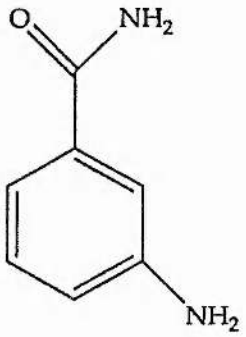

Figure 2.17. Structure of 3-aminobenzamide.

The effects of 3AB on the induction of chromosomal aberrations by X-rays in CHO and *xrs* cells has been examined [Darroudi and Natarajan, 1987a; b]. In these studies it was found that 3AB potentiated the induction of aberrations in G_1 and G_2 cells in irradiated CHO, *xrs-5* and *xrs-6* cells. The potentiation observed was greatest in G_1 irradiated cells with a reduced level of potentiation in the mutants compared to the wild type. However, this potentiation was inversely proportional to X-ray dose. This was attributed to the saturation of the frequency of aberrations at higher doses.[Darroudi and Natarajan, 1987a]. 3AB also enhanced the spontaneous induction of sister chromatid exchanges (SCEs) but not radiation induced SCEs [Darroudi and Natarajan, 1987b]

CHO and *xrs-5* cells were treated in the following experiments with 7 and 1 Gy γ-rays respectively. Various concentrations of 3AB were added post-irradiation to examine for a possible effect of PARP inhibition on the induction of micronuclei. Since agents added to irradiated cells might either affect repair of lesions or expression of damage the 3AB was present for either the initial 2 hours or the entire 24 hours of the experiment.

Figures 2.18 and 2.19 show the results of 3AB on the induction of micronuclei per binucleate, per damaged cell and on the binucleate index. There were no significant effects of 3AB on any of these parameters either in the unirradiated or irradiated samples at either 2 hours or 24 hours exposure to 3AB.

This is in contrast to previous workers who found that 3AB potentiated both the induction of aberrations in CHO and *xrs* cells [Darroudi and Natarajan, 1987a] and repair of DSB in rat thymocytes [Smit and Stark, 1994]. The doses of γ-rays used in the experiments described in this chapter were greater than those used for chromosomal aberration studies and so the saturation effect observed by Darroudi and Natarajan [1987a] may come into effect. The

repair studies of Smit and Stark [1994] were performed at similar doses to those used in this study but repair was only followed over the first hour. The repair may therefore be delayed but not completely blocked by 3AB. The micronucleus assay extends for 24 hours and so aberration causing lesions might be fully repaired in the timescale of these experiments. Treatment of human lymphocytes has, however, shown that micronucleus frequencies can be enhanced by 3AB treatment [Catena et al., 1992] although here 3AB was included in the culture medium both prior to and post-irradiation. The prior treatment with 3AB was avoided in this study due to the possibilty of inhibition of PARP inducing changes in chromatin which would increase the initial level of DNA damage. This would prove deleterious to interpretations of data since both CHO and *xrs* cells apparently exhibit similar levels of damage immediately after irradiation [Kemp et al., 1984, Costa and Bryant, 1991b]. Further work would be necessary to determine the precise role, if any, PARP plays on the repair of DSB and formation micronuclei, and the repair defect observed in *xrs* cells.

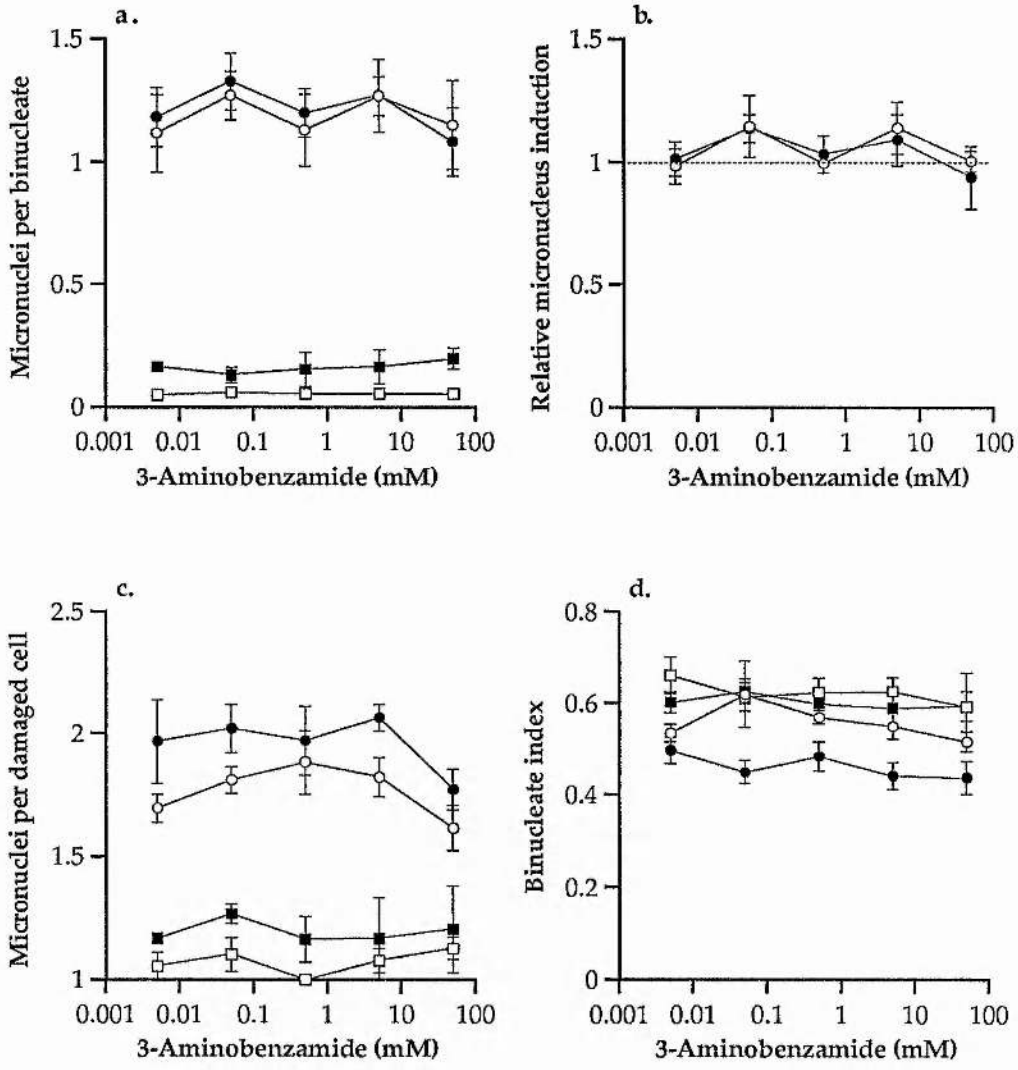

Figure 2.18. Effect of 2 hours exposure to 3-aminobenzamide on unirradiated (□,■) and irradiated (○, ●) CHO (○, □)and *xrs-5* cells (●, ■).
Irradiated samples exposed to 7 (CHO) or 1 Gy (*xrs-5*) ^{137}Cs γ-rays. Error bars represent the standard error of the mean of a minimum of 3 independent experiments.
a) Micronuclei per binucleate cell. Irradiated data corrected by subtraction of unirradiated values. One-way ANOVA indicates no significant effect on the frequency with dose for either the unirradiated (CHO, p=0.960, F=0.19, df=5; *xrs-5*, p=0.932, F=0.25, df=5) or irradiated samples (CHO, p=0.926, F=0.26, df=5; *xrs-5*, p=0.784, F=0.48, df=5).
b) Relative micronucleus induction (relative to unirradiated samples). One-way ANOVA indicates no significant effects with dose (CHO, p=0.436, F=1.04, df=5;*xrs-5*, p=0.621, F=0.72, df=5). GLM analysis indicates no significant differences between the response of CHO and *xrs-5* cells (p=0.981, F=0.14, df=5).
c) Frequency of micronuclei per damaged binucleate cell. One-way ANOVA indicates no significant effect on the frequency with dose (CHO, p=0.565 F=0.81, df=5, *xrs-5*; p=0.996, F=0.07, df=5).
d) Binucleate index. One-way ANOVA indicates no significant decreases with dose for control (CHO, p=0.441, F=1.10, df=5; *xrs-5*, p=0.593, F=0.76, df=5) or irradiated samples (CHO, p=0.630, F=0.71, df=5; *xrs-5*, p=0.645, F=0.68, df=5).

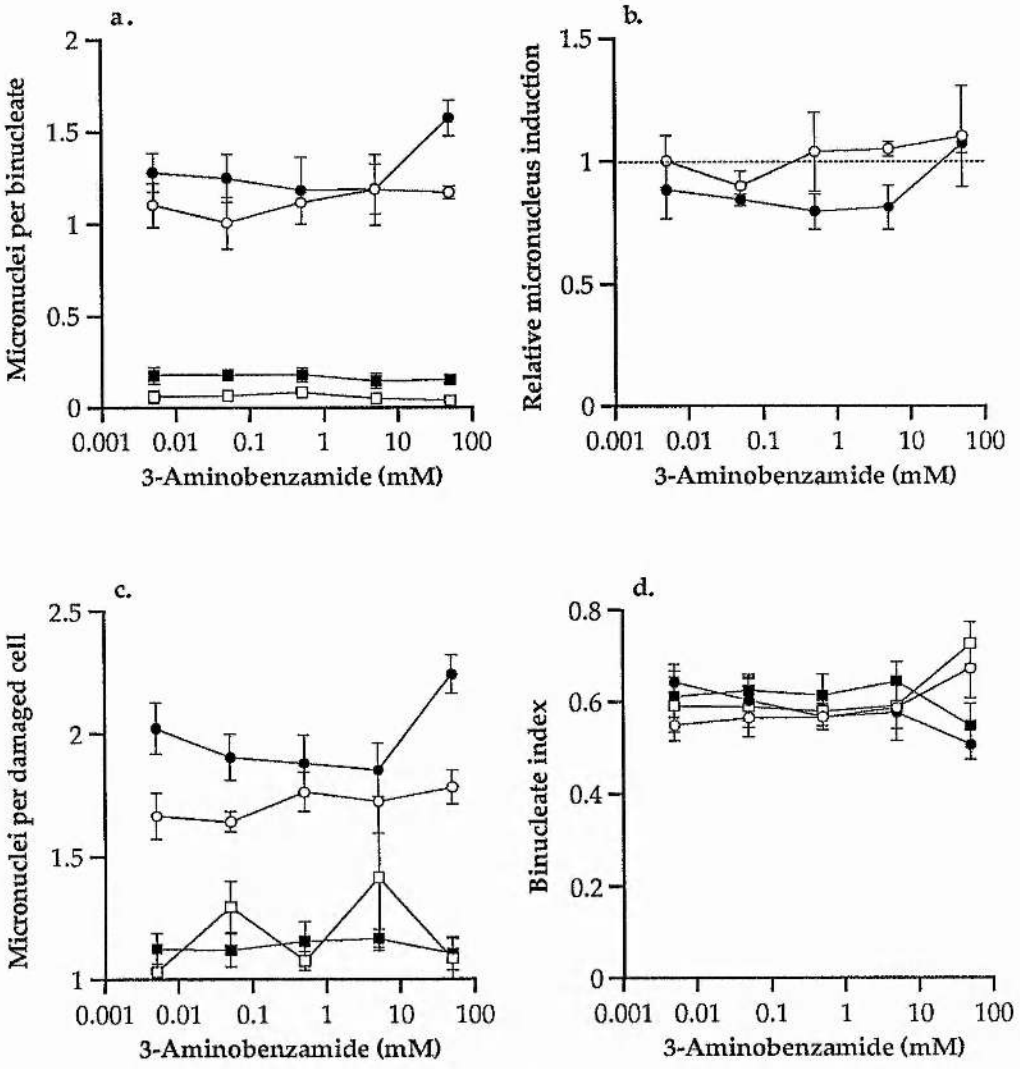

Figure 2.19. Effect of 24 hours exposure to 3-aminobenzamide on unirradiated (□,■) and irradiated (○, ●) CHO (○, □)and *xrs-5* cells (●, ■).
Irradiated samples exposed to 7 (CHO) or 1 Gy (*xrs-5*) ^{137}Cs γ-rays. Error bars represent the standard error of the mean of a minimum of 3 independent experiments.
a) Micronuclei per binucleate cell. Irradiated data corrected by subtraction of unirradiated values). One-way ANOVA indicates no significant effect on the frequency with dose for either the unirradiated (CHO, p=0.567, F=0.81, df=5; *xrs-5*, p=0.960, F=0.19, df=5) or irradiated samples (CHO, p=0.942, F=0.23, df=5; *xrs-5*, p=0.257, F=1.51, df=5).
b) Relative micronucleus induction (relative to unirradiated samples). One-way ANOVA indicates no significant effects with dose (CHO, p=0.884, F=0.33, df=5;*xrs-5*, p=0.086, F=2.55, df=5). GLM analysis indicates no significant differences between the response of CHO and *xrs-5* cells (p=0.705, F=0.59, df=5).
c) Frequency of micronuclei per damaged binucleate cell. One-way ANOVA indicates no significant effect on the frequency with dose for irradiated CHO (p=0.883 F=0.33, df=5) and a significant effect in *xrs-5*; (p=0.05, F=3.10, df=5).
d) Binucleate index. One-way ANOVA indicates no significant decreases with dose for control (CHO, p=0.400, F=1.12, df=5; *xrs-5*, p=0.588, F=0.77, df=5) or irradiated samples (CHO, p=0.123, F=2.19, df=5; *xrs-5*, p=0.339, F=1.27, df=5).

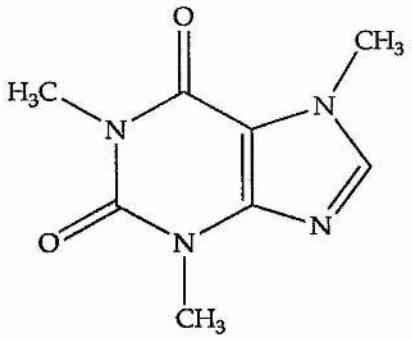

Figure 2.20. Structure of caffeine (1,3,7-trimethylxanthine).

Caffeine (1, 3, 7-trimethylxanthine) acts in a synergistic manner with many-DNA damaging agents. The drug is capable of over-riding the G_2 delay exhibited by many cells in response to ionising radiation. The precise cause of the G_2 block is still uncertain, although protein extracts derived from irradiated mitotic cells exhibit inhibitory activities [Mikkelsen and Gentry, 1992]. The inhibitor is induced by radiation and its induction is prevented by treatment with caffeine. Several candidates for the target of caffeine have been proposed including a cyclin B protease, tyrosine phosphatase $p80^{cdc25}$, cyclic AMP phosphodiesterase, maturation promoting factor (MPF) and other agents involved in the control (via phosphorylation /dephosphorylation of cell cycle proteins) of the transition from G_2 to M phase. Caffeine has also been identified as a topoisomerase II inhibitor *in vitro* and *in vivo* [Warters et al., 1989]. This enzyme has been identified as a requisite for entry into mitosis through its role in permitting condensation of chromosomes [Hirano et al., 1993].

DSB repair is also influenced by the presence of caffeine with repair of radiation induced damage, as measured by neutral filter elution and visco-elastic assays, and is inhibited by caffeine [Rowley and Kort, 1988; Wun and Shafer, 1982]. This inhibition is manifested as an inhibition in the slow component to repair whilst the fast component remains unaffected [Rowley and Kort, 1988]. Similarly, the recoiling of DNA in irradiated cells after irradiation, as measured by nucleoid sedimentation is inhibited by caffeine, possibly through inhibition of topoisomerase II or the presence of non-repaired DSB [Warters et al., 1989].

The resulting decrease in survival of irradiated caffeine treated HeLa cells compared to irradiated controls can be reversed by the liposomal mediated introduction of the bacterial RecA protein [Spivak et al., 1991]. This protein, derived from *Escherichia coli*, is believed to be involved in the repair of DNA damage via recombination events. Introduction of RecA into irradiated cells which were not treated with caffeine had no effect. It was therefore postulated that eukaryotic cells posses a protein similar to RecA which is effective in the

repair of DNA damage. Treatment with caffeine inhibits the pathway involving this protein. The introduction of exogenous, bacterial RecA compensates for this loss.

The possible effect of this DSB repair inhibition and/or cell cycle block inhibition is the reduction in the survival of irradiated cells treated with caffeine [Utsumi and Elkind, 1991]. Enhanced killing occurs because of the conversion of potentially lethal damage to lęthal damage (i.e. inhibition of PLDR).

Darroudi and Natarajan [1987a], examined the influence of caffeine on the production of radiation induced chromosomal aberrations and G_2 blocks in CHO, *xrs-5* and *xrs-6* cells. The relative speed at which irradiated S phase or G_2 phase cells progressed into mitosis in the presence of caffeine was greater in CHO than the two mutants. Caffeine counteracted the G_2 delay in CHO cells and *xrs-5*, but not *xrs-6*, although the *xrs-5* block was significantly less susceptible to caffeine release than the CHO block. Caffeine elevated the levels of chromosomal aberrations in G_2 CHO cells with approximately 1.7-2 fold more aberrations. *Xrs-5* and *xrs-6* cells exhibited virtually no potentiation of aberrations after caffeine treatment.

The defect in *xrs-5* cells may therefore involve the pathway affected by caffeine. As noted above, caffeine inhibits the slow DSB repair pathway. Thus it is the repair of these DSB which appears to be defective in *xrs-5*. Because caffeine also affects cell cycle events it was an interesting agent to examine with the micronucleus assay described in this chapter.

When the effect of caffeine on micronucleus induction per binucleate cell was examined (Figure 2.21a, b) there was a significant increase in the frequency of micronuclei in CHO cells but not in *xrs-5*. This would support the findings of Darroudi and Natarajan [1987a]. After 5 mM caffeine and 7 Gy γ-rays CHO cells expressed 1.67 (± 0.226) fold more micronuclei than cells treated with γ-rays alone. *Xrs-5* cells irradiated with 1 Gy and incubated with 5 mM caffeine expressed only 1.14 (± 0.070) fold more micronuclei. The frequency of micronuclei per damaged cell also increased significantly in a dose dependent manner in both CHO and *xrs-5* (Figure 2.21c). When correlated to the frequency per binucleate (data not shown) the elevation in CHO was observed to match the expected values based on a Poisson distribution of damage. *Xrs-5* values appeared to deviate from this expected distribution. These results would indicate that although caffeine elevated the frequency of micronuclei per binucleate in CHO, this increase followed a random distribution throughout the population of cells, with no particular sub-population exhibiting a differential sensitivity. *Xrs-5* cells, although not producing significantly more micronuclei per binucleate did exhibit a deviation from the random distribution of damage. This would indicate that while a sub-population of cells might expresses more damage this may be counterbalanced by a reduction in another sub-population.

Caffeine was a potent inhibitor of the binucleate index by itself (Figure 2.21d). Both the mutant and wild-type exhibited a dose dependent decrease in the proportion of cells passing through one mitosis in 24 hours (the initial increase in the binucleate index in *xrs-5* and CHO cells at low doses could be attributed to elevated frequency of tetranucleates in these experiments). Any effect that caffeine might have on radiation induced cell cycle delay was not observed, possibly due to any caffeine induced delay masking any such release from the radiation induced delay.

Therefore, caffeine would appear to be limited in its effects on the induction of micronuclei in *xrs-5* cells. This result would reinforce the possibility of *xrs* cells possessing a defect in a repair pathway which can be inhibited by caffeine in normal cells.

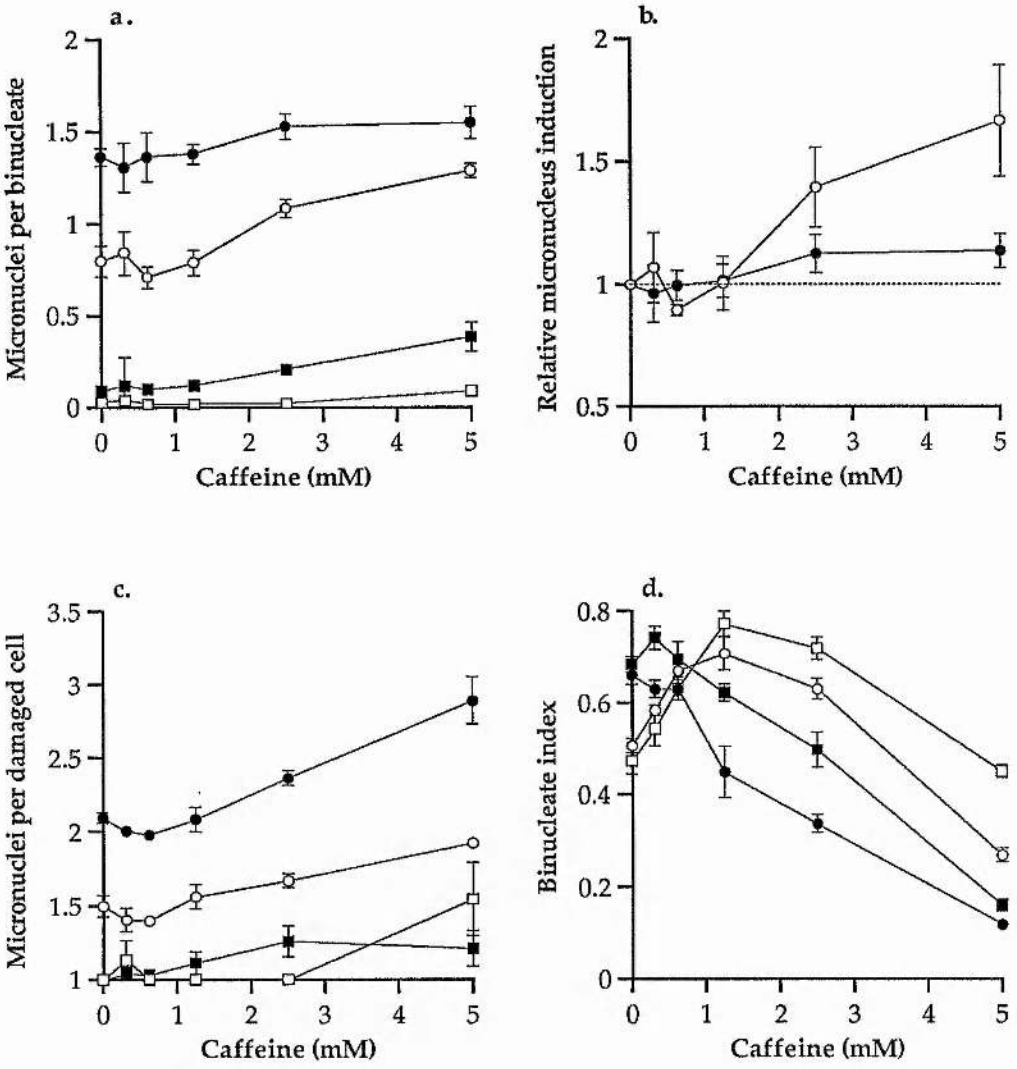

Figure 2.21. Effect of 24 hours exposure to caffeine on unirradiated (□,■) and irradiated (○, ●) CHO (○, □)and *xrs-5* cells (●, ■).
Irradiated samples exposed to 7 (CHO) or 1 Gy (*xrs-5*) ^{137}Cs γ-rays. Error bars represent the standard error of the mean of a minimum of 3 independent experiments.
a) Micronuclei per binucleate cell. Irradiated data corrected by subtraction of unirradiated values. One-way ANOVA indicates significant increases in frequency with dose for both the unirradiated (CHO, p=0.002, F=7.54, df=5; *xrs-5*, p≤0.001, F=10.40, df=5) and irradiated CHO (p=0.001, F=8.97, df=5) but not *xrs-5* (p=0.397, F=1.13, df=5).
b) Relative micronucleus induction (relative to unirradiated samples). One-way ANOVA indicates significant increases with dose for CHO (p=0.013, F=4.75, df=5) but not for *xrs-5* (p=0.474, F=0.97, df=5). GLM analysis indicates no significant differences between the response of CHO and *xrs-5* cells (p=0.085, F=2.23, df=5).
c) Frequency of micronuclei per damaged binucleate cell. One-way ANOVA indicates significant increases in frequency with dose (CHO; p≤0.001 F=10.58, df=5, *xrs-5*; p≤0.001, F=15.19, df=5).
d) Binucleate index. One-way ANOVA indicates significant effects with dose for control (CHO, p≤0.001, F=26.04, df=5; *xrs-5*,p≤0.001, F=63.68, df=5) or irradiated samples (CHO, p≤0.001, F=53.75, df=5; *xrs-5*, p<0.001, F=56.34, df=5).

2.3.3.3. Effect of distamycin-A on the resposne of irradiated CHO and xrs-5 cells.

The possible involvement of nuclear structure [Yasui et al., 1991; 1994; Schwartz et al., 1990, 1993] and/or associated components such as topoisomerase II [Jeggo et al., 1989; Darroudi and Natarajan, 1989b; Warters et al., 1991; Caldecott et al., 1993] in the sensitivity of *xrs* cells implicate DNA-protein interactions as a possible target for the modulation of radiation sensitivity. The binding of proteins to DNA can be modified in a variety of ways including protein phosphorylation, acetylation and DNA methylation, supercoiling and sequence/structure specificities. It is this latter, sequence/structure specificity that is indirectly investigated in this section using the micronucleus assay and the compound distamycin-A (DST).

DST is an antibiotic which binds to the minor-groove of DNA. The drug-DNA interaction widens this groove and induces a bend in the double helix with little or no long-range distortion. DST expresses a specificity for oligo (dA)•oligo (dT) tracts with hydrogen bonding to and electrostatic interactions with DNA bases.

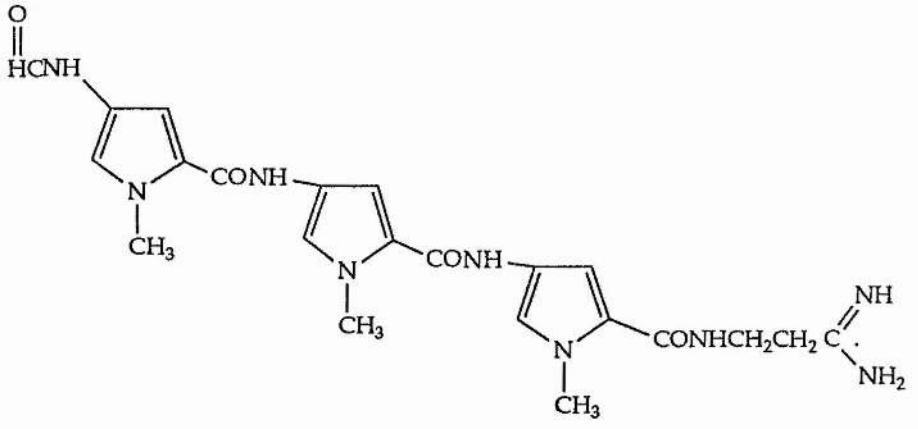

Figure 2.22. Structure of distamycin-A.

Oligo (dA)•oligo (dT) tracts are associated with several important structures of chromatin. These include the scaffold/matrix attachment regions (SARs/MARs) which are involved in the binding of loops of chromatin in eukaryotic cells, and specific histone H1 binding sites [Gasser and Laemmli, 1986; Izaurralde et al., 1988]. The binding of DST to these tracts has been shown to abolish the interaction between SARs and the nuclear scaffold and histone H1 from these and other oligo (dA)•oligo (dT) stretches [Käs et al., 1989; 1993]. The drug also inhibits the activities of topoisomerases I and II and DNA ligases I and III. [Beerman et al., 1991; Käs et al., 1993; Montecucco et al., 1993]. Chromatin is observed to be more accessible to restriction endonucleases in internucleosomal linker regions as a result of unfolding of the chromatin fibre and removal of histone H1. This localised opening of oligo (dA)•oligo (dT) tracts can spread to other regions via disruption of highly cooperative H1-H1 interactions

[Käs et al., 1993]. The removal of H1 from SARs by DST can stimulate the cleavage of SAR DNA by topoisomerase II until levels of DST rise sufficiently to inhibit this activity as well. The inhibitory action of DST on topoisomerase I and II sets it aside from other inhibitors such as etoposide, m-AMSA and camptothecin all of which inhibit the cleavage-rejoining reaction of these drugs resulting in an accumulation of strand breaks [Liu, 1989].

To examine the effect of DST on the radiosensitivity of *xrs-5*, cells were γ-irradiated and incubated with varying concentrations of DST for either 2 or 24 hours post-irradiation. DST was added post-irradiation to specifically examine the effects of the drug on the response to DNA damage rather than any effects that altering protein binding to DNA might have on levels of DNA damage.

The results for a 2 hour incubation with DST revealed no significant effect of the drug either on its own or after irradiation in any of the parameters examined (Figure 2.23).

24 hours incubation with the drug produced different results (Figure 2.24). Treatment with the drug alone produced a slight, but significant increase in the frequency of micronuclei in *xrs-5* cells with the frequency per binucleate rising from the background of 0.15 (± 0.027) to 0.30 (± 0.041) after 100 μg ml^{-1}. This increase was not observed in CHO cells. High doses of DST also produced a reduction in the binucleate indices of both cell lines (Figure 2.24d) with this effect most marked in *xrs-5*. In addition to these effects it should be noted that DST treated cells appeared abnormal at high doses with increased levels of chromatin bridges between cells (not quantified).

The effect of DST on γ-irradiated cells revealed a significant protective action of the drug with regards to micronucleus induction (Figure 2.24a, b). After exposure to 100 μg ml^{-1} DST frequencies of micronuclei per binucleate are decreased from 0.90 (±0.075) to 0.73 (±0.036) in CHO cells and from 1.18 (±0.097) to 0.72 (±0.096) in *xrs-5* cells. It should be remembered that the initial γ-ray dose was 7 Gy for CHO and 1 Gy for *xrs-5* and so this represented only a partial restoration of radioresistance for the mutant.

The distribution of this damage was similar in the two cell lines with only a slight deviation from the expected Poisson distribution (data not shown).

DST also produced a larger reduction in the binucleate indices of both CHO and *xrs-5* in irradiated compared to non-irradiated samples (figure 2.24d). *Xrs-5* would appear to exhibit some resistance to this block to the formation of binucleates but exact comparisons between the two cell lines are difficult to quantify.

Therefore, while DST appeared to reduce the frequency of micronuclei in both CHO and *xrs-5* cells this reduction could not be precisely accounted for from the experiments performed here.

The reduction in induced micronuclei may relate to the corresponding effect on the binucleate indices of the two cell lines indicating that there may be a synergistic effect of irradiation and DST on cell cycle blocks. Damaged cells may be inhibited from passing through into mitosis by the effects of distamycin-A on proteins such as ligases and topoisomerases and any possible influence these proteins have on the repair of DNA damage.

Further work is required to determine whether DST is acting in a positive or negative manner on damaged cells, possibly by DNA repair studies.

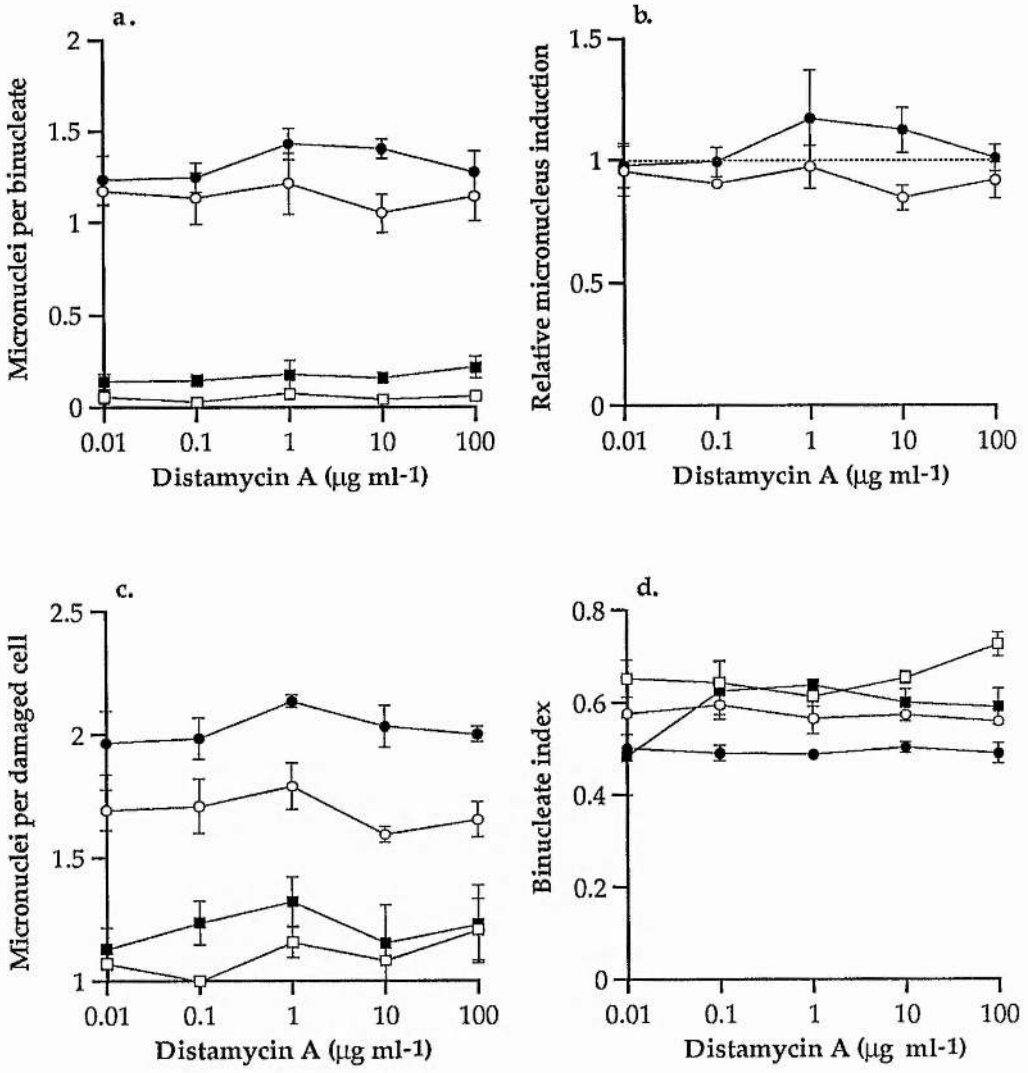

Figure 2.23. Effect of 2 hours exposure to distamycin-A on unirradiated (□,■) and irradiated (○, ●) CHO (○, □)and *xrs-5* cells (●, ■).
Irradiated samples exposed to 7 (CHO) or 1 Gy (*xrs-5*) ^{137}Cs γ-rays. Error bars represent the standard error of the mean of a minimum of 3 independent experiments.
a) Micronuclei per binucleate cell. Irradiated data corrected by subtraction of unirradiated values. One-way ANOVA indicates no significant effects on the frequency with dose for both the unirradiated (CHO p=0.810, F=0.45, df=5; *xrs-5*, p=0.739, F=0.55, df=5) and irradiated (CHO p=0.910, F=0.29, df=5; *xrs-5*, p=0.704, F=0.60, df=5).
b) Relative micronucleus induction (relative to unirradiated samples). One-way ANOVA indicates no significant effects with dose (CHO p=0.634, F=0.70, df=5;*xrs-5*, p=0.696, F=0.61, df=5). GLM analysis indicates no significant differences between the response of CHO and *xrs-5* cells (p=0.594, F=0.75, df=5).
c) Frequency of micronuclei per damaged binucleate cell. One-way ANOVA indicates no significant effects on the frequency with dose (CHO, p=0.613 F=0.73, df=5, *xrs-5*, p=0.774, F=0.50, df=5).
d) Binucleate index. One-way ANOVA indicates no significant effects with dose for either control (CHO, p=0.141, F=1.92, df=5; *xrs-5*, p=0.324, F=1.31, df=5) or irradiated samples (CHO, p=0.518, F=0.88, df=5; *xrs-5*, p=0.908, F=0.29, df=5).

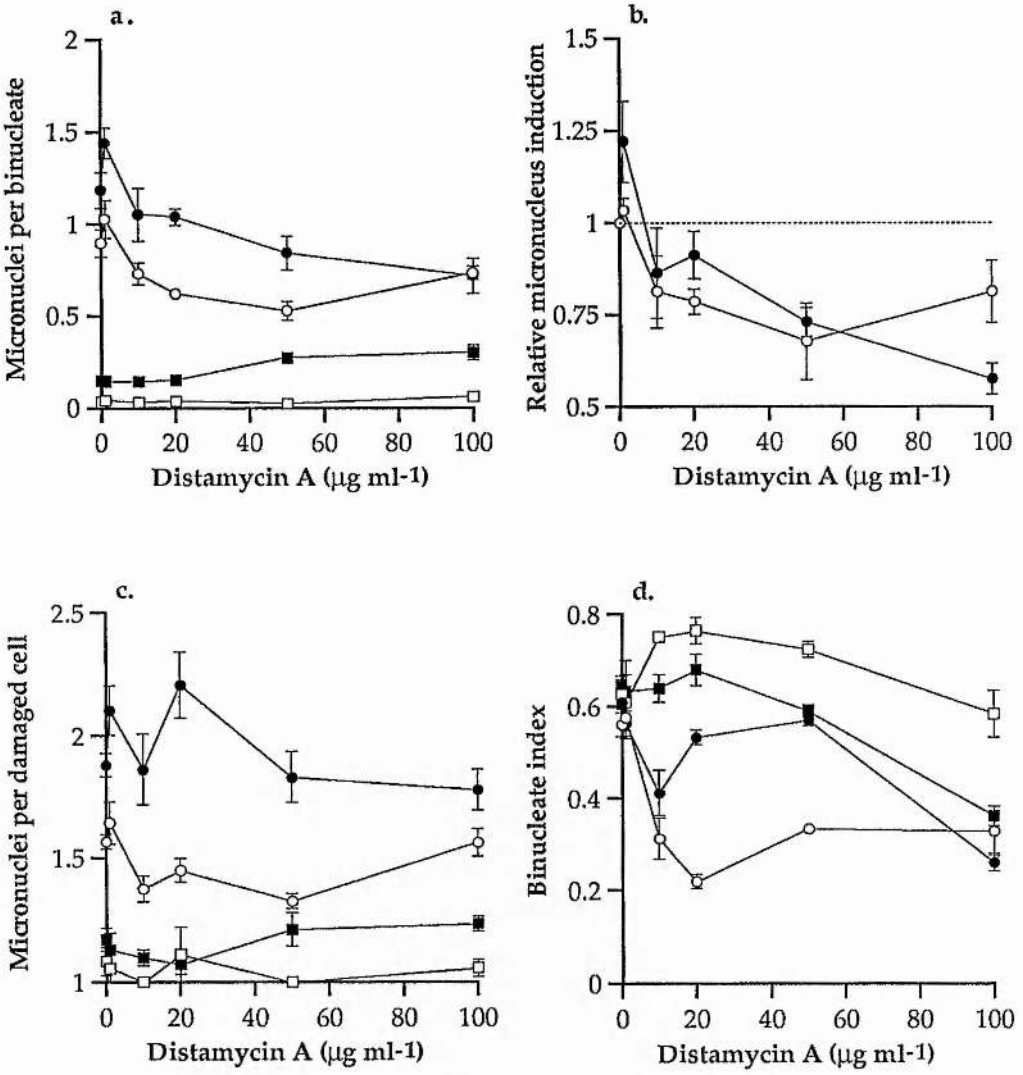

Figure 2.24. Effect of 24 hours exposure to distamycin-A on unirradiated (□,■) and irradiated (○, ●) CHO (○, □)and *xrs-5* cells (●, ■).

Irradiated samples exposed to 7 (CHO) or 1 Gy (*xrs-5*) ^{137}Cs γ-rays. Error bars represent the standard error of the mean of a minimum of 3 independent experiments.

a) Micronuclei per binucleate cell. Irradiated data corrected by subtraction of unirradiated values. One-way ANOVA indicates no significant effect on the frequency with dose for unirradiated CHO ($p=0.176$, $F=1.65$, $df=7$) and a significant decrease in unirradiated *xrs-5* ($p=0.002$, $F=4.98$, $df=7$) and irradiated CHO ($p\leq0.001$, $F=7.03$, $df=7$) and *xrs-5* ($p=0.009$, $F=3.72$, $df=7$).

b) Relative micronucleus induction (relative to unirradiated samples). One-way ANOVA indicates significant decrease with dose for both cell lines (CHO, $p=0.002$, $F=5.10$, $df=7$; *xrs-5*, $p\leq0.001$, $F=6.52$, $df=7$). GLM analysis indicates no significant differences between the response of CHO and *xrs-5* cells ($p=0.196$, $F=1.49$, $df=7$).

c) Frequency of micronuclei per damaged binucleate cell. One-way ANOVA indicates significant decrease in frequency with dose for CHO ($p=0.012$, $F=3.52$, $df=7$) but not *xrs-5* ($p=0.099$, $F=2.03$, $df=7$).

d) Binucleate index. One-way ANOVA indicates significant effects with dose for control (CHO, $p=0.016$, $F=3.30$, $df=7$; *xrs-5*, $p\leq0.001$, $F=9.53$, $df=7$) and irradiated samples (CHO, $p\leq0.001$, $F=15.26$, $df=7$; *xrs-5*, $p<0.001$, $F=7.12$, $df=7$).

2.3.3.4. Effect of okadaic acid on the response of irradiated CHO and xrs-5 cells.

The control of the cell cycle and several related events often involves phosphorylation and dephosphorylation of nuclear proteins [reviewed in Pines and Hunter, 1991; Wollfe, 1991; Pallen et al., 1992; Meek and Street, 1992; Murray 1992]. These events regulate both direct interactions of proteins with DNA and chromatin proteins with each other and indirectly via activation/suppression of kinases/phosphatases themselves. Examples of phosphorylation driven events include phosphorylation of nuclear lamina proteins, resulting in nuclear envelope breakdown at mitosis [Peter et al., 1990; Moir and Goldman, 1993], phosphorylation of histones with a resulting alteration in DNA binding affinities which can result in transcriptional regulation and chromatin condensation [Yasuda et al., 1987; Wolffe, 1991], and activation of topoisomerase II [Cardenas and Gasser, 1993]. The control of phosphorylation events would appear to involve the formation of an equilibrium between phosphorylation by protein kinases and dephosphorylation by protein phosphatases [Cohen, 1989; Black et al., 1991; Lee et al., 1991]. Alterations in the activities of one of these may result in dramatic shifts in this equilibrium. Many phosphorylation pathways involve both negative and positive feedback mechanisms whereby phosphorylation events on only a few proteins can activate rapid phosphorylations/dephosphorylations on many other proteins [Lorca et al., 1992; Hubbard and Cohen, 1993].

Phosphorylation events have been postulated as central to the response of cells to damage by ionising radiation or other DNA damaging agents [Fónagy et al., 1977; Zhivotovsky et al., 1988; Lock and Ross, 1990; Kim et al., 1992; Tauchi et al., 1992; Teale et al., 1992]. This may have the dual effect of both altering chromatin structure and causing cell cycle delays permitting repair of damage.

Agents which affect the phosphorylation status of cells have been described. These include inhibitors of kinases and phosphatases [reviewed in Pardee and Keyomarski, 1992].

One of these,okadaic acid (OA), is a monocarboxylic acid extracted from the common black sponges of the genus *Halichondria* [Bialojan and Takai, 1988]. It is a potent inhibitor of two phosphatases, protein phosphatase 1 (pp1) and protein phosphatase 2a (pp2a). These are both serine/threonine phosphatases and are involved in the regulation of the cell cycle at several points [reviewed in Cohen, 1989]. This inhibition is non-competitive or mixed in nature. OA rapidly stimulates protein phosphorylation in intact cells [Haystead et al., 1989]. The protein kinases responsible for this elevated phosphorylation probably include cyclic-AMP dependent protein kinase, AMP-activated protein kinase, casein kinase II, and glycogen synthase kinase-3 [Haystead et al., 1989]. Pp2a is more readily inhibited by OA than pp1 with 50% inhibition occurring at 0.2 and 20 nM respectively.

The effect on the cell of this elevated phosphorylation status are varied and include premature chromosome condensation of G_2 cells via indirect MPF activation [Yamashita et al., 1990; Gavin et al., 1991], mitotic arrest [Zheng et al., 1991; Ghosh et al., 1992], hepatocyte DNA replication inhibition [Mellgren et al., 1993], and alterations in the transcription and regulation of several oncogenes and tumour suppressor genes such as p53, retinoblastoma protein, c-*fos* and c-*jun*, [Black et al., 1991; Scheidtmann et al., 1991a; b; Schönthal et al., 1991; Ludlow et al., 1993]. These effects may be the cause of the observed tumour promoting activity of OA [Tauchi et al., 1992].

CHO and *xrs-5* cells were exposed in the following experiments to concentrations of OA which reportedly inhibit pp2a but not pp1 [Haystead et al., 1989]. This was for the practical reason of the amount of OA that would be required for pp1 inhibition in the cellular systems examined. Exposure was for either 2 or 24 hours post-irradiation (Figures 2.25. and 2.26.).

No effect of OA could be observed in any parameters examined in either cell line after the two exposure times. This included binucleate indices.

OA has been shown to be ineffective in enhancing transformation of Balb/c 3T3 cells [Tauchi et al., 1992]. In addition, mitotic arrest only occurs at concentrations greater than 1 nM and thus presumably via inhibition of pp1 [Ghosh et al., 1992]. The concentrations used in this study were therefore probably too low to produce effective cell cycle delay. The entry into mitosis may be stimulated by inhibition of pp2a and subsequent premature activation of MPF. The lack of effect of OA on the binucleate index in these experiments may therefore indicate that pp2a does not influence G_2 arrest that might produce extended cell cycle times and a corresponding decrease in binucleate index.

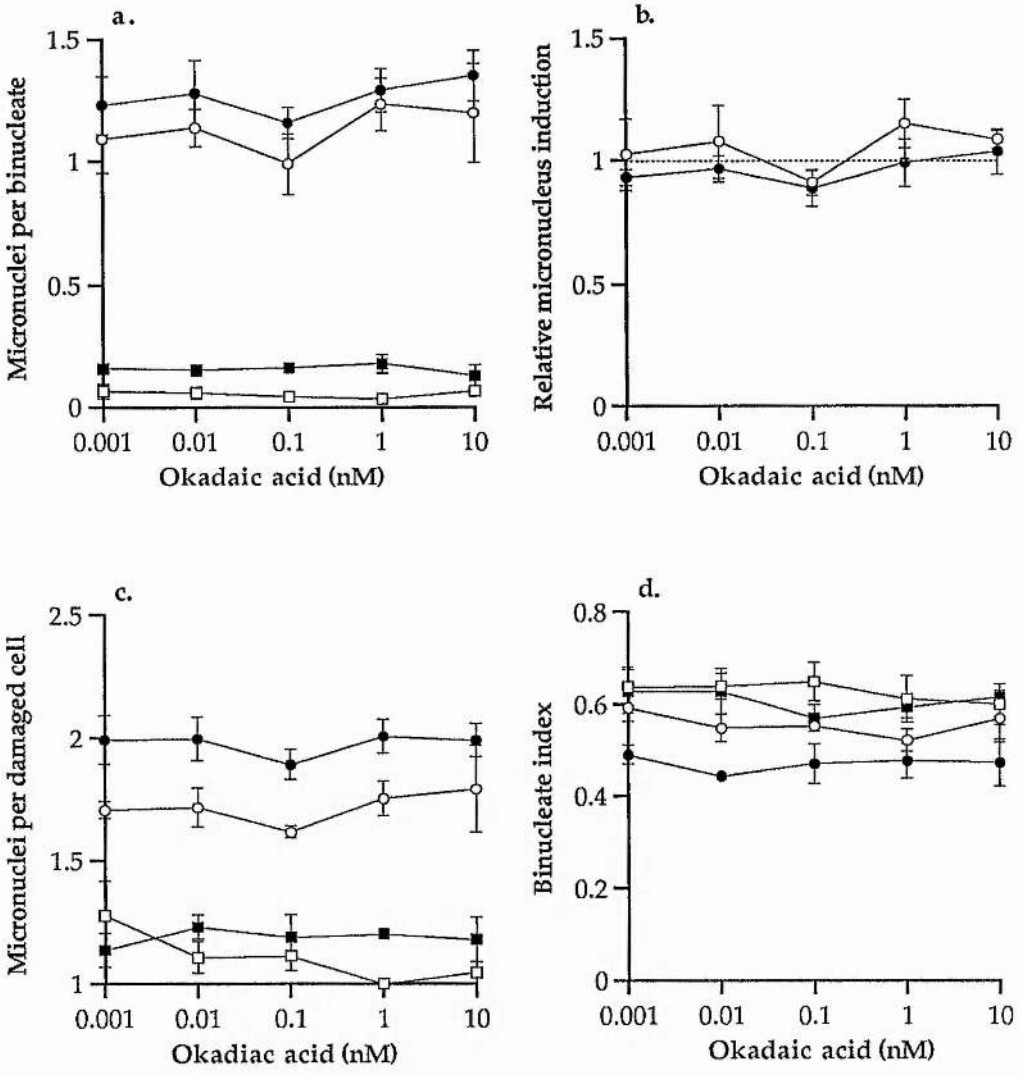

Figure 2.25 Effect of 2 hours exposure to okadaic acid on unirradiated (□,■) and irradiated (○, ●) CHO (○, □)and *xrs-5* cells (●, ■).
Irradiated samples exposed to 7 (CHO) or 1 Gy (*xrs-5*) ^{137}Cs γ-rays. Error bars represent the standard error of the mean of a minimum of 3 independent experiments.
a) Micronuclei per binucleate cell. Irradiated data corrected by subtraction of unirradiated values. One-way ANOVA indicates no significant effects on the frequency with dose for both the unirradiated (CHO, p=0.943, F=0.23, df=5; *xrs-5*, p=0.930, F=0.25, df=5) and irradiated (CHO, p=0.863, F=0.36, df=5; *xrs-5* , p=0.815, F=0.44, df=5).
b) Relative micronucleus induction (relative to unirradiated samples). One-way ANOVA indicates no significant effects with dose (CHO, p=0.625, F=0.71, df=5;*xrs-5*, p=0.682, F=0.63, df=5). GLM analysis indicates no significant differences between the response of CHO and *xrs-5* cells (p=0.934, F=0.25, df=5).
c) Frequency of micronuclei per damaged binucleate cell. One-way ANOVA indicates no significant effects on the frequency with dose (CHO, p=0.794 F=0.47, df=5, *xrs-5*, p=0.617, F=0.73, df=5).
d) Binucleate index. One-way ANOVA indicates no significant effects with dose for either control (CHO, p=0.942, F=0.24, df=5; *xrs-5*, p=0.821, F=0.43, df=5) or irradiated samples (CHO, p=0.659, F=0.66, df=5; *xrs-5*, p=0.915, F=0.28, df=5).

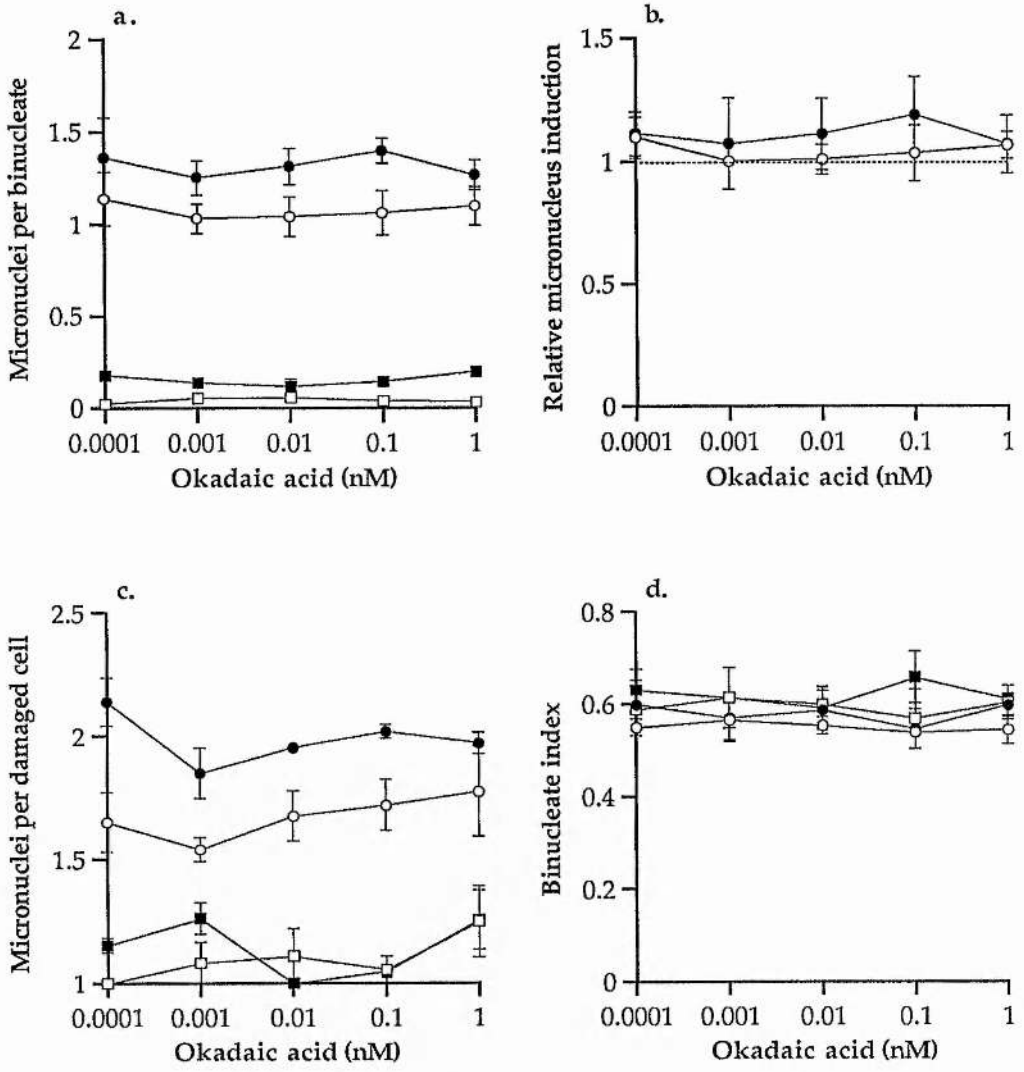

Figure 2.26. Effect of 24 hours exposure to okadaic acid on unirradiated (□,■) and irradiated (○, ●) CHO (○, □)and *xrs-5* cells (●, ■).

Irradiated samples exposed to 7 (CHO) or 1 Gy (*xrs-5*) ^{137}Cs γ-rays. Error bars represent the standard error of the mean of a minimum of 3 independent experiments.

a) Micronuclei per binucleate cell. Irradiated data corrected by subtraction of unirradiated values). One-way ANOVA indicates no significant effects on the frequency with dose for both the unirradiated (CHO, p=0.348, F=1.24, df=5; *xrs-5*, p=0.145, F=2.04, df=5) and irradiated (CHO, p=0.973, F=0.16, df=5; *xrs-5*, p=0.945, F=0.22, df=5).

b) Relative micronucleus induction (relative to unirradiated samples). One-way ANOVA indicates no significant effects with dose (CHO, p=0.861, F=0.37, df=5;*xrs-5*, p=0.941, F=0.23, df=5). GLM analysis indicates no significant differences between the response of CHO and *xrs-5* cells (p=0.966, F=0.18, df=5).

c) Frequency of micronuclei per damaged binucleate cell. One-way ANOVA indicates no significant effects on the frequency with dose (CHO, p=0.748 F=0.53, df=5, *xrs-5*, p=0.411, F=1.10, df=5).

d) Binucleate index. One-way ANOVA indicates no significant effects with dose for either control (CHO, p=0.980, F=0.14, df=5; *xrs-5*, p=0.907, F=0.30, df=5) or irradiated samples (CHO, p=0.503, F=0.92, df=5; *xrs-5*, p=0.938, F=0.24, df=5).

2.3.3.5. Effect of staurosporine on the response of irradiated CHO and xrs-5 cells.

As described above, many cellular processes involve phosphorylation / dephosphorylation pathways. Protein kinases are responsible for the phosphorylation side of the equilibrium produced in conjunction with phosphatases [Cohen, 1989; Meek and Street, 1992]. Many protein kinases have been identified which are regulated during the cell cycle. These form parts of phosphorylation pathways and cascades with one protein kinase activating a whole series of downstream events including other kinases and phosphatases.

Staurosporine (STP) is a microbial alkaloid derived from *Streptomyces* sp. with anti-fungal activities. It is a non-competitive inhibitor of a wide range of protein kinases including phospholipid/Ca^{++} dependent protein kinase (protein kinase C; PKC), cyclic-AMP dependent protein kinase (protein kinase A; PKA) [Tamaoki et al., 1986], cyclic-GMP dependent protein kinase, tyrosine protein kinase, calcium/calmodulin-dependent protein kinase, $p34^{cdc2}$/cyclins and $p33^{cdk2}$/cyclin A kinase [Th'ng et al., 1994]. STP is a more potent inhibitor than other PKC inhibitors such as chlorpromazine, terifluorperazine and polymixin B which are all competitive inhibitors. STP also does not inhibit binding of phorbol esters which are recognised activators of PKC activity.

Incubation of cells with STP produces an inhibition of growth which is dependent on both STP concentration and length of exposure. 100% inhibition of HeLa S3 cells was observed at concentrations > 100 ng ml^{-1} after 1 hour and > 1 ng ml^{-1} after 72 hours exposure to the drug [Tamaoki et , 1986].

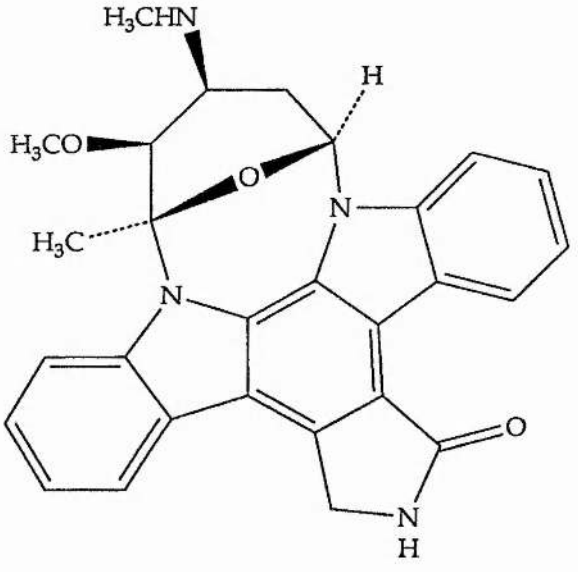

Figure 2.27. Structure of staurosporine. [Redrawn from Tamaoki et al., 1986].

This growth inhibitory effect is probably related to effects staurosporine has on the cell cycle and also toxic effects. STP, in doses of 1-10ng ml^{-1} has been demonstrated to arrest non-

transformed cells at G_1, having no effect on many transformed cells. Higher doses (50-75 ng ml^{-1}) arrested cells in both G_1 and G_2 (G_2 only for transformed cells). STP also induced decondensation of chromosomes in metaphase arrested cells via a decrease in phosphorylation of histones H1 and H3 by their respective kinases [Th'ng et al., 1994]. In addition to this cell cycle arrest STP also produced apoptotic death in a number of cell lines in concentrations of >0.47 ng ml-1 [Bertrand et al., 1994; Jarvis et al., 1994]. This would indicate regulation of protein kinases in the activation of programmed cell death.

CHO and *xrs-5* cells were incubated with varying concentrations of STP for either 2 hours (Figure 2.27) or 24 hours (Figure 2.28) post-irradiation. No significant effect was observed in irradiated and unirradiated cells in either the frequency of micronuclei or the binucleate index after 2 hours incubation. The doses used in the 2 hour incubations covered both the concentrations required to produce G_1 and G_2 blocks. Although there was a slight increase in the binucleate index in unirradiated *xrs-5* cells and a slight increase in irradiated CHO cells at doses > 1 ng ml^{-1} these effects were not significant. This would indicate that 2 hours is an insufficient time for any significant cell cycle effects to occur.

24 hour incubations were performed with lower doses of STP ($\leq$ 5 ng ml^{-1}). There was no significant effect STP on its own (Figure 2.28a-d). In irradiated cells (Figure 2.28a) STP produced a significant effect on the frequency of micronuclei per binucleate in CHO cells but not *xrs-5*. At 1.75 ng ml^{-1} the frequency decreased. This was followed by an increase at higher doses. However, after corrections for the effect of STP on unirradiated cells (Figure 2.28b) the significance of the CHO results was lost. This also resulted in no significant differences in the micronucleus between CHO and *xrs-5* as estimated by a two-way analysis of variance of the relative micronucleus induction. The distribution of the damage in both cell lines did not deviate significantly from the Poisson (data not shown). Therefore any possible difference in the response of these two cell lines is uncertain.

24 hour incubations with STP again did not produce significant differences in the binucleate index (Figure 2.28d). The doses examined in these experiments would be expected to produce G_1 arrest [Tamaoki, 1986; Th'ng et al., 1994] . That no decrease in the binucleate index could be observed might indicate that any such block occurs only after cells have passed through one cell cycle after the addition of the drug. Cells which are positioned prior to G_1 checkpoint prior to the addition of STP may be blocked but the proportion of the whole population that these cells represent may be too small to be detected by this technique.

The micronucleus assay, as performed in the above experiments, does not take into account the possibilty of the removal of cells by cellular death, either apoptotic or otherwise. Only cells which are attached to the tissue-culture plates at the end of the experiment are scored.

Therefore, if STP is producing significant levels of cell death then this may be the cause of the inconclusive results obtained in these experiments.

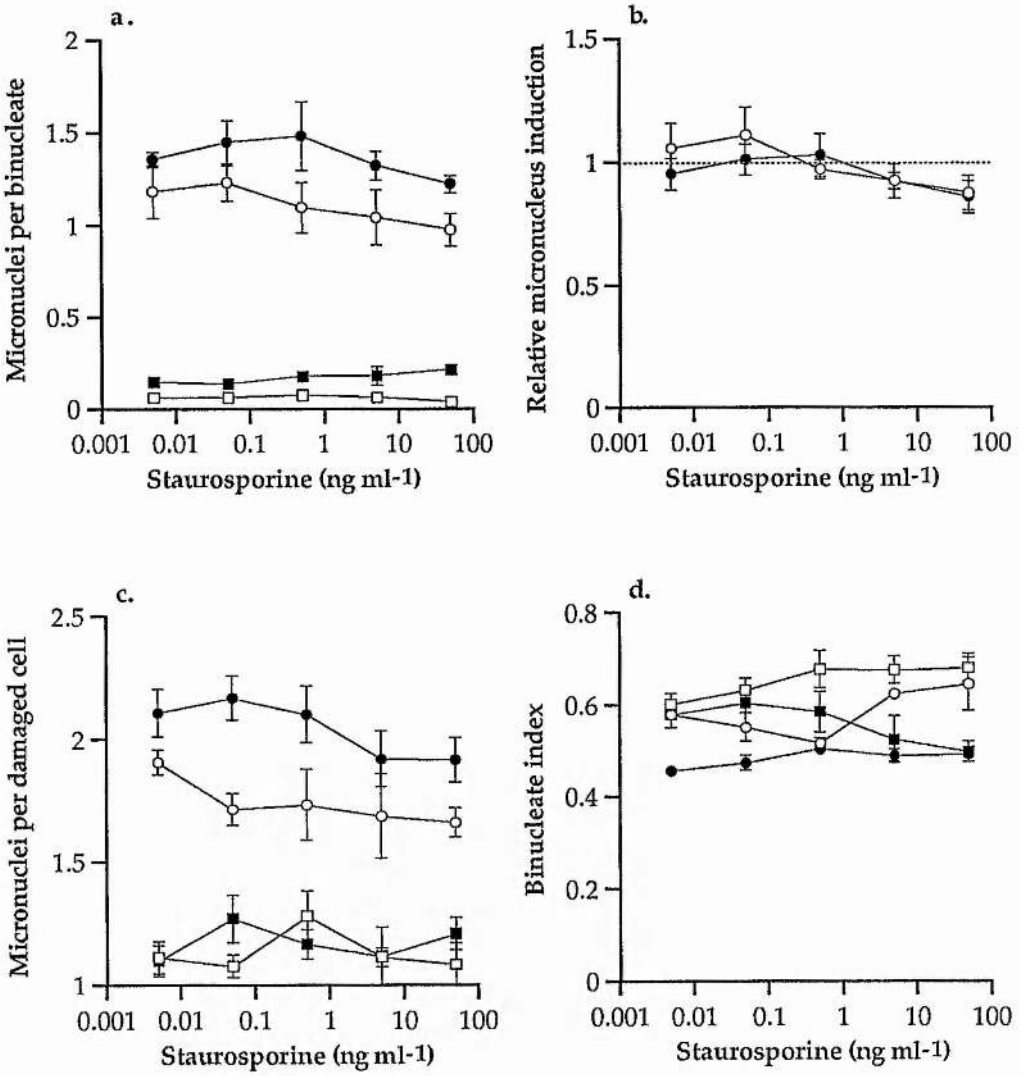

Figure 2.28. Effect of 2 hours exposure to staurosporine on unirradiated (□,■) and irradiated (○, ●) CHO (○, □)and *xrs-5* cells (●, ■).
Irradiated samples exposed to 7 (CHO) or 1 Gy (*xrs-5*) ^{137}Cs γ-rays. Error bars represent the standard error of the mean of a minimum of 3 independent experiments.
a) Micronuclei per binucleate cell. Irradiated data corrected by subtraction of unirradiated values. One-way ANOVA indicates no significant effects on the frequency with dose for both the unirradiated (CHO, p=0.805, F=0.45, df=5; *xrs-5*, p=0.463, F=0.99, df=5) and irradiated (CHO, p=0.729, F=0.56, df=5; *xrs-5*, p=0.505, F=0.91, df=5).
b) Relative micronucleus induction (relative to unirradiated samples). One-way ANOVA indicates no significant effects with dose (CHO, p=0.326, F=1.30, df=5;*xrs-5*, p=0.376, F=1.18, df=5). GLM analysis indicates no significant differences between the response of CHO and *xrs-5* cells (p=0.820, F=0.43, df=5).
c) Frequency of micronuclei per damaged binucleate cell. One-way ANOVA indicates no significant effects on the frequency with dose (CHO, p=0.689 F=0.62, df=5, *xrs-5*, p=0.324, F=1.31, df=5).
d) Binucleate index. One-way ANOVA indicates no significant effects with dose for either control (CHO, p=0.384, F=1.13, df=5; *xrs-5*, p=0.494, F=0.93, df=5) or irradiated samples (CHO, p=0.064, F=2.85, df=5; *xrs-5*, p=0.411, F=1.10, df=5).

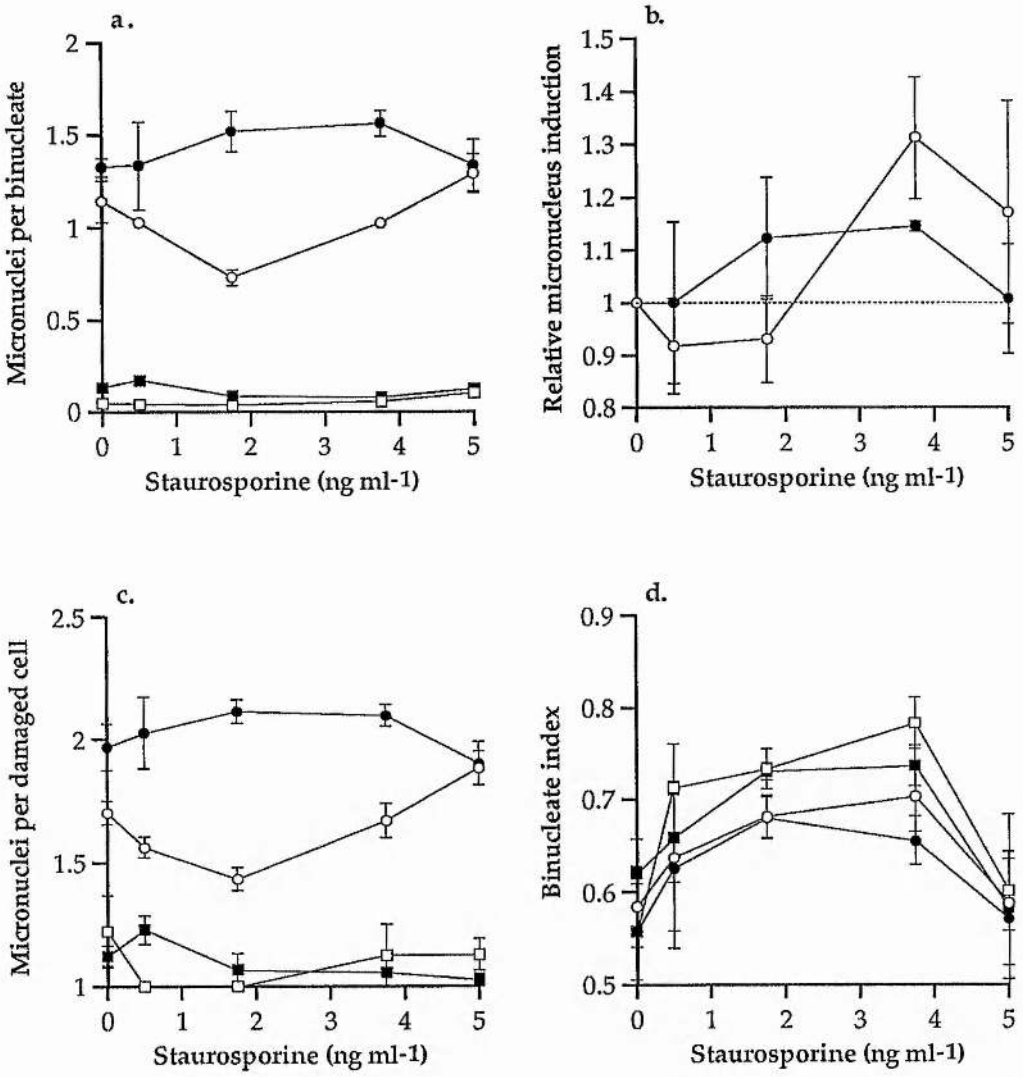

Figure 2.29. Effect of 24 hours exposure to staurosporine on unirradiated (□,■) and irradiated (○, ●) CHO (○, □)and *xrs-5* cells (●, ■).

Irradiated samples exposed to 7 (CHO) or 1 Gy (*xrs-5*) ^{137}Cs γ-rays. Error bars represent the standard error of the mean of a minimum of 3 independent experiments.

a) Micronuclei per binucleate cell. Irradiated data corrected by subtraction of unirradiated values. One-way ANOVA indicates no significant effects on the frequency with dose for unirradiated samples (CHO, p=0.189, F=1.66, df=7;*xrs-5*, p=0.058, F=2.54, df=7) or irradiated samples *xrs-5* (p=0.847, F=0.46, df=7) but a significant increase in irradiated CHO (p=0.004, F=4.96, df=7).

b) Relative micronucleus induction (relative to unirradiated samples). One-way ANOVA indicates no significant effects with dose (CHO, p=0.067, F=2.43, df=7;*xrs-5*, p=0.886, F=0.40, df=7). GLM analysis indicates no significant differences between the response of CHO and *xrs-5* cells (p=0.573, F=0.83, df=7).

c) Frequency of micronuclei per damaged binucleate cell. One-way ANOVA indicates a significant effect on the frequency with dose for CHO (p=0.033 F=2.98, df=7) but not *xrs-5* (p=0.887, F=0.40, df=7).

d) Binucleate index. One-way ANOVA indicates no significant effects with dose for either control (CHO; p=0.185, F=1.68, df=7; *xrs-5*; p=0.601, F=0.80, df=7) or irradiated samples (CHO; p=0.274, F=1.39, df=7; *xrs-5*; p=0.549, F=0.87, df=7).

2.3.3.6. Effect of T4 DNA ligase on irradiated and PvuII treated CHO and xrs-5 cells.

The structure of DSBs may play an important part in the mechanisms by which cells repair this damage. Ionising radiation and agents such as bleomycin produce a wide range of damage which, in addition to cleaving the phosphodiester back bone of DNA, can also produce damage to the bases and sugars of DNA. For example; a common strand break end-structure that is observed with BLM and ionising radiation are 3'phosphoglycolates and 5' phosphate groups at either end of the break. These result from damage to the deoxyribose moiety which produces cleavage of the sugar ring structure and also base loss. These "dirty" structures compare with so called "clean" DSB whereby only the phosphodiester backbone is cleaved to produce 3' phosphates and 5' hydroxyl groups. In order to reproduce the correct DNA structure the former damage requires processing of the ends, including excision of the phosphoglycolate moiety and re-synthesis of the subsequent missing base pairing. In contrast, "clean" breaks can be repaired, *in vitro*, by simple ligation reactions by DNA ligases in an ATP dependent reaction.

To examine whether the DNA repair defect in *xrs-5* resulted from a deficiency in processing of "dirty" ends or from a lack of endogenous ligase activity experiments were attempted whereby exogenous DNA ligase (T4 bacteriophage ligase) was introduced into cells via SLO mediated poration. DNA damage was introduced either by γ-irradiation or by the co-introduction of the restriction endonuclease *PvuII* along with the T4 DNA ligase. T4 DNA ligase introduced by osmolytic shock along with *PvuII* has been shown to significantly increase cell survival of C3H10T1/2 cells [Durante et al., 1991]. This occurred as a result of an increase in potentially lethal damage repair.

Figure 2.30 shows the frequency of micronuclei produced in CHO and *xrs-5* cells by 4 Gy and 0.5 Gy respectively (approximately equi-clastogenic doses). Although there was an apparent rise in micronucleus frequency in *xrs-5* and a reduction in CHO; neither of these were significant compared to the control values. There was no significant effect of T4 ligase on the distribution of damage either relative to dose (Figure 2.30c) or to the frequency of micronuclei per binucleate (data not shown) or the binucleate indices of the two cell lines (Figure 2.30d).

From these results it would appear that T4 ligase has no effect on the response of CHO or *xrs-5* to γ-rays. This may be due to insufficient levels entering the cells or rapid degradation of T4 ligase occurring between introduction and irradiation. Alternatively, since the predominant types of DSB end structures caused by ionising radiations are "dirty" then the repair of these may involve processing followed by ligation. The ligation step may not be affected by exogenous ligase.

Exposure of CHO and *xrs-5* cells to BLM as opposed to γ-rays similarly failed to show any effect of T4 ligase. Since valid statistical analysis could not be performed on this data due to lack of repeats (CHO = 1 experiment, *xrs-5* = 2 experiments) this data is not shown.

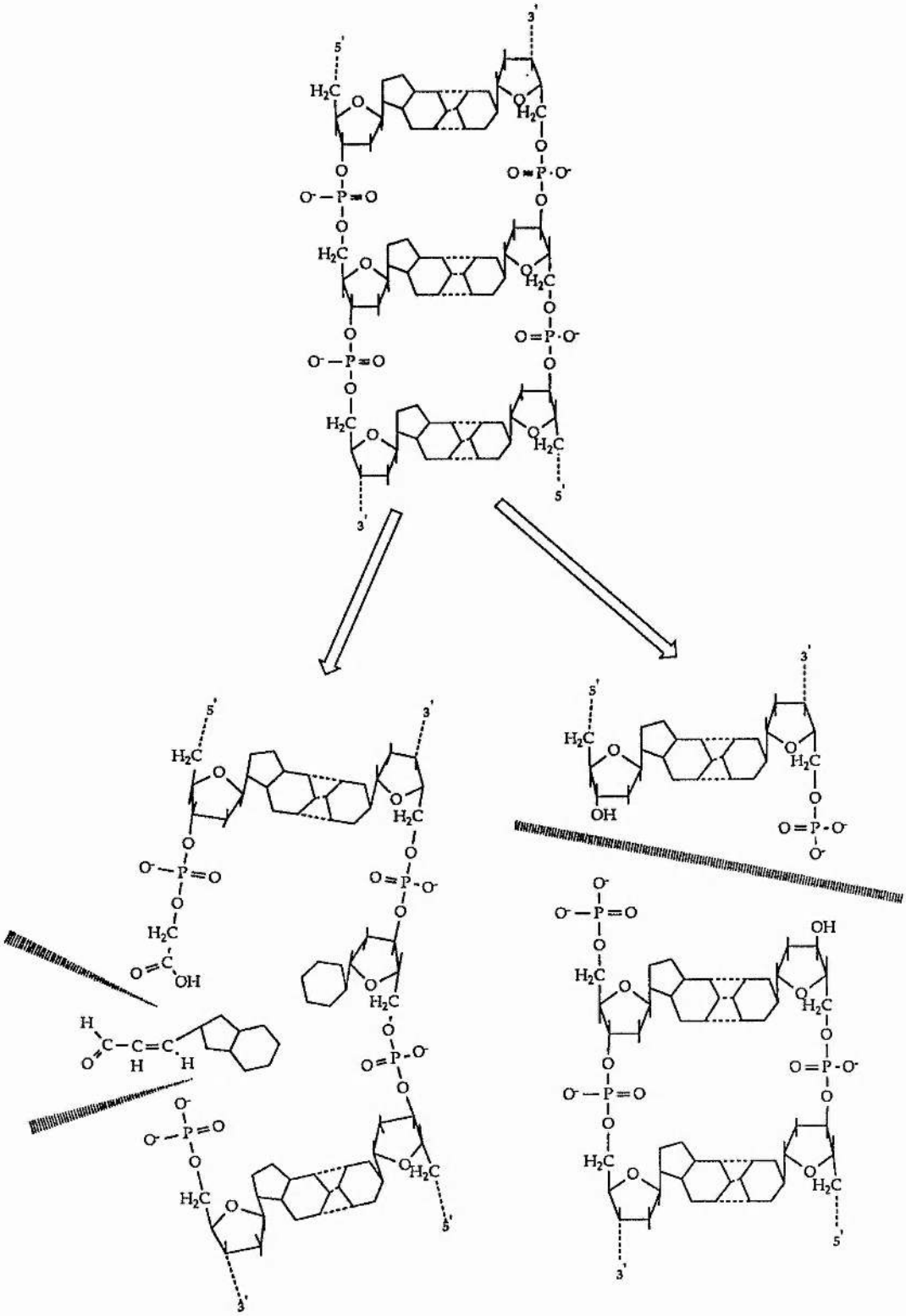

"Dirty" ended SSB
(3'-phosphoglycolate)
e.g. Ionising radiation
Bleomycin

"Clean" ended DSB
e.g. Ionising radiation
Restriction endonucleases

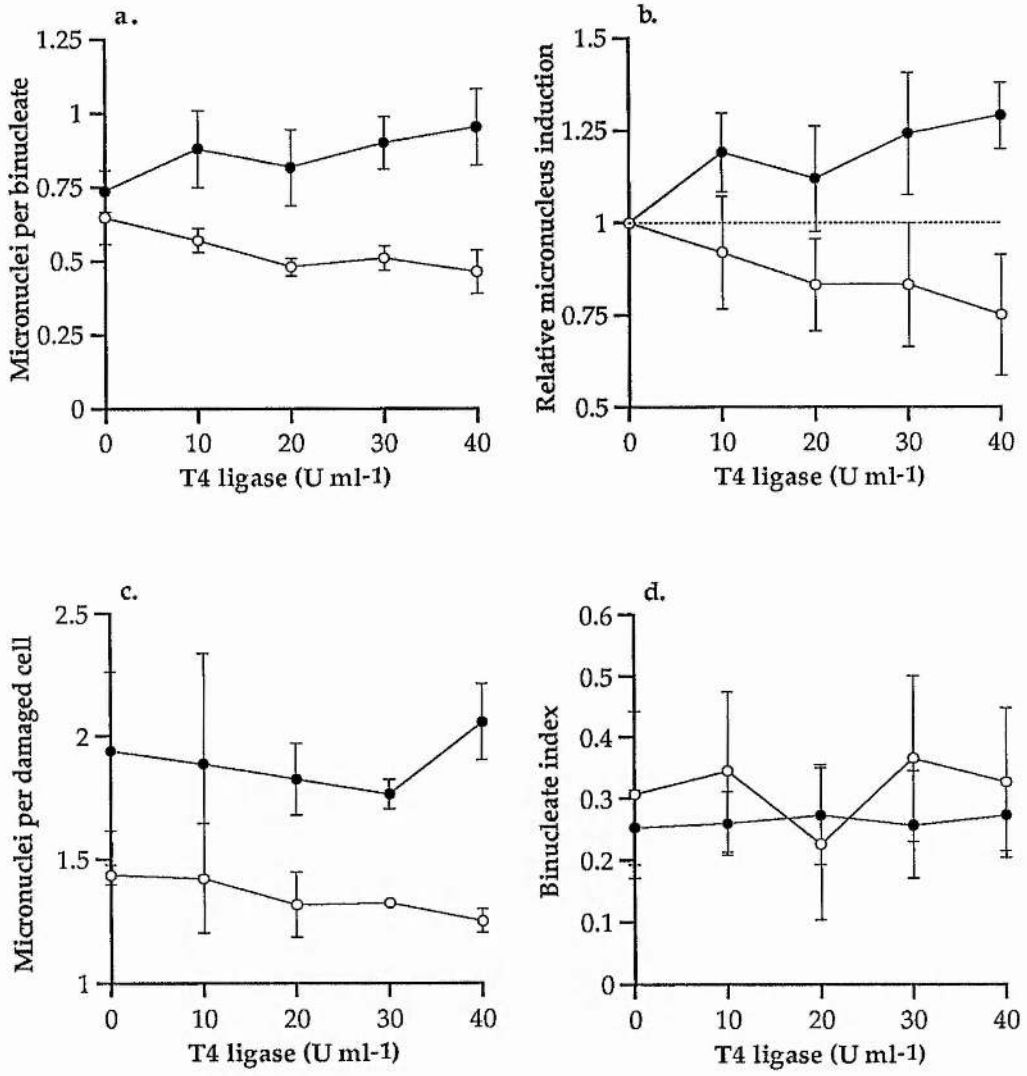

Figure 2.30. Effect of the streptolysin-O mediated introduction of T4 DNA ligase on irradiated CHO (○)and *xrs-5* cells (●).

Irradiated samples exposed to 4 (CHO) or 0.5 Gy (*xrs-5*) ^{137}Cs γ-rays. Error bars represent the standard error of the mean of a minimum of 3 independent experiments.

a) Micronuclei per binucleate cell. Irradiated data corrected by subtraction of unirradiated control. One-way ANOVA indicates no significant effects on the frequency with dose for (CHO; p=0.297, F=1.44, df=4) or *xrs-5* (p=0.702, F=0.55, df=4).

b) Relative micronucleus induction (relative to unirradiated samples). One-way ANOVA indicates no significant effects with dose (CHO, p=0.749, F=0.48, df=4;*xrs-5*, p=0.460, F=0.98, df=4). GLM analysis indicates no significant differences between the response of CHO and *xrs-5* cells (p=0.317, F=1.27, df=4).

c) Frequency of micronuclei per damaged binucleate cell. One-way ANOVA indicates no significant effects on the frequency with dose (CHO, p=0.765 F=0.46, df=4, *xrs-5*, p=0.945, F=0.18, df=4).

d) Binucleate index. One-way ANOVA indicates no significant effects with dose for either CHO (p=0.966, F=0.13, df=4) or *xrs-5* (p=0.999, F=0.02, df=4).

Experiments with T4 DNA ligase in conjunction with *PvuII* produced contradictory results. Figure 2.31 shows the results from three sets of experiments. Figure 2.31a and 2.31b show the effect of varying concentrations of T4 ligase on the micronucleus induction caused by the introduction of unit amounts of *PvuII*. One set of results(fig. 2.31.a.) resulted in a decrease in the levels of micronuclei in both CHO and *xrs-5* cells. This is the result which would be expected from the results of Durante et al., [1991]. The decrease was similar in both CHO and *xrs-5* and thus it would appear from these experiments that the defect in *xrs-5* is not one of a defect in ligase activity but of a prior processing step [Bryant and Johnston, 1993]. However, when it was attempted to repeat this set of experiments (Figure 2.31b) no such decrease was observed, with CHO actually expressing an elevation in frequency. To determine whether this was the result of the increased concentrations of *PvuII* used in the second set of experiments the third set of experiments (Figures 2.31c and d) examined the effect of varying the concentration of *PvuII* while maintaining a constant concentration (40 U ml^{-1}) of T4 ligase. Here no apparent effect of T4 ligase could be observed in either CHO or *xrs-5*. This lack of reproducability means that no further analysis has been perfomed on this data. The precise cause of this non-reproducability has not been elucidated. The first set of experiments were performed at the same time, and with the same batches of enzymes as the γ-ray experiments described above. In subsequent experiments the supplier of enzymes was changed. The results of both the γ–ray experiments and restriction endonuclease experiments must therefore be treated with extreme caution.

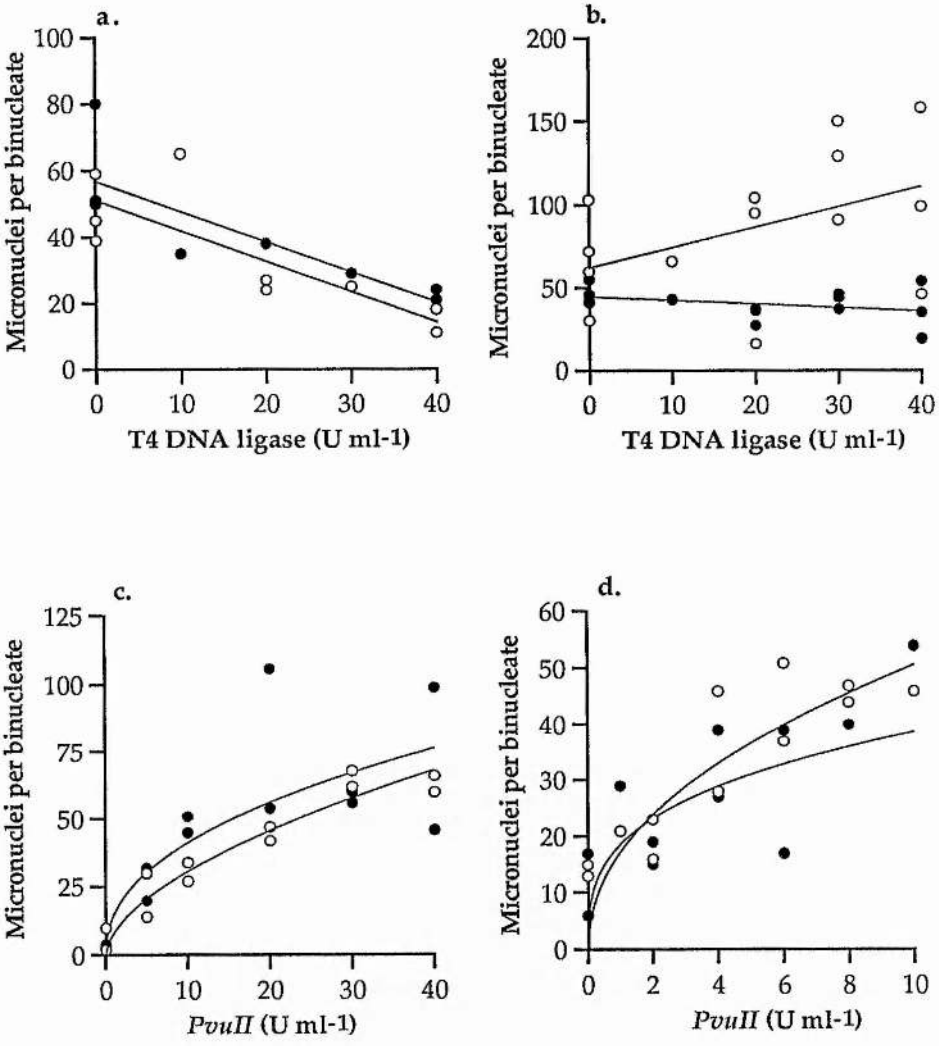

Figure 2.31. Effect of the streptolysin-O mediated introduction of T4 DNA ligase and *PvuII* on CHO and *xrs-5* cells . Data points represent independent values. Results pooled from 1-2 independent experiments.

a), b). T4 ligase dose response. Graphs represent the frequency of micronuclei per binucleate (not corrected for background) after treatment with *PvuII* introduced concommitantly with varying units of T4 DNA ligase. a) CHO (○) = 30 U ml^{-1} and *xrs-5* (●) = 7.5 U ml^{-1}. b) CHO = 40 U ml^{-1}, *xrs-5* = 10 U ml^{-1}.

c), d) *PvuII* dose response. c) CHO. d) *xrs-5*. Graphs represent the frequency of micronuclei per binucleate (not corrected for background) after treatment with (●) and without (○) 40 U ml^{-1} T4 ligase concommitantly with varying units of *PvuII*.

2.3.3.7. Effect of nuclear extract on the response of CHO and xrs-5 cells.

Chapter 4 of this thesis describes experiments performed on nuclear extracts derived from the two cell lines CHO and *xrs-5*. The original aims for the extraction of nuclear proteins had been to complement the radiation sensitivity of *xrs-5* by the introduction of protein extracts into irradiated cells using streptolysin-O (SLO). Complementation of xeroderma pigmentosum (XP) cells has been performed by the introduction of cell free extracts [Wood et al., 1988]. The protein extracts described in the following experiments were obtained by elution with a variety of salt concentrations of nuclei released by cell homogenisation. The following experiments described in this chapter were preliminary experiments to determine if there was any effect of these extracts could be observable on the induction of micronuclei by bleomycin. BLM was chosen as the clastogenic agent because of the failure of the radiation source at the time of the experiments. Entry of the nuclear proteins was facilitated by SLO poration as described above. Cells were exposed to the extracts and BLM added 30 minutes later. This time interval allowed resealing of the pores produced by SLO and allowed for entry of proteins into the nucleus. Although it would also permit degradation of proteins within the cell it was preferable that the proteins be present during the period of damage.

Figure 2.32. shows the results of the exposure of *xrs-5* cells to one such series of extracts and 1 $\mu g\ ml^{-1}$ BLM. The precise procedure for extraction of the proteins is described in full in chapter 4. Briefly, the extracts examined were obtained by stepwise exposure of washed nuclei to 420 mM KCl, 600 mM KCl or 6 M urea. After each extraction step the nuclei were spun down and washed three times in the relevant extraction buffer. These supernatants were pooled and concentrated by centrifugal ultrafiltration (10 kDa exclusion limit Amicon-10 filters). Prior to poration the buffers were changed for HBSS, again by ultrafiltration (see procedure for restriction endonuclease purification, Section 2.2.3). During this procedure it was observed that precipitation of proteins occurred, particularly from the 6M urea fraction. These were removed by centrifugation. 20 $\mu g\ ml^{-1}$ of protein was used to treat the cells.

There was no significant effect of the proteins on either the frequencies of micronuclei or the binucleate indices. The reason for this could be one of many including insufficient protein, denaturation/degradation during the experiment (protease inhibitors were removed prior to poration into cells), proteins not entering the nucleus or simply that the protein extracts did not contain an *xrs* complementing activity. It was decided that further characterisation and possible purification of nuclear proteins was desirable prior to further attempts at cell free complementation experiments.

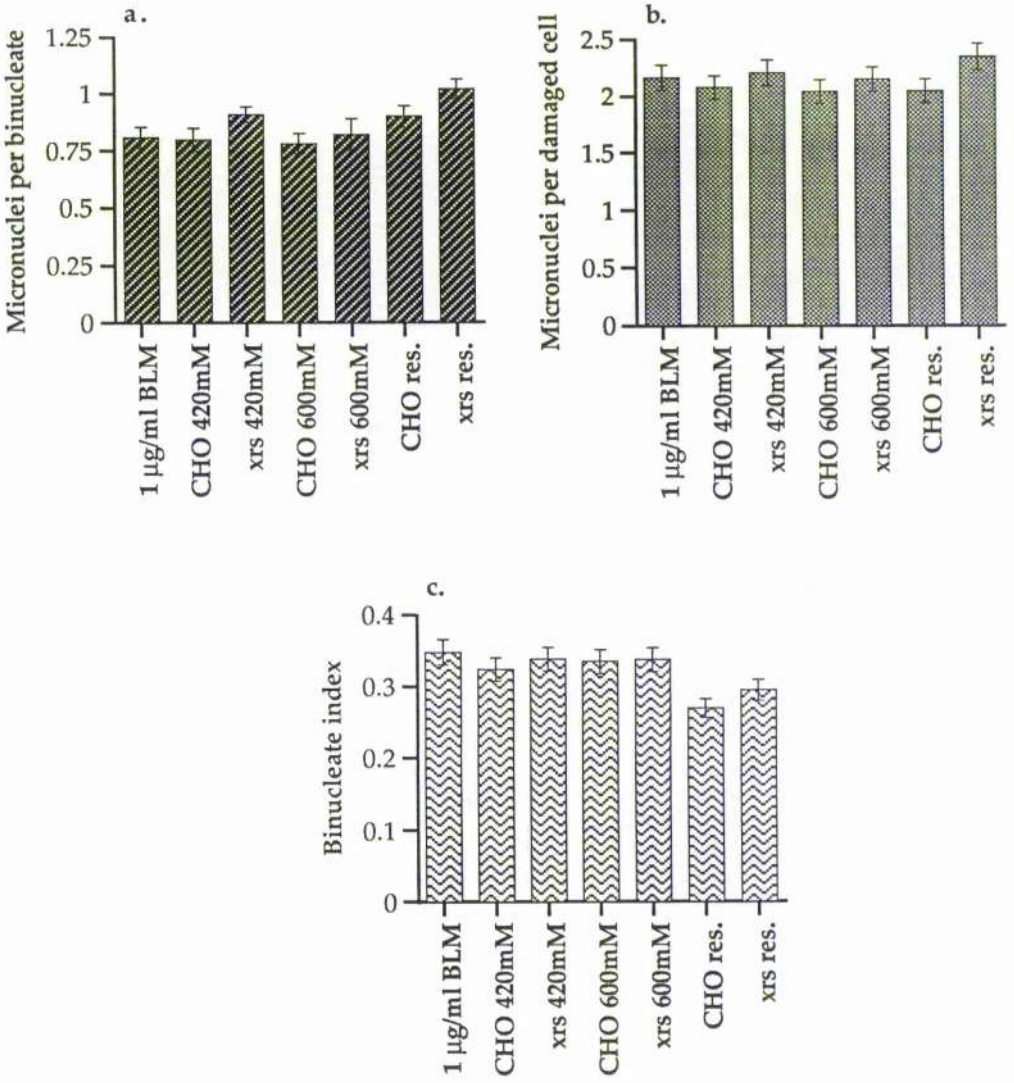

Figure 2.32. Effect of nuclear extracts (CHO and *xrs-5*) introduced into bleomycin (1 µg ml^{-1}) treated *xrs-5 cells using* streptolysin-O.

BLM treatment 30 min post-extract exposure. *Xrs-5* cells exposed to nuclear extracts from CHO or *xrs-5* cells. Extracts = 420 mM KCl wash, 600 mM KCl wash or residual (res) proteins extracted with 6 M urea. Error bars represent the standard error of the mean of a minimum of 3 independent experiments.

a) Micronuclei per binucleate cell. Irradiated data corrected by subtraction of unirradiated values. Student t-test indicates no significant effects on the frequency with dose.

b) Frequency of micronuclei per damaged binucleate cell. Student t-test indicates no significant effects on the frequency with dose.

c) Binucleate index. Student t-test indicates no significant effects on the frequency with dose.

2.3.3.8. Summary of the modulation of micronucleus induction in CHO and xrs-5 cells.

The chemical modulation of micronucleus induction and the associated parameters by chemical agents is summarised in table 2.2. Of the five agents tested, three produced significant effects on the cell lines examined; caffeine, staurosporine and distamycin A. The other two chemical agents; okadaic acid and 3-aminobenzamide, and the introduction of T4 DNA ligase or nuclear extracts into clastogen treated cells were either not effective or the results too inconclusive to allow them to be classified as modulators of the response of CHO or *xrs-5* cells to damage.

Both cell lines exhibited a reduction in the micronucleus frequency on exposure to distamycin-A post-irradiation. This reduction was not preferential to either cell line although the different doses applied to CHO and *xrs-5* may hide any relative difference in the mode of action of DST in the wild type and mutant. The decrease in micronucleus frequency could not attributed to protection of a specific sub-population of cells since the distribution of damage did not deviate from the expected pattern (data not shown). However, the decrease in the binucleate indices of both cell lines, which was concomitant with the decrease in micronucleus frequency, may indicate that a cell cycle delay is induced which prevents damaged cells from undergoing mitosis. This may involve either an extension of an existing check-point mechanism, possibly due to repair inhibition, or a separate mechanism possibly involving synergistic effects of DST and DNA damage on cell cycle progression.

The other two modulators of the micronucleus response, caffeine and staurosporine, produced elevated frequencies of micronuclei but only in CHO cells.

With STP this effect was unaccompanied by any effect on the cell cycle. This is surprising since STP has been shown repeatedly to cause cell cycle inhibition. This may, however be the result of an insensitivity of the assay to delays induced by STP, possibly because the assay examines cells only up to the first division. In addition, the elevation in γ-ray induced micronucleus frequencies by STP was not statistically valid after correction was made for effects of STP on its own. Therefore the effect of STP is, to a certain extent, uncertain in this study. That there may be a specificity for CHO may indicate that the protein kinases inhibited by STP may be involved in the defective mechanism present in *xrs-5*.

The effect of caffeine treatment was more definite. Here, the elevated frequencies of micronuclei in CHO remained after correction for clastogenic effects of caffeine itself. This agrees with the work of Darroudi and Natarajan [1987a]. Caffeine produced a reduction in the binucleate frequency which was similar in both CHO and *xrs-5* and independent of irradiation, indicating that the pathway involved in the expression of micronuclei is not

necessarily linked directly with the inhibition of the cell cycle measured by reductions in the binucleate index.

Table 2.2. Summary of the chemical modulation of the induction of micronuclei in CHO and *xrs-5* cells.

	3-Amino-bezamide	Caffeine[3]	Distamycin-A	Okadaic acid	Stauro-sporine
Micronuclei per binucleate[1].	No effect at either 2 or 24 hours incubation post-irradiation)	Increase in irradiated CHO and unirradiated CHO and *xrs-5* cells No effect in irradiated *xrs-5*.	Decreases in both cell lines after 24 hours exposure but not 2 hours. Observed in unirradiated *xrs-5* but not unirradiated CHO.	No significant effect at either 2 or 24 hours incubation post-irradiation)	No effect of 2 hr exposure. Significant effect in irradiated CHO cells (24 hrs exposure) No significant effect in *xrs-5*.
Relative micronucleus induction[2].	No effect at either 2 or 24 hours incubation post-irradiation). No differences between CHO and *xrs-5*.	Significant increase in CHO but not *xrs-5*. But no significant difference between CHO and *xrs-5*.	Decrease in both cell lines. But no significant difference between CHO and *xrs-5*.	No effect at either 2 or 24 hours incubation post-irradiation). No differences between CHO and *xrs-5*.	No effect of 2 or 24 hr exposure. No significant difference between CHO and *xrs-5*.
Micronuclei per damaged cell.	No effect at either 2 or 24 hours incubation post-irradiation) except an increase in irradiated *xrs-5* cells after 24 hrs exposure.	Increases in both CHO and *xrs-5*.	Decreased frequency in both cell lines.	No significant effect at either 2 or 24 hours incubation post-irradiation)	No effect of 2 hr exposure. Significant effect in irradiated CHO cells (24 hrs exposure) No significant effect in *xrs-5*.
Binucleate Index·	No effect at either 2 or 24 hours incubation post-irradiation)	Decrease proportional to dose in both cell lines. Response similar in both cell lines and irradiated / unirradiated cells.	Reduction in BI in both CHO and *xrs-5* cell (24 hrs exposure).	No significant effect at either 2 or 24 hours incubation post-irradiation)	No significant effect at either 2 or 24 hours incubation post-irradiation)

1) Micronuclei per binucleate. Effect of agents based on statistical analysis of the frequency of micronuclei per binucleate cell after corrections for background levels of micronuclei in untreated-unirradiated controls..
2) Relative micronucleus induction. Effect of agents on the induction of micronuclei by γ-rays based on statistical analysis after normalising data for both background levels of micronuclei and any clastogenic activity of the agents on their own.
3) Caffeine results for 24 hour exposure only.

2.4. *Discussion.*

From the results obtained from the above sections it is plain that the use of the cytokinesis block technique to assay damage to cells can produce varied results depending on the parameters used to asses sensitivity. The cytokinesis block technique proved efficient at determining relative levels of sensitivity CHO and *xrs-5* cells after treatment with clastogens. here the three main parameters examined; frequency of micronuclei per binucleate or per damaged cell and the effect of the agents on the binucleate index revealed significant differences between the wild-type and *xrs-5*.

However, the use of the binucleate index proved least useful since reductions in frequency sometimes did not appear to correlate with levels of expressed micronuclei. This is likely to be due several of the agents having effects not only on DNA damage but also on other cellular components some of which are likely to be involved in cell cycle progression themselves. In spite of this problem the use of the binucleate index did reveal interesting differences between CHO and *xrs-5*. From Section 2.2.1. it was apparent that the both the rate of progression into mitosis and the proportion of cycling cells was reduced in *xrs-5* cells following treatment. However, when treated with several of the clastogens, the proportion of the cycling cells which were subsequently blocked from completing one mitosis was reduced in the mutant. It might be expected that a cell line which exhibits both reduced growth properties and a DNA repair defect might exhibit a hypersensitivity to clastogen induced reductions in binucleate index. Indeed, it has been demonstrated that G_1 arrest is extended after DNA damage in *xrs-5* [Jeggo, 1985] presumably due to extended lifetimes of lesions in these cells. The results shown above would indicate therefore that there may be a defect in the arrest of cells in G_2 and or S phase. The S-phase specificity of DSB formation of CPT would support this. The question should therefore be asked as to whether *xrs-5* cells pass through G_2 with an elevated level of damage compared to CHO.

If this were the case then at high doses of clastogen, when such cell cycle effects are activated, *xrs-5* cells might be expected to express higher levels of damage compared to CHO even though the population as a whole may contain equal levels of damage. Evidence for this may exist in the results obtained with G_2 chromosomal aberration assays [MacLeod and Bryant; 1990a, b]. Here, although the kinetics of repair of aberrations are similar in mutant and wild-type, the levels of aberration are 4 fold greater in *xrs* cells. It has been recently shown that the repair of DSB in G_2 cells is also not defective in G_2 *xrs-5* cells compared to G_1 cells [Mateos and Bryant, 1994]. It may be that the elevated levels of expressed damage in the form of aberrations is the result of a decrease in the normal checkpoints involved in preventing heavily damaged cells entering mitosis. It is possible that the threshold level for the damage that is permissible is higher in *xrs-5* than CHO. Alternatively the position of

the checkpoint may vary between cell lines. A checkpoint which occurs earlier in G2 will allow a greater proportion of damaged cells into mitosis. This may be the reason for the higher minimum binucleate index observed in *xrs-5* cells after treatment with CPT or etoposide.

Therefore the *xrs* radiosensitive phenotype may be comprised not only of a DSB repair defect (predominant in G_1) but also a cell cycle checkpoint defect which permits an elevated level of damage expression after irradiation in G_2.

Further evidence for a cell cycle defect is evidenced by the lack of effect of CFN on *xrs-5* cells (and possibly STP as well) as demonstrated in this study and for CFN by Darroudi and Natarajan [1987a]. The effect of CFN on inhibition of G_2 arrest after irradiation is well documented, although a direct link between this activity and elevated aberration frequencies is still inconclusive [Rowley and Kort, 1988]. In addition CFN produced a reduction in binucleate indices of both irradiated and unirradiated cells with no difference between mutant and wild-type. This may occlude any possible effect that CFN has on the G_2 arrest. However that CFN is ineffective at enhancing *xrs-5* micronucleus frequencies would imply that the CFN sensitive pathway is inoperative in the mutant, and that this pathway may act via a G_2 arrest mechanism in the wild type.

There is a link between CFN and STP in that both have been demonstrated to alter protein phosphorylation levels in cells [Jung and Streffer, 1992; Tamaoki et al., 1986; Th'ng et al. 1994]. The possibility therefore exists of the *xrs* defect involving phosphorylation of proteins, possibly by alterations in the equilibrium between protein kinase and phosphatase activity. Treatment with doses of OA which are sufficient to inhibit pp2a but not pp1 produce no effect on the induction of micronuclei in CHO or *xrs-5*. However, the possible involvement of pp1 and other phosphatases on the response to radiation can not be ruled out. Although, sensitivity of cells could be determined by examining the induction and distribution of damage and the effect on the binucleate indices, these parameters may not possess sufficient sensitivity to permit accurate identification of modulators of damage response pathways. More specific methods might be more appropriate for precise determinations. However, by taking note of all of the parameters examined here then this assay may prove useful in general screening of compounds and cell lines. Particularly, since the technique does exhibit some sensitivity to a broad range of parameters including cell cycle kinetics and damage expression.

2.5. *Conclusions.*

The sensitivity of CHO and *xrs-5* cell lines to a number of clastogenic agents and modulators of the response to irradiation by a micronucleus assay which includes cell cycle and damage distribution in its mode of analysis reveals significant differences in the response of the *xrs-5* cell line. These include, not only elevated levels of damage expressed but also a possible cell cycle defect which may involve the progression of damaged *xrs-5* cells through check-points which normally prevent entry into mitosis.

The assays used to determine cellular sensitivity may provide a rapid and convenient technique for the screening of agents and cells. It also reveals an important cautionary note in that the measurement of expressed damage may be derived from only a small proportion of the total population of cells and that this proportion may vary depending on the nature of the clastogen and the type of cells examined. Therefore, in assays of radiosensitivity it is important to observe multiple parameters including ones which assess cell cycle kinetics.

Chapter 3.

Relationship of the nuclear matrix to the repair of DNA double-strand breaks.

Summary.

The structure of chromatin is implicated as having an important role in many of the normal functions of the nucleus including DNA replication and transcription. The roles of higher order nuclear structures in the repair of ionising radiation induced damage are still uncertain. This chapter reviews the organisation of chromatin within the nucleus and presents evidence for a structural component to the DNA double-strand break (DSB) repair defect in *xrs-5*.

A modification of the neutral filter elution technique was used to examine ionising radiation induced damage. Elution of DNA was measured from nucleoids extracted using high salt and non-ionic detergent. Lesions involving the release of DNA fragments from *xrs-5* nucleoids were identified as possibly of major importance in sensitivity to ionising radiation. A mathematical model based on the Poisson distribution of ionising radiation induced breaks was developed to help identify the structures involved in this defect. This points to the accumulation of DSB within large Mbp sized domains as critical in the repair defect of *xrs-5* and in the rate of repair in wild-type cells.

3.1. Introduction.

The identification of DNA as the main target of ionising radiation implicates the disruption of genomic material as important in its biological effects. It is convenient to imagine the DNA of cells as relatively homogeneous in structure and the effect of damage similar wherever it occurs. Indeed, the possibility that cell killing may be brought about by a single DSB [Frankenberg et al., 1981] would suggest that the position of the break within the genome is not of great importance. However, this is based not on the induction of a single DSB but on the presence of a single unrepaired DSB. As in *xrs* cells, the reduced ability to repair DSB has been associated with an increased sensitivity to ionising radiation [Jeggo and Kemp, 1983; Kemp et al., 1984]. Ionising radiation produces a random distribution of breaks within the genome [Blöcher and Pohlit, 1982]. That subsequent chromosomal abnormalities have also been demonstrated to occur randomly in chromosomes supports this [Kovacs et al., 1994]. However, thethe possibility remains that repair processes are less random. Lesions, albeit induced randomly throughout the chromatin of a cell, can take many different forms such as DSB, single strand breaks (SSB), base damage, protein-protein and protein-DNA crosslinks and combinations of these [reviewed Prise, 1994; Goodhead, 1994]. Regions of chromatin might express differential repair capacities for lesion variants. Differential repair could then super-impose an ordered pattern of DSB lethality on an initial random distribution of lesions.

3.1.1. The organisation of eukaryotic chromatin.

DNA possesses a very organised structure within the nucleus of eukaryotic cells. This structure builds up in complexity from the molecular structure of DNA itself to the organisation of the nucleus. A complex organisation is essential since the average haploid mammalian cell contains approximately 3×10^9 nucleotides which would result in a molecule of approximately one meter in length. To package this into a nucleus with a diameter of approximately 10 μm clearly requires a great deal of organisation in order to allow the proper functioning of the genome.

The final structure of chromatin is the end-product of a great number of individual events. The fundamental component is, of course, DNA. However variations in the structure of DNA itself can result in subsequent variations in the final organisation of the nucleus. DNA molecules can assume a variety of forms, with these being the result of both the nucleotide sequence, modifications to DNA and local conditions. In addition to the conventional B-form of the double helix, DNA can produce helices with different periodicities, shape and direction. In addition, triple helices and cruciforms structures exist [reviewed in van Holde and Zlatanova, 1994]. The cause of these variations can be attributed to the nucleotide

sequence, local ionic conditions and modifications such as methylation of e.g. cytosine residues. These processes can affect subsequent DNA-protein interactions and lead to regulation of both chromatin structure, DNA modifications and gene expression [Koudelka et al., 1988; Homberger, 1989; Breneman et al. 1993; D'Erme et al., 1993; Englander et al., 1993; Tate and Bird, 1993].

It is the sequence of DNA that comprises the blue-print for the formation of proteins via transcription and translation. However, the majority of DNA in a nucleus does not code for proteins. Genes themselves contain sequences involved in transcriptional control such as promoter regions and also sequences within the transcribed segments which are lost prior to translation (e.g. introns). Approximately 30% of the remaining, non-transcribed, DNA consists of highly repeated sequences including satellite DNAs, interspersed repeated DNAs and telomeric sequences [Lewin, 1990].

The next level of chromatin organisation is the formation of nucleosomes. These are fundamental subunits of chromatin structure in all eukaryotes [reviewed in van Holde, 1989; Baldwin, 1992; Ramakrishnan, 1994]. A nucleosome contains approximately 200 base pairs of DNA organised by a central complex of eight basic proteins into a bead like structure. Core histones are proteins with molecular weights of between 11 and 16 kDa and fall into four groups H2A, H2B, H3 and H4. The core histones form a tetramer from the arginine rich H3 and H4 histones ($H3_2 \cdot H4_2$) and two dimers formed from one of each of the slightly lysine rich H2A and H2B histones (H2A·H2B). These three polypeptide complexes combine to form the octamer. 146 base pairs of DNA wind around the core histones making approximately 1.8-1.9 turns per nucleosome. The remaining DNA forms "linker" DNA which separates individual nucleosomes. The length of linker DNA varies in a tissue and species specific manner with lengths ranging from 0 to 70 bp. The carboxy "tail" regions of H2A and H2B are considered to be able to interact with the ends of the nucleosomal DNA and parts of linker DNA outside the nuclesome core [Allan et al., 1982] The ($H3_2 \cdot H4_2$) tetramer associates with the central regions of the core particle DNA. Interactions between histones and DNA occur through hydrogen bonding between the positively charged amino acids (lysine, arginine and histidine) of the proteins and the negatively charged phosphates in the DNA helix.

Nucleosomes are found in both transcriptionally active and inactive DNA and also bind to both positively and negatively supercoiled DNA. Preferences for different forms of DNA do exist however, with histone octamers preferentially transferring from the positively supercoiled to negatively supercoiled DNA. This may be due to octamers relieving negative supercoiled stresses but enhancing positive supercoiling. During the movement of DNA binding proteins such as RNA polymerase, along a stretch of DNA, positive supercoiling in front and negative supercoiling behind the protein may be formed [Tsao et al., 1989; Dröge,

1994]. The preference of nucleosomes for negatively supercoiled DNA may be responsible for the chromatin rearrangement that occurs during the transcriptional process. Nucleosomes also exhibit short range mobility in their position on DNA [Meersseman et al., 1992]. Movement along the DNA, possibly in a cork-screw manner, is observed with several binding positions possible for an individual nucleosome. These positions are within certain boundaries demarcated by local ionic conditions and the position of neighbouring nucleosomes and other DNA binding proteins. Adenine rich regions can also act as boundaries to nucleosome positioning since nucleosomes preferentially bind to GC rich regions [Englander et al., 1993]. Although nucleosomes do exist on active and inactive DNA their actual positioning can be affected by the transcriptional status of the sequence they are attached to. The presence of nucleosomes within enhancer/repressor regions of DNA may affect the binding of enhancer/repressor proteins. Methylation of CpG islands in promoter regions of genes can cause enhanced repression of transcription by enhancing core particle binding *in vitro* [Englander et al., 1993].

A string of nucleosomes can therefore be produced forming the "beads on a string" structure also known as the 10 nm fibre. By altering ionic conditions *in vitro*, or, *in vivo* by the binding of linker histones; further packing can be induced to form the 30 nm fibre [van Holde, 1989; Allan et al., 1981].

Linker histones are a family of lysine rich proteins with molecular weights of approximately 23 kDa. There are approximately six H1 sub-types plus more distantly related $H1^0$ and H5 linker histones [reviewed in Breneman et al., 1993]. The six H1 sub-types are found associated with inactive DNA and are partially depleted on active chromatin. The sub-types can be segregated into two families H1A and H1B depending on their electrophoretic mobility. Under this classification H1A is associated with the nuclear periphery and H1B is distributed evenly throughout the nucleus. $H1^0$ is concentrated around the nucleolus and may be associated with potentially active genes. H5 is only found to be enriched in nucleated erythrocytes as found in avians, reptiles and amphibians. It is thought to be associated with the near complete repression of gene activity in these cells.

Linker histone bind to 22 bp of DNA as it leaves the core particle and the resulting structure is termed a chromatosome. H1 associates with the central turn of the nucleosomal DNA as well as either 11 bp from each end of the chromatosome DNA or 22 bp from just one end [Allan et al., 1980; Baldwin, 1992]. The precise structure of the 30 nm fibre is still uncertain since the structure is readily disturbed during isolation procedures resulting in artefactual structures. The 30 nm fibre follows a highly contorted path within the nucleus and would appear to be in the form of either a highly flexible dinucleosomal ribbon with linker DNA zig-zagging across the fiber axis or in the form of a solenoid comprised of six chromatosomes per turn with

histone H1 lying along the central axis surrounded by the nucleosomes [Swedlow et al., 1993; Horowitz et al., 1994]. Both of these models involve H1 positioned centrally [Grazianio et al., 1994].

The binding of histones to DNA can be modified by a number of post-translational alterations including phosphorylation, acetylation, poly(ADP-ribose)ylation and proteolysis. These events can occur in both a cell cycle and DNA damage dependent manner [Fónagy et al., 1977; Yasuda et al., 1987; Robérge et al., 1990; Gaziez and Kutsyi, 1992; Wolffe, 1991]. By these modifications the functional status and accessibility of DNA can be altered resulting in changes in transcriptional status, structure and repairability of the DNA.

In circular DNA or linear molecules fixed at both ends, topological changes may occur including supercoiling [Bauer, 1978]. These can be detected by either the electrophoretic mobility or the rate of centrifugal sedimentation of DNA. Intercalative drugs such as ethidium bromide (EtBrd) and propidium iodide (PI) when bound to DNA remove supercoils that are present and if the concentration of these drugs rise sufficiently they will induce supercoils opposite to those originally present. The concentration of EtBrd required to remove all supercoils is indicative of the level of supercoiling in the DNA molecule [Hinton and Bode, 1975a; b].

When nuclei were isolated and extracted with non-ionic detergents and high salt concentrations, protein depleted structures which retained several of the properties of the nuclei were formed. The DNA contained within these "nucleoids", as they were termed, proved to contain supercoils [Cook and Brazell, 1975; Ide et al., 1975]. Since eukaryotic DNA is formed from linear, not circular molecules, this indicated that the DNA molecules in eukaryotic nuclei were fixed in such a way as to permit this supercoiling [Cook and Brazell, 1975; 1976, Cook et al., 1976]. By the use of salt gradients during nucleoid extraction [Levin et al., 1978] it was possible to selectively remove different DNA binding proteins. At low salt concentrations a low level of positive supercoiling existed [Levin and Cook, 1981a]. As salt concentration rose it was the H2A and H2B histones which were released first. The loss of these did not affect the supercoiling levels. At a critical concentration of NaCl of between 0.92 and 0.95 M negative supercoiling became apparent in the nucleoids. This occurred without the loss of the remaining H3 and H4 histones and could be attributed to a conformational change in the histone-DNA complex. A further increase in salt concentration removed the remaining histones without producing an increase in supercoiling levels. Therefore it would appear that negative supercoiling is induced into DNA by the binding of histones, in particular the $(H3_2 \cdot H4_2)$ tetramer. Supercoils exist within both intra and internucleosomal DNA and it is the presence of the nucleosomal proteins that locks this free energy within the DNA. Although it was found that the binding of $(H3_2 \cdot H4_2)$ to DNA

caused this supercoiling, histone H2A and H2B were found to bind more readily to supercoiled DNA than relaxed [Levin et al., 1978; Levin and Cook; 1981a, b]. It therefore appears that the binding of ($H3_2$·$H4_2$) induces negative supercoils which promote the subsequent binding of H2A and H2B. The 1.8-1.9 turns that DNA makes around the nucleosomal core should induce a similar number of negative supercoils in protein free DNA. Instead, only 1 supercoil is observed per nucleosome on removal of histones. This discrepancy is likely to be caused by structural alterations in DNA which decreases the periodicity of the DNA helix from 10.5 bp to 10 bp per turn. On removal of the histones the free energy of supercoiling is partially absorbed by unwinding of the DNA helix to reform the 10.5 bp periodicity [Lewin, 1990].

Since eukaryotic DNA is not circular there must be some form of fixation of the molecule along its length to allow formation of supercoils. A looped structure of DNA was postulated to occur by Cook and Brazell [1976; 1978] and Hartwig [1978] with chromatin fastened at the base of the looped domains by non-histone proteins [Ide et al., 1975; Adolph et al., 1977a; b; Laemmli et al., 1978]. These loops could be observed by electron-microscopy in protein depleted metaphase chromosomes and interphase nucleoids [Paulson and Laemmli, 1977; Laemmli et al., 1978]. The loops extended from a proteinaceous network termed in the nuclear "scaffold" metaphase cells or the nuclear "matrix" in interphase cells. Two major component proteins of both of these structures have been identified termed SC1 and SC2 [Lewis and Laemmli, 1982]. The SC1 protein has been identified as DNA topoisomerase II in both metaphase scaffolds [Earnshaw et al., 1985; Gasser et al., 1986] and the interphase nuclear matrix [Berrios et al., 1985]. Topoisomerase II, when bound to DNA can cause the formation of a transient protein linked DNA double strand break. Another intact DNA duplex can subsequently be passed through this strand break with the effect of either reducing the torsional stresses induced by supercoiling or separating two catenated DNA molecules [Cozzarelli, 1980; Wang, 1987]. Topoisomerase II binds to specific sequences of DNA which are enriched with AT regions termed scaffold and matrix attachment regions (SAR and MAR respectively) [Gasser and Laemmli, 1986; Mirkovitch et al., 1987; 1988; Izaurralde et al., 1988, Vassetzky, 1989]. It was originally postulated that topoisomerase II might act as the loop attachment protein in nuclei. However, whilst the proper functioning of topoisomerase II is apparently required for events such as condensation of chromosomes at mitosis and possibly segregation of sister chromatids [Charron and Hancock, 1990; 1991, Sumner, 1992] it is not required for the scaffolding of mitotic chromosomes in *Xenopus* extracts [Hirano et al., 1993]. Illegitimate recombination events have also been linked to dysfunction of matrix attachment regions and topoisomerase II [Charron and Hancock, 1991; Sperry et al., 1989]. Incorporation of exogenous supercoiled DNA into the nuclear scaffold is also linked to the presence of topoisomerase II [Tsutsui et al., 1988; 1989]. This would indicate that while topoisomerase II may be important in loop metabolism via the SAR and MAR sites on DNA it is not necessarily responsible for maintaining the loop structure. The siting of SAR/MAR sequences at the base of the loop

places topoisomerase II in an ideal position to respond to the induction of topological stresses. It is also evident that different isoforms of topoisomerase, the α- and β-isoforms, are present to differing degrees in nuclei of varying proliferative state. Topoisomerase IIα is retained almost exclusively in the nuclear matrix of proliferating cells. Topoisomerase IIβ is present in resting cells and then predominantly in the nucleolus and euchromatic regions [Zini et al., 1994]. This indicates differing roles for the isoforms in cell division and transcription.

The high-mobility group protein HMG-1/Y also binds preferentially to SAR sequences with over 15 binding sites identified in 657 bp histone SAR sequence [Saitoh and Laemmli, 1994]. Immunolocalisation of HMG-1/Y indicates that it is associated with topoisomerase II.

Yet another, abundant, SAR binding protein was identified by Romig et al. [1992]. This 120 kDa protein, termed scaffold attachment factor A (SAF-A), was identified as a component of eukaryotic nuclear matrices and scaffolds. This protein, in addition to SAR binding activity promoted the formation of looped DNA structures.

In interphase cells, the attachment sites of the looped domains are associated with the nuclear membrane via the internal nuclear lamina [reviewed in McKeon, 1987]. The nuclear membrane is contiguous with the endoplasmic reticulum. It is comprised of two layers of bilipid membrane punctured by the nuclear pore complexes which permit communication and transport between the nucleus and the cytoplasm [Alberts et al., 1983]. The inner nuclear membrane contains transmembrane proteins which act as receptors for the nuclear lamina [Worman et al., 1988; Simos and Georgeatos, 1992]. The lamina is formed from a meshwork of intermediate filaments; a family of structural proteins including cytoplasmic proteins such as vimentin, desmin and the cytokeratins [Franke, 1987]. There are three main lamin groups A, B and C. The B lamins, although capable of direct interaction with the inner nuclear lipid bilayer via an isoprenyl group [Krohne et al., 1989], are also associated with the nuclear membrane via the aforementioned receptor proteins. The B-lamin-receptor protein complex acts as the anchor for the lamin mesh. The A and C lamins are transcribed from a single gene; lamin C as a truncated form of lamin A [Riedel and Werner, 1989]. These proteins appear to have affinities for both DNA and lamin B [Hakes and Berezney, 1991; Shoeman and Traub, 1990]. The presence of lamins is variable in both a developmental and cell cycle dependent manner [reviewed in Moir and Goldman, 1993]. Lamins A and C would appear to preferentially co-locate with the condensed heterochromatin within the nucleus [Bridger et al., 1993]. Decondensed euchromatin regions are relatively depleted of lamins. The dependence of heterchromatin structure on the presence of lamins A and C is evidenced by the lack of these proteins in the highly euchromatic nuclei of undifferentiated cells and certain haematopoeitic cells [Guilly et al., 1990; Röber et al., 1990]. It is only on differentiation with the resulting appearance of heterochromatin that lamins A and C appear to be expressed

[Weber et al., 1990; Paulin-Levasseur, 1989]. In differentiated cells there are further cell cycle alterations in lamin A/C distribution within the nucleus. In G_0 cells lamins A/C are uniformly distributed around the inner surface of the nuclear membrane. In G_1 cells this perinuclear array is disrupted with the lamins appearing in discrete foci and fibres. These are associated not with the nuclear membrane, but with regions of condensed chromatin. These foci disappear as cells progress into S-phase [Bridger et al., 1993]. This data indicates that after the reformation of the nucleus following mitosis, lamins A/C initially form fibres and foci in association with heterochromatin. As the cell cycle progresses, or the cells enter G_0 the lamin-heterochromatin complexes associate with the nuclear membrane, possibly via lamin B. The presence of lamins A/C may therefore be essential not to the structure and function of active regions of DNA but in the packaging of the non-transcribed regions of the genome.

During metaphase the nuclear lamina becomes disrupted along with the nuclear membrane. Lamin B remains associated with the fragmented membrane. Lamins A and C are partially dispersed into the cytoplasm the remainde associated with the surface of the condensed chromosomes [Jost and Johnson, 1981; Glass and Gerace, 1990]. At telophase the reformation of the nuclear membrane is not dependent on the presence of lamins [Newport et al., 1990; Ulitzer et al., 1992]. The rearrangement of chromatin may be targeted to the nuclear membrane by lamin-lamin and lamin-chromatin interactions. Binding to chromatin by lamin A may be mediated by specific binding to polynucleosomes [Yuan et al., 1991].

Therefore chromatin structure would appear to depend on specific DNA binding proteins. These proteins can be located to specific regions of the nucleus depending on the transcriptional status of the chromatin with transcribed regions of DNA generally having fewer associated proteins and exhibiting a more expanded structure compared to non-transcribed regions. However, even though chromatin structure can be imposed on cells by these DNA binding proteins the sequences and lineage of the DNA itself would also appear to be important. A striking example of this is observed in the structure of chromosomes formed from the fusion of fragments of fission yeast chromosomes into mouse chromosomes [McManus et al., 1994]. Here the yeast fragments maintain a different structure to the surrounding mouse chromatin on condensation indicating that either the yeast DNA sequences/modifications or certain structural components could be carried over into the mammalian chromosome.

Figure. 3.1. Interphase Chromatin Structure.

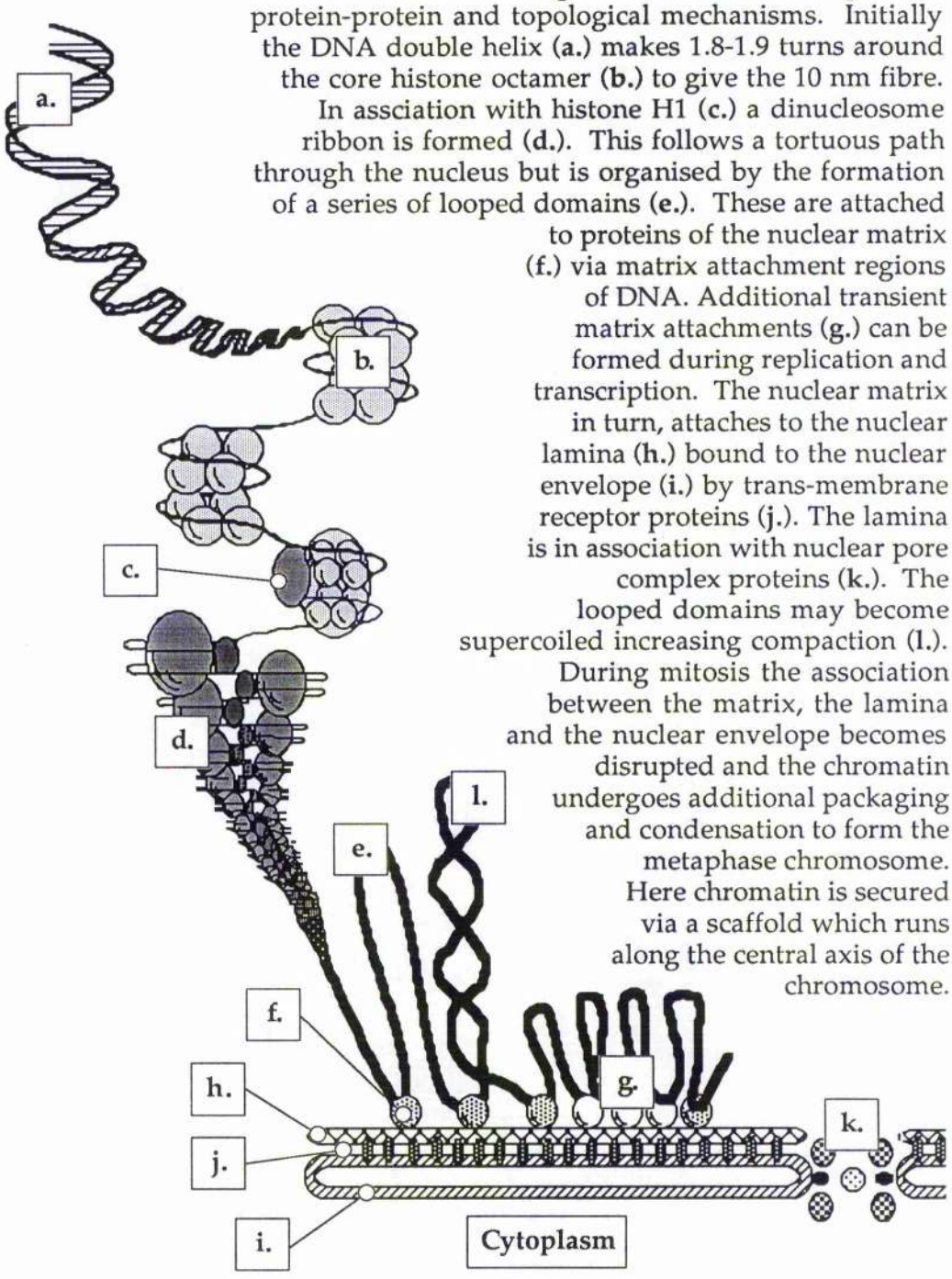

The structure of chromatin follows several levels of DNA folding based around DNA-protein, protein-protein and topological mechanisms. Initially the DNA double helix (**a.**) makes 1.8-1.9 turns around the core histone octamer (**b.**) to give the 10 nm fibre. In assciation with histone H1 (**c.**) a dinucleosome ribbon is formed (**d.**). This follows a tortuous path through the nucleus but is organised by the formation of a series of looped domains (**e.**). These are attached to proteins of the nuclear matrix (**f.**) via matrix attachment regions of DNA. Additional transient matrix attachments (**g.**) can be formed during replication and transcription. The nuclear matrix in turn, attaches to the nuclear lamina (**h.**) bound to the nuclear envelope (**i.**) by trans-membrane receptor proteins (**j.**). The lamina is in association with nuclear pore complex proteins (**k.**). The looped domains may become supercoiled increasing compaction (**l.**). During mitosis the association between the matrix, the lamina and the nuclear envelope becomes disrupted and the chromatin undergoes additional packaging and condensation to form the metaphase chromosome. Here chromatin is secured via a scaffold which runs along the central axis of the chromosome.

3.1.2. *The relationship of structure to function*

As mentioned above, the organisation of the nucleus is essential for the proper functioning of replication and transcription and other nuclear processes. The looped structure of chromatin would appear instrumental in these processes [McCready et al., 1980; 1982; reviewed in van Holde, 1989].

3.1.2.1. Replication and transcription.

Structural studies have revealed that during replication of DNA distinct complexes of proteins are associated with the nuclear matrix/lamina [Hozák et al., 1993]. By pulsed labelling of newly replicated DNA these complexes can be co-located with the origins of replication of DNA. Similarly the replication forks themselves are consistently organised within the nuclear matrix [Vaughn et al., 1990]. Since these replication sites in the matrix are apparently static in position then it is proposed that it is the DNA that moves relative to the complexes as opposed to the complexes moving along the DNA helix. The looped structure of DNA provides a mechanism for matrix associated processing of DNA via the attachment points at the matrix. A model was proposed whereby DNA could be spooled through attachment sites and the associated replication machinery [McCready et al., 1980; McCready et al., 1982]. This model not only maintains the higher order structure of DNA but may permit control of the extent of replication via the ordered activation of specific origins of replication. It has been estimated that there are 100-300 replication centres within nuclei each of which containing 300-1000 replication forks [Mills et al., 1989; Adachi and Laemmli, 1992]. Indeed, it has been observed that there is a defined sequence to replication of different sites during S-phase. Replicating foci are initially distributed throughout the euchromatin followed in late S-phase by replication of perinuclear then intranuclear heterochromatin [Fox et al., 1991].

With pulse labelling studies of nascent RNA it has been demonstrated that transcription also occurs at the nuclear matrix with the transcription complex, nascent RNA transcripts, RNA polymerase and actively transcribed genes all closely associated with the nuclear matrix [McCready et al., 1982; Vogelstein et al., 1982; Jackson and Cook, 1985]. However, other work has indicated that RNA polymerase and transcription complexes are not actually bound to the nuclear matrix and that transcriptional machinery may in fact move around the DNA loops during transcription [Roberge et al., 1988]. Actively transcribed genes have been located lying close to the nuclear matrix [Cook et al., 1982, Cijek et al., 1983]. The location of MAR/SAR sequences were subsequently mapped to non-transcribed enhancer regions of genes, both 5′ and 3′ to transcribed regions in both highly transcribed regions and regions of low transcriptional activity [reviewed in Mirkovitch et al., 1987]. These attachment regions

have been reported to be constant regardless of the transcriptional activity of a specific gene. Nor do they differ between interphase and mitosis. SARs can contain several individual topoisomerase recognition sequences along regions up to 1 kbp in length. The distance between adjacent SARs varies between 4.5 and 112 kbp, with one or several differentially regulated genes occurring between these sequences. Approximations of loop sizes have been made [reviewed in Pienta and Coffey, 1984; Paulson and Laemmli, 1977] with an estimate of the average loop 60 kbp in length within a range of 30-100 kbp (45,000-150,000 loops per haploid cell). These values are approximated on the basis of direct measurements of halo size, SAR spacings and replicon size. However, by the use of centrifugal nucleoid sedimentation to measure the reduction in supercoiling by irradiation, estimates of domain size are placed of approximately 2-7 Mbp (or approximately 750-2625 supercoiled domains/haploid cell). This approximation is made on the basis of one DNA strand break causing relaxation of one supercoiled domain [Cook and Brazell, 1975; van Rensburg et al., 1985; 1987; Hartwig, 1978; Walicka and Godlewska, 1989]. This discrepancy between the "replicon" domain size and "supercoiled" domain size has been explained by the Mbp supercoiled domains experiencing additional structuring so as to be comprised of approximately 50-60 of the smaller 60 kbp domains [Hartwig, 1978]. A single strand break in the DNA of one of these 60 kbp loops may cause relaxation of supercoiling in all the loops of that cluster. The techniques used to measure supercoiling disrupts membrane structures while leaving protein structures mainly intact. It was proposed, that *in vivo*, individual replicons are maintained via protein-membrane interactions. On lysis of the cells the membrane supporting structure is removed but the individual replicons retain their basic form. The loss of the membrane allows supercoiling stresses to be communicated between replicons. If the nucleoids are exposed to protein denaturants such as sodium dodecyl sulphate, β-mercaptoethanol or enzymic proteolysis the replicons are further disrupted giving rise to domains the size of the sum of the replicon sizes.

Therefore it would appear that the "replication factories" observed in the nuclei of replicating cells [Hozák et al., 1993] may be comprised of functionally independent clusters of replicons each of which is a separate looped domain. The basis for the replicons is supposedly MAR mediated attachment to the nuclear membrane via the nuclear matrix. The regulation of this level of chromatin packaging may be further controlled by lower order chromatin structures such as the position of nucleosomes and histone H1 within MARs. For example, histone H1 can apparently mask MARs from topoisomerase II [Käs et al., 1989; 1993]. Thus the packaging of DNA could conceivably be altered by relatively minor alterations in the positions of proteins along the length of the chromatin. This would have implications on both the structure of the nucleus and the metabolism of DNA.

The precise control of incorporation of MAR sequences into the nuclear matrix is cell cycle regulated. It has been observed that certain origin of replication sequences (*ors*) associate with the nuclear matrix preferentially at the G_1/S transition and during early S-phase [Mah et al., 1993]. Other origins of replication associate with less temporal control throughout S-phase and then only transiently, presumably during replication initiation of specific segents. These results support a dynamic higher order structure with specific sequences recruited and lost at time points throughout replication of DNA.

3.1.2.2. Repair of DNA damage.

Since the major processes involving DNA occur at the matrix it would be convenient for repair processes to also occur here. Some evidence for matrix associated repair mechanisms does exist, however, this work has mainly been performed on UV repair mechanisms. UV repair has the advantage over ionising radiation repair mechanisms in that large regions of DNA polymerisation are formed via the long-patch excision repair process. This permits labelling studies to be used to localise the site of repair in the nucleus. Ionising radiation results in only short (1-3 bp) regions of polymerisation preventing the application of these techniques. The sites of replication in response to low doses of UV indicate that repair polymerisation does occur at the matrix. Newly synthesised DNA was seen to occur predominantly in association with the nuclear matrix. In addition the position of the patches did not appear to alter with time indicating that the repaired regions remained attached to the matrix [McCready and Cook, 1984]. The patches produced by low dose UV can be co-localised with actively transcribing genes which are also positioned at the matrix [Mullenders et al., 1988]. However, if high doses of UV were given the distribution of repair patches became more random with the ratio of matrix versus loop associated repair patches decreasing. This evidence implied preferential repair of actively transcribed regions of DNA which are permanently associated proximal to the matrix instead of the transient binding of more distally damaged sites [Mullenders et al., 1988; Hanawalt, 1990; Mullenders et al., 1990;]. Evidence from two UV sensitive cell lines (Cockaynes' syndrome and Xeroderma pigmentosum-C) indicates that two partially independent pathways exist for the repair of active and inactive DNA. Repair of UV lesions is also more rapid on the transcribed strand of DNA compared to the non-transcribed strand and even between damaged nucleotides separated by only a few bases [Gao et al., 1994; Tornaletti and Pfiefer, 1994].

The importance of the higher order chromatin structures on transcription, replication and repair of UV damage indicate that the repair of ionising radiation induced damage might also be affected by chromatin structure. Work, upto the present, has been confined to correlations between radiation sensitivity and visible and implied alterations in the structure of chromatin. Many radiosensitive cell lines express similar frequencies of initial

lesions to cells of normal sensitivity. It is the subsequent processing of breaks including repair and misrepair that is likely to determine the radiosensitivity. It is in these processes that chromatin structure may therefore play a role.

Several techniques which are used for the detection of DNA strand breaks have also identified nuclear structure as an indicator of ionising radiation sensitivity [reviewed in Olive, 1992]. Techniques which appear to be sensitive to chromatin structure include neutral filter elution, nucleoid sedimentation and alkaline DNA unwinding. The parameters measured by these techniques are all sensitive to the conditions of lysis and measurement to which the cells are exposed. As higher order structures are removed by lysis conditions differences between sensitive and resistant cell lines diminish. Generally, these techniques infer a correlation between sensitivity and DNA structure without identifying specific causative structures. Attempts have been made to correlate the size of supercoiled domains with the radiosensitivity of cells. In comparing the sizes and proportions of differently sized Mbp supercoiled domains a relationship between cells containing a higher proportion of intermediate or large domains (2-7Mbp) and cellular radiosensitivity was found for thymocytes and peripheral lymphocytes sub-types [Filipovitch et al., 1982; van Rensburg et al., 1985]. This is not the case for all radiosensitive cells; the L5178Y-R and L5178Y-S lymphoma cell lines show no such correlation [Walicka and Godlewska, 1989].

As described in chapter one, structural differences between CHO and *xrs-5* are also observed including altered metaphase chromosome and interphase nuclear structure, accessibility to nuclease digestion, alkaline DNA unwinding and ethidium bromide induction of positive supercoils [Schwartz et al., 1990; 1993; Yasui et al., 1991; 1994]. However, no definite evidence of a structural component to the defect in the repair of DSB in *xrs-5* has yet been identified.

It was decided to develope an assay whereby structural analysis could be combined with DSB measurement. The importance of the position of breaks in relation to higher order nuclear structures and to other DSB in the repair of DSB was examined. To study the spatial orientation of breaks and their relationship to cellular repair mechanisms it is first necessary to have a method of identifying where in the DNA a break is occurring. Techniques of DSB measurement do not, at present, posses this accuracy. The majority make an assessment of the overall reduction in the size of DNA molecules caused by strand breakage. The reduction in size is measured by a variety of physico-chemical techniques including changes in sedimentation during centrifugation, electrophoretic mobility, and passage through filters [Iliakis et al., 1991; Olive, 1992] The conditions under which these techniques are performed generally attempt to remove most of the structures normally associated with chromatin by the use of ionic detergents and in some cases proteolysis. This results in formation of a

homogenous DNA "gel". From the physico-chemical properties of this gel an estimate or in the case of low speed centrifugal sedimentation, a quantification of the numbers of strand breaks present in the DNA can be made.

As described above, by extracting nuclei in high salt and non-ionic detergent, structures retaining the looped domains of interphase nuclei can be obtained. A strand break, either single or double stranded in one of the histone depleted loops will release any free energy of supercoiling maintained in that loop. Individual DSB within a loop will not release any DNA since attachment of the DNA is maintained to the matrix. However, if two or more DSB occur within the same domain then the segment of DNA not linked to the matrix might be extracted from the matrix. Release of this fragment could be measured using one of several techniques including filter elution and agarose pulsed-field gel electrophoresis. The technique of filter elution lends itself to measurement of these fragments since alterations to the conditions under which the nucleoids are retained on the filter can be readily made and the high salt conditions required for nucleoid production can be maintained throughout elution. Filter elution has already proved versatile in the variety of treatments that can be performed on the DNA of cells [Johnston and Bryant, 1991]. The main disadvantages of filter elution are the lack of sensitivity at low doses and the lack of quantitative information of numbers of strand breaks and DNA sizes. Electrophoretic techniques pose difficulties both in the handling and processing of nucleoids and in the buffers that can be used during electrophoresis. However, they do permit estimations of the size of DNA fragments and in the case of the "comet" assay can provide information on the levels of strand breakage and cell cycle position for individual cells [Östling et al., 1987; Olive et al., 1992; Smith and Sykes, 1992]. It was decided therefore to use a modified filter elution technique since the flexibility of this technique would prove most useful.

Conventional "neutral" filter elution is performed at a pH of 9.6 and uses harsh lysis conditions involving proteolysis and denaturing detergents [Bradley and Kohn, 1979] or heat [Okayasu et al., 1989] in order to minimise protein-DNA interactions [Bradley and Kohn, 1979; Okayasu et al., 1989]. A pH of 7.5 was chosen for the lysis and elution procedures to prevent conversion of alkali-labile base damage to strand breaks. Lysis and elution was performed using a buffer including the non-ionic detergent Triton X-100. Another potential problem was the action of proteases, nucleases and possible alterations to nuclear structure if elution was performed at room temperature. To minimise these effects all elutions involving nucleoids were performed at 4°C in the presence of the divalent cation chelating agent EDTA. To distinguish conventional elution of deproteinised DNA and elution from nucleoids the term non-ionic neutral filter elution (NINFE) is used denoting the use of non-ionic detergents in the extraction of nucleoids. Elutions performed on protein depleted DNA "gels" were termed ionic neutral filter elution (INFE) to denote that ionic detergent was used.

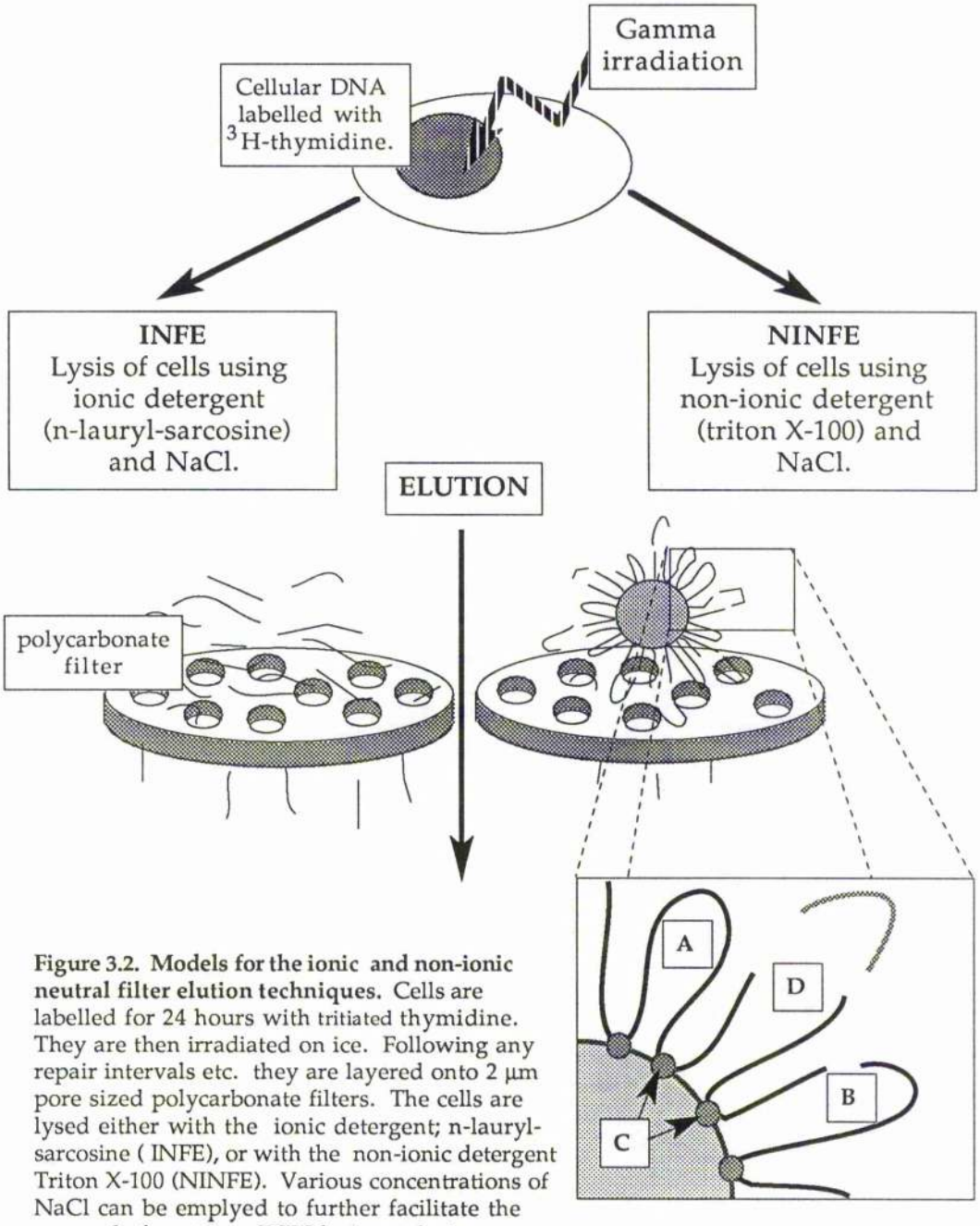

Figure 3.2. Models for the ionic and non-ionic neutral filter elution techniques. Cells are labelled for 24 hours with tritiated thymidine. They are then irradiated on ice. Following any repair intervals etc. they are layered onto 2 μm pore sized polycarbonate filters. The cells are lysed either with the ionic detergent; n-lauryl-sarcosine (INFE), or with the non-ionic detergent Triton X-100 (NINFE). Various concentrations of NaCl can be emplyed to further facilitate the removal of proteins. INFE lysis results in disruption of the majority of the DNA-protein interactions and produces a "gel" of DNA on thefilter. The rate of elution through the filter will be proportional to the number of DSB within the DNA. NINFE lysis retains the matrix-DNA interactions and thus also maintains the looped domains of DNA which can spill out from the residual nucleus to produce the nucleoid (see inset). Loops which contain either no DSB (**A**) or one DSB (**B**) retain all their DNA by means of the matrix binding sites (**C**). Loops containing two or more DSB (**D**) may lose the non-matrix associated segment of DNA (〰〰〰). It is these segments which can be eluted from the filter.

3.2. *Materials and methods.*

3.2.1. *Cell Culture and irradiation.*

Cells in exponential growth were labelled for 24 hours with 0.1 μCi ml^{-1} (3.7 kBq ml^{-1}) [methyl-^{3}H]-thymidine (^{3}H-TdR) at 37°C. The cells were then washed twice with fresh medium and medium containing 1 μM unlabelled thymidine added . The cells were incubated for 16 hours to chase any unincorporated ^{3}H-TdR. For dose response experiments cells were trypsinised as normal and washed twice in HBSS at 4°C. They were then resuspended in HBSS at 10^6 cells ml^{-1} in 7 ml plastic bijou and irradiated on ice. In repair experiments, cells in 25 cm^2 flasks were placed on ice for 15 minutes followed by gamma irradiation on ice. The medium was exchanged for fresh medium pre-incubated to 37°C and the flasks returned to 37°C for the repair period. This was followed by trypsinisation and washing in HBSS as above.

3.2.2. *Filter elution.*

Filter elution was based on the technique of Bradley and Kohn [1979] with some modifications. Swinnex filter units were loaded with 45 mm diameter, 2 μm pore size polycarbonate filters (Nucleopore), previously moistened with PBS. 1 ml of ice cold PBS was added to the units and connected to 50 ml syringe barrels and a peristaltic pump (Watson Marlow 202U/AA) via silicon tubing. 15 ml of ice cold PBS was added to the syringe reservoirs and the system cleared of air bubbles. Cells were added to the reservoirs and allowed to flow onto the filters under gravity. Just prior to all of the fluid flowing out of the reservoir a further 10 ml of PBS was added and allowed to flow out completely. The filter units were subsequently clamped off.

3.2.2. 1. *Ionic neutral filter elution (INFE).*

INFE was based on the modified neutral elution procedure used by Okayasu et al. [1989] with several modifications. The Swinnex filter units were disconnected from the apparatus and 1 ml of INFE buffer , pre-warmed to 60°C, added to the units.

INFE buffer= **40 mM tris; pH 7.5**
10 mM Na-EDTA
2.5% (w/v) N-lauryl-sarcosine (NLS)

The units were capped to prevent evaporation and incubated at 60°C for 1 hour. They were then reconnected to the pump, unclamped and 40 ml of INFE buffer (room temperature) added to the reservoirs. In contrast to the technique used by Okayasu et al. [1989], no proteases were

included in the lysis buffer and elution was performed in the same buffer as lysis. Elution was performed in the dark at a rate of 2.6 ml hr^{-1} until all the buffer had passed through the filters. The eluate was collected as a single fraction.

3.2.2.2. Non-ionic neutral filter elution (NINFE).

1 ml of NINFE buffer, pre-chilled to 4°C, was added to the Swinnex filtration units.

NINFE buffer = **40 mM tris-HCl; pH 7.5**
10 mM Na-EDTA
0.25% (v/v) Triton X-100

These were unclamped and 40 ml of NINFE buffer (4°C) added to the reservoirs. Elution was then performed at a rate of 2.6 ml hr^{-1} in a refrigerator at 4°C until all the buffer had passed through the filters. The eluate was again collected as a single fraction.

3.2.2.3. Sequential elution.

NINFE was performed as above. The filter units were then disconnected from the apparatus and 1 ml of INFE buffer pre-warmed to 60°C was added. Lysis and elution then followed the INFE method described above except that elution was performed at 4°C. The eluates from NINFE and INFE were collected separately.

3.2.3. Calculation of DNA damage.

The filters were removed from the units and placed in plastic scintillation vials. 5 ml of Filter-count (Packard) was added and the vials thoroughly vortexed for 1 minute prior to scintillation counting. The volume of eluate was measured and 5 ml removed and placed in plastic scintillation vials. 5 ml of distilled water was added; to prevent precipitation of NaCl from the eluate, and 10 ml of Optiphase MP (LKB) added. Radioactivity was determined by scintillation counting.

The fraction DNA eluted, FE was calculated using the equation

$$FE = \frac{DPM_{eluate}}{DPM_{total}} \qquad (3.1)$$

Here DPM_{eluate} are the total number of disintegrations per minute calculated by correcting the DPM in the 5 ml sample tested for the total volume eluted. DPM_{total} are the total number of DPM in the eluate plus the DPM contained on the filter. To correct for background levels of elution, which would include background damage and unincorporated ^{3}H-thymidine, the relative fraction eluted (RFE) was calculated by using Equation (3.2).

did not permit examination of the effect of salt concentration on elution since virtually all DNA was released from the filter at each salt concentration. The concentration of NaCl of 2 M was chosen for all further experiments. This concentration was used in both NINFE and INFE lysis and eluting buffers.

3.3.2. *Induction of elution by gamma-rays.*

As expected, the amount of DNA eluted by NINFE was much lower than by INFE. To examine this further, dose response curves were generated for both elution condition types (Figure 3.5).

Ionic neutral filter elution in the presence of 2 M NaCl produced a dose response curve similar in magnitude and shape to those reported by other workers [e.g. Iliakis et al., 1992]. For the initial 100 Gy, elution was relatively linear with dose. After 100 Gy, virtually all DNA was eluted from the filter resulting in saturation of the response. The response for *xrs-5* was not significantly different for that of CHO indicating equal numbers of DSB are induced in the two cell lines.

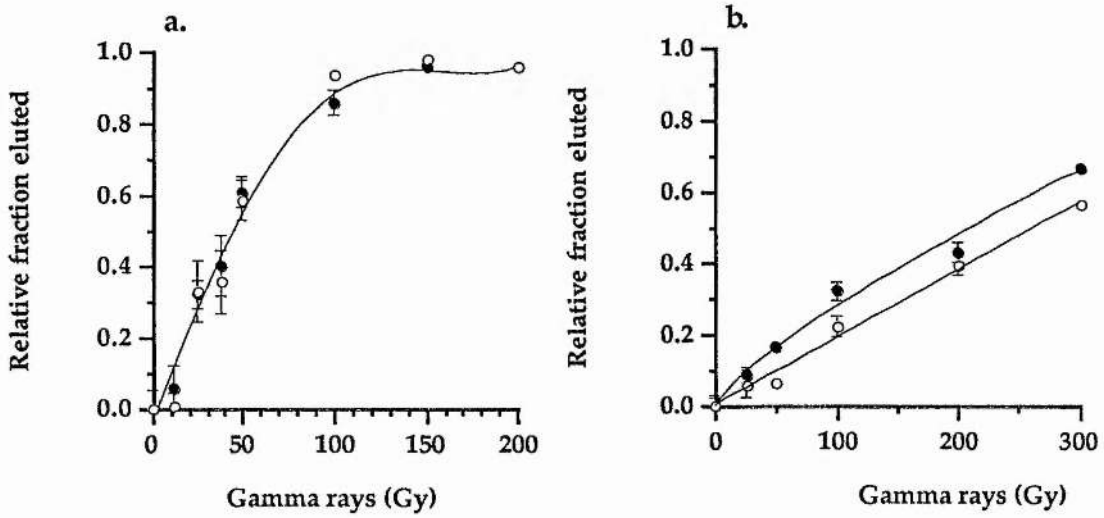

Figure 3.5. Gamma ray dose response. CHO (o) and *xrs-5* (•) cells were irradiated on ice and a) INFE or b) NINFE lysis and elution were performed. The graph shows the relative fraction of DNA eluted from the filter versus dose of γ-rays. Error bars shown the SEM of a minimum of 3 independent experiments. Two-way analysis of variance indicates no significant difference between the two cell lines after INFE or NINFE (INFE; $p = 0.978$, $F = 0.22$, $df = 7$. NINFE; $p = 0.891$, $F = 0.33$, $df = 5$). Curves fitted by eye.

Under non-ionic neutral filter elution conditions the response remained relatively linear over the entire dose range examined. The amount of DNA eluted was markedly reduced compared to INFE. NINFE released approximately one sixth of the DNA released by INFE per Gy over the linear region of the INFE curve. *Xrs-5* repeatedly showed more DNA eluted than CHO but this difference did not prove significant. The linear increase in elution with dose

indicates that release of DNA from nucleoids may occur via a "one-hit" process. The linearity observed may however be the result of too few data points for precise curve fitting to be performed.

To enable comparisons to be made between cell lines, after different doses or after repair intervals **RFE** values were converted to dose equivalents (**Deq**). **Deq** were defined as the dose of γ-rays that would produce the **RFE** value in question. **Deq** can be calculated by extrapolation from the above dose response curves. These are termed $\mathbf{Deq_{ninfe}}$ and $\mathbf{Deq_{infe}}$ depending on the technique used to determine the **RFE** values.

Direct comparisons cannot be made between the two techniques since the elution of DNA will be dependent on different factors. The expected model of elution from nucleoids involves two DSB existing within the same looped domain. These allow the intervening DNA segment to be released and eluted from the filter. Loops containing a single DSB would not cause DNA to elute from the filter. Therefore elution under NINFE would be the result of at least two DSB while under INFE only one DSB would be required to affect elution. The DNA remaining on the filter after NINFE should therefore also contain DSB from both loops which originally only contained one DSB and from the loops which contained two or more DSB and released segments of DNA. It was decided to examine whether DSB remained in the residual nucleoids left by NINFE. This was performed by first exposing irradiated cells to NINFE lysis and elution. After this an additional step of exposure to INFE lysis and elution was performed with the eluants collected separately. The results of these experiments are shown in Figure 3.6.

An exponential dose response was observed for both cell types with no significant difference between the two. There remained a significant fraction of DNA on the filter even at doses of 200 Gy where approximately 30% was retained. Using INFE alone virtually all DNA could be eluted from the filter at these doses. There are possible explanations for a fraction of DNA remaining on the filter; firstly rejoining of DSB is occurring during the NINFE stage. This is unlikely since all procedures are carried out at 4°C or less in the presence of 10 mM Na-EDTA, 2 M NaCl and 0.25% (v/v) Triton X-100. These conditions are likely to prevent rejoining processes involving extractable proteins, energy utilisation or soluble factors such as nucleotides etc. It may not prevent passive events involving the insoluble matrix proteins. The second possibility was that fixation of DNA to the filter occurs, possibly by retention or alteration of remnants of nucleoid structure during the initial INFE and/or subsequent NINFE. This is more likely since matrix DNA binding has been shown to be stabilised in the presence on 10 mM Na-EDTA. Whether or not this causes retardation of the DNA segments released from the matrix by two DSB occurring in the same looped domain is uncertain. The process of

elution of DNA from filters is still not understood. Therefore this two phased elution process may produce a reduction in the total amount of DNA eluted via an unknown mechanism.

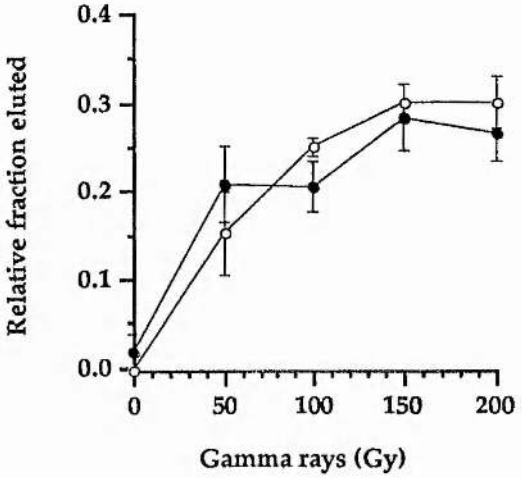

Figure 3.6. Ionic neutral filter elution of DNA from nucleoids after non-ionic neutral filter elution. Subsequent to NINFE irradiated CHO (°) and *xrs-5* (•) cells were lysed and eluted under INFE conditions. The relative fraction of DNA eluted versus γ-ray dose is shown. Error bars represent the SEM of a minimum of 3 independent experiments. Two-way analysis of variance shows no significant difference between CHO and *xrs-5* ($p = 0.889$, $F = 0.28$, 4 degrees of freedom).

3.3.3. *Repair of damage* .

To examine repair of damage a dose of 200 Gy was given. This dose was chosen since it gave a significantly high level of elution under NINFE and also gave elution within the saturated portion of the INFE dose response curve. This would mean that the main factor affecting the rate of elution would be release from the nuclear matrix as opposed to passage through the filter. After irradiation, the cells were incubated at 37°C for a repair interval of up to 16 hours. The cells were sampled at intervals and elution performed by either INFE or NINFE. The results are shown in Figure 3.7.

The relative fraction of DNA eluted as measured by INFE decreased with time in a biphasic exponential manner in both CHO and *xrs-5*. There was a sharp initial decrease in the relative fraction of DNA eluted over the first hour. This was followed by a reduced rate of decrease in CHO over the subsequent 15 hours. *Xrs-5* did not exhibit such a decrease, with a possible increase in elution after 4 hours repair.

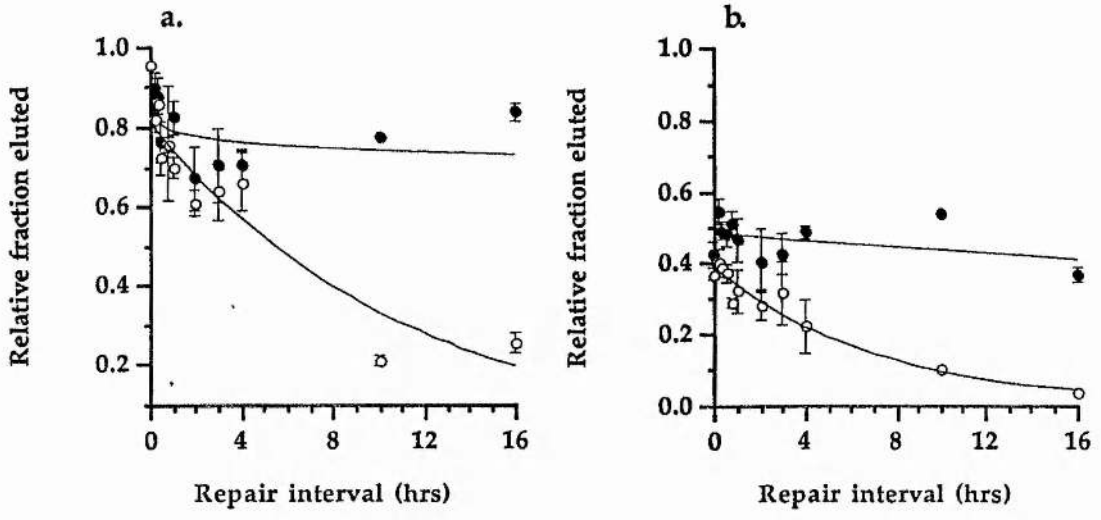

Figure 3.7. Repair of damage measured by ionic and neutral filter elution. CHO (°) and *xrs-5* (•) cells were irradiated with 200 Gy γ-rays on ice and then incubated at 37°C for the repair interval. The relative fraction of DNA eluted was measured at repair intervals using INFE (a.) or NINFE (b.). Error bars show the SEM a minimum of 3 independent experiments. Two-way analysis of variance shows a significant difference between cell lines in INFE ($p < 0.001$, $F = 18.75$, $df = 10$) and NINFE ($p < 0.001$, $F = 4.46$, $df = 10$). Curves fitted by eye.

NINFE appeared to reveal a different picture. Elution of CHO produced only a single exponential component to repair as opposed to the biphasic repair observed with INFE. *Xrs-5* did not exhibit any significant reduction in the level of DNA eluted. By conversion of the data to the dose equivalent amounts of damage remaining further detail of the repair processes are discernible (Figure 3.8). For INFE measured repair a biphasic pattern is distinguishable [e.g. Iliakis et al., 1991; Dahm-Daphi et al., 1993]. Both CHO and *xrs-5* exhibit a fast component of repair. At approximately 1 hour post-irradiation a slower rate of repair becomes apparent. In CHO the decrease in levels of damage remaining continues up to the limits of the experiment with 23.1 (± 1.56) Gy equivalents of damage remaining at 16 hours. In *xrs-5* this slow component is very much reduced over the same time period: Between 2 and 4 hours repair interval a plateau of approximately 60 Gy equivalent remains. After this time there was a slight rise with 86.5 (± 6.24) Gy equivalent remaining after 16 hours.

NINFE elution did not measure a fast component of repair in either CHO or *xrs-5*. CHO cells showed a single exponential component of repair falling to 19.1 (±3.11) Gy equivalents after 16 hours. No significant repair occured in *xrs-5*. From inspections of these graphs it would appear that whilst INFE measured lesions which were repaired by a biphasic process NINFE measured only a slow component to repair.

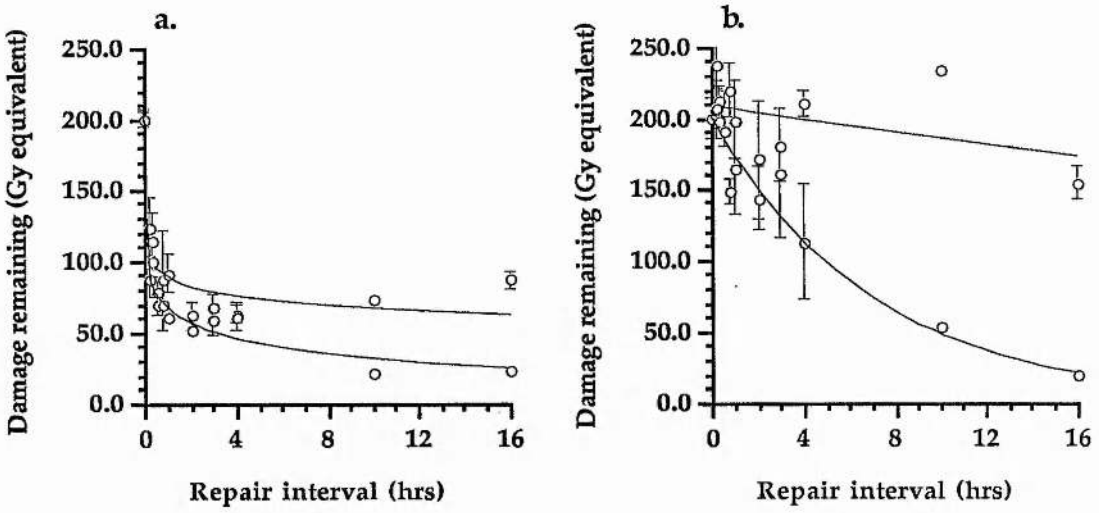

Figure 3.8. Repair of damage , dose equivalent. Graph shows the dose equivalent amount of damage remaining at various repair intervals after 200 Gy γ-rays. **RFE** values (as in fig. 6.) were converted to $\mathbf{Deq_{infe}}$ (a.) or $\mathbf{Deq_{ninfe}}$ (b.) for CHO (○) and *xrs-5* (•). Error bars show SEM of a minimum of 3 independent experiments. One-way analysis of variance indicated no significant reduction in damage in *xrs-5* cells as measured by NINFE ($p = 0.061$, $F = 1.94$, $df = 10$). Curves fitted by eye.

3.3.4. Residual damage.

It has been reported that in *xrs-5* the fraction of DNA damage left unrepaired increases with dose [Iliakis et al., 1992; Dahm-Daphi et al., 1993]. To examine whether NINFE might also reveal a dose dependent component to repair the damage remaining after 16 hours for a variety of doses was measured. These results are shown in Figure 3.9.

There was a significant difference between the levels of DNA eluted from CHO and *xrs-5* cells measured by both INFE and NINFE. The values of **RFE** were converted again to dose equivalents to permit a closer examination of the kinetics of residual damage (Figure 3.10). INFE does reveal an increasing fraction of unrepaired lesions with dose with the rise linear quadratic in appearance. This rise is more pronounced when measured by NINFE. The level of unrepaired lesions was approximately 100% with NINFE at high doses with a slight quadratic function. In CHO whilst there was an increase in the level of damage remaining this increase was very much reduced compared to *xrs-5*. The levels of damage remaining was similar with both techniques for CHO cells.

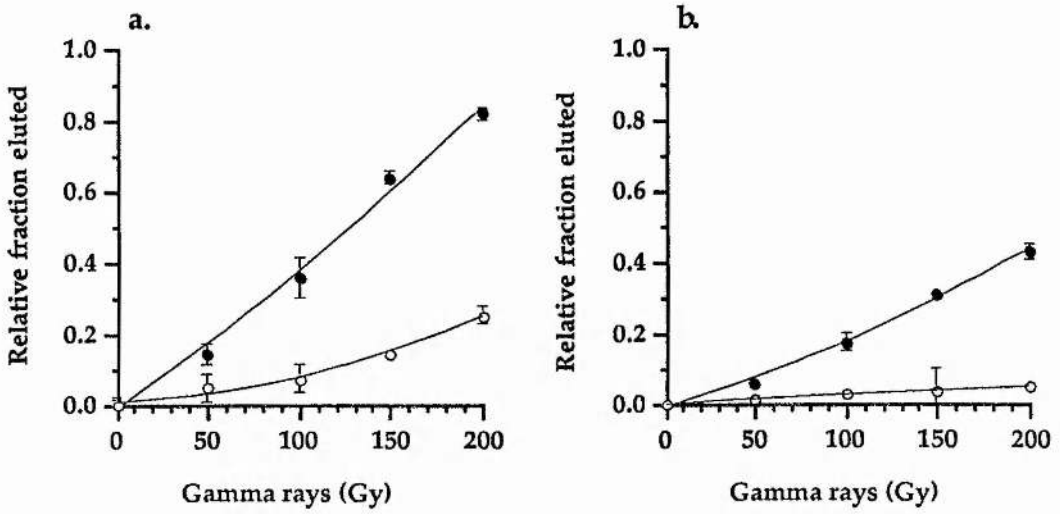

Figure 3.9. Residual damage as measured by ionic and non-ionic neutral filter elution. CHO (°) and *xrs-5* (•) were irradiated on ice and subsequently incubated at 37°C for 16 hours. Cells were then subjected to either INFE (a.) or NINFE (b.). Error bars show the SEM of the relative fraction DNA eluted from a minimum of 3 independent experiments. Curves fitted by eye.

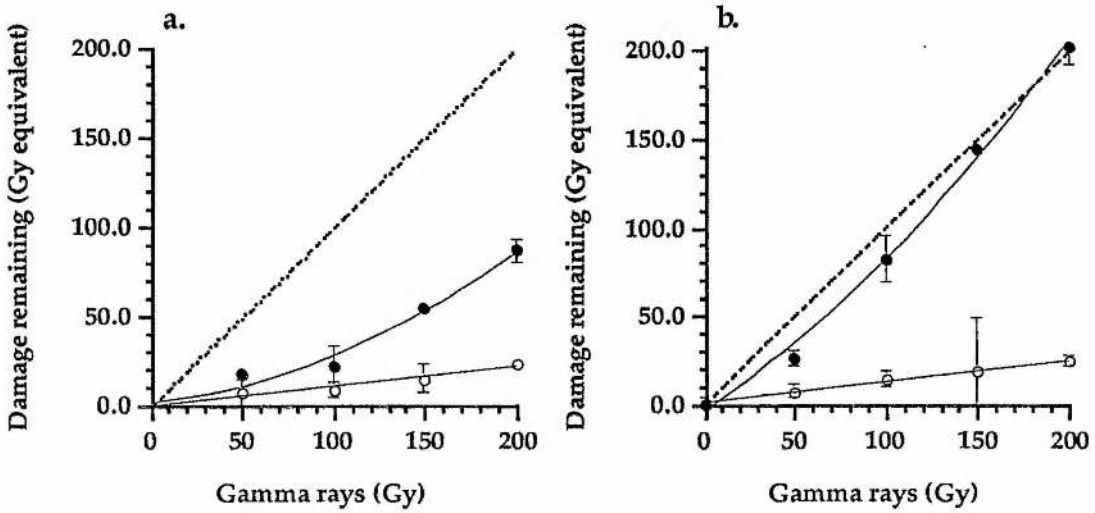

Figure 3.10. Residual damage as measured by ionic and non-ionic neutral filter elution, dose equivalent. CHO (°) and *xrs-5* (•) were irradiated on ice and subsequently incubated at 37°C for 16 hours. Cells were then subjected to either INFE (a.) or NINFE (b.). Graph shows the level of damage remaining in dose equivalents versus the initial dose. Error bars show the SEM from a minimum of 3 independent experiments. CHO curves fitted by eye. Also shown are lines of parity (·····) which approximates the level of damage corresponding to no repair.

The repair curves indicated that NINFE only measured the slow component of repair. However since it can only determine the level of damage released from the matrix there existed the possibility that the defect observed in *xrs-5* was the result of DSB mis-repair:

The release of DNA fragments could be caused by the joining of two adjacent DSB at the matrix with the loss of the intervening segment. This form of repair would be exhibited as a reduction in the total numbers of DSB, as estimated by INFE, but would not be shown by NINFE which would still measure the release of the fragment. A sequential NINFE followed by INFE protocol was performed as above, on cells irradiated with 200 Gy and permitted to repair for 16 hours. This is shown in Figure 3.11.

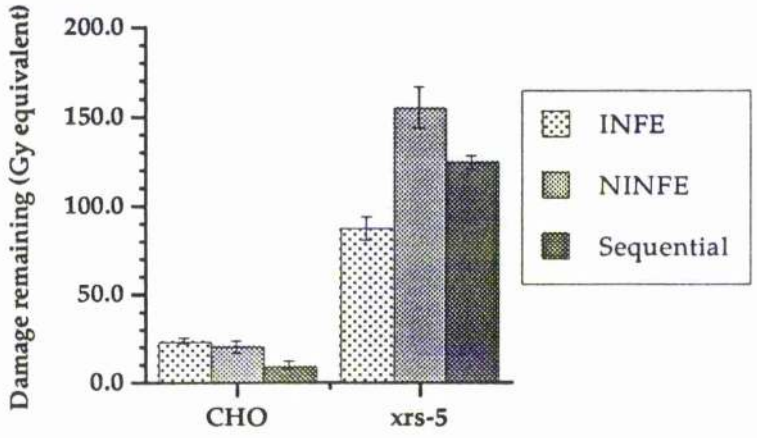

Figure 3.11. Residual damage as measured by INFE, NINFE and sequentially eluted nucleoids. CHO and *xrs-5* cells were irradiated with 200 Gy and incubated at 37°C for 16 hours. Dose equivalents were calculated from the relative fractions of DNA eluted after INFE, NINFE or the sequential INFE of nucleoids exposed previously to NINFE conditions and elution (**Deq** values for sequential elution calculated from data presented in figure 3.3.). Error bars show the SEM of a minimum of 3 independent experiments.

CHO exhibits a significant reduction in the level of damage remaining after this sequential elution. *Xrs-5* also shows a significant reduction however, this repair does not approach that observed with CHO cells. This would indicate that in *xrs-5* the repair of lesions in the portion of DNA retained on the filter after non-ionic detergent treatment is also defective.

3.4. *Discussion*

The results from the experiments described above indicate that the technique of NINFE reveals a possible correlation between the spatial orientation of DSB within chromatin and associated nuclear structures and the ability of cells to repair these lesions. The original hypothesis of the mechanism of DNA release from a nucleoid postulated that two DSB would be required within the same looped domain. In the initial experiments cells were lysed and eluted in the presence of a variety of NaCl concentrations. After 200 Gy γ-irradiation it was found that the amount of DNA eluted from the filter was dependent on this salt concentration. There was a rapid rise in the amount of DNA eluted between 0.75 M and 1.0 M.

In order for DNA to be released from the matrix it is necessary for the two ends of the DSB to dissociate. It is possible that this process may be limited by protein-DNA and protein-protein interactions with proteins effectively bridging the strand break. Therefore the increase in elution with increasing salt concentration may reflect the removal of these proteins hence exposing the DSB. Alternatively, the ends of the breaks may be revealed but, the segments of DNA may be held within the still relatively compact nucleoid by higher order structures including protein-DNA or protein-protein interactions some distance from the site of damage. The rise in fraction of DNA eluted between 0.75 and 1.0 M NaCl may indicate the involvement of histones H2A and H2B and/or histones H3 and H4. The binding of DNA to nucleosomes may help maintain the association of the two ends of a DSB. The release of the free energy of supercoiling by the disruption of H3- and H4-DNA interactions may also permit elution of DNA by relaxing the chromatin. The experiments performed here cannot distinguish the exact cause of the retardation of elution at low salt concentrations.

3.4.1. *Modelling the distribution of DSB using a Poisson based model.*

In order to describe the events involved in the elution of DNA from nucleoids a mathematical model of the processes involved in the measurement of the induction and repair of DSB by NINFE and INFE was produced.

On the assumption of a random distribution of DSB within DNA the probability of a break occurring within a defined target distance can therefore be modelled using Poisson distribution mathematics [Hartwig, 1978]. Models of DSB induction [Charlton et al., 1989] and their relationship to cell survival [Blöcher and Pohlit, 1982], and the measurement of DNA strand breaks by nucleoid sedimentation [Hartwig, 1978], pulsed field electrophoresis [Blöcher, 1990] and filter elution [Balbi et al., 1986; Nicolini et al., 1983] have all been proposed. These models have generally assumed one strand break (either DSB or SSB) per target or have modelled the effect of a reduction in size of DNA on its physico-chemical properties.

As described above; the DNA of eukaryotic cells is in the form of linear molecules as opposed to the circular genomes of bacteria etc. The introduction of topological configurations requires the genome to be constrained. In mammalian cells this occurs at two main levels; the replicon and the replicon cluster. A replicon is a stretch of DNA approximately 60 kbp in length containing one or more genes which is formed into a looped domain by attachment to the nuclear matrix via matrix attachment regions [Pienta and Coffey, 1984; Paulson and Laemmli, 1977; Mirkovitch et al., 1987]. These can be considered to be the fundamental unit of DNA replication and transcription [van Holde, 1989]. Supercoiling can occur within a replicon independent of the surrounding looped domains. These replicons are further organised into clusters, each of which may contain tens of individual replicons [Hartwig, 1978]. Under certain experimental conditions the supercoiling of all the component replicons of a cluster can be released by a single strand break within the cluster indicating that additional attachment to the matrix occurs by a different mechanism to that securing individual replicons. This attachment may involve the nuclear membrane which is removed during nucleoid extraction.

3.4.2. *Non-ionic neutral filter elution.*

The aim of producing the following model was to attempt to describe the observed results with non-ionic neutral filter elution on the basis of the induction of two DSB within a single domain and to determine some of the properties of that domain. In order that a Poisson based model could be formed it was necessary to make the following assumptions:

i) The distribution of DSB within the genome is random and follows a Poisson distribution. This assumes that although an ionising radiation track may produce multiple DSB, these are distributed throughout the genome. This is unlikely to be completely valid since, for example, track end structures etc. may result in localised regions of multiple damage types [Goodhead, 1994].

ii) The numbers of DSBs induced within a nucleus increases linearly with dose and is proportional to the DNA content of the cell. For this model the value of 21 DSB Gy^{-1} per haploid nucleus is used [Iliakis et al., 1991]. The size of the haploid CHO genome is taken as $\approx 3.8 \times 10^9$ bp (2.5×10^{12} D) [Buongiorno-Nardelli et al., 1982].

iii) The presence of single strand breaks and other DNA lesions have no influence on either the induction or repair of DSB.

iv) The genome consists of a number of equally sized "targets" or looped domains. Damage within one of these domains has no effect on either the induction or repair of lesions in neighbouring domains.

Although these assumptions restrict the validity of the model to some extent, they are necessary in order to produce the initial model.

Based on these assumptions the probability (p_n) of an individual target domain containing n DSB can be calculated from an adaptation of the equation of Poisson distribution [Wardlaw, 1985];

$$p_n = \frac{b^n e^{-b}}{n!} \tag{3.3}$$

Here n is the number of DSB within an individual domain and b is the mean number of breaks per domain for the whole nucleus given by

$$b = \frac{yd}{a} \tag{3.4}$$

With d the dose of radiation (Gy), y the yield of DSB Gy-1 nucleus^{-1} and a the number of domains per nucleus given by

$$a = \frac{g}{q} \tag{3.5}$$

Where q is the size of an independent domain (bp) and g is the size of the genome (bp).

Equation (3.3) gives the probabilty of any domain containing n DSB. This probability will be equivalent to the fraction of the total numbers of domains within a cell containing n DSB (f_n). Therefore the fraction of domains with no DSB, f_0 is given by

$$f_0 = \frac{b^0 e^{-b}}{0!}$$

$$= e^{-b} \tag{3.6}$$

The fraction of domains with 1 DSB, f_1 is

$$f_1 = \frac{b^1 e^{-b}}{1!}$$

$$= be^{-b} \tag{3.7}$$

And since q is the size of a domain (in bp) the sum of the fraction of domains with more than 1 DSB, f_Δ is

$$f_\Delta = \frac{b^2 e^{-b}}{2!} + \frac{b^3 e^{-b}}{3!} \ldots + \frac{b^q e^{-b}}{q!}$$

$$= \sum_{n=2}^{q} \frac{b^n e^{-b}}{n!} \qquad (3.8)$$

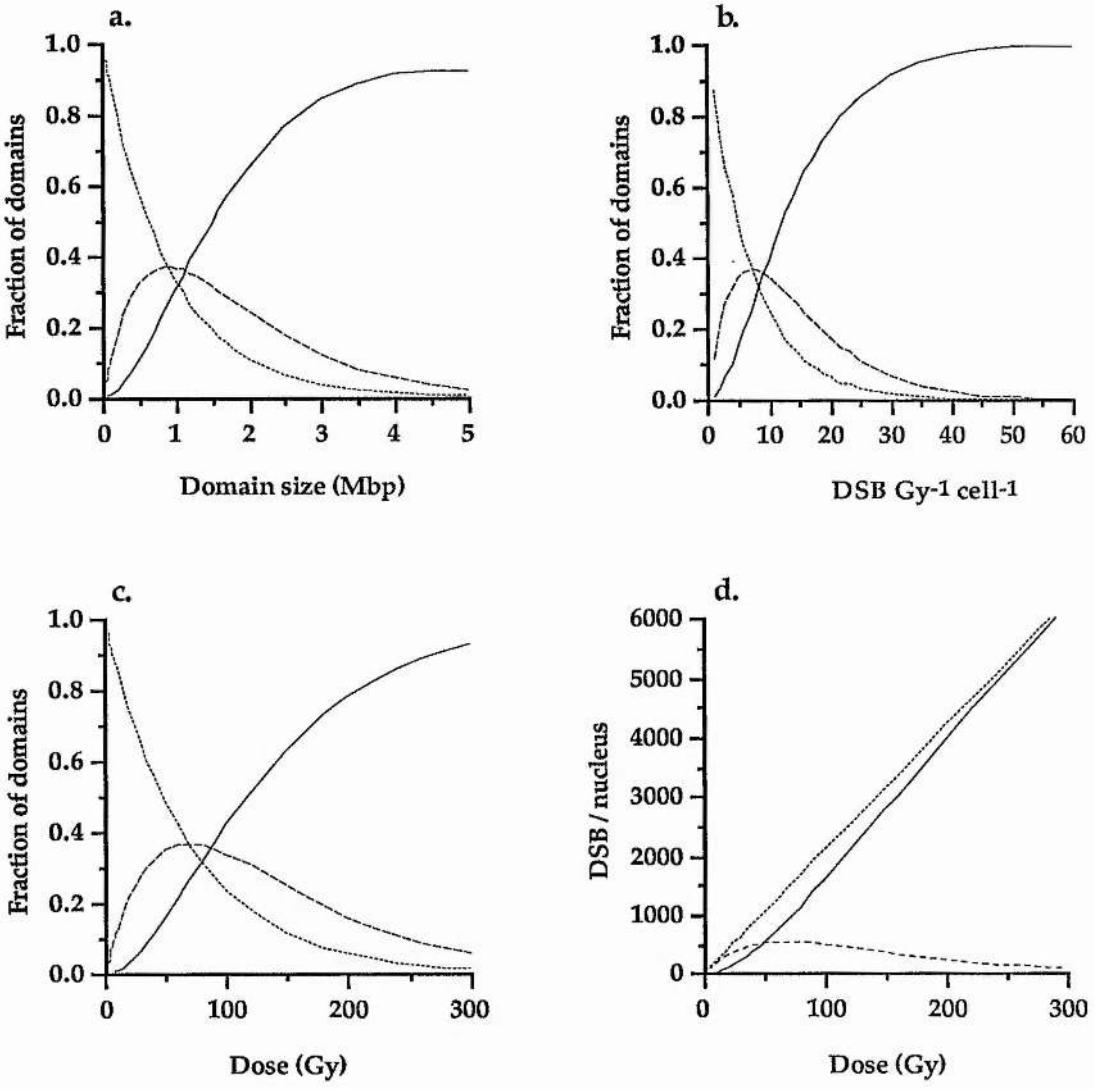

Figure 3.12. Modelling of the induction of DSB. **a.)** Effect of domain size on the fraction of domains containing 0 (·····), 1 (----) or >1 DSB (——). Dose = 200 Gy, yield = 21 DSB Gy^{-1}.
b.) Effect of the yield of DSB Gy^{-1} $nucleus^{-1}$ on the fraction of domains containing 0 (·····), 1 (----) or >1 DSB (——). Dose = 200 Gy, domain size = 2.6 Mbp.
c.) Effect of dose on the fraction of domains containing 0 (·····), 1 (----) or >1 DSB (——). Yield = 21 DSB Gy^{-1}, domain size = 2.6 Mbp.
d.) Numbers of DSB per nucleus within domains containing 1 (----) or >1 DSB (——). Total numbers of DSB given by the line (·····). Yield = 21 DSB Gy^{-1}, domain size = 2.6 Mbp.

Although, theoretically, the value of f_Δ could equal the size of a domain (q) for practical reasons calculations of f_Δ were normally calculated using n values of 2-18 DSB per domain. In Figures 3.12 the effect of loop size, dose and the yield of DSB induced per Gy on the fraction of

loops containing 0, 1 and more than 1 DSB domain^{-1} and the total numbers of DSB contained within these domains are shown.

These graphs show that altering any of the three main parameters; domain size; dose or yield of DSB per Gy, affects the distribution of DSB within domains. Generally, the fraction of domains containing more than 1 DSB is minimal at low doses but can rapidly rise until the majority of the domains contain more than 1 DSB. After an initial lag, the numbers of DSB contained within domains containing more than 1 DSB increases in an almost linear fashion, approaching 100% at high doses.

3.4.2.1. Fraction of DNA eluted under NINFE.

The premise made with the non-ionic filter elution technique was that DNA would be eluted only from looped domains containing two or more DSB. The fraction of DNA eluted from the filter can therefore be expected to be directly proportional to the fraction of domains containing two or more DSB. However, again assuming a random distribution of breaks along the length of the domain, two DSB in a loop will not release all of the DNA from that domain. The mean size of the segment of DNA that is left unattached to the site of fixation to the matrix will be given by

$$i_n = \frac{q(n-1)}{(n+1)} \qquad (3.9)$$

Where i_n is the amount of DNA released (bp) by n DSB in that domain and q is the size of the domain (bp). From Equation (3.9) one DSB will release zero DNA; 2 DSB 1/3 of the domain; 3 DSB 2/4 etc.

Since the fraction of domains containing more than 1 DSB f_Δ can be calculated using Equation (3.8), an estimate can be made of the fraction of the total amount of DNA that will become unattached from the matrix and hence available for elution from a cell and therefore from the filter. This is performed by substituting the size of the domain q by the fraction of domains with more than 1 DSB given by f_Δ. This gives the following equation for the estimation of the fraction of DNA eluted under NINFE conditions, FE_{ninfe}

$$FE_{ninfe} = \frac{f_\Delta(b_\Delta-1)}{b_\Delta+1} \qquad (3.10)$$

Where b_Δ is the mean number of DSB per domain containing more than1 DSB. Since the number of DSB is given by yd, the number of domains by a (Equation 3.5), the fraction of domains with only one DSB is given by f_1 (Equation 3.7) and the fraction with more than one DSB given by f_Δ (Equation 3.8) then b_Δ will be given by

$$b_{\Delta} = \frac{yd - af_1}{af_{\Delta}} \quad (3.11)$$

At the chosen dose of 2M NaCl; NINFE produced a measurable level of elution from irradiated nucleoids over a dose range of 25-300 Gy. These values of RFE are shown in Figure 3.13 along with calculated values of the fraction of DNA that can be expected to elute from the filter based on the above model. It gives the calculated values of FE_{ninfe} for loop sizes ranging from 325 kbp to 5.2 Mbp over a dose range of 0-300 Gy.

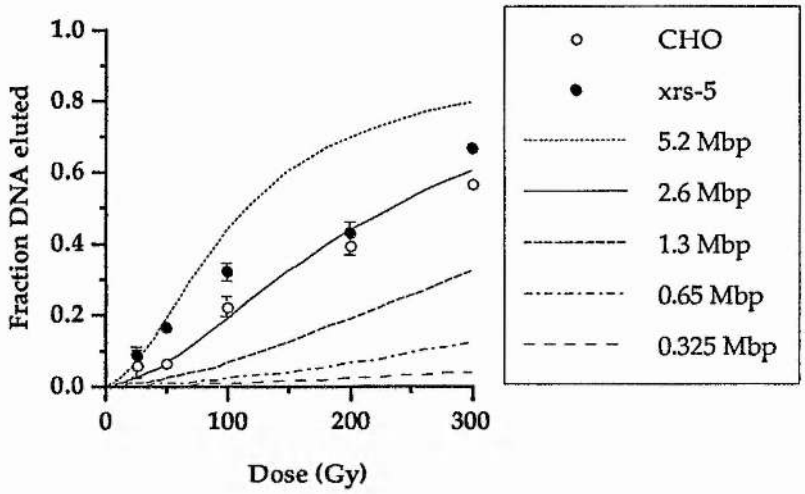

Figure 3.13. Estimation of the fraction of DNA eluted from a filter. Graph shows calculated values of the fraction of DNA eluted from nuclei with mean domain sizes ranging from 0.325 Mbp-6 Mbp. The assumption of a yield of 21 DSB Gy^{-1} $nucleus^{-1}$ was made. Also shown are the values of RFE measured for CHO and *xrs-5* cells by NINFE. Error bars show the standard error of the mean of a minimum of 3 independent experiments.

The shapes of the curves of the measured dose response and the model values show a possible correlation, with the best fit made by CHO cells. From this model estimates of the domain size involved in the elution from CHO and *xrs-5* cells lie between 2.4 and 3.4 Mbp (≈1100-1600 individual domains). This would place the domain size within the range of the clusters of replicons. The size of the individual replicons (approximately 100 kbp) is too small to produce significant levels of elution from the range of doses used in this study.

The measured values of RFE_{ninfe} for the two cell lines were not significantly different (see Results Section) although *xrs-5* consistently produced increased levels of elution compared to CHO. It could therefore be concluded, from the basis of this model, that both CHO and *xrs-5* posses similarly sized structures which, when containing two or more DSB, can potentially release the segments not attached to the nuclear matrix. For the purposes of further calculations the assumption was made that the domain size for the initial induction of elutable fragments of both CHO and *xrs-5* cells was 2.6 Mbp.

The values of f_Δ can give an indication of the dose required to produce a mean of one domain within a cell containing 2 or more DSB. This can be calculated from the inverse of the f_Δ which, when equal to the number of domains, will indicate the mean dose required to produce 1 domain per cell containing 2 DSB. For the range of domain sizes estimated for the two cell lines this gives a dose of around 2.55 Gy. This value is within the dose range used for calculation of survival curves

3.4.2.2. Repair/residual breaks.

If irradiated CHO and *xrs-5* cells were allowed to repair damage prior to performing NINFE then a large difference in the amount of DNA eluted was noticeable between the two cell lines. Two possibilities can explain this i) The domain size is decreased resulting in a decrease in the probability of more than 1 DSB occurring in given domain. ii) The DSB causing elution under NINFE are rejoined. Both of these hypotheses would result in a decrease in f_Δ and therefore the amount of DNA eluted from a cell. These hypotheses were modelled and compared to the data measured in CHO and *xrs-5* cells using NINFE. The measured $\mathbf{RFE_{ninfe}}$ values for the damage remaining after 16 hours repair interval for different doses are plotted along with calculated values of $\mathbf{FE_{ninfe}}$ in Figure 3.14.

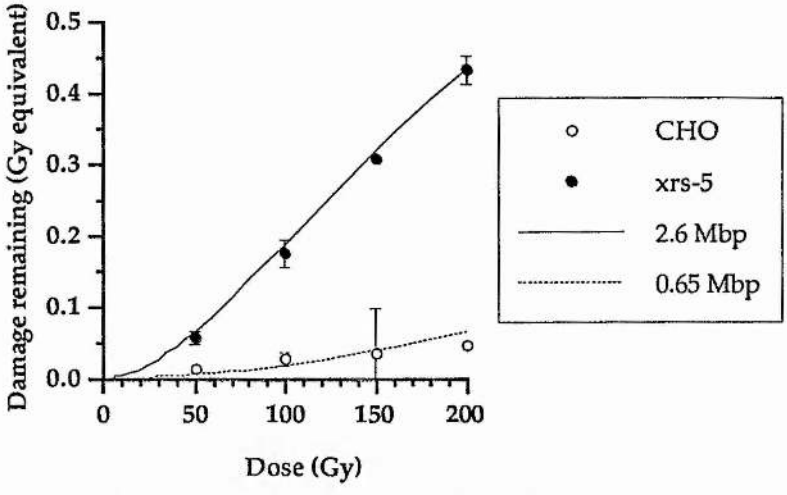

Figure 3.14. Fraction of DNA eluted after 16 hours repair interval. RFE values for CHO and *xrs-5* are plotted versus dose of γ-rays. Error bars represent the standard error of the mean of a minimum of 3 independent experiments. Curves represent the calculated values of $\mathbf{FE_{ninfe}}$ based on domain sizes of 2.6 Mbp and 0.65 Mbp.

The estimates of target size that correlate with the measured values are 0.65 and 2.6 Mbp for CHO and *xrs-5* respectively. Thus the apparent repair observed in CHO cells by the NINFE technique could be explained by a four-fold reduction in the target size. *Xrs-5*, which does not exhibit repair under NINFE, exhibits no such reduction.

The second hypothesis was modelled by comparing the kinetics of the measured reduction in elution with an exponential repair model described by the equation

$$r_t = r_0 e^{-\beta} \quad (3.12)$$

Here r_0 is the initial amount of damage, r_t is the amount of damage remaining after a repair interval t (hours) and β is the time constant given by

$$\beta = \frac{t}{\delta} \quad (3.13)$$

With t the repair interval (hours) and δ the repair constant (time for damage to equal e^{-1} initial r_0)

Based on calculated dose equivalents using Equation (3.12), Figure 3.15 shows the residual damage after 16 hours repair interval for different doses and the repair kinetics of the reduction of damage based on an initial dose of 200 Gy and varying values of δ. Also shown are the Deq_{ninfe} values for CHO and *xrs-5* after 200 Gy. From this model approximations of the values of repair constant; δ, are 7.5 and greater than 120 hours for CHO and *xrs-5* respectively. The repair constant for *xrs-5* indicates that negligible repair of this form of damage occurs in the mutant cell line .

The model described above is based purely on the Poisson distribution of DSB within a genome comprised of a number of discrete domains or targets. It would appear that the elution of DNA under NINFE can be described by this model. It is therefore proposed that the induction of two DSB per domain results in a fragment of DNA which can subsequently be eluted from the bulk of the genome. In CHO cells these lesions can undergo "repair". This can be described by an exponential equation with a repair constant of approximately 7.5 hours which corresponds to a half life of the elutable fragment of approximately 5.2 hours. This repair could be due to the physical rejoining of at least one of the causative DSB. It should be remembered that the repair of only one DSB is required to prevent the elution of the fragment from the nucleoid. The alternative suggestion is that a structural rearrangement occurs within the nucleus which results in the reduction of the mean domain size. This would have the effect of reducing the probability of two DSB occurring within the same domain, and so the fraction of DNA that can be eluted. This possibility can be described by a four-fold reduction in the mean domain size. With this hypothesis no actual rejoining of DSB is required and the kinetics of repair can be related to the rate of change of domain size. In *xrs-5* cells no repair is observed with similar levels of damage remaining after 16 hours repair interval in the dose range of 50-200 Gy.

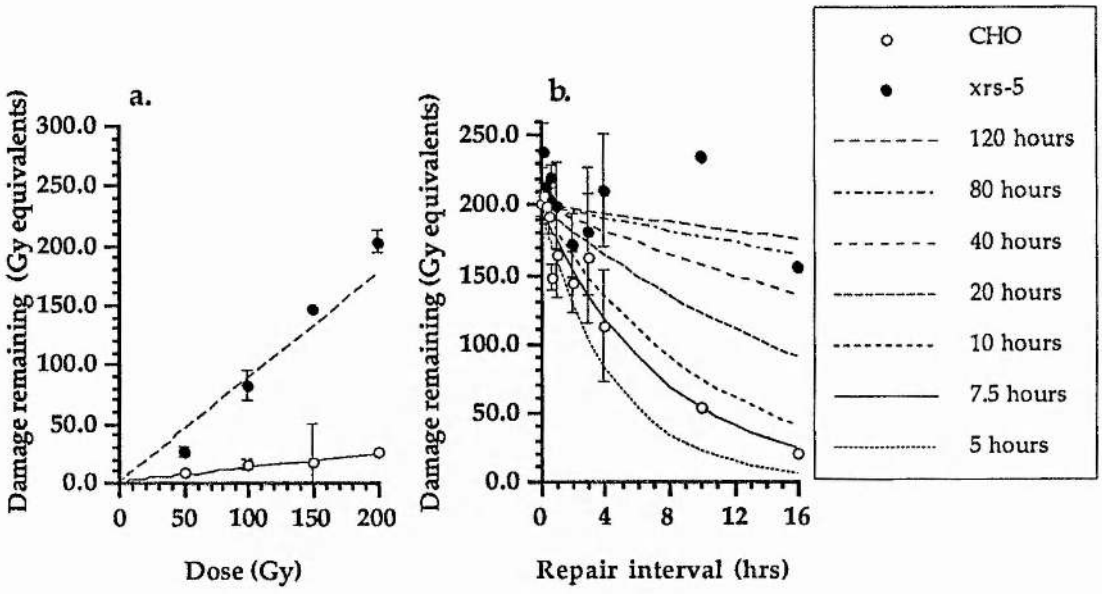

Figure 3.15. Model of the repair of DSB as measured by NINFE. **a.)** Damage remaining (Gy equivalents) after 16 hours as measured by NINFE for CHO and *xrs-5* irradiated with different doses of γ-rays. Error bars represent the mean of a minimum of three independent experiments. Curves represent the calculated $\mathbf{Deq_{ninfe}}$ values using Equation (3.12) Repair constants (δ) = 7.5 and 120 hours.
b.) Damage remaining (Gy equivalents) after different repair intervals as measured by NINFE for CHO and *xrs-5* irradiated with 200 Gy of γ-rays. Error bars represent the mean of a minimum of three independent experiments. Curves represent the calculated $\mathbf{Deq_{ninfe}}$ values using Equation (3.12) Repair constants (δ) range from 5-120 hours.

3.4.3. *Ionic neutral filter elution.*

NINFE measures only DNA fragments released from domains containing two or more DSB with the fragment of DNA that is eluted proximal to both DSB. The elution of DNA by INFE is supposed to be proportional to the total numbers of DSB within a genome. Actually modelling the effect of individual DSB on INFE elution is far more complex than for NINFE and various models have been described which have attempted to explain the behaviour of DNA on a filter [Nicolini et al., 1983; Balbi et al., 1986; Olive, 1992]. However, it might be expected that elution would be proportional to the size of DNA fragments which decreases exponentially with increasing numbers of DSB (Figure 3.16). The mean size of DNA fragments (k) produced by a given dose of γ-rays can be described by the equation;

$$k = \frac{g}{yd+c+1} \qquad (3.14)$$

Here g is the size of the genome (bp) and c is the number of chromosomes per cell.

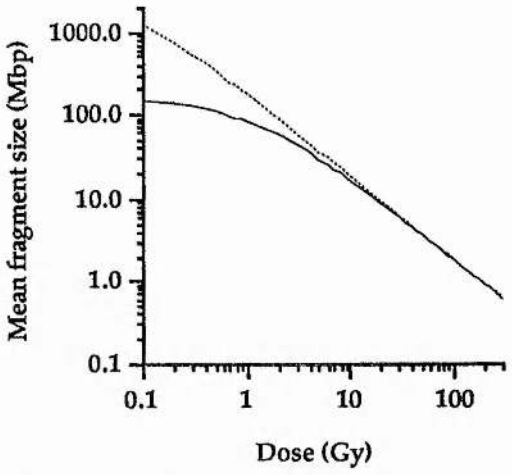

Figure 3.16. Mean size of fragments of DNA after irradiation. Graph shows the calculated mean fragment length (Mbp) of DNA using Equation (3.14) Calculations based on a yield of 21 DSB Gy^{-1} per nucleus; a total genome length of 3.8 Gbp which is in the form of either a single linear molecule (——) or consists of 23 chromosomes (·····).

That the genome is segregated into chromosomes can make a significant difference to the mean fragment size of DNA after low doses of irradiation. The assumption that genomic DNA is in the form of a single molecule of DNA produces a linear regression as a function of $\log_{10}$(dose) versus $\log_{10}$(fragment size). By dividing the genome into chromosomes, a shoulder in this curve is observed at low doses. If INFE measures DSB induction by the amount of elution being proportional to the relative difference in size between irradiated and unirradiated samples then this shoulder might affect the detection of DSB at these low doses. Shoulders are observed with NFE under certain lysis condition [Radford, 1985; 1988]. However, the doses used in this study are all outside this shoulder region (i.e. 12.5-300 Gy) and so it is assumed that fragment size decreases constantly in proportion to dose.

The limit of resolution for INFE is approximately 5 Gy and it can be observed that the mean fragment size produced by this minimum dose is approximately 30 Mbp. At the other end of the range, where elution approaches 100% (≈ 100 Gy) the mean fragment size is approximately 2 Mbp. The mean size of fragments released by 2 DSB in a single domain under NINFE will be approximately 0.9 Mbp (from Equation (3.10) based on domains of 2.6 Mbp). This lies within the saturation portion of the INFE range. This supports the assumption that the main factor affecting NINFE elution will be the relative frequency of 2 or more DSB in a single domain and the size of these domains.

Equation (3.14) allows examination of the results from the sequential elution involving first exposing irradiated cells to INFE and then to NINFE conditions. The final amount of DNA eluted after this sequential elution was consistently lower than after INFE alone. The first

stage of the sequential elution would remove fragments released from the domains containing more than 1 DSB. This would presumably leave the DSB contained in domains with a single DSB plus effectively one DSB per domain which originally contained more than 1 DSB. Therefore the total number of DSB within the nucleoid retained on the filter will be given by;

$$s = a(f_1+f_\Delta) \tag{3.15}$$

By substituting s in the expression for **yd** in Equation (3.14) and since the amount of DNA left on the filter will equal the original amount minus that which elutes, the mean fragment size of the DNA left on the filter (residual mean fragment size; $k_{retained}$) will be given by

$$k_{retained} = \frac{g(1-FE_{ninfe})}{s+c+1} \tag{3.16}$$

Where the value of $(1-FE_{ninfe})$ gives the fraction of DNA retained on the filter as calculated from Equation (3.10).

The mean fragment size of the DNA eluted from the filter (k_{eluted}) can be obtained by

$$k_{eluted} = \frac{q}{b_\Delta+1} \tag{3.17}$$

The mean fragment sizes of these two fractions of DNA are plotted in Figure 3.17. This graph shows the mean size of the fragments relative to the mean size of DNA given by Equation (3.14).

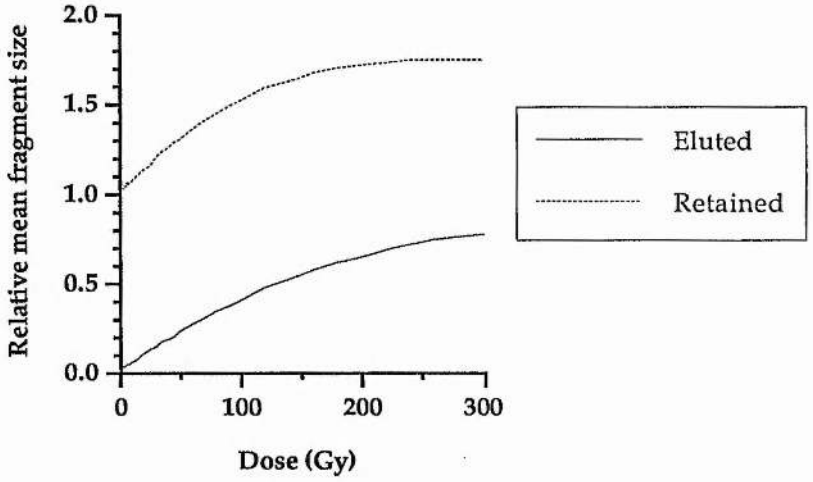

Figure 3.17. Relative size of the DNA fragments during NINFE. Graph shows the effect of dose on the calculated mean size of the fragments of DNA which are retained on the filter or eluted from the filter relative to the overall mean fragment size given by Equation (3.14).

This shows that compared to the overall mean fragment size, the mean fragment size of DNA left on the filter is larger and the mean fragment size of DNA eluted is smaller. If, under INFE, small fragments normally enhance the elution of larger fragments then this could explain the results obtained with the sequential elution of irradiated DNA.

3.4.3.2. Repair/residual breaks.

When the repair curves seen with INFE are examined they appear to be biphasic with two exponential components. The monophasic slow repair observed in CHO cells with NINFE could be assumed to form the slower of these two components since it is absent in both INFE and NINFE experiments with *xrs-5*. The next logical assumption would be that the slow component observed with INFE is therefore due to the repair of DSB within domains containing 2 or more DSB, while the faster component is due to the repair of domains with only one DSB. When the fractions of loops containing 1 or >1 DSB are examined (Figure 3.12) e.g. for 200 Gy, it would appear that only 16% of the domains contain 1 DSB only while 78% contain 2 or more DSB, based on a domain size of 2.6 Mbp. In terms of dose equivalents, the domains with multiple DSB contain 188.7 Gy equivalents while only 11.3 Gy equivalents occur singly. However, the measurements of $\mathbf{Deq_{infe}}$ would indicate that the slow component is responsible for the repair of approximately 60 Gy equivalents of the initial damage. If elution under INFE is proportional only to the numbers of DSB this would indicate that the fast component of repair involved DSB within domains containing both single and multiple DSB; in contradiction to the results obtained with NINFE. Modelling of the mean fragment sizes of irradiated DNA to the sequential results indicate that elution of DNA may not be proportional to the numbers of DSB but also to the distribution of these DSB. The repair of DSB may therefore cause disproportionate decreases in amounts of DNA eluted according to their position in relationship to other DSB. As shown in Figure 3.17 the mean fragment size of DNA retained on the filter after NINFE (as given by Equation (3.14)) is larger than that of the fragments which are eluted (as given by Equation (3.16)). This effect is particularly noticeable at low doses. The repair of a single DSB within a domain containing only one DSB will therefore result in a larger decrease in the fraction of DNA eluted than that produced by the repair of a DSB within a multiply damaged domain. Caution must therefore be taken when extrapolating the amount of damage represented by a given fraction of DNA eluted. At low doses, when the proportion of domains with more than 1 DSB is low, this effect will be negligible since the majority of lesions will occur singly and repair will cause a proportionate decrease in elution. As f_Δ increases the importance of the disproportionate sizes of fragments on the measurement of repair will increase. The practical aspects of this may be the cause of the apparently large fast component to repair. The actual numbers of DSB involved in this component may be much fewer than calculated by extrapolating from the apparent dose equivalent graph.

The repair constant for the slow component, δ'' measured by NINFE was approximated to 7.5 hours. By making the assumption that the slow component observed with INFE is also the repair of DSB within domains containing multiple DSB the repair data measured can be adjusted to actual numbers of DSB. This can be performed by the following equations

$$r_t = r_0' e^{-\beta' w'} + r_0'' e^{-\beta'' w''} \quad (3.18)$$

Where r_t is the damage remaining after repair interval t, r_0' is the damage repaired by fast component, r_0'' is the damage repaired by slow component, β' and w' are the fast component constants and β'' and w'' are the slow component constants.

The constants w' and w'' are estimates of the possible effect of the disproportionate mean sizes of the fragments produced by the DSB repaired by the two components and are approximated by the equation;

$$w = \frac{\text{Apparent damage}}{\text{Actual damage}} \quad (3.19)$$

Where the apparent damage is the fraction of damage repaired by a given component estimated from the repair curves measured. The actual damage is the calculated fractions of damage contained within either the domains with a single DSB (fast component) or the domains with multiple DSB (slow component).

By making the above approximations, Equation (3.18) can describe the repair of DSB measured by INFE as shown in Figure 3.18.

The approximations of the repair constants for the slow component are 15 and 240 hours for CHO and *xrs-5* respectively. The value for CHO is twice that measured by NINFE and may indicate that while only one DSB is required for the repair to be measured by NINFE, INFE requires the repair of two DSB to produce the same reduction in elution. The approximations of the repair constants, δ for the fast component are 12 and 21 minutes for CHO and *xrs-5* respectively.

However, it should be noted that several major assumptions have been made with regards the correction of INFE measurements to actual figures of damage. That correcting factors (w) are required to produce a model that fits the measured data implies that these cannot be considered an accurate model. Further work on the actual levels of DSB represented by the two components is required. The non-Poisson effects of differently positioned DSB make modelling of the induction and repair of lesions measured by INFE complex, and therefore difficult to predict using the Poisson based model which describes NINFE.

Because of the large number of assumptions made in the above model of repair as measured by INFE, it is necessary to consider possibilities for the lesions repaired by the fast and slow components other than a demarcation based solely on whether DSB occur singly or in multiples within a domain. Any hypothesis is required to fulfil both the observation that in *xrs-5* no slow repair is observed and with INFE *xrs-5* exhibits only the fast component to repair. i.e. The lesions repaired by a fast component with INFE must have no effect on the elution of fragments measured by NINFE.

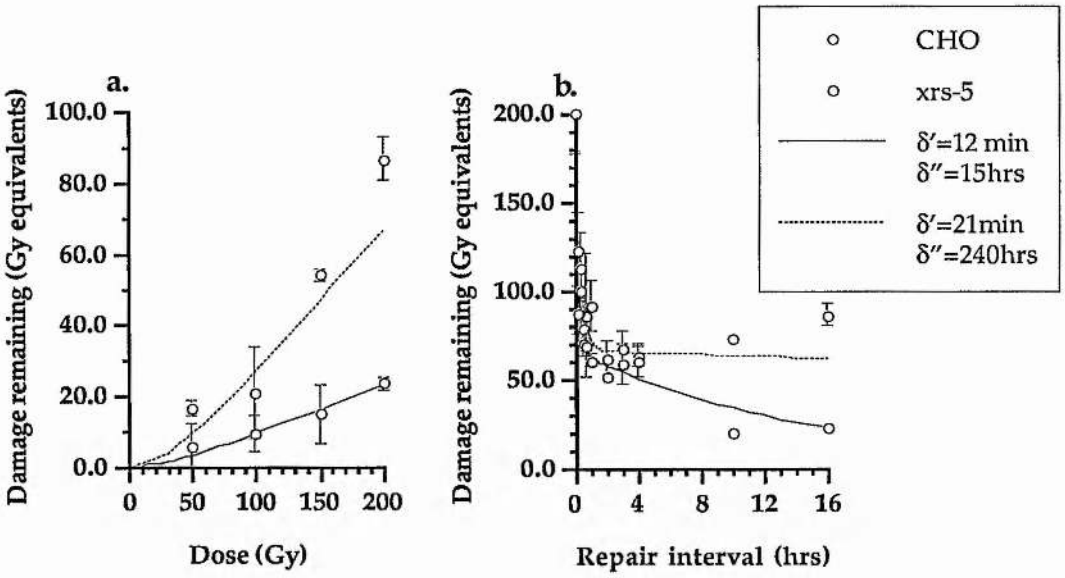

Figure 3.18. Model describing the repair of damage measured by INFE. Graph shows the measured values of the damage remaining (in dose equivalents) measured by INFE.
a.) Effect of dose on residual damage in cells subsequently allowed to repair for 16 hrs.
b.) Effect of repair interval on repair of DSB in cells irradiated with 200 Gy γ-rays. Error bars represent the standard error of the mean of a minimum of 3 independent experiments. Lines indicate the calculated values of the damage remaining using Equation (3.17). Adjustment constants (w' and w") based on approximations of the fast and slow components of repair equalling 134 and 66 Gy equivalents respectively. These approximations estimated from the minimum values of repair obtained for *xrs-5*.

In addition to the repair of DSB within domains with no other DSB, hypotheses are limited to the additional numbers of DSB comprising DSB rejoined between the fragments of DNA released under NINFE or by the repair of DSB within the residual DNA not eluted by NINFE; e.g. between the matrix associated ends at the point of detachment of fragments released by NINFE (Figure 3.19). Both of these models produce a decrease in the total numbers of breaks without the prerequisite of rejoining of released fragments to the bulk of the DNA attached to the matrix. It would be difficult to find evidence for or against the former model without specifically examining the size of the fragments released by NINFE at different time points. The latter model can be examined within the scope of the experiments performed in this study. Since it is proposed that DSB are rejoined at the matrix during the

fast component then a similar reduction in the elution of DNA from the sequentially treated residual nucleoids in both CHO and *xrs-5* should have been observed. Figure 3.11. indicated no such decrease.

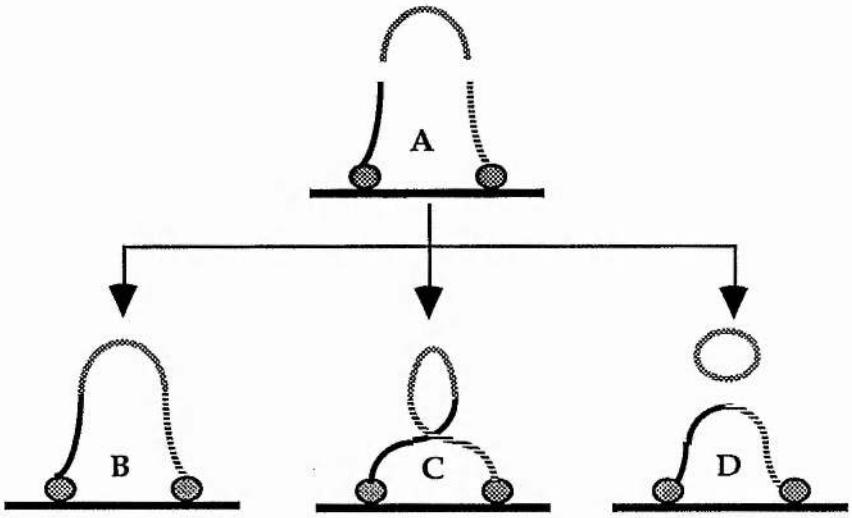

Figure 3.19. Possible repair structures in a DNA looped domain containing 2 DSB. If a loop of DNA contains 2 DSB; **A**, then there are four ends, two matrix bound ends and two non-matrix bound ends. These can be rejoined in one of three ways. **B**; repair proceeds correctly with each end of the DSB rejoining its sister end. **C**; Rejoining of the matrix bound ends occurs to the wrong non-matrix bound end resulting in an inversion of the non-matrix bound segment of DNA. **D**; Rejoining occurs between the matrix bound ends and/or between the non-matrix bound ends resulting in deletive rejoining with the non-matrix bound segment possibly forming a circular structure.

A fourth hypothesis can also be put forward for the lesions repaired by the fast component. At present it has been assumed that the DSB contained within irradiated DNA come solely from the direct effects of the radiation. However, the possibility exists that radiation induced DSB cause additional DSB via a cellular mechanism. Again these DSB would have to exist in such a manner so as not to contribute to elution under NINFE. DSB are routinely introduced into DNA as a part of the normal metabolism of DNA via topoisomerse II. This enzyme produces protein linked DSB during the strand passing reaction which occurs during decatenation of interlinked circular DNA molecules and also during the relaxation of supercoils. Normally, these DSB are transient and are only observed after inhibition of the rejoining reaction by drugs such as etoposide and m-AMSA. In addition, these DSB require the harsh denaturation processes associated with INFE to be revealed. The *in vivo* state of DNA involves the maintenance of positive supercoiling within the looped domains which indicates that topoisomerase is in a non-active state. Alterations in the *status quo* supercoiling levels may cause the enzyme to attain an active state with the resultant cleavage of DNA. It is therefore conceivable that the relaxation of DNA that occurs by radiation induced DSB may result in DNA strand cleavage at the nuclear matrix by

topoisomerase II. Again no direct evidence for this can be observed from the above experiments so it remains as a conjectural point.

3.5. Conclusions.

By the use of a mathematical model based on Poisson distribution it has been possible to describe the events leading to elution under NINFE. This model suggests that the genome of both CHO and *xrs-5* cells is segregated into independent domains approximately 2.6 Mbp in length. When two or more DSB occur within a domain then elution of a fragment of that domain occurs. It is these fragments which are postulated to be the basis of the measurement of damage by NINFE. The size of these domains places them in the range of the intermediate domains described by several workers for different cell lines [reviewed in Walicka and Godlewska, 1989]. These domains exist as independent supercoiled units after extraction of nucleoids with Triton X-100 and 2 M NaCl. They may, in turn be composed of 20-30 individual sub-domains approximately 100 kbp in length. [Hartwig, 1978]. The sub-domains, although independent of each other to a large extent *in vivo* , lose this independence on extraction.

3.6. *Glossary of mathematical terms, constants and equations.*

Numbers in parentheses indicates equations by which terms are calculated.

a : Number independent domains per nucleus (3.5).

b : Mean number of DSB per domain for the whole nucleus (3.4).

b_Δ : Mean number of DSB per domain which contain more than 1 DSB.

β : Time constant (3.13).

β′ : Fast component time constant.

β″ : Slow component time constant.

c : Mean number of chromosomes per cell.

d : Dose of radiation (Gy).

δ : Repair constant (hours).

δ′ : Fast component repair constant (hours).

δ″ : Slow component repair constant (hours).

Deq : Dose of γ-rays that would produce a given **RFE** value.

Deq_{infe} : Dose of γ-rays that would produce a given **RFE** value under INFE conditions.

Deq_{ninfe} : Dose of γ-rays that would produce a given **RFE** value under NINFE conditions.

DPM : Disintegrations per minute.

DPM_{eluate}: Disintegration per minute in the total volume of buffer eluted through a filter.

DPM_{total} : Disintegrations per minute remaining on a filter plus DPM_{eluate}.

f_n : Fraction of the total number of domains containing n DSB.

f_0 Fraction of the total number of domains containing no DSB. (3.6).

f_1 Fraction of the total number of domains containing 1 DSB. (3.7).

f_Δ Fraction of the total number of domains containing more than 1 DSB. (3.8).

FE : Fraction of DNA eluted from a filter (3.1).

$FE_{control}$: Fraction DNA eluted by an unirradiated control (3.1).

FE_{ninfe} : Calculated fraction of DNA eluted from a filter under NINFE conditions (3.10).

g: Size of the genome (bp)

i_n : Amount of DNA released (bp) by **n** DSB within that domain (3.9).

k: Mean size of DNA fragments produced by a given dose of radiation (3.14).

$k_{retained}$: Mean DNA fragment size of DNA left on the filter after NINFE lysis and elution.(3.16).

k_{eluted} : Mean fragment size of DNA eluted under NINFE conditions (3.17).

n: Number of DSB within an individual domain.

p_n : Probability of an individual target domain containing **n** DSB (3.3)

q: Size of an independent domain (bp).

r_t : Amount of damage remaining after a repair interval **t**. (3.12).

r_0 : Initial amount of damage.

RFE: Relative fraction eluted (FE corrected for background damage) (3.2)

RFE_{infe} : Relative fraction of DNA eluted under INFE conditions.

RFE_{ninfe} : Relative fraction of DNA eluted under NINFE conditions.

s: Total number of DSB retained on the filter after NINFE lysis and elution (3.15).

t: Repair interval (minutes)

w: Fragment size correction factor (3.19).

w' : Fast component correction factor.

w'' : Slow component correction factor.

y: Yield of DSB Gy^{-1} nucleus $^{-1}$.

(3.1) $$FE = \frac{DPM_{eluate}}{DPM_{total}}$$

(3.2) $$RFE = \frac{FE-FE_{control}}{1-FE_{control}}$$

(3.3) $$p_n = \frac{b^n e^{-b}}{n!}$$

(3.4) $$b = \frac{yd}{a}$$

(3.5) $$a = \frac{g}{q}$$

(3.6) $$f_0 = \frac{b^0 e^{-b}}{0!} = e^{-b}$$

(3.7) $$f_1 = \frac{b^1 e^{-b}}{1!} = be^{-b}$$

(3.8) $$f_\Delta = \frac{b^2 e^{-b}}{2!} + \frac{b^3 e^{-b}}{3!} \ldots + \frac{b^q e^{-b}}{q!} = \sum_{n=2}^{q} \frac{b^n e^{-b}}{n!}$$

(3.9) $$i_n = \frac{q(n-1)}{(n+1)}$$

(3.10) $$FE_{ninfe} = \frac{f_\Delta(b_\Delta-1)}{b_\Delta+1}$$

(3.11) $$b_\Delta = \frac{yd-af_1}{af_\Delta}$$

(3.12) $$r_t = r_0 e^{-\beta}$$

(3.13) $$\beta = \frac{t}{\delta}$$

(3.14) $$k = \frac{g}{yd+c+1}$$

(3.15) $$s = a(f_1+f_\Delta)$$

(3.16) $$k_{retained} = \frac{g(1-FE_{ninfe})}{s+c+1}$$

(3.17) $$k_{eluted} = \frac{q}{b_{\Delta}+1}$$

(3.18) $$r_t = r_0' e^{-\beta' w'} + r_0'' e^{-\beta'' w''}$$

(3.19) $$w = \frac{\text{Apparent damage}}{\text{Actual damage}}$$

Chapter 4

DNA binding activities of proteins extracted from *xrs-5* .

Summary.

Results presented in this chapter indicate that the mutation in *xrs-5* may involve an alteration in the DNA binding activity of extractable nuclear proteins. The affinity of proteins for double-stranded calf thymus DNA was measured in nuclear extracts of CHO and *xrs-5* cells. There was an alteration in the DNA binding activity of extractable proteins from *xrs-5* as measured by a filter binding assay. By the use of the technique of tricine-SDS-PAGE and South-Western blotting, it was possible to identify the approximate molecular weights of these DNA binding proteins.

Differences were found in DNA binding between proteins from CHO and *xrs-5* extracts of both non-irradiated and irradiated (10 Gy ^{137}Cs γ-rays + 30 minutes incubation at 37°C) cells. Two proteins with apparent molecular weights of 32.2 and 31.8 kDa exhibited a lower DNA binding activity in *xrs-5* than proteins of similar extracts from CHO. The amount of the higher molecular weight protein was less in the *xrs-5* extracts than in the CHO extracts, as measured by Coomassie blue staining. The two proteins have not yet been identified but comprise a major DNA binding activity in CHO extracts obtained by detergent-free extraction procedures. There is circumstantial evidence that suggests these two polypeptides may form part of the histone H1 family.

4.1. Introduction.

While the radiosensitive phenotype in *xrs* cells has been extensively examined [reviewed in Jeggo, 1990; Collins; 1993] the cause of this sensitivity is not fully understood. The enhanced frequencies of induced chromosomal aberrations and reduced survival in response to radiation and other DNA damaging agents has been correlated to the defective repair of DSB [Kemp et al., 1984; Dahm-Daphi et al., 1993]. In turn, the structural differences observed between the wild-type and *xrs* cells [Yasui et al., 1991; 1994; Schwartz et al., 1992; 1993] would appear to be linked to this repair deficiency. The question must be asked whether these structural alterations are coincidental to the repair defect or are causally related. The results from chapter 3 suggest that the position of DSB within higher order structures influences the repair of these lesions. It was postulated that in *xrs-5*, DSB which exist in multiples within a single looped domain may not be repaired. In contrast, these lesions are repaired (with slow kinetics) in the wild-type. These results do not identify specific mechanisms for the repair of multiple lesions only that they are non-reparable in the mutant.

Two of the main possibilities for the *xrs-5* DSB repair defect are i) components of a multiple DSB repair mechanism are defective or absent in *xrs-5*. This model would require that there is a separate repair mechanism for single and multiple DSB and the repair pathway for the multiple DSB might be defective due to the loss a critical repair enzyme. ii) A structural component renders DSB non-reparable even though *xrs-5* maintains a full complement of repair enzymes. Here there is not necessarily a pre-requisite for separate repair mechanisms for single and multiple lesions. However, the coincidence of multiple DSB within a single looped structure, possibly combined with a structural defect in the mutant may produce a lesion which cannot be repaired.

The work described in this chapter examines nuclear protein extracts from CHO and *xrs-5* in an attempt to identify differences between the two cell lines in terms of both functional characteristics of these extracts and the constituent protein composition. Extractable proteins from these two cell lines have been compared previously. Topoisomerase II was examined by Warters et al. [1991] and Caldecott et al. [1993] and electrophoretic properties investigated by Yasui et al. [1994]. These have not produced results which explain the radiation sensitivity of *xrs* cells.

Cellular protein extracts have been examinated in connection with other radiation sensitive cell lines [Wood et al., 1988, Eker et al., 1992]. These studies have generally considered the *in vitro* DNA repair capacity of extracts [e.g. North et al., 1990] and purified proteins although others, for example for ataxia telangiectasia and xeroderma pigmentosum cell lines, have

examined properties such as DNA binding and topoisomerase activity [Singh et al., 1988; Mohamed and Levin, 1989; Smith and Makinson, 1989; Eker et al., 1992].

The original objective in the extraction of nuclear proteins from CHO cells had been to complement the radiation sensitivity of *xrs-5* by the introduction of wild-type protein extracts into irradiated cells using streptolysin-O (SLO). Complementation of UV sensitivity of xeroderma pigmentosum (XP) cells has been performed by the introduction of cell extracts [Wood et al., 1988]. However, for *xrs-5* cells, as described in chapter 2, introduction of wild-type cell extract proved to be ineffective in complementing the radiosensitivity. This failure could probably be accounted for by any of a number of reasons including the crude nature of the extracts used, the mode of introduction and the protocol used to identify alterations in radiation sensitivity. As seen with experiments involving the introduction of *PvuII* and T4 DNA ligase into cells the effect of the introduction of proteins into damaged cells was difficult to quantify using the micronucleus assay. It was therefore decided to investigate the *in vitro* properties of nuclear proteins extracted from CHO and *xrs-5* in an attempt to identify specific polypeptides or activities which differed between the mutant and wild-type. These proteins could then be purified further, characterised and only then might SLO mediated complementation be attempted.

The problem with this course of action was to produce a method for the identification of proteins which might be involved in repair. As described below this involved screening extracts for possible "repair" activities including ligation and nuclease activities. During the course of performing these assays an additional property was identified where differences between the cell lines was noticeable. This was the DNA binding activity of proteins in extracts. The major part of this chapter therefore deals with this aspect of the investigation.

4.2. *Materials and Methods.*

4.2.1. *Materials.*

All reagents were of analytical or molecular biological grade unless otherwise stated. Solutions for cell culture were prepared under normal sterile conditions. A cocktail of proteinase inhibitors (PPLACD) was made by dissolving, in DMSO, 5 mg ml^{-1} each of pepstatin-A, leupeptin, antipain, chymostatin (all Sigma). To this dithiothreitol (DTT) and phenyl methyl sulphonyl fluoride (PMSF) were added to give final concentrations of these of of 50 mM. The storage concentrations were 500 times the working concentrations. PPLACD was stored in aliquots at -20°C. PPLACD was included in all protein extractions and subsequent procedures involving protein extracts.

4.2.2. *Cell culture.*

Chinese hamster ovary (CHO-K1 strain) and *xrs-5* cells were routinely maintained as exponentially growing monolayers in tissue culture flasks in EMEMS (Eagles' minimal essential medium supplemented with Earles' salts (Gibco), 10% (v/v) newborn calf serum (Gibco), 100μM $FeCl_3$ (to saturate transferrin), 50 IU ml^{-1} penicillin (Gibco) and 50 mg ml^{-1} streptomycin (Gibco)). All incubations were performed at 37°C in an atmosphere of 5% CO_2 unless otherwise stated. Cells were passaged or collected for treatment by trypsinisation. Briefly; cell monolayers were rinsed twice with 0.05% trypsin (Difco Laboratories), 0.7mM sodium ethylenediaminetetraacetic acid (EDTA) in phosphate buffered saline (PBS; 140 mM NaCl, 2.5 mM KCl, 8.1 mM Na_2HPO_4, 1.5 mM KH_2PO_4). The flasks were incubated at 37°C for 6 minutes and cells resuspended in EMEMS. Determination of cell numbers was performed by Coulter counting. The extraction of proteins required large numbers of cells. These were grown in batches, in 150 cm^2 flasks, maintaining exponential growth. The cells were trypsinised at routine intervals as above and resuspended in medium at $5x10^7$ cell ml^{-1}. Irradiation and incubation at 37°C was performed as necessary and the cells stored under liquid nitrogen prior to extraction procedures. Cells were stored for a maximum of 1 month.

4.2.3. *Irradiation.*

The cells were irradiated on ice using a ^{137}Cs IBL437C γ-irradiator (CIS UK Bio International) at a dose rate of 4.6 Gy min^{-1}. Dosimetry was checked by a ferrous sulphate method [Frankenberg, 1969].

4.2.4. *Micronucleus assay.*

The mass cell culture required for protein extraction placed increased pressure on the *xrs-5* cell line to revert [Jeggo and Holliday, 1986]. To routinely assay for radiosensitivity aliquots of

cells from each batch were removed prior to storage in liquid nitrogen and seeded, in triplicate, into 25 cm^2 flasks. These were irradiated with 1 Gy ^{137}Cs γ-rays and exposed to 3 $\mu g\ ml^{-1}$ cytochalasin B for 24 hours at 37°C. Trypsinisation was performed and the cells spun onto glass slides using a Cytospin 2 (Shandon). After drying in air, slides were fixed for 10 minutes in methanol, dried again and stained for 20 minutes in 10% (v/v) filtered Giemsa (BDH). The frequency of micronuclei were scored using a Zeiss 63x planapochromatic objective (aperture = 1.4). If *xrs-5* cells exhibited signs of reversion to wild-type sensitivity the batch of cells to which they belonged and the previous two batches would be discarded and fresh stocks of cells grown up from storage. The above procedure ensured that revertant stocks were detected prior to protein extraction procedures.

4.2.5. Protein extraction.

Cells frozen in EMEM under liquid nitrogen were gently defrosted and stabilised to ice-cold conditions. All subsequent procedures were also performed on ice or at 4°C where appropriate. Extraction procedures were based on those of North et al. [1990] with several modifications. Generally, extraction was performed on the basis of sequential centrifugal washes of homogenisation extracted nuclei in buffers of increasing salt concentration. Several variations on this procedure were used, these are detailed later. The procedure below is for one such protein extraction.

The cells were washed 3x by centrifugation (5 minutes at 4°C in a Chilspin 2; MSE, at 1450 RPM) with Hanks Balanced Salt Solution (HBSS). $5x10^8$ cells were placed in v-tubes (Nunc), centrifuged and the pellet resuspended in buffer A + 250 mM sucrose. The cells were maintained at 4°C for 10 minutes prior to centrifugation. The supernatant was aspirated and the pellet resuspended in 2.5 ml buffer B.

Buffer A =
20 mM tris (pH 7.5)
0.5 mM $MgCl_2$
0.5 mM KCl
20 mM NaEDTA

Buffer B =
20 mM tris (pH 7.5)
0.5mM $MgCl_2$
100 mM KCl
20 mM NaEDTA
0.6 mM spermine HCl (Sigma)
2 $\mu l\ ml^{-1}$ PPLACD

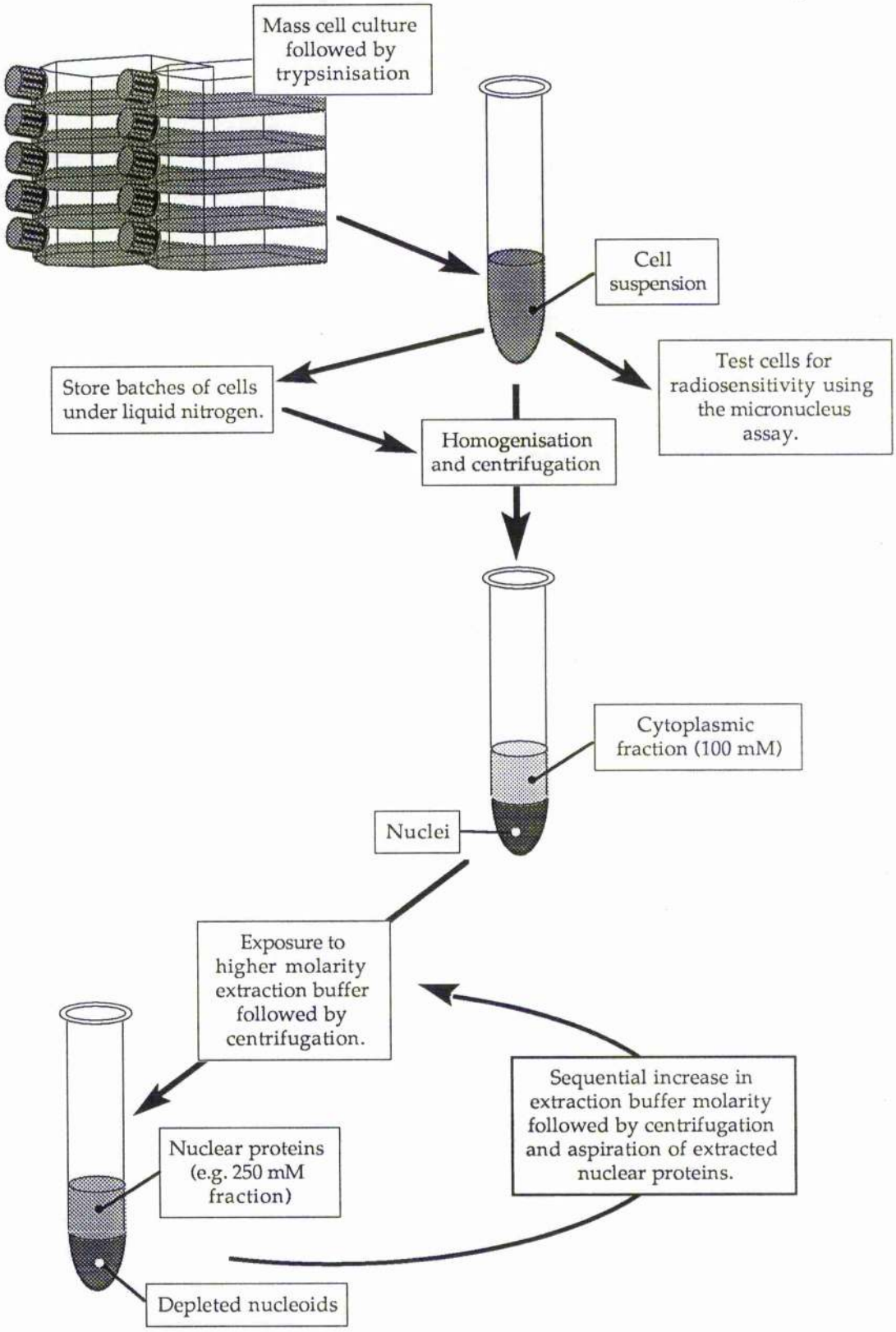

Figure 4.1. Diagramof the protein extraction procedure.

The cell suspension was homogenised using a Dounce homogeniser with 20 strokes pestle B followed by 40 strokes pestle A. Homogenisation was performed in an ice-water bath to prevent excessive heat generation. Disruption of cell membranes was confirmed using a haemocytometer, ensuring that greater than 99% of cells were disrupted. The nuclear suspension was centrifuged at 2000 RPM in a Chilspin for 5 minutes and the supernatant aspirated and retained. The pellets were washed in 3 x 0.5 ml buffer B with the supernatants pooled with the initial aspirate.

The nuclei were resuspended in 2 ml buffer C and were held on ice for 20 minutes with gentle agitation.

Buffer C = **20 mM tris (pH 7.5)**
250 mM $MgCl_2$
0.5 mM KCl
20 mM NaEDTA
0.6 mM spermine HCl (Sigma)
2 µl ml^{-1} PPLACD

This suspension and the 100 mM extract were then transferred into 1.5 ml microfuge tubes (Treff) and centrifuged at 25,000g in a Beckman JA 18.1 rotor for 30 minutes at 4°C to remove membrane fragments etc. The supernatants from the two fractions were aspirated and transferred into 10 kDa pore sized ultra-centrifugal micro-concentrators (Amicon). These were centrifuged at 8000g in a Beckman JA 20 rotor at 4°C, with 2x1.5 ml washes in the respective buffers over 16 hours to reduce the volume of the fractions to 50-300 µl. These fractions were designated according to the salt concentration used during extraction i.e. the above procedure produced a 100 mM KCl and a 250 mM $MgCl_2$ fraction.

Protein concentrations were estimated by a Bradford colorimetric assay (BioRad) using bovine serum albumin (BSA) as a standard. Protein fractions were diluted to a maximum of 12.5 mg ml^{-1} in their respective extraction buffers. To avoid repetitive cycles of freeze-thawing, the samples were split into aliquots and frozen at -20°C for storage with each aliquot used once only.

The above procedure describes the extraction of one set of proteins; 100 mM KCl and 250 mM $MgCl_2$ fractions in the presence of 6 mM spermine. Other procedures involved extraction of 400 and 600 mM NaCl and 8 M urea fractions in the absence of spermine and 100, 400, 600, 800, 1000 and 2000 mM NaCl and 6M urea fractions in the presence of 6 mM spermine. The latter set of fractions were obtained by sequentially resuspending the nuclear pellet in increasing concentrations of NaCl. It should be noted that spermine was originally included to

facilitate extraction by maintaining a compact nuclear structure. Extractions performed in the absence of spermine resulted in the formation of a DNA gel and low protein yields. At high salt concentrations however, (>800 mM NaCl) it was difficult to resuspend the nuclear pellet and the yield of proteins at these concentrations was reduced. This problem could have been resolved by the use of DNAase treatment however this would have prevented the use of DNA binding assays etc. The use of non-ionic detergents was similarly avoided since these are difficult to remove from extracted proteins [Helenius and Simons, 1975] and might similarly affect DNA binding assays.

4.2.6. In vitro assays of nuclear protein extract activity.

Nuclear extracts were examined for the following activities i) exo/endonuclease, ii) topoisomerase , iii) DNA ligase. Assays were performed by incubation of a variety of commercially available DNA with 1 µg of extract and examining the results using agarose electrophoresis of the samples. These activities were examined by the use of the following DNA.

Table 4.1. ***In vitro*** **assays of nuclear protein activity.**

Enzyme activity assayed.	DNA molecule used.	Buffer	µg of DNA	Evidence of activity
Endonuclease	pBR322	D/E	0.25	Closed circular to linear form
Exonuclease	λ (*HindIII/EcoR1* digest)	F	2	Smearing of bands
Topoisomerase	pBR322	D	0.25	Uniform "ladder" formed from topoisomeric forms ranging from closed circular to open circular forms
DNA ligase	λ (*HindIII/EcoR1* digest)	F	2	Loss of bands or formation of additional high M.W. bands.

Reactions were performed in a total volume of 20 µl at 37°C for 1 hour. The reactions were terminated by addition of 2 µl of DNA sample buffer and by placing the samples on ice. Samples were run on 0.8% agarose gels at 30 V (constant voltage) overnight in tris-borate-EDTA (TBE) buffer. Gels were run in the absence of ethidium bromide unless otherwise stated, in order to visualise topoisomers. DNA was visualised by staining gels after electrophoresis with 2 µg ml^{-1} ethidium bromide (in TBE) for 1 hour at 4°C. Gels were then

destained for 2 hours in 10% (w/v) ammonium acetate (in TBE) and visualised under UV light.

Buffer D =	**20 mM tris HCl, pH 7.5.**
	0.5 mM KCl
	10 mM Na-EDTA
	10 mM Na-EGTA
	2 µl ml^{-1} PPLACD
Buffer E =	**20 mM tris HCl, pH 7.5.**
	5 mM $MgCl_2$
	0.5 mM KCl
	5 mM $CaCl_2$
	2 µl ml^{-1} PPLACD
Buffer F =	**50 mM tris HCl, pH 7.6**
	10 mM $MgCl_2$
	1 mM ATP
	2 µl ml^{-1} PPLACD
	5% (v/v) polyethylene glycol-8000
DNA sample buffer =	**10 mM tris pH 8.0**
	1 mM NaEDTA
	50% (v/v) glycerol
	10% (w/v) SDS
	0.025% bromophenol blue.
TBE buffer=	**89 mM tris**
	1.1% (w/v) boric acid
	2.5 mM Na-EDTA

4.2.7. "DNA-Eppendorf" binding assays

Initial experiments on possible DNA synthetic activities of extracts (not shown) revealed a DNA binding activity of the extracts which was evidenced by binding of radio-labelled CHO genomic DNA to the walls of plastic Eppendorf tubes in the presence of protein extracts. Briefly, this activity was quantified as follows;

The DNA of exponentially growing CHO cells was labelled using 0.05 μCi ml^{-1} [methyl ^{14}C]-dTTP (Amersham, 50 μCi ml^{-1}, 51.4 mCi $mmol^{-1}$) for 24 hours. Cells were trypsinised and washed 3x with HBSS followed by resuspension in TEN buffer plus 100 μg ml^{-1} proteinase K plus 1% (w/v) SDS at 10^7 cells ml^{-1}.

TEN buffer = **10 mM tris pH 8.0**
1 mM Na-EDTA
150 mM NaCl

The DNA was incubated overnight at 37°C with gentle agitation. The DNA was subsequently phenol-chloroform extracted and precipitated using 2.1 M ammonium acetate and 60 ethanol. The DNA was washed with 70% ethanol, dried and redissolved in TE buffer. This crude DNA extract was purified using RNAase (1μg ml^{-1}, 37°C for 1 hour) and further phenol-chloroform extractions until the purity (as measured by absorbence at 260 and 280 nm) was greater than 1.80.

2 μg of the purified [^{14}C]-labelled DNA was added to plastic Eppendorfs (Treff) containing a reaction mixture comprising of various concentrations of nuclear extract in buffer G to a final volume of 50 μl.

Buffer G = **25 mM tris pH 8.0**
10 mM $MgCl_2$
1 mM DTT
50 μM each dATP, dCTP, dGTP and dTTP

(Buffer G contained nucleotides since the reactions were originally DNA synthesis reactions.)

The reaction was incubated at 37°C for 2 hours and terminated by the addition of 200 μl ice cold trichloroacetic acid (10% w/v). This was then removed and added to a scintillation vial containing 4 ml Optiphase "MP" (Packard) scintillation fluid. The Eppendorf was rinsed 3x200 μl 10% TCA and these washes added to the scintillation vial. The plastic Eppendorf was placed in a separate scintillation vial containing 4 ml Optiphase "MP". Free and bound radioactivity was determined by scintillation counting.

4.2.8. ^{32}P labelling of DNA.

25 ng of single-stranded calf thymus DNA (phenol-chloroform extracted, SIGMA) was labelled by random priming ("Ready to Go" random prime labelling reaction kit, Pharmacia) using 50 μCi [α-^{32}P]dCTP (Amersham, 10 mCi ml^{-1}, 3000 Ci $mmol^{-1}$). Unincorporated label was removed by passing through a "Nick" spin column (Sephadex G-50, DNA grade; Pharmacia) and the activity per ng calculated using scintillation counting.

4.2.9. *DNA filter binding assays.*

DNA binding reactions were carried out in wells of round bottomed multi-well plates (Nunc). Non-specific protein binding to the plastic of the plates was minimised by pre-rinsing with 5% (w/v) acetylated bovine serum albumin (Sigma) in buffer D followed by 3 rinses with buffer D.

Dilutions of calf thymus DNA (double-stranded, Sigma) were made up in the wells using buffer H.

Buffer H = **20 mM tris HCl, pH 7.5.**
0.5 mM $MgCl_2$
0.5 mM KCl
10 mM Na-EDTA
10 mM Na-EGTA
2 µl ml^{-1} PPLACD

To this, 2.5 ng ml^{-1} [^{32}P]-labelled calf thymus DNA and 100 µg ml^{-1} protein extract were added. The final concentration of DNA (labelled + unlabelled) ranged from 2-200 µg ml^{-1}. The final reaction volume was 100 µl. The multi-well plate was transferred to a water bath maintained at 37°C in an humidified environment and incubated for 1 hour. The plate was then placed on ice. Samples were then blotted onto nitrocellulose filters (Hybond-C; Amersham or 0.45 µm pore 25 mm diameter filter; Whatman) using either a slot-blot manifold (BRL) or a circular filter manifold under vacuum. The wells of the reaction plates were rinsed 3x 200 µl buffer H and the rinses added to the filters. The filters were rinsed *in situ* with buffer D (3x 200 µl for slot-blots, 3x 4 ml for circular filters. The filters were then air dried and the activity which was bound to nitrocellulose counted using 4 ml "Filter count" (Packard).

4.2.10. *Calculation of DNA binding activity.*

To calculate the DNA binding activity of the extracts the amount of DNA bound per µg of protein extract was calculated. This was based on the assumption that the extract bound the labelled and unlabelled DNA with equal efficiency. The total amount of DNA bound was therefore the fraction of DNA bound multiplied by the total amount of DNA present.

$$B_{DNA} = \frac{CPM_{bound}}{CPM_{total}}(D_{total}) \qquad (4.1)$$

Here CPM_{bound} is the activity on filter in counts per minute, CPM_{total} is the activity of labelled DNA in counts per minute and D_{total} is total amount of DNA (labelled + unlabelled) in µg.

The unit of DNA binding activity was defined as the amount of DNA (μg) bound per μg of extract.

$$= \frac{B_{DNA}}{\text{amount of extract}} \qquad (4.2)$$

4.2.11. Protein gel electrophoresis.

Electrophoretic separation of proteins was performed using the tricine-SDS polyacrylamide gel electrophoresis (TSDS-PAGE) procedure [Schägger and von Jagow, 1987]. The use of tricine (N-tris[hydroxymethyl]methyl-glycine) has several advantages over conventional glycine-SDS-PAGE including an increased protein loading capacity, high salt tolerance and a broader polypeptide size range which can resolved without the need for gradient gels. Briefly, a 1.5 mm thick gel was cast after degassing of the acrylamide solutions (20 minutes under partial vacuum) using 0.05% (w/v) ammonium persulphate (Fluka) and 0.05% (v/v) N,N,N,N'-tetramethylethylenediamine (TEMED; Sigma) for polymerisation. A water saturated iso-butanol overlay on the polymerising resolving gels formed an air-tight seal and prevented meniscus formation. This was removed by rinsing in distilled water prior to pouring the stacking gel. The stacking gel length was 1 cm (from bottom of well). The resolving gel length was 12 cm. Urea was included in the gels and sample buffer to facilitate protein denaturation without the use of high temperatures and to maintain protein solubility during electrophoresis.

Resolving gel =	**1 M tris-HCl, pH 8.45**
	1% (w/v) sodium dodecyl sulphate (SDS)
	6 M urea
	8-12% T, 3% C acrylamide/bisacrylamide (37:1)
Stacking gel =	**0.75 M tris-HCl, pH 8.45**
	0.75% (w/v) (SDS)
	6 M urea
	4-6% T, 3% C acrylamide/bisacrylamide (37:1)
Protein sample Buffer =	**25 mM tris-HCl pH 7.5**
	12 M urea
	25 mM bromophenol blue (Sigma)
	20% (v/v) glycerol
	10% β-mercaptoethanol

Approximately 20 μl of protein extract (4-250 μg) was added to 20 μl of sample buffer and mixed thoroughly. This was then placed on ice for 30 minutes to permit denaturation of

proteins. The sample was briefly centrifuged (2 min 6500 RPM; MSE microcentaur) prior to loading. The gel was run in a discontinuous buffer system at 30 V for 1 hour followed by approximately 4 hours at 130 V in a V15.17 electrophoresis tank (Life Technologies Inc.). When the bromophenol blue marker reached the end of the gel, the gel was removed.

Anode buffer = **0.2 M tris-HCl, pH 8.9 (adjusted with HCl)**

Cathode buffer = **0.1 M tris, pH 8.25 (no correction of pH)**
0.1 M tricine
0.1% (w/v) SDS

The gel could now be processed for visualisation of proteins using Coomassie blue staining , South-Western blotting for visualisation of DNA binding proteins or Western blotting for the visualisation of nuclear lamins.

4.2.12. Coomassie blue staining.

The staining procedure used was followed that of Neuhoff et al. [1988]. This technique uses Coomassie blue G-250 (as opposed to the more conventional R-250). Coomassie blue G-250 forms a colloidal suspension in the presence of ammonium acetate and methanol. Protein staining with this dye produces enhanced resolution with ng sensitivities. It also produces very little background staining.

The gel was placed in 12.5% (w/v) trichloroacetic acid at 4°C and allowed to fix for 1 hour. The gel was rinsed briefly in distilled water and placed in staining buffer over-night at 4°C with gentle agitation. The gel was briefly destained using 25% (v/v) methanol until a clear background was obtained. The gel could then be stored in 20% (v/v) ammonium sulphate at 4°C indefinitly.

Staining buffer = **0.8% (w/v) coomassie blue G-250 (BDH)**
1.6% (w/v) phosphoric acid
8% (w/v) ammonium sulphate
20% (v/v) methanol (added fresh)

Molecular weights could be estimated by standard weight marker proteins (Dalton Mark VII-l, Sigma) run alongside the extracts.

4.2.13. South-Western blotting.

South-Western blotting analysis of DNA binding was performed based on the technique of Mazan et al. [1989] with some modifications. Gels run as above were removed from the electrophoresis set and placed in 300 ml of electrophoretic transfer buffer for 20 minutes at 4°C

with gentle agitation. The gel was then subjected to semi-dry electrophoretic transfer (Multiphor II Nova Blot, Pharmacia LKB Biotechnology) at a constant 0.8 mA cm^2 onto nylon supported nitrocellulose membrane (Hybond-C extra; Amersham).

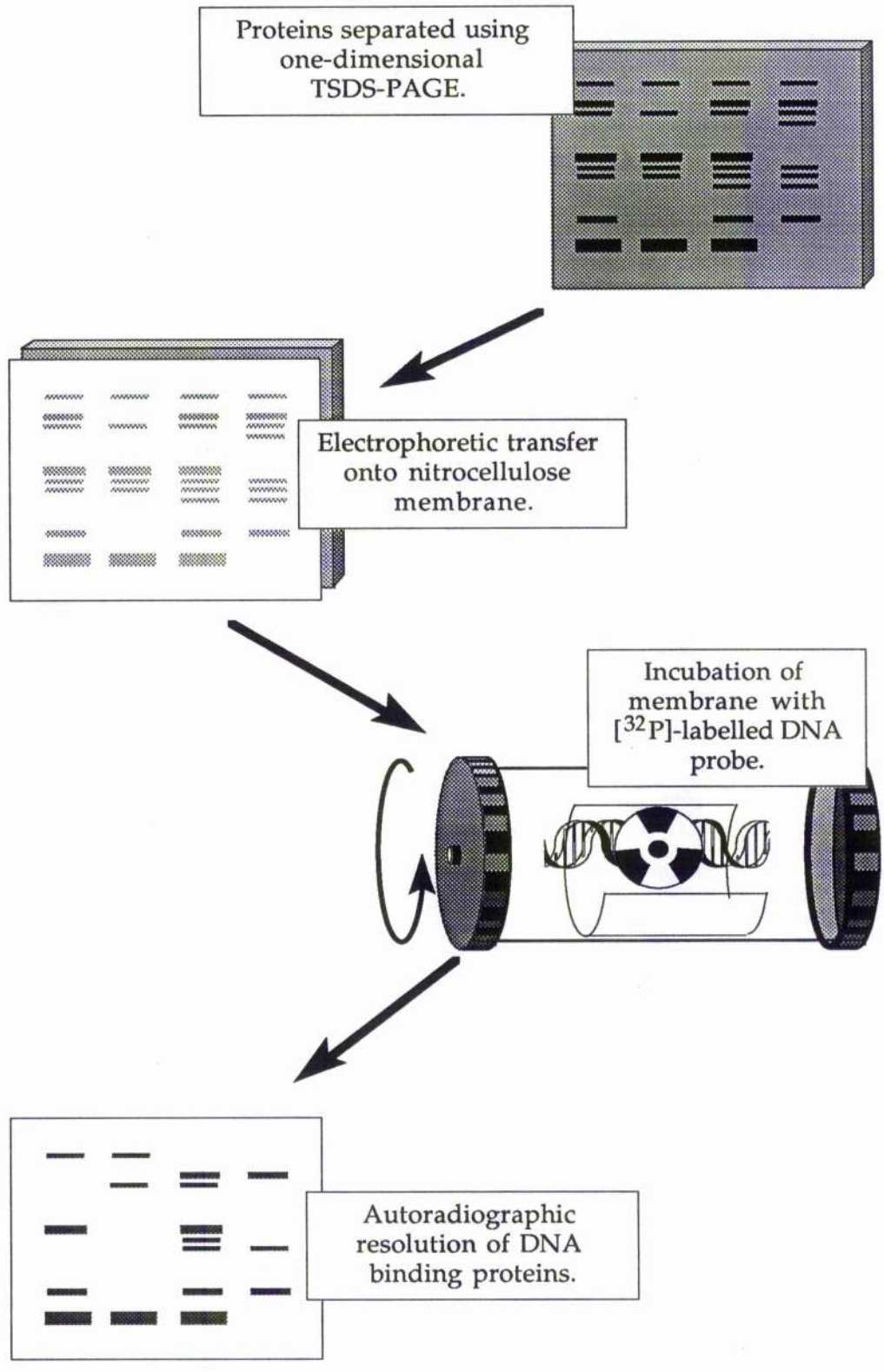

Figure 4.2. Diagram of the South-Western blotting procedure.

Electrophoretic transfer buffer=25 mM tris
192 mM glycine
0.0375% (w/v) SDS
20% (v/v) methanol

Transfer efficiency was estimated by transfer of prestained marker proteins (Sigma) run alongside the samples. The gel was also stained using Coomassie blue as above to determine transfer efficiency of the individual extracted proteins. Figure 4.3a shows two duplicate gels one of which was blotted onto nitrocellulose prior to Coomassie blue staining. This indicates that although the majority of proteins are transferred to the nitrocellulose the efficiency of transfer decreases with increasing molecular weight.

The blotted membrane was placed on hybridisation mesh inside a hybridisation bottle in an oven (Techne Hybridiser HB-1) and washed 3x20 ml buffer H to remove acrylamide. The membrane was then incubated for 16 hrs at 37°C in 10 ml buffer H plus 5% (w/v) non-fat milk powder (NFM, Marvel™) to allow renaturation of proteins and to block the membrane.

The membrane then was washed 3x10 ml buffer H plus 0.25% NFM followed by a two hour incubation at 37°C with 10 ml buffer H plus 0.25% NFM plus 25 ng [^{32}P]-labelled DNA probe (approximately 3x10^{7} CPM). Additional competing unlabelled DNA could also be added. Two types of South-Western were performed. The first (type A) was carried out using 25 ng of radio-labelled probe alone (to give an approximate protein:DNA ratio of 6000-80,000:1 This would theoretically detect the majority of DNA binding proteins including non-specific binding. The second (type B) was performed using the same quantity of [^{32}P]-labelled probe but additional unlabelled calf thymus DNA was included in mg quantities (to give an approximate protein:DNA ratio of 0.33:1). This latter "competitive" South-Western used similar protein:DNA ratios that were used in the filter binding assay. The competing unlabelled DNA would help saturate the less specific DNA binding proteins.

After the 2 hour incubation the labelling solution was removed and the membrane washed 3x20 ml buffer H plus 0.25% NFM for five minutes each at room temperature. The membrane was then removed, air-dried and wrapped in cling-film (Saran-wrap™, Dow Chemical Company). Autoradiography was performed (without intensifying screens) using Hyperfilm-MP X-ray film for 1-240 hours at -60°C. The length of exposure depended on the activity of the filter. Generally the type A South-westerns required only 1-24 hour exposure and the type B South-Westerns required 24-240 hour exposures. Subsequently, background exposure was greater in the type B South-Westerns resulting in a reduction in quality of the auto-radiographs.

Figure 4.3b-d shows South-Western blots along with the corresponding Coomassie blue stained duplicate gels for negative controls (= molecular weight marker proteins; bovine α-lactalbumin, soybean trypsin inhibitor, bovine trypsinogen, bovine carbonic anhydrase, rabbit glyceraldehyde-3-phosphate dehydrogenase, egg albumin and bovine albumin, (all Sigma)) and two positive controls (purified calf thymus histone H1 and histone H2a (Sigma)). No DNA binding activity was observed for the marker proteins (Figure 4.3b). Histone H1 (Figure 4.3c) and to a lesser extent histone H2a (Figure 4.3d) exhibited several DNA binding bands. The resolution of South-Western blots was less than that observed using Coomassie blue staining making molecular weight approximations more difficult.

4.2.14. Western blotting.

By use of Western blotting versus lamins A and C, which are markers of the nuclear matrix, it was possible to confirm that the salt extraction (at least the 100 mM KCl and 250 mM $MgCl_2$ fractions) did not contain significant nuclear matrix proteins (Figure 4.3e). This was to be expected since the nuclear lamins are retained in the nuclear matrix after extraction with 2 M NaCl and non-ionic detergent. The procedure used for Western blotting is as follows.

Proteins were separated and blotted onto a nylon supported nitrocellulose membrane as above. The membrane was subsequently washed 3x20 ml buffer I for 5 minutes each at room temperature in a hybridisation bottle.

Buffer I = **10 mM tris pH 8.0**
150 mM NaCl
0.05% Tween-20 (Sigma)

The membrane was then incubated for 30 minutes at room temperature in 10 ml buffer I plus 1% (w/v) BSA. The membrane was rinsed 3x20 ml buffer I and incubated for 30 minutes at rom temperature with 10 ml buffer I plus a 1:2000 dilution of LS-1 human anti-lamin A/C antibody (received as a gift from Dr F. D. McKeon; Department of Physiology and Biophysics, Harvard Medical School) [McKeon et al., 1983]. The membrane was washed 3x20 ml buffer I for 5 minutes each followed by addition of 10 ml buffer I plus 1:100 horseradish peroxidase (HRP) conjugated sheep polyclonal anti-human IgG (Scottish Antibody Production Unit) for 30 minutes at room temperature. The unbound antibody was removed by washing with 3x20 ml buffer I.

The membrane was removed from the hybridisation and placed in a plastic box along with 20 ml HRP colour development solution; buffer J. The membrane was briefly agitated to ensure the entire membrane was covered in developing solution and then left in the dark, without agitation for 10 minutes at room temperature. The membrane was removed and briefly rinsed

in deionised water. The membrane was photographed while damp to ensure maximum contrast.

Buffer J = **1 mg ml^{-1} 3',3-diaminobenzidine (DAB, Sigma)**
0.03% (w/v) nickel sulphate
0.06% (v/v) H_2O_2

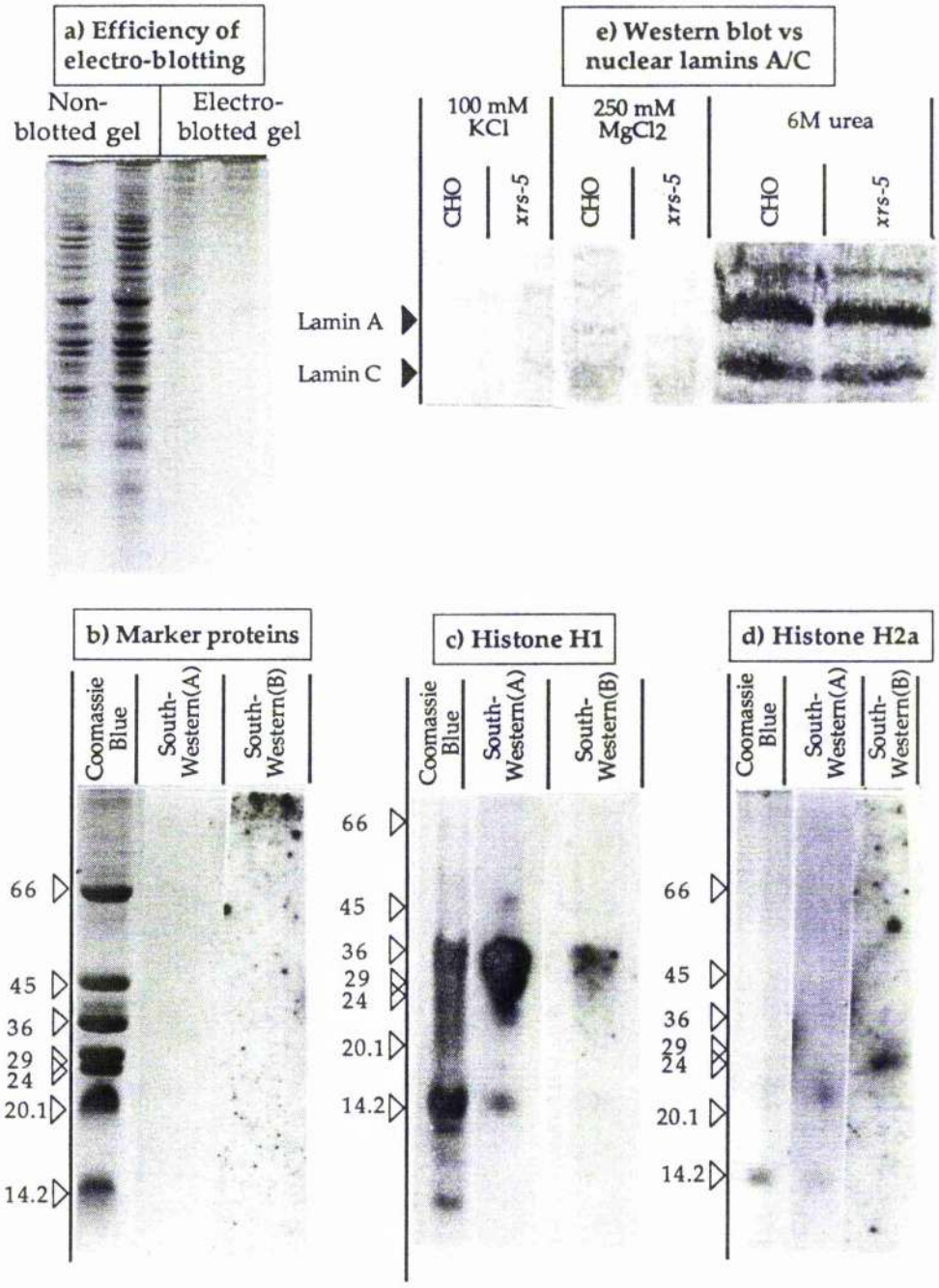

Figure 4.3a) Efficiency of electrophoretic transfer (blotting). 2x12 µg of nuclear extracts were separated, in duplicate, on a TSDS-PAGE gel. The gel was divided and one half subjected to Coomassie blue staining and the other electro-blotted onto nitrocellulose prior to Coomassie blue staining.

b-d) South-western blots of negative control proteins (b), and the positive control proteins histone H1 (c) and histone H2a (d). Figures represent TSDS-PAGE separations performed in triplicate and each subjected to either Coomassie blue staining or South-western blotting type A (non-competitive) or type B (competitive). Note type B blots have run short. Figures to the left represent the positions of marker proteins (Molecular weights given in kDa)

e) Western blot of nuclear extracts derived from CHO and *xrs*-5 cells versus lamins A and C.

4.3. Results.

4.3.1. In vitro activity of protein extracts derived from CHO and xrs-5.

Figures 4.4a-c show examples of the activities of nuclear protein extracts obtained from CHO and *xrs-5* cells. Incubation of the plasmid pBR322 with extracts in the absence of the chelating agents EDTA or EGTA and presence of $MgCl_2$ plus $CaCl_2$ indicated divalent cation dependent exonuclease activity in the extracts (Figure 4.4a). This activity could be greatly reduced by the removal of divalent cations and inclusion of EDTA and EGTA.

The majority of the extracts exhibited topoisomerase activities on closed circular pBR322, as evidenced by "ladders" of topoisomers appearing between the closed circular and open (i.e. relaxed) forms of the plasmid (Figure 4.4b). These represent stepwise relaxation of the multiply supercoiled plasmid [Caldecott et al., 1993]. The presence of ladders indicates that this activity is not the result of nicking activity since nicking would produce only the open circular form without the intervening topoisomeric forms. The absence of linear forms indicates that endonuclease activity is also minimal in these extracts. There was limited evidence of topoisomerase activity in extracts obtained by extraction with 6 M urea. Since the main topoisomerase activity of nuclei is located with the nuclear matrix and is resistant to salt extraction [Berezney and Coffey, 1977; Gasser and Laemmli, 1986] it might have been expected that the 6 M urea fraction would produce a large activity. The lack of detectable activity indicates that the extracted proteins are denatured by this procedure and that the concentration of urea remaining in the reaction mixture is inhibiting any activity. The identity of the topoisomerase responsible for relaxation was not determined. However, since ATP was not include in the reaction mixture then the responsible enzyme is likely to be the ATP-independent topoI rather than the ATP dependent topoII [Mattern et al., 1987; Stewart and Schütz, 1987]. There did not appear to be significant differences between extracts from CHO and *xrs-5*.

Incubation of extracts with λ (*HindIII/EcoR1* digest) failed to identify any major ligase activity in the extracts (Figure 4.4c). This may indicate that the levels of ligase which might be present in these crude extracts are to low to be detectable using this assay. The assay conditions were designed using T4 DNA ligase as a positive control, although incubations were performed at 37°C as opposed to the optimum temperature of 22°C. These conditions might not be optimal for mammalian DNA ligases. Again, with this assay no significant differences could be observed between CHO and *xrs-5* extracts.

Therefore, although the extracts appeared to retain activity as observed by topoisomerase activity no obvious differences between the two cell lines could be observed using these techniques.

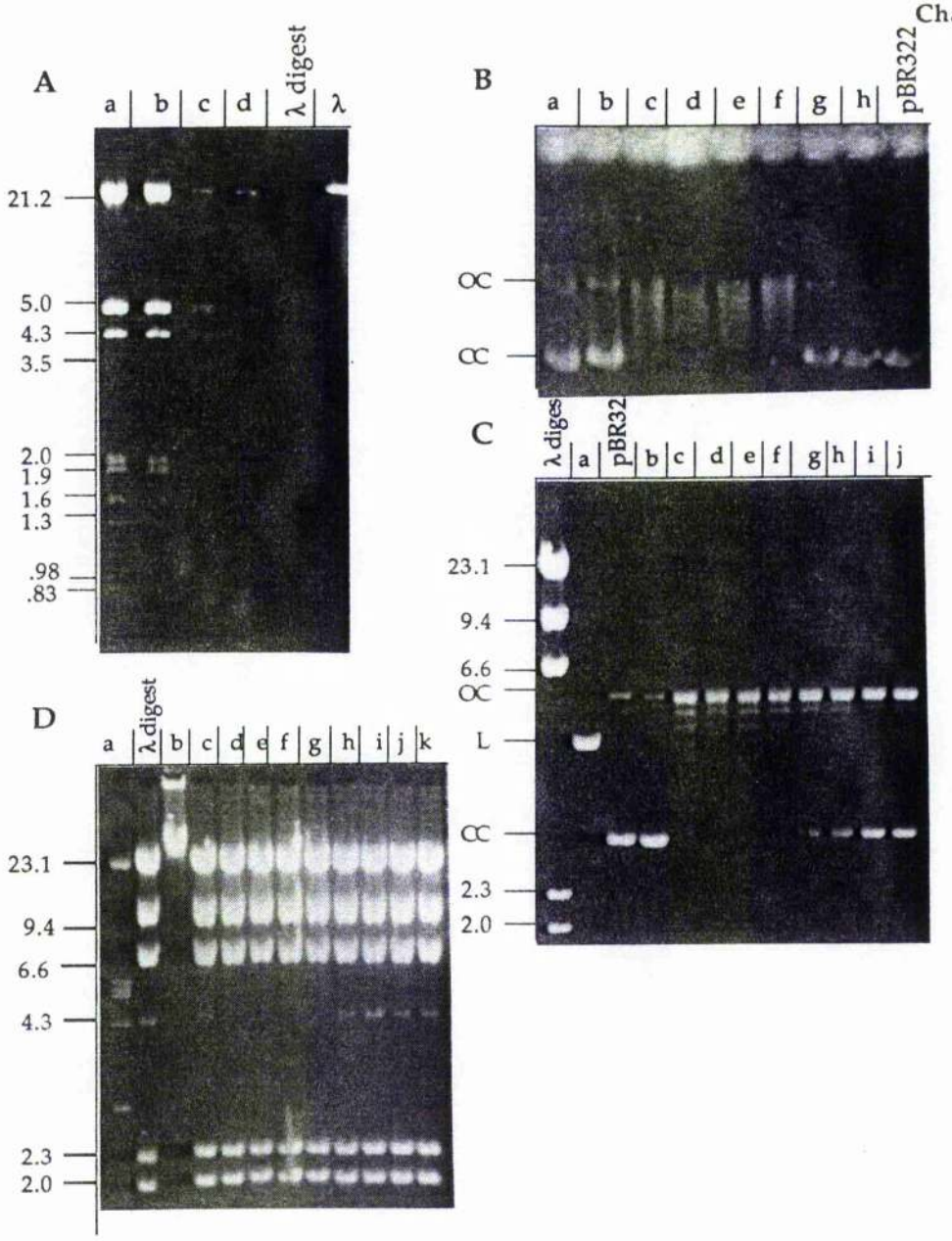

Figure 4.4. ***In vitro*** **activities of extracts derived from CHO and *xrs-5* cells.**
Numbers represent molecular weights (kbp).

A) Assay of exonuclease activity Incubation of λ *HindIII/EcoR1* digest with 600 mM NaCl extract in the presence or absence of divalent cations. a, c) CHO. b, d) *xrs-5*, a, b) + EDTA/EGTA. c, d) + Mg^{2+}/Ca^{2+}. Also shown is the result of digestion with exonuxlease III and control λ DNA.

B, C) Assay of endonuclease and topoisomerase activity. Incubation of extracts with pBR322 plasmid DNA. CC = closed circular, OC = open circular, L = linear.

B) 400 mM NaCl (lanes e,f), 600 mM NaCl (lanes c, d) and 6 M urea (lanes a, b) extracts of CHO (lanes a, c, e) and *xrs-5* (b, d, f). Lanes g, h = 400 and 600 mM buffers only.

C) 100 mM KCl (lanes c-f) and 250 mM $MgCl_2$ (lanes g-i) extracts derived from CHO (lanes c, d, g, i) and *xrs-5* (lanes d, f, h, j) cells. λ digest = *HindIII* digest. Lane a = *PvuII* digest of pBR322. Lane b = buffer D only.

D) Assay of ligase and exonuclease activity. Incubation of λ *HindIII* digest with 100 mM KCl (lanes d, e), 100 mM irradiated (f, g) 250 mM $MgCl_2$ (lanes h, i) and irradiated 250 mM $MgCl_2$ (lanes j, k) extracts derived from CHO (lanes d, f, h, i) and *xrs-5* (lanes e, g, i, k) Lane a = exonuclease III, lane b = T4 DNA ligase, lane c = buffer F only.

4.3.2. *DNA binding activity of CHO and xrs-5 extracts.*

During experiments designed to measure DNA synthetic activity of nuclear extracts (not shown) it was observed that high concentrations of extract mediated the binding of a significant fraction of the DNA in a reaction to the walls of plastic Eppendorf tubes. When DNA binding activity was quantified for 600 mM NaCl fractions from CHO and *xrs-5* (Figure 4.5a) there appeared to be a significant difference between the two cell lines, with *xrs-5* extract binding less DNA than CHO extracts. However, the "DNA-Eppendorf" assay required large quantities of protein and so a more sensitive assay was required.

The filter binding assay used was a modification of that described by Mohamed and Lavin [1989]. The assay involved incubation of nuclear extracts with [^{32}P]-labelled DNA. Passage of the reaction mixture through a nitrocellulose filter traps proteins and any protein-associated DNA. Unbound DNA passes through the filter. Quantification of DNA binding activity can be achieved by incubation with increasing amounts of DNA with a unit amount of extract which produces saturation of the available binding sites.

Figure 4.5b and c shows results obtained using this assay on 100 mM KCl (4.5b) and 250 mM $MgCl_2$ (4.5c) fractions. No difference was observed between CHO and *xrs-5* cells with the 100 mM KCl fraction. The 250 $MgCl_2$ mM fractions revealed saturation at high DNA concentrations indicating possible specific DNA binding kinetics. CHO cells show higher levels of binding compared to *xrs-5*.

Figures 4.6a and 4.6b show the binding of DNA by a wider range of salt extractable proteins (extracted in the presence of spermine). Figure 4.6a represents the DNA binding activity per µg of extract in a reaction involving 1 µg of extract and 3 µg of DNA. This indicates that for these extracts there is no difference between CHO and *xrs-5* in terms of activity per µg of protein. Figure 4.6b shows the results of these experiments with NaCl extractable proteins in terms of the total DNA binding activity extracted per 10^7 cells. These results would indicate that in addition to an increased activity of *xrs-5* proteins per µg extracted, the concentration of salt required to extract these proteins is greater than for CHO with the peak extraction efficiency occurring at 600 mM and 800 mM NaCl respectively. It should be noted, however, that the results of the NaCl extract experiments were obtained from a single extraction.

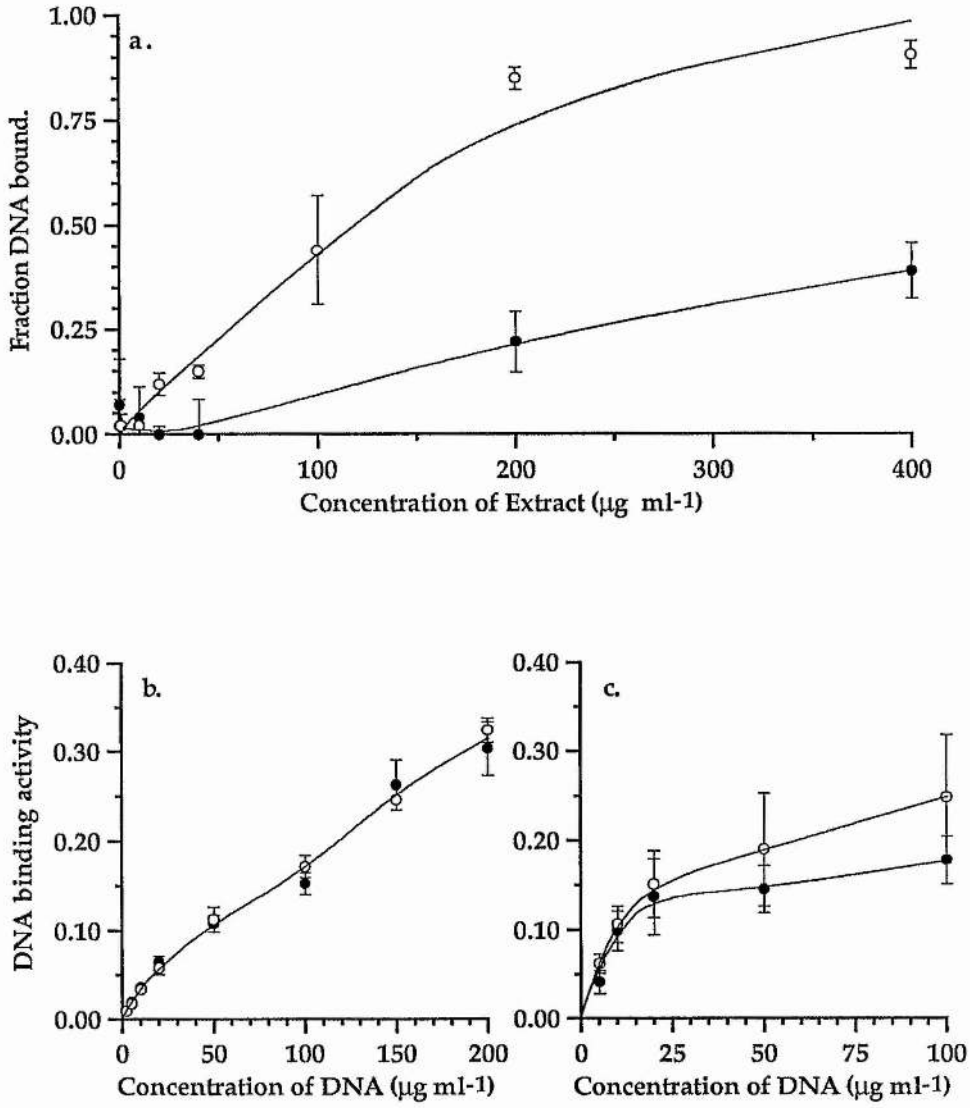

Figure 4.5. a) DNA binding to plastic Eppendorf tubes mediated by 600 mM NaCl protein extracts of CHO (○) and *xrs-5* (●) cells. Graph represents the fraction of double-stranded ^{14}C-labelled CHO genomic DNA bound by varying concentrations of extract with constant amounts of extract. Errors represent the SEM of a minimum of 3 experiments performed on a single batch of extract. Curves fitted by eye.
b) and c). Filter binding assay of 100 mM KCl (b) and 250 mM MgCl2 extracts derived from CHO (○) and xrs-5 (●) cells. Graphs represent the DNA binding activity of extracts in the presence of varying concentrations of double-stranded calf thymus DNA. Error bars represent the SEM of a minimum of 4 experiments performed with 1-3 batches of extract. Curves fitted by eye.

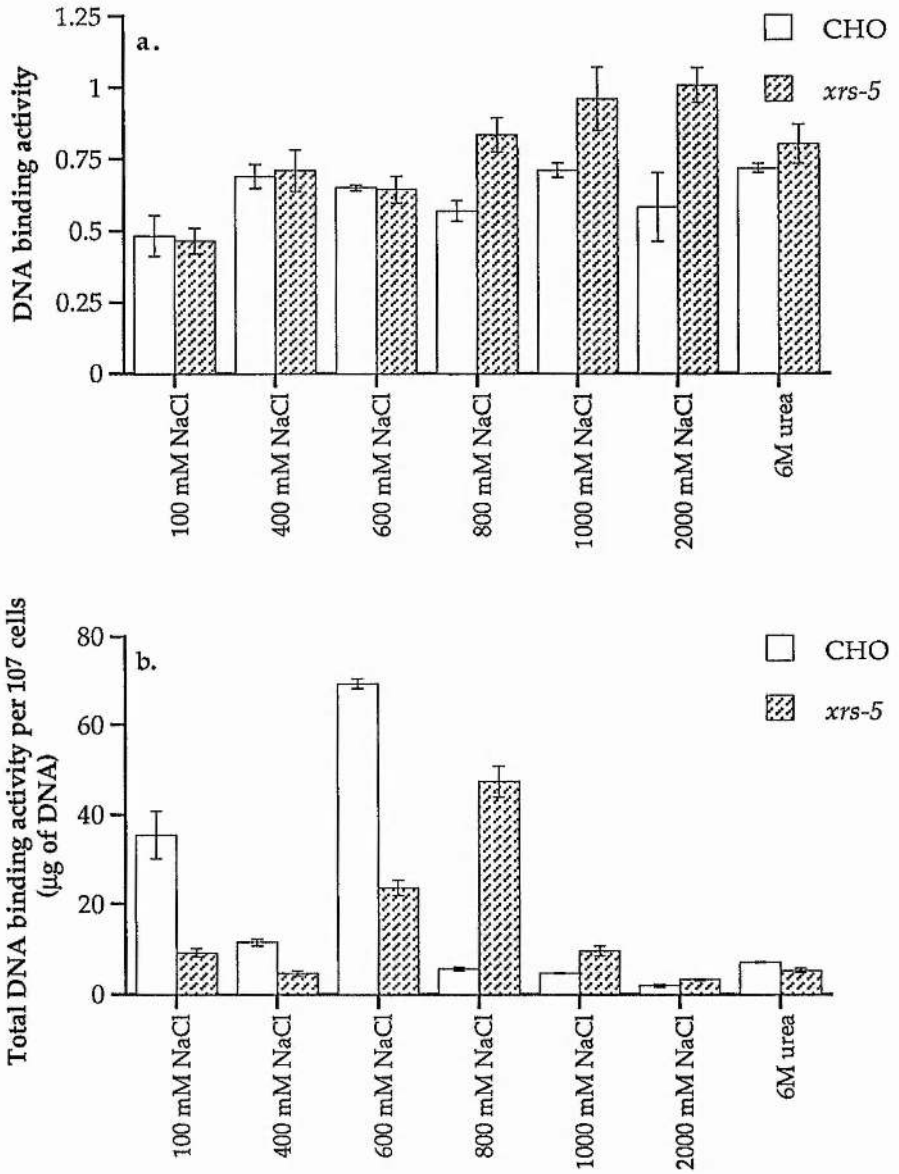

Figure 4.6. a) Filter binding assay of extracts derived from CHO and xrs-5 cells in the presence of varying concentrations of NaCl plus 6 mM spermine. Graphs represent the DNA binding activity of extracts in the presence of a unit concentration of double-stranded calf thymus DNA. Error bars represent the SEM of 3 experiments performed with a single batch of extract.

b) DNA binding activity per 10^7 cells of extracts derived from CHO and xrs-5 cells in the presence of varying concentrations of NaCl plus 6 mM spermine. DNA binding activity expressed as the total activity per 10^7 cells calculated by multiplying the DNA binding activity per µg by the amount of protein extracted from 10^7 cells. Error bars represent the SEM of 3 experiments performed with a single batch of extract.

The lower protein extraction efficiency that occurs at high salt concentrations for both cell lines is possibly attributable to the physical changes that occurred to the nuclear pellet during extraction. As the nuclear pellets were sequentially exposed to higher salt concentrations the pellet became increasingly compacted and resuspension of the nucleoids after centrifugation became more difficult. The salt concentration at which this occurred coincided with the observed reduction in extractable DNA binding activity (Figure 4.6b). This compaction may have prevented the extraction of proteins from the salt extracted nuclei. Treatment of nuclear pellets with DNAaseI reduced the compaction. However, this treatment would not have been apprpriate for extracts which would subsequently be used for DNA binding assays.

The two spermine-facilitated extraction procedures employed (100 mM KCl/250 mM $MgCl_2$ and the NaCl sequence) produced different results (Figure 4.5 and 4.6). The 250 mM $MgCl_2$ *xrs-5* extracts exhibited a lower DNA binding activity while the *xrs-5* NaCl extracts did not appear to be deficient in DNA binding activity, with high salt concentration extracts exhibiting higher levels of binding per μg than CHO. To determine the polypeptide composition and to identify DNA binding polypeptides TSDS-PAGE of the extracts was performed to determine the cause of this and the resulting polyacrylamide gels subjected to either Coomassie blue staining or South-Western blotting [Mazan et al., 1989]. It must be noted that denaturation of proteins is necessitated for electrophoresis and therefore only those DNA binding proteins which renature on the nitrocellulose filter will be identified. This contrasts with the filter binding assay where no denaturation was involved other than might occur during extraction procedures.

The Coomassie blue stained gels and the autoradiographs of the South-Western blots of duplicate gels of protein fractions extracted under different conditions are shown in Figures 4.8 to 4.11. Also shown are similar figures for 100 mM KCl and 250 mM $MgCl_2$ extracts derived from cells irradiated with 10 Gy and subsequently incubated for 30 minutes at 37°C for 30 minutes prior to extraction (Figures 4.12 and 4.13). Also shown are the scanning laser densitometer traces of b) Coomassie blue and c) South-Western blots (type A) for a selection of lanes. Although the amount of protein loaded onto these gels might vary between the different fractions the amount loaded for CHO and *xrs-5* for the same fraction was always the same. This permits comparisons between the cell lines.

As indicated by both visual analysis and densitometry, the protein banding pattern generally appeared similar in the two cell lines. No obvious differences were observed at first, in the pattern of banding. The densitometry confirmed that, with a few exceptions, similar amounts of protein were loaded for the two cell lines. Also obvious is the large numbers of individual polypeptides in the extracts.

Comparisons between CHO and *xrs-5* revealed that consistent differences could be observed by South-Western analysis in apparent molecular weight ranges of 30-35 kDa. In CHO this region exhibited the greatest DNA binding activity of the majority of the fractions. Two protein bands were involved in DNA binding at these molecular weights. In the majority of extracts where DNA binding in this region occurred, *xrs-5* appeared to bind less DNA than CHO. In some extracts, e.g. the 2000 mM NaCl fractions it appeared that *xrs-5* exhibited a lower DNA binding activities in the higher molecular weight band and a relative increase in the lower molecular weight band (not shown). However, the resolution of the South-Western blots was too poor to permit accurate densitometric resolution of these bands.

When a closer examination was made of the Coomassie blue staining pattern of the region exhibiting differences in DNA binding between the two cell lines, distinct differences could be observed in two bands in CHO and *xrs-5* with apparent molecular weights of 32.2 and 31.8 kDa (= p32.2 and p31.8 respectively). The densitometric traces of these two bands are shown in more detail in Figures 4.8-4.13d. In extracts derived from *xrs-5* the p32.2 band was decreased in intensity compared to CHO with densitometry with relative intensity of *xrs-5* extracts of 0.21 to 0.83% with a mean relative intensity over all extracts shown in Figures 4.15 of 0.45. In contrast, the lower molecular weight band, p31.8, was either similar or elevated in intensity in *xrs-5* fractions compared to CHO with a mean relative intensity of 1.17 over all the extracts represented in Figure 4.15. Since both the overall levels of protein loading and the intensity of the p31.8 bands were similar in the two cell lines the decrease in p32.2 intensity would appear to be constitutive. From the South-Western blots it would appear that p32.2 is a major DNA binding polypeptide in the size range of polypeptides resolved by the acrylamide concentrations used.

The histones, H1 and H2a, had been used as positive controls for the South-Western blot procedure (Figure 4.3c and 4.3d). Histone H1 proved to be more efficient at binding than H2a and when compared to the Coomassie blue and South-Western profiles of the extracts, histone H1 DNA binding activity and polypeptide banding patterns corresponded with p32.2, p31.8 and an additional DNA binding polypeptide band at approximately 16 kDa. The DNA binding bands of histone H1 are designated by the black triangles on the electrophoretographs in Figures 4.8 to 4.13.

Other DNA binding proteins could be observed but none appeared to show the consistency of differences that could be observed between the p32.2 bands in CHO and *xrs-5* extracts as measured by both Coomassie blue staining and South-Western blotting. The main polypeptides concerned with DNA binding appeared at molecular weights of greater than 66 kDa. In several of the NaCl extracts from *xrs-5* exhibited greater DNA binding activity in this region than CHO. The extracts obtained using 250 mM $MgCl_2$ did not exhibit as much

DNA binding activity in this region as the NaCl extracts and it appeared that $MgCl_2$ was more specific in its extraction of the three bands which corresponded to histone H1. Therefore it is possible that the decreased filter binding observed with the 250 mM $MgCl_2$ (plus spermine) fractions and the similar or elevated DNA binding activity of NaCl fractions (also plus spermine) for *xrs-5* may be due to different quantities of the high molecular weight polypeptides and the p32.2 and p31.8 bands.

Irradiated extracts did not appear to differ significantly from non-irradiated extracts (Figures 4.12 and 4.13) except for a low molecular weight band (approximately 10 kDa) which exhibited an increase in both Coomassie blue staining and DNA binding activity. However, this band was only observed after large amounts of protein were loaded. Nor was there any significant difference between the overall DNA binding activity of the irradiated cell extracts compared to the non-irradiated extracts as measured by the filter binding assay (data not shown).

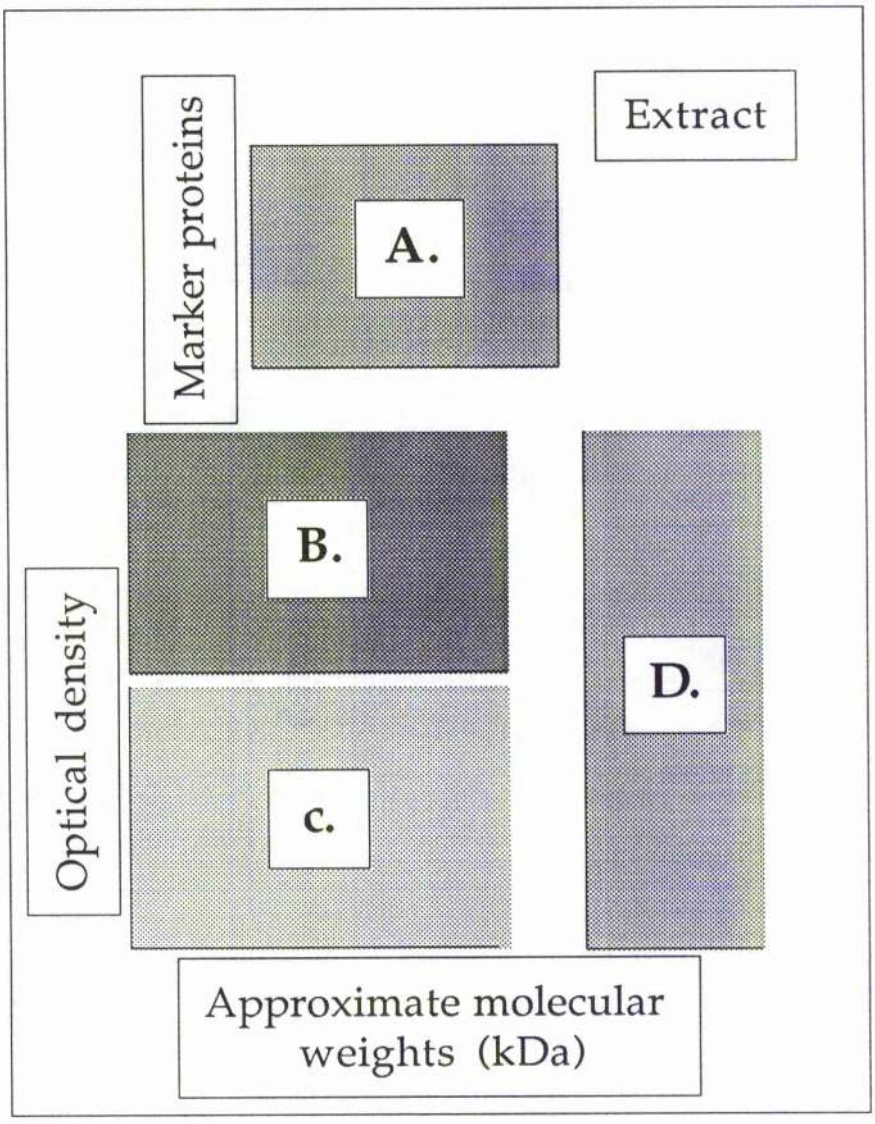

Figure 4.7. Explanation of figures 4.8 to 4.13.
A) TSDS-PAGE separation of extracts and South-Western blotting. Equal amounts (shown in parentheses) of extract were loaded in triplicate and separated by TSDS-PAGE. The resulting gels were subjected to either Coomassie blue staining or South-Western blotting (type A = non-competitive, type B = competitive). Marker protein molecular weights indicated by open triangles (Δ). Closed triangles (▲) represent the position of major DNA binding bands of purified calf thymus histone H1.
B-D) Densitometric traces of B) Coomassie blue electrophoretograph, C) South-Western blot (type A) and D) expanded trace of the Coomassie blue electrophoretograph of p32.2 and p31.8. CHO = solid line and *xrs-5* = dotted line. Y-axis represents the optical density of the bands, the X-axis represents the approximate molecular weights of the bands as calculated from the position of the marker proteins. When different levels of protein loading are represented densitometry was performed on the lowest protein concentration.

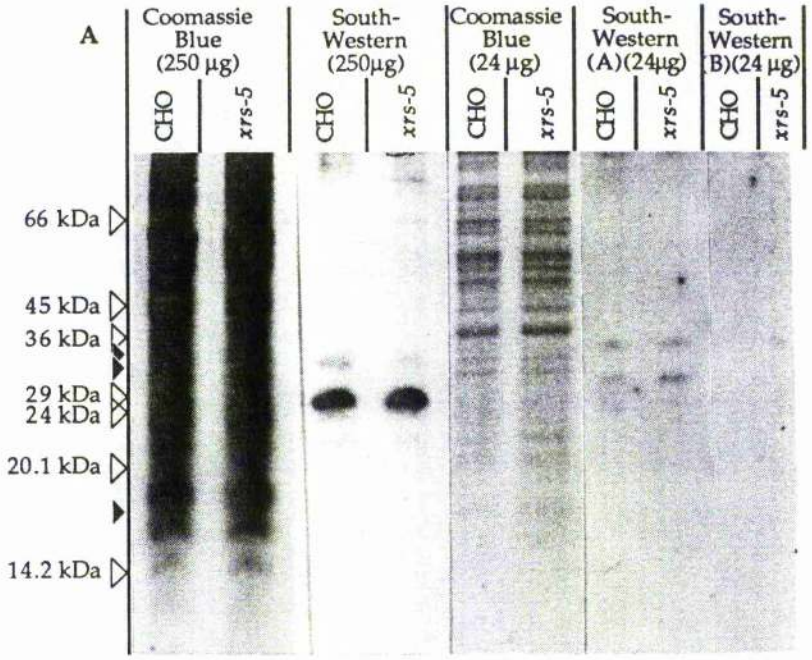

Figure 4.8.
100 mM KCl

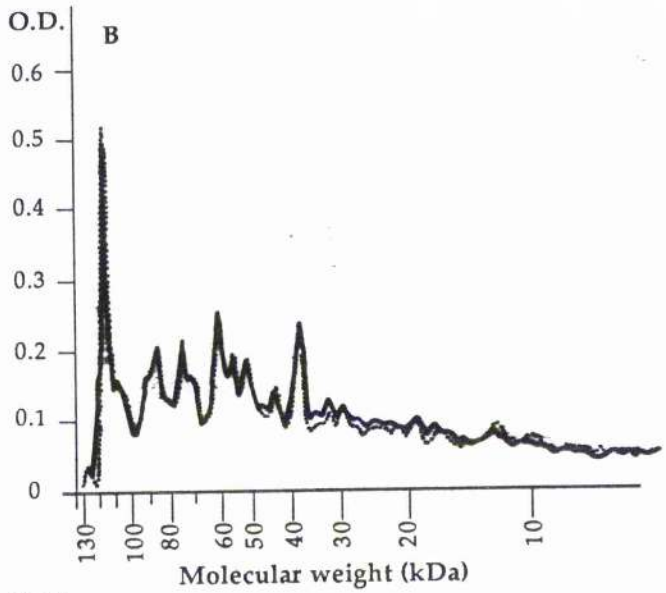

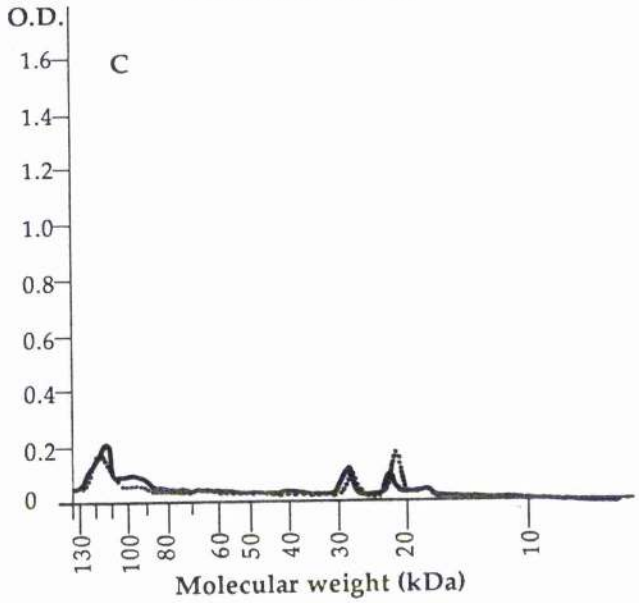

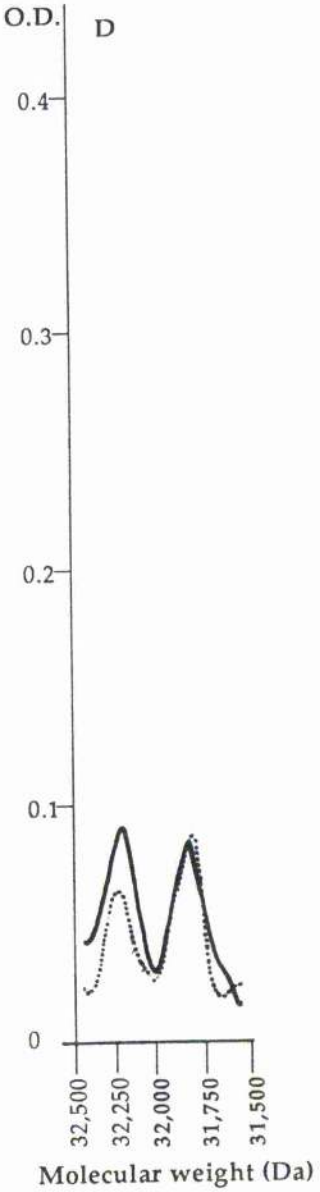

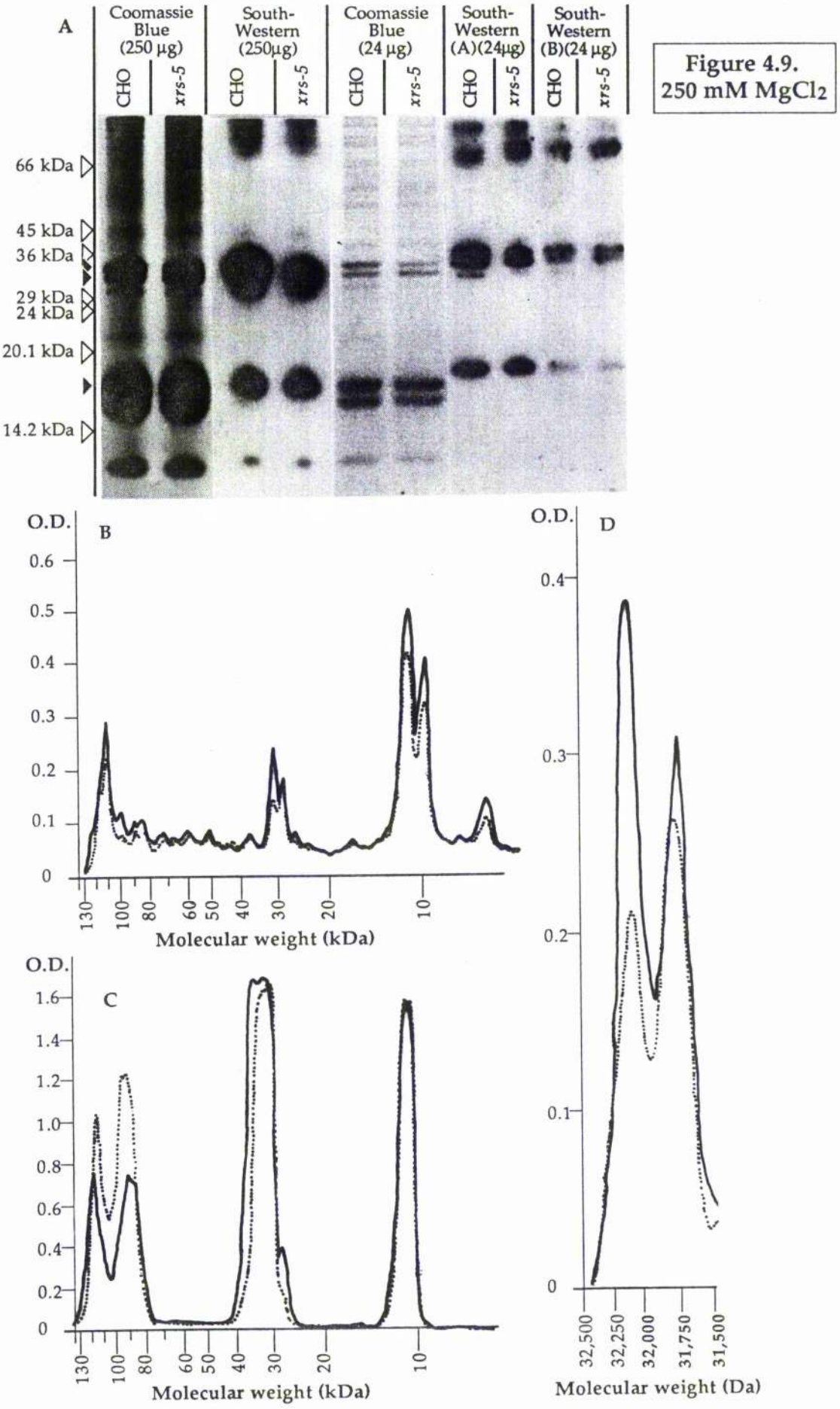

Figure 4.9.
250 mM $MgCl_2$

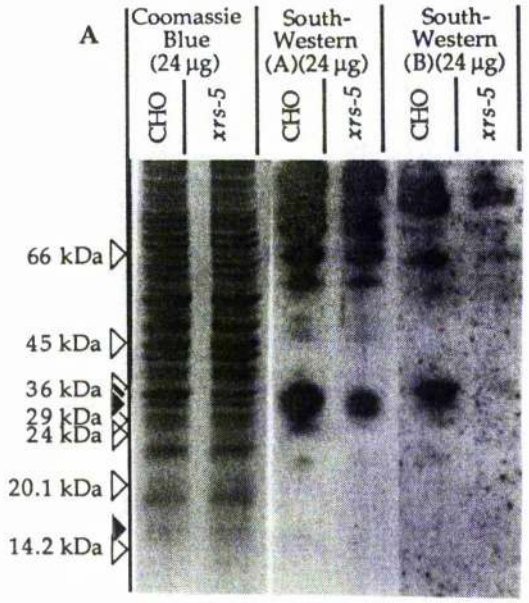

Figure 4.10.
600 mM NaCl

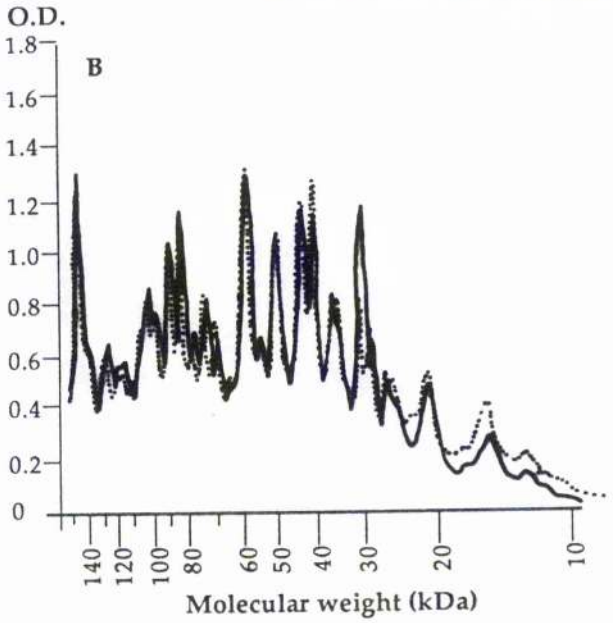

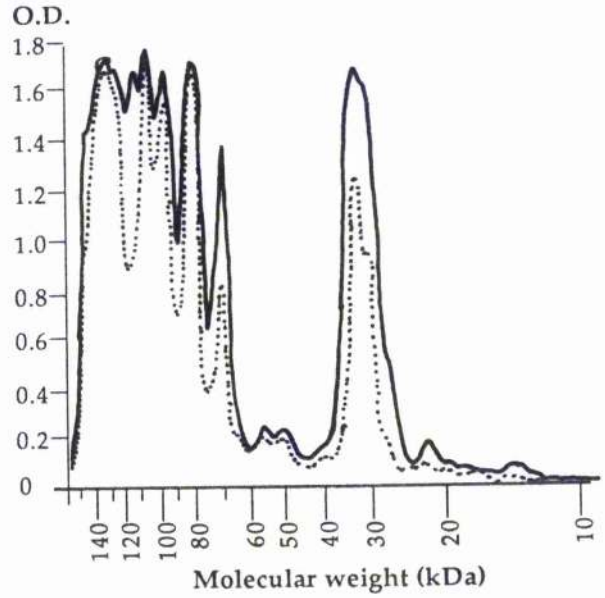

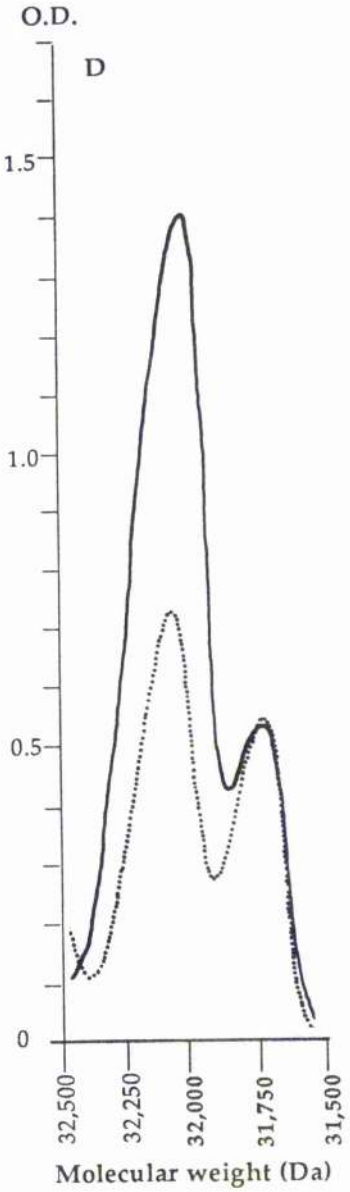

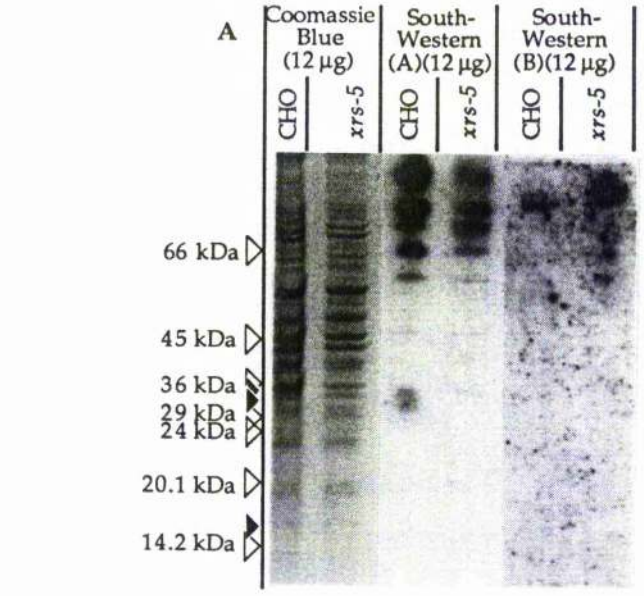

Figure 4.11.
800 mM NaCl

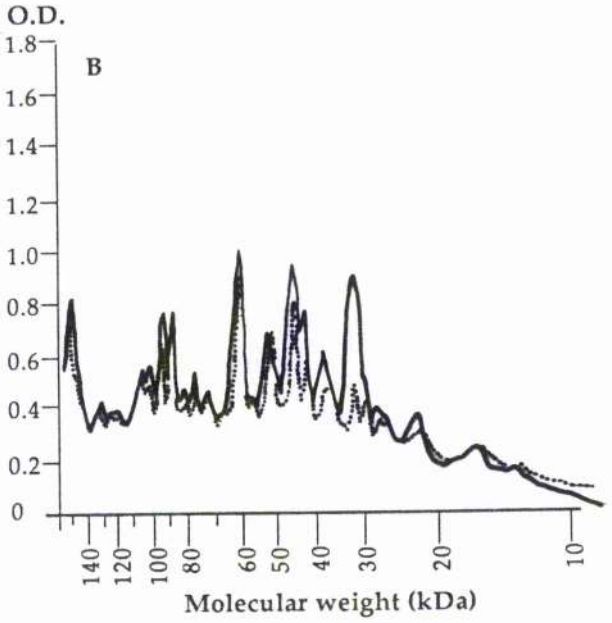

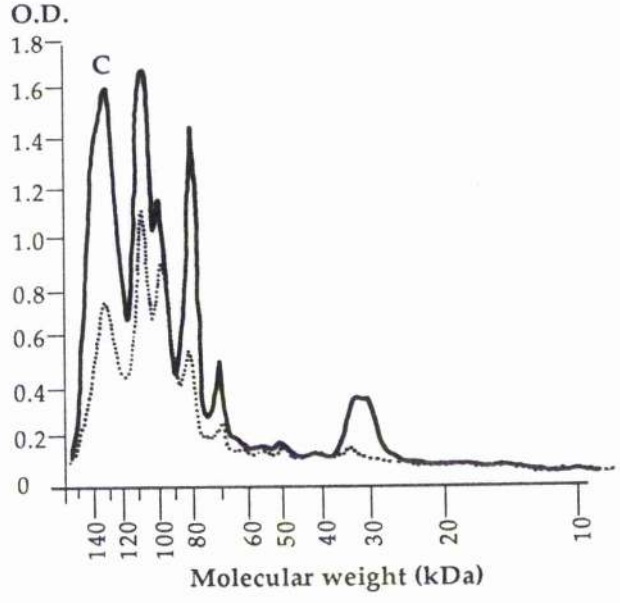

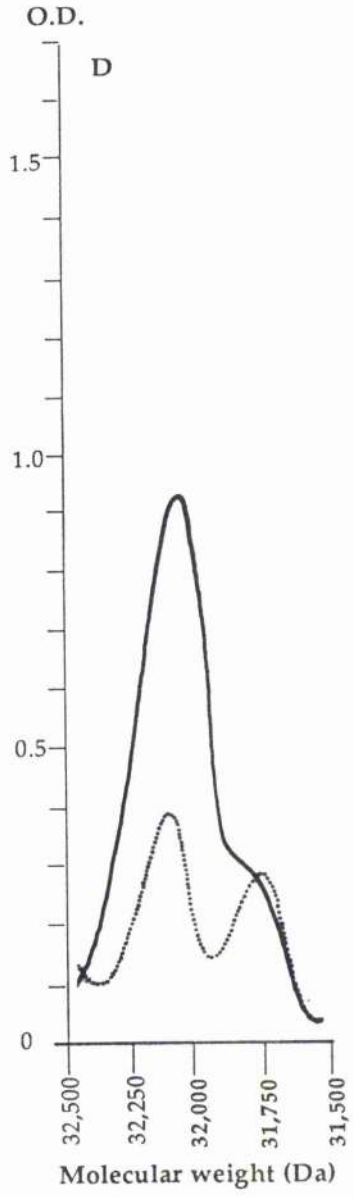

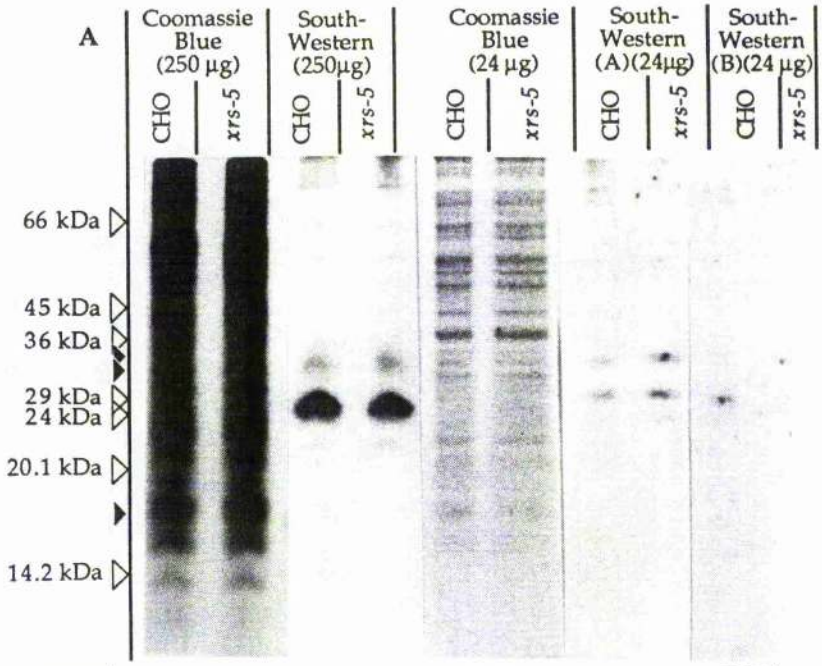

Figure 4.12.
100 mM KCl
(irradiated cell extract)

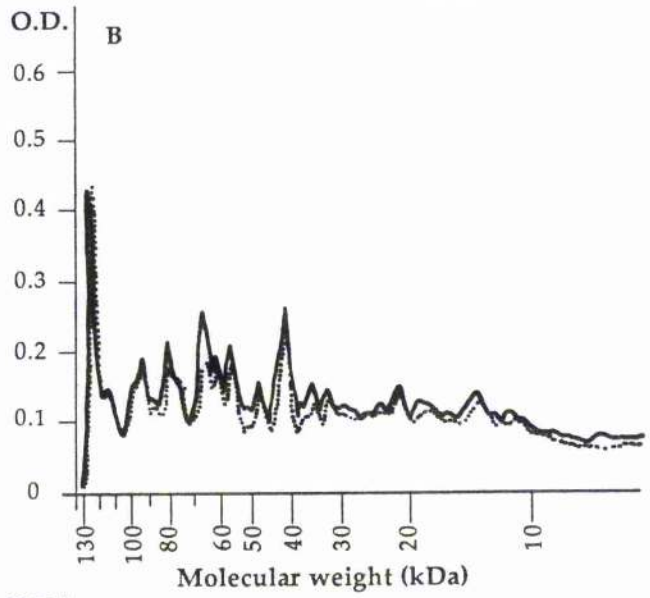

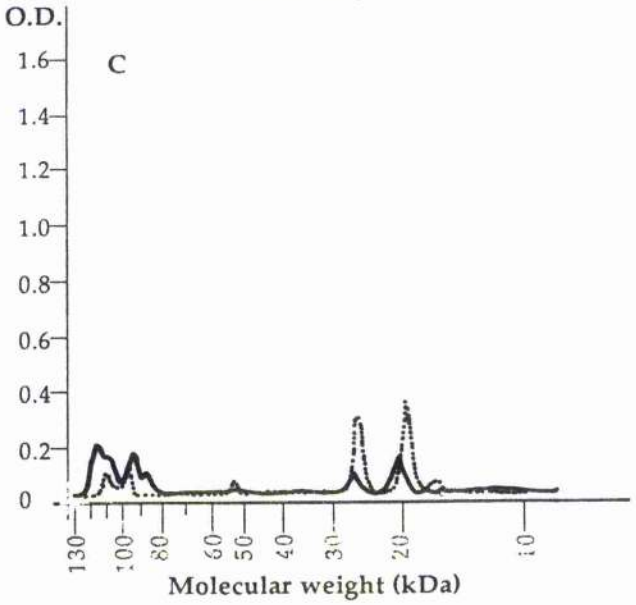

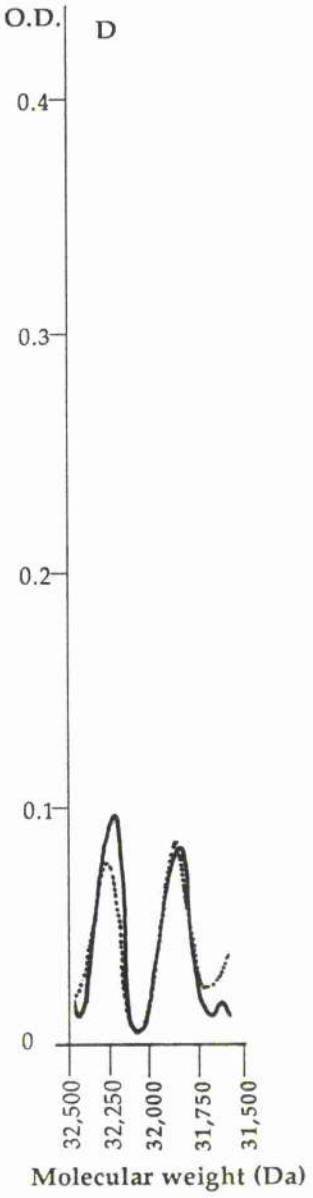

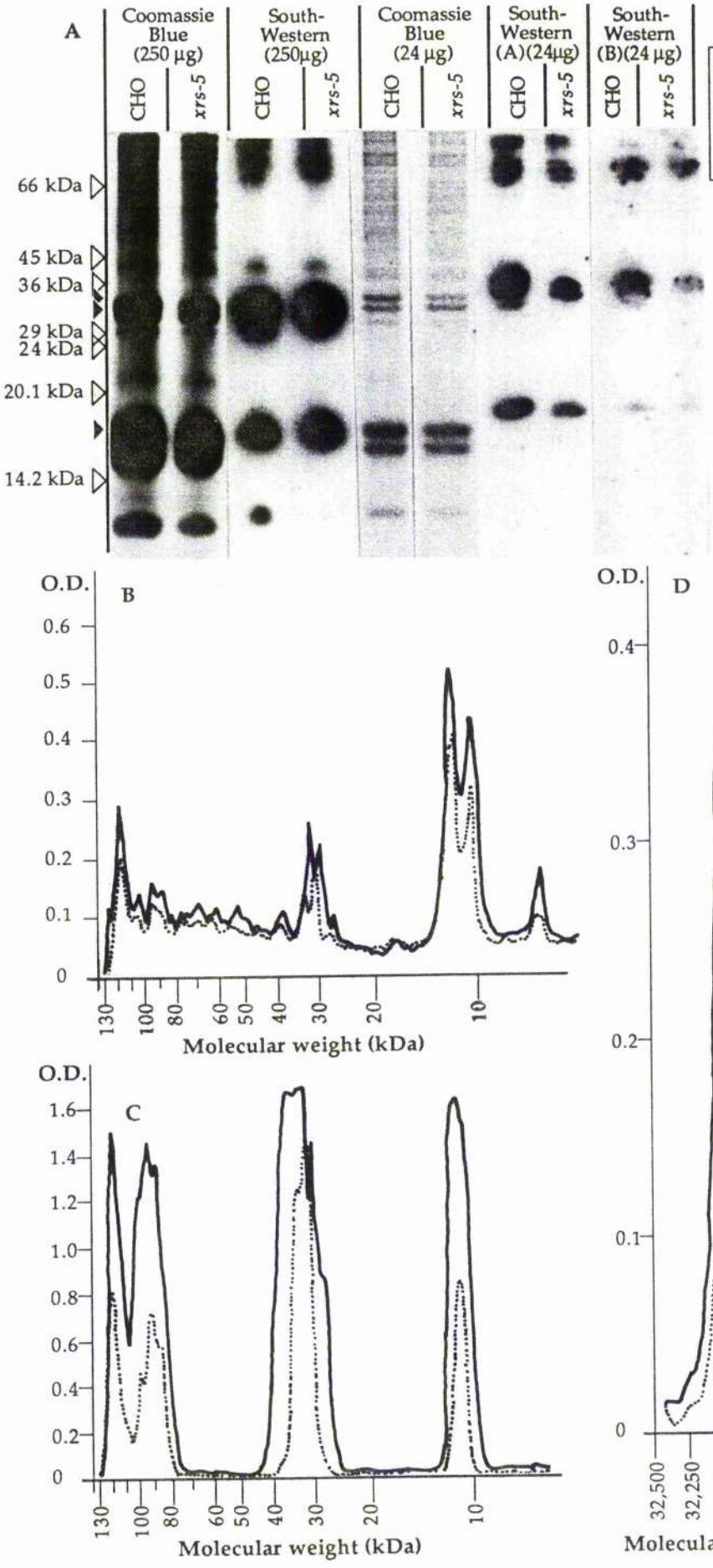

Figure 4.13.
250 mM $MgCl_2$
(irradiated cell extract)

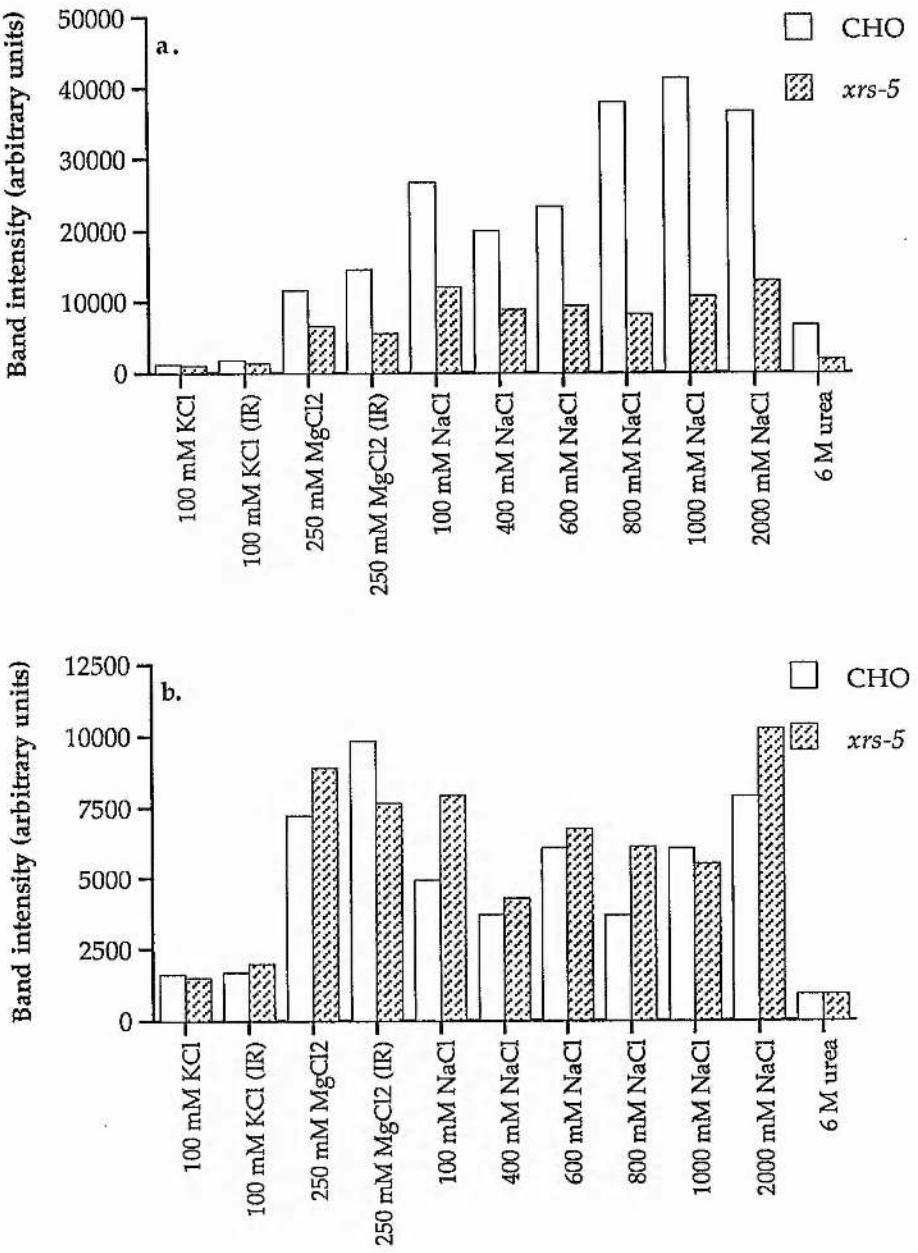

Figure 4.14. Amounts of the Coomassie blue stained a) p32.2 and b) p31.8 bands in various extracts derived from CHO and *xrs-5* cells. Graph represents the calculated area under the densitometric traces (in arbitrary units) which is proportional to the amount of protein present in the band.

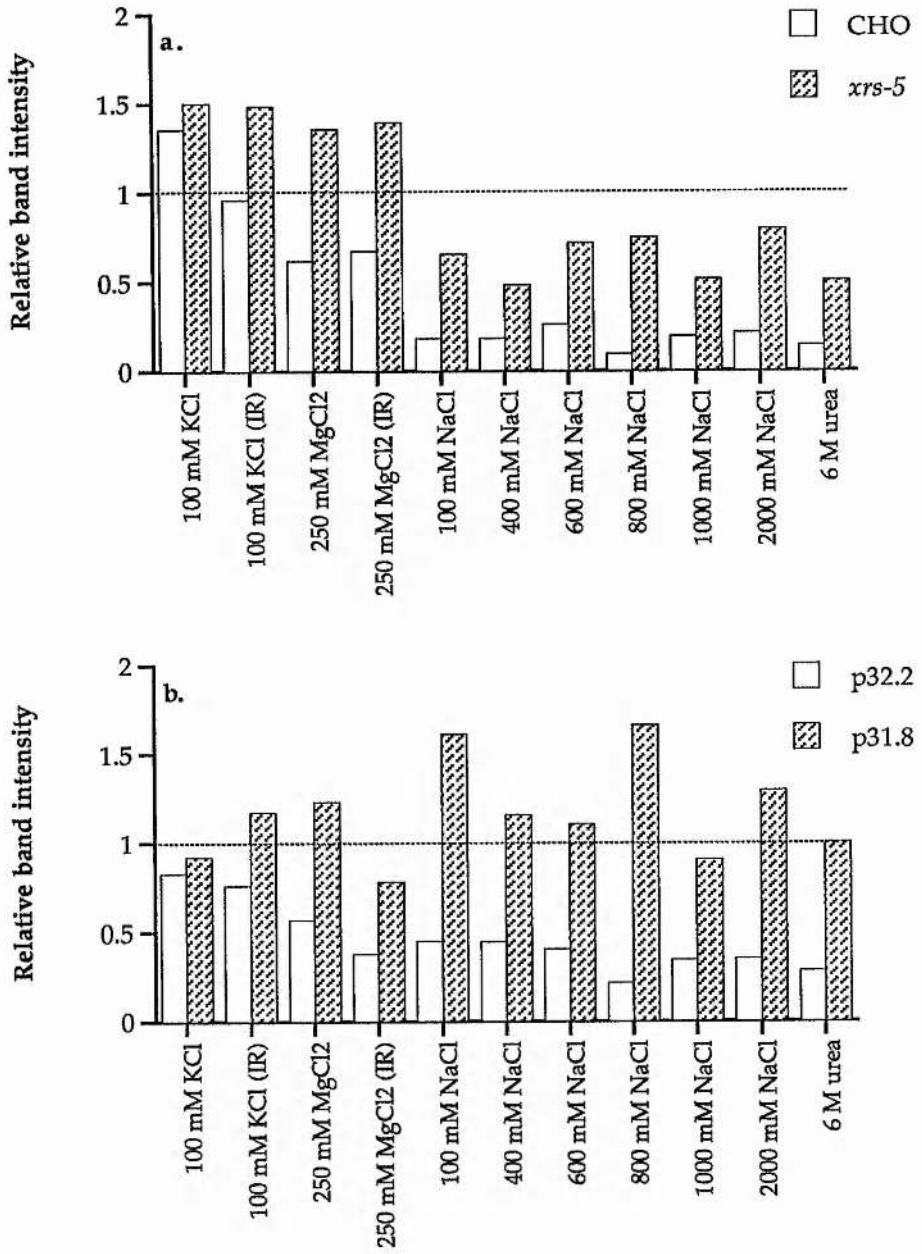

Figure 4.15. a) Ratio of the intensity of the Coomassie blue stained p31.8 band intensity relative to the p32.2 band for various extracts derived from CHO and *xrs-5*. Here a value of 1 indicates that the bands are similar in intensity.
b) Intensity of the Coomassie blue p32.2. and p31.8 bands for *xrs-5* extracts relative to CHO extracts. Here a value of 1 indicates that the component proteins exist in similar quantities in *xrs-5* and CHO extracts.

4.4. Discussion.

The protein extracts described above were relatively crude with a large number of constituent proteins. The *in vitro* analyses of activity that were performed failed to identify any obvious activity that could be directly related to the actual repair of DNA lesions.

The DNA binding activities of the extracts were estimated using a filter binding technique and the "DNA-Eppendorf" technique. These revealed that differences in both the total DNA binding activity extractable with the techniques employed, and the activity per μg of protein differed between the two cell lines examined (Figures 4.5 and 4.6). These differences appeared to be dependent on the type of extraction procedure used.

TSDS-PAGE separation of the fractions obtained by a variety of detergent-free extraction procedures identified differences in both the intensity and DNA binding activities of at least two polypeptide bands, designated p32.2 and p31.8. *Xrs-5* extracts were depleted in the level of the most prevalent; p32.2, with a corresponding decrease in DNA binding activity at this molecular weight. The second band; p31.8, although apparently occurring at similar levels relative to CHO appeared to exhibit a decreased binding activity in *xrs-5*. The protein bands represented by p32.2 and p31.8 correspond with the major DNA binding polypeptides in a commercially purified calf thymus histone H1 extract. Although exact identification of p32.2 and p31.8, requires much further work this data provides circumstantial evidence as to their identity.

The procedures used to extract proteins from the nuclei of CHO and xrs-5 cells involved alterations in ionic strength and, in the majority of extracts, the actions of the polyamine spermine. It is therefore unlikely that extracts obtained by these procedures will contain structural components of the nuclear matrix such as the nuclear lamins which remain attached to nuclear DNA even in the presence of 2 M NaCl and non-ionic detergents [Berezney and Coffey, 1977]. Western blot analysis of 100 mM KCl and 250 mM $MgCl_2$ extracts using an anti-lamin A/C antibody failed to identify the presence of these proteins in these extracts. In contrast, the residual nucleoids (extracted with 6 M urea) were positive for lamins A/C. The other main chromatin proteins such as histones are less stably attached and can be readily removed by increasing salt concentrations [Levin et al., 1978; Levin and Cook, 1981].

Histone H1, as described in chapter 3 comprises an abundant family of polypeptides which bind to linker regions of DNA. They are lysine rich proteins with approximate molecular weights of 23 kDa although as observed in Figure 4.3c, these proteins separate anomalously under SDS-PAGE conditions with higher than expected apparent molecular weights. Although there exists at least 6 H1 sub-types plus the more distantly related H^0 and H5

linker histones [Breneman et al., 1993] these polypeptides can be separated into three main bands using SDS-PAGE; H1A; H1B and $H1^0$. The former two may correspond with p32.2 and p31.8 respectively. Histone H1 is linked to the control of chromatin structure and gene regulation via its binding to specific linker regions [Allan et al, 1980; Käs et al., 1989; Levine et al., 1993]. These sites include MARs and similar AT rich sequences. The relative levels of the different H1 subtypes vary in both quantity and location throughout the nucleus [Breneman et al., 1993]. They are also subjected to cell cycle regulation via post-translational modifications which can act to control both position within chromatin and DNA binding activity and the associated effect on chromatin structure and function. Histone H1 proteolysis, poly(ADP)ribosylation and phosphorylation have all been identified to be affected after DNA damage [Fónagy et al., 1977; Roberge et al., 1990; Gaziez and Kutsyi, 1992; Panzeter et al., 1993]. This would imply that removal from or modification of histone H1 involvement with chromatin may be required during the cellular response to damage. This may permit repair enzymes access to sites of damage.

However, before more speculation on the possible involvement of histone H1 in the *xrs-5* defect can be made an identification of the proteins observed in this study is required. The difference in levels of the two protein bands p32.2 and p31.8 may have no connection with the sensitivity of *xrs-5* to ionising radiation. Instead they may be a pleiotropic effect of the *xrs* gene. The lower p32.2 levels in *xrs-5* may be due to a reduction in transcription of the respective gene, as observed for other genes [Zhu et al., 1992; 1993] or it may be the result of the increased proportion of non-cycling cells observed in chapter 2. That the p32.2 protein appears to be one of the major DNA binding polypeptides in the extracts would indicate that it may be of importance in the basic structure and functioning of chromatin.

The differences in the structure of *xrs-5* nuclei and chromatin that have been observed [Yasui et al., 1991; 1994; Schwartz et al., 1992; 1993] may therefore be due to altered levels of DNA binding proteins and/or the specificity of these proteins for DNA sequences. This may in turn alter the processing of DNA damage in *xrs-5* cells. Similarly an altered specificity of DNA binding proteins for specific sequences might be the cause of reduced activation of transcription observed in *xrs* cells [Zhu et al., 1992; 1993]. Phosphorylation of linker histones and deacetylation of core histones have been demonstrated to make DNA accessible to *trans*-acting transcription factors [reviewed in Wolffe, 1991]. Similarly histone H1 binding to SAR recognition sequences can alter higher order structures via inhibition of matrix attachment [Käs et al., 1989; 1993].

4.5. Conclusions.

By the use of *in vitro* DNA binding assays and electrophoretic analysis of the protein composition of extracts obtained from the nuclei of CHO and *xrs-5* cells at least one polypeptide has been identified which is reduced in concentration in extracts derived from *xrs-5* cells compared to similar extracts from CHO cells. In the wild-type extracts this protein is a major DNA binding protein. In *xrs-5* extracts the level of DNA binding by this polypeptide (or group of polypeptides) appears to be reduced. The apparent molecular weight of this polypeptide band (32.2 kDa) indicates that it may form part of the histone H1 family. Hence the defect in *xrs-5* may be related to a reduction in the levels of DNA binding proteins which may play a role in chromatin structure and function. However, this study did not identify any direct involvement of the proteins observed to differ in the two cell lines in the radiation sensitivity phenotype of *xrs-5*.

Chapter 5.

General conclusions.

The aims of this thesis were to examine the radiosensitive phenotype of the CHO mutant *xrs-5* via a number of approaches at both cellular and molecular levels. By the examination of the response of *xrs-5* cells to a number of clastogens using the cytokinesis block micronucleus assay a possible cell cycle defect was identified in addition to elevated levels of expressed chromosome damage. This was in addition to a constitutive elevation of the frequency of non-cycling cells in *xrs-5*. *Xrs-5* cells appeared to be partially defective in damage dependent cell cycle checkpoints. In the wild-type cell line these checkpoints inhibit the passage of cells into mitosis after treatment with clastogens. The position of this checkpoint defect in *xrs-5* in the cell cycle was postulated to occur within the G_2 phase since it has been demonstrated that the G_1/S inhibition of entry into S phase in response to DNA damage is more severe in *xrs* cells [Jeggo, 1985]. In addition, caffeine, an inhibitor of the G_2 check point in wild-type cells, was ineffective in *xrs-5* cells after irradiation. The increased levels of expressed damage in *xrs-5* may therefore be due to these cells passing into mitosis with an elevated level of DNA damage. That repair of DSB is apparently normal in G2 *xrs-5* cells [Mateos et al., 1994] and that the kinetics of the repair of chromatid breaks [MacLeod and Bryant, 1990] would support this.

That there might be cell cycle related components to the *xrs-5* phenotype does not diminish the importance of the DSB repair defect that can be observed in exponentially growing and G_1 cells [Kemp et al., 1984; Dahm-Daphi et al., 1993, Mateos et al., 1994]. Chapter 3 described experiments whereby the repair of DSB was dependent on the spatial orientation of these breaks in relation to both other DSB and to higher order structures within the chomatin. Very large structures, Mbp in length, containing multiple DSB exhibited slow DSB repair kinetics in the wild-type. In the *xrs-5* cells this repair was absent. In contrast, repair of DSB which occurred individually within these structures could be repaired proficiently and with fast kinetics in both CHO and *xrs-5* cells. These results indicate that the structural differences observed in the nuclei of *xrs* cells [Yasui et al, 1991; 1994; Schwartz et al., 1992; 1993] may indeed play a part in the repair defect of these cells. The nature of the role of nuclear structure in the repair of DSB is still unclear since it is not certain whether it is a constitutive structural component or an induced change in nuclear structure that is responsible for the repair of a proportion of DSB in the wild-type but not the *xrs-5* cells.

Further evidence of a constitutive alteration in nuclear structure of *xrs-5* cells was presented in chapter 4. Using salt and polyanion elutable nuclear extracts the DNA binding activities of these proteins was examined and found to be altered in the *xrs-5* extracts. One major DNA binding polypeptide band, with an apparent molecular weight 32.2 kDa, exhibited both a decrease in levels and DNA binding activity compared to CHO extracts. The position of the bands coincided with a DNA binding polypeptide band in purified calf thymus histone H1

preparations. This speculative identification would indicate that the *xrs-5* structural defects, and possibly the structure dependent DSB repair defect, may involve altered levels of consitutive chromatin proteins. That these may be related to the histone H1 family of linker proteins would provide possible roles for ubiquitous chromatin proteins in the response of cells to ionising radiation. Similarly, the cell cycle component of the *xrs-5* phenotype may be related to the structural component via the regulatory mechanisms which exist, such as protein phosphorylation levels. The *xrs-5* characteristics observed in the DNA repair and protein studies described in this thesis may therefore be related not to defects in classical repair pathways involving DSB processing but via events which lie either upstream or downstream from these. Upstream events might involve chromatin structure alterations which prevent either damage recognition and/or repair processes whilst downstream events might involve subsequent effects of damage on cell cycle related events which in turn may involve chromatin structural alterations.

The human gene which complements the *xrs* phenotype (*XRCC5*) has recently been identified [Taccioli et al., 1994 in press]. By the laborious task of positional cloning [Jeggo et al., 1992; Hafezparast et al., 1993] and molecular cloning techniques involving human gene libraries of the identified chromosomal regions [Taccioli et al., 1994 in press] the *XRCC5* has been identified as the *Ku 80* gene. The gene product of this gene, Ku 80, is along with Ku 70, one part of a heterodimeric polypeptide which is the DNA-binding subunit of a DNA dependent protein kinase. The Ku heterodimer binds to the ends of DNA and as such may play a part in the repair of DSB. That this polypeptide is also linked with a protein kinase may imply that the absence of this protein prevents the recognition of DSB and that subsequent events involved in the repair of DSB are defective. This may link up with the cell cycle related component of the *xrs* phenotype via protein kinase regulation of cell cycle progression.

Therefore, although the gene responsible for the *xrs* phenotype has been identified it is clear that much additional work is required to identify the relationship betwen Ku 80 and DSB and other mechanisms and interacting proteins which will undoubtably be involved in the repair and response of cells to ionising radiation. Hopefully this thesis has made some headway in this direction.

Bibliography.

Adachi, Y., Käs, E. and Laemmli, U. K., 1989, Preferential, cooperative binding of DNA topoisomerase II to scaffold-associated regions. *EMBO J.*, **8**, 3997-4006.

Adachi, Y. and Laemmli, U. K., 1992, Identification of nuclear pre-replication centers poised for DNA synthesis in *Xenopus* egg extracts: Immunolocalisation study of replication protein A. *J. Cell Biol.*, **119**, 1-15.

Adolph, K. W., Cheng, S. M. and Laemmli, U. K., 1977, Role of nonhistone proteins in metaphase chromosome structure. *Cell*, **12**, 805-816.

Adolph, K. W., Cheng, S. M., Paulson, J. R. and Laemmli, U. K., 1977, Isolation of a protein scaffold from mitotic HeLa cell chromosomes. *Proc. Natl. Acad. Sci. USA.*, **74**, 4937-4941.

Ahnström, G. and Ljungman, M., 1988, Effects of 3-aminobenzamide on the rejoining of DNA-strand breaks in mammalian cells exposed to methyl methanesulphonate; role of poly(ADP-ribose) polymerase. *Mutat. Res.*, **194**, 17-22.

Alberts, B., Bray, D., Lewis, J., Raff, M., Roberts, K. and Watson, J. D., 1983, *Molecular biology of the cell.* (Garland Publishing Inc., New York).

Allan, J., Cowling, G. J., Harborne, N., Cattini, P., Craigie, R. and Gould, H., 1981, Regulation of the higher-order structure of chromatin by histones H1 and H5. *J. Cell Biol.*, **90**, 279-288.

Allan, J., Harborne, N., Rau, D. C. and Gould, H., 1982, Participation of core histone "tails" in the stabilisation of the chromatin solenoid. *J. Cell Biol.*, **93**, 285-297.

Allan, J., Hartman, P. G., Crane-Robinson, C. and Aviles, F. X., 1980, The structure of histone H1 and its location in chromatin. *Nature*, **288**, 675-679.

Alper, T., 1979, *Cellular radiobiology.* (Cambridge University Press, Cambridge).

Balbi, C., Pala, M., Parodi, S., Figari, G., Cavazza, B., Trefiletti, V. and Patrone, E., 1986, A simple model for DNA elution from filters.

Baldwin, J. P., 1992, Protein-nucleic acid interactions in nucleosomes. *Curr. Opin. Structural Biol.*, **2**, 78-83.

Bauer, W. R., 1978, Structure and reactions of closed duplex DNA. *Ann. Rev. Biophys. Bioeng.*, **7**, 287-313.

Beerman, T. A., Woynarowski, J. M., Sigmund, R. D., Gawron, L. S., Rao, K. E. and Lown, J. W., 1991, Netropsin and bis-netropsin analogs as inhibitors of the catalytic activity of mammalian DNA topoisomerase II and topoisomerase cleavable complexes. *Biochim. Biophys. Acta*, **1090**, 52-60.

Belehradek Jr, J., Orlowski, S., Poddevin, B., Paoletti, C. and Mir, L. M., 1991, Electrochemotherapy of spontaneous mammary tumours in mice. *Eur. J. Cancer*, **27**, 73-76.

Berezney, R. and Coffey, D. S., 1977, Nuclear matrix. Isolation and characterisation of a framework structure from rat liver nuclei. *J. Cell Biol.*, **73**, 616-637.

Berrios, M., Osheroff, N. and Fisher, P., 1985, *In situ* localisation of DNA topoisomerase II, a major polypeptide of the *Drosophila* nuclear matrix. *Proc. Natl. Acad. Sci. USA.*, **82**, 4142-4146.

Bertrand, R., Solary, E., O'Connor, P., Kohn, K. W. and Pommier, Y., 1994, Induction of a common pathway of apoptosis by staurosporine. *Exp. Cell Res.*, **211**, 314-321.

Bialojan, C. and Takai, A., 1988, Inhibitory effect of a marine-sponge toxin, okadaic acid, on protein phosphatases. *Biochem. J.*, **256**, 283-290.

Black, E. J., Street, A. J. and Gillespie, D. A. F., 1991, Protein phosphatase 2A reverses phosphorylation of c-Jun specified by the delta domain in vitro: correlation with oncogenic activation and deregulated transactivation activity of v-jun. *Oncogene*, **6**, 1949-1958.

Blöcher, D., 1982, DNA double strand breaks in Ehrlich ascites tumour cells at low doses of X-rays. I. Determination of induced breaks by centrifugation at reduced speed. *Int. J. Radiat. Biol.*, **42**, 317-328.

Blöcher, D., 1988, DNA double-strand break repair determines the RBE of α-particles. *Int. J. Radiat. Biol.*, **54**, 761-771.

Blöcher, D., 1990, In CHEF electrophoresis a linear induction of dsb corresponds to a non-linear fraction of extracted DNA with dose. *Int. J. Radiat. Biol.*, **57**, 7-12.

Blöcher, D. and Pohlit, W., 1982, DNA double strand breaks in Ehrlich ascites tumour cells at low doses of X-rays, II. Can cell death be attributed to double strand breaks? *Int. J. Radiat. Biology.*, **42**, 329-338.

Bradley, M. O. and Kohn, K. W., 1979, X-ray induced DNA double strand break production and repair in mammalian cells as measured by neutral filter elution. *Nucleic Acids Res.*, **7**, 793-804.

Breneman, J. W., Yau, P., Teplitz, R. L. and Bradbury, E. M., 1993, A light microscopic study of linker histone distribution in rat metaphase chromosomes and interphase nuclei. *Exp. Cell Res.*, **206**, 16-26.

Bridger, J. M., Kill, I. R. and Hutchison, C. J., 1993, Internal structures within G1 nuclei of human dermal fibroblasts. *J. Cell Sci.*, **104**, 297-306.

Bryant, P. E., 1984, Enzymatic restriction of mammalian cell DNA using Pvu II and Bam H1: evidence for the double strand break origin of chromosomal aberrations. *Int. J. Radiat. Biol.*, **43**, 459-464.

Bryant, P. E., 1985, Enzymatic restriction of mammalian cell DNA: evidence for double strand breaks as potentially lethal lesions. *Int. J. Radiat. Biol.*, **48**, 55-60.

Bryant, P. E., 1992, Induction of chromosomal damage by restriction endonuclease in CHO cells porated with streptolysin O. *Mutation Res.*, **268**, 27-34.

Bryant, P. E., Birch, D. A. and Jeggo, P. A., 1987, High chromosomal sensitivity of Chinese hamster xrs 5 cells to restriction endonuclease induced DNA double-strand breaks. *Int. J. Radiat. Biol.*, **52**, 537-554.

Bryant, P. E. and Christie, A. F., 1989, Induction of chromosomal aberrations in CHO cells by restriction endonucleases: effects of blunt- and cohesive-ended double-strand breaks in cells treated by "pellet" methods. *Mutat. Res.*, **213**, 233-241.

Bryant, P. E. and Johnston, P. J., 1993, Restriction-endonuclease-induced DNA double strand breaks and chromosomal aberrations in mammalian cells. *Mutation Res.*, 299, 289-296.

Buckingham, L. and Duncan, J. L., 1983, Approximate dimensions of membrane lesions produced by streptolysin S and streptolysin O. *Biochim. Biophys. Acta*, **729**, 115-122.

Buongiorno-Nardelli, M., Micheli, G., Carri, M. T. and Marilley, M., 1982, A relationship between replicon size and supercoiled domains in the eukaryotic genome. *Nature*, 298, 100-102.

Busk, H., Thomsen, B., Bonven, B. J., Kjeldsen, E., Nielsen, O. F. and Westergaard, O., 1987, Preferential relaxation of supercoiled DNA containing a hexadecameric recognition sequence for topoisomerase II. *Nature*, 327, 639-640.

Byfield, J. E., Lee, Y. C. and Kulhanian, F., 1976, Molecular interactions of the combined effects of bleomycin and x-rays on mammalian cell survival. *Cancer Res.*, 36, 1138-1143.

Byrnes, R. W., Templin, J., Sem, D., Lyman, S. and Petering, D. H., 1990, Intracellular DNA strand scission and growth inhibition of Ehrlich ascites tumour cells by bleomycins. *Cancer Res.*, **50**, 5275-5286.

Caldecott, K., Banks, G. and Jeggo, P., 1993, The induction and reversal of topoisomerase II cleavable complexes formed by nuclear extract from the CHO DNA repair mutant, xrs1. *Mutation Res.*, 293, 259-267.

Cantoni, O., Cattabeni, F., Stocchi, V., Meyn, R. E., Cerutti, P. and Murray, D., 1989, Hydrogen peroxide insult in cultured mammalian cells: relationships between DNA single-strand breakage poly(ADP-ribose) metabolism and cell killing. *Biochim. Biophys. Acta*, **1014**, 1-7.

Cardenas, M. E. and Gasser, S. M., 1993, Regulation of topoisomerase II by phosphorylation: a role for casein kinase II. *J. Cell Sci.*, **104**, 219-225.

Cardenas, M. E., Walter, R., Hanna, D. and Gasser, S. M., 1993, Casein kinase II copurifies with yeast topoisomerase II and re-activates the dephosphorylated enzyme. *J. Cell Sci.*, **104**, 533-543.

Catena, C., Conti, D., del Nero, A. and Righi, E., 1992, Inter-individual differences in radiation response shown by an *in vitro* micronucleus assay: effects of 3-aminobenzamide on X-ray treatment. *Int. J. Radiat. Biol.*, 62, 687-694.

Charleton, D. E., Nikjoo, H. and Humm, J. L., 1989, Calculation of initial yields of single-and double-strand breaks in cell nuclei from electrons, protons and alpha particles. *Int. J. Radiat. Biol.*, 56, 1-19.

Charron, M. and Hancock, R., 1990, DNA topoisomerase II is required for formation of mitotic chromosomes in chinese hamster ovary cells: studies using the inhibitor 4'-demethylepipodophyllotoxin 9-(4,6-o-thenylidene-ß-D-glucopyranoside). *Biochemistry*, 29, 9531-9537.

Charron, M. and Hancock, R., 1991, Chromosome recombination and defective genome segregation induced in Chinese hamster cells by the topoisomerase II inhibitor VM-26. *Chromosoma*, **100**, 97-102.

Ciejek, E. M., Tsai, M. and O'Malley, B. W., 1983, Actively transcribed genes are associated with the nuclear matrix. *Nature*, **306**, 607-609.

Ciriolo, M. R., Peisach, J. and Magliozzo, R. S., 1989, A comparative study of the interactions of bleomycin with nuclei and purified DNA. *J. Biol. Chem.*, **264**, 1443-1449.

Cohen, P., 1989, The structure and regulation of protein phosphatases. *Annu. Rev. Biochem.*, **58**, 453-508.

Collins, A. R., 1993, Mutant rodent cell lines sensitive to ultraviolet light, ionising radiation and cross-linking agents: a comprehensive survey of genetic and biochemical characteristics. *Mutat. Res.*, **293**, 99-118.

Cook, P. R. and Brazell, I. A., 1975, Supercoils in human DNA. *J. Cell Sci.*, **19**, 261-279.

Cook, P. R. and Brazell, I. A., 1976, Conformational constraints in nuclear DNA. *J. Cell Sci.*, **22**, 287-302.

Cook, P. R. and Brazell, I. A., 1978, Spectrofluorometric measurement of the binding of ethidium to superhelical DNA from cell nuclei. *Eur. J. Biochem.*, **84**, 465-477.

Cook, P. R., Brazell, I. A. and Jost, E., 1976, Characterisation of nuclear structures containing superhelical DNA. *J. Cell Sci.*, **22**, 303-324.

Cook, P. R., Lang, J., Hayday, A., Lania, L., Fried, M., Chiswell, D. J. and Wyke, J. A., 1982, Active viral genes in transformed cells lie close to the nuclear cage. *EMBO J.*, **1**, 447-452.

Costa, N. D. and Bryant, P. E., 1988, Repair of DNA single-strand and double-strand breaks in the Chinese hamster xrs 5 mutant cell line as determined by DNA unwinding. *Mutation Res.*, **194**, 93-99.

Costa, N. D. and Bryant, P. E., 1990, The induction of DNA double-strand breaks in CHO cells by Pvu II: kinetics using neutral filter elution (pH 9.6). *Int. J. Radiat. Biol.*, **57**, 933-938.

Costa, N. D. and Bryant, P. E., 1991a, Differences in the accumulation of blunt and cohesive ended double-strand breaks generated by restriction endonucleases in electroporated CHO cells. *Mutation Res.*, **254**, 239-246.

Costa, N. D. and Bryant, P. E., 1991b, Elevated levels of DNA double strand break (DSB) in restriction endonuclease treated xrs 5 cells correlates with the reduced capacity to repair DSB. *Mutation Res.*, **255**, 219-226.

Costa, N. D. and Thacker, J., 1993, Response of radiation-sensitive human cells to defined DNA breaks. *Int. J. Radiat. Biol.*, **64**, 523-529.

Cozzarelli, N. R., 1980, DNA gyrase and the supercoiling of DNA. *Science*, **207**, 953-960.

D'Erme, M., Santoro, R., Allegra, P., Reale, A., Marenzi, S., Strom, R. and Caiafa, P., 1993, Inhibition of CpG methylation in linker DNA by H_1 histone. *Biochim. Biophys. Acta*, **1173**, 209-216.

Dahm-Daphi, J., Dikomey, E., Pyttlik, C. and Jeggo, P. A., 1993, Reparable and non-reparable DNA strand breaks induced by X-irradiation in CHO K1 cells and the radiosensitive mutants *xrs1* and *xrs5*. *Int. J. Radiat. Biol.*, **64**, 19-26.

Darroudi, F. and Natarajan, A. T., 1987a, Cytological characterisation of Chinese hamster ovary X-ray-sensitive mutant cells xrs 5 and xrs 6. I. Induction of chromosomal aberrations by X-irradiation and its modulation with 3-aminobenzamide and caffeine. *Mutation Res.*, **177**, 133-148.

Darroudi, F. and Natarajan, A. T., 1987b, Cytological characterisation of Chinese hamster ovary X-ray sensitive mutant cells, xrs 5 and xrs 6. II. Induction of sister-chromatid exchanges and chromosomal aberrations by X-rays and UV-irradiation and their modulation by inhibitors of poly(ADP-ribose) synthetase and α-polymerase. *Mutation Res.*, **177**, 149-160.

Darroudi, F. and Natarajan, A. T., 1989a, Cytogenetical characterisation of Chinese hamster ovary X-ray sensitive mutant cells xrs 5 and xrs 6. III. induction of cell killing, chromosomal aberrations and sister chromatid exchanges by bleomycin, mono-and bi-functional alkylating agents. *Mutation Res.*, **212**, 123-135.

Darroudi, F. and Natarajan, A. T., 1989b, Cytogenetical characterisation of Chinese hamster ovary X-ray sensitive mutant cells, xrs 5 and xrs 6. IV. Study of chromosomal aberrations and sister-chromatid exchanges by restriction endonucleases and inhibitors of DNA topoisomerase II. *Mutation Res.*, **212**, 137-148.

Darroudi, F. and Natarajan, A. T., 1989c, Cytogenetical characterisation of Chinese hamster ovary X-ray sensitive mutant cells xrs 5 and xrs 6. VII. Complementation analysis of X-irradiated wild-type CHO-K1 and xrs mutant cells using the premature chromosome condensation technique. *Mutation Res.*, **213**, 249-255.

Darroudi, F., Natarajan, A. T., Schans, G. P. v. d. and Loon, A. A. W. M. v., 1990, Biochemical and cytological characterisation of Chinese hamster ovary X-ray-sensitive mutant cells xrs 5 and xrs 6. V. The correlation of DNA starnd breaks and base damage to chromosomal aberrations and sister-chromatid exchanges induced by X-irradiation. *Mutation Res.*, 235, 119-127.

Denekamp, J., Whitmore, G. F. and Jeggo, P., 1989, Biphasic survival curves for XRS radiosensitive cells: subpopulations or transient expression of repair competance? *Int. J. Radiat. Biol.*, 55, 605-617.

Dewey, W. C., Noel, J. S. and Dettor, C. M., 1972, Changes in radiosensitivity and dispersion of chromatin during the cell cycle of synchronous chinese hamster cells. *Radiat. Res.*, 52, 373-394.

Downes, C. S. and Johnson, R. T., 1988, DNA topoisomerases and DNA repair. *Bioessays*, 8, 179-184.

Dröge, P., 1994, Protein tracking-induced supercoiling of DNA: A tool to regulate DNA transaction *in vivo*. *Bioessays*, **16**, 91-99.

Durante, M., Grossi, G. F., Napolitano, M. and Gialanella, G., 1991, Repair of potentially lethal damage by introduction of T4 DNA ligase in eucaryotic cells. *Int. J. Radiat. Biol.*, **59**, 963-971.

Earnshaw, W. C., Halligan, B., Cooke, C. A., Heck, M. M. S. and Liu, L. F., 1985, Topoisomerase II is a structural component of mitotic chromosome scaffolds. *J. Cell Biol.*, **100**, 1706-1715.

Eker, A. P. M., Vermeulen, W., Miura, N., Tanaka, K., Jaspers, N. G. J., Hoejimakers, J. H. J. and Bootsma, D., 1992, Xeroderma pigmentosum group A correcting protein from calf thymus. *Mutation Res.*, **274**, 211-224.

Englander, E. W., Wolffe, A. P. and Howard, B. H., 1993, Nucleosome interactions with a human Alu element. Transcriptional repression and effects of template methylation. *J. Biol. Chem.*, **268**, 19565-19573.

Evans, H. J., 1977, Molecular mechanisms in the induction of chromosome aberrations. In: *Progress in genetic toxicology.* Edited by: D. Scott, B. A. Bridges and F. H. Sobles, (Elsevier, Amsterdam), pp. 55-74.

Falk, S. J. and Smith, P. J., 1992, DNA damaging and cell cycle effects of the topoisomerase I poison camptothecin in irradiated human cells. *Int. J. Radiat. Biol.*, **61**, 749-757.

Farrance, I. K. and Ivarie, R., 1985, Ethylation of poly(dG-dG) poly(dC-dG) by ethylmethanesulphonate stimulates the activity of mammalian DNA methyltransferase *in vitro*. *Proc. Natl. Acad. Sci. USA*, **82**, 1045-1049.

Fenech, M. and Morley, A. A., 1985, Measurement of micronuclei in lymphocytes. *Mutation. Res.*, **147**, 29-36.

Filipovitch, J. V., Sorokina, N. J., Soldatenkov, V. A. and Romantzev, E. F., 1982, Supercoiled DNA repair in thymocyte fractions differing in radiosensitivity. *Int. J. Radiat. Biol.*, **42**, 31-44.

Fónagy, A., Ord, M. G. and Stocken, L. A., 1977, Phosphorylation of rat thymus histones, its control and the effects theron of γ-irradiation. *Biochem. J.*, **162**, 171-181.

Fonck, K., Barthel, R. and Bryant, P. E., 1984, Kinetics of recombinational hybrid formation in X-irradiated mammalian cells: a possible first step in the repair of DNA double strand breaks. *Mutat. res.*, **132**, 113-118.

Fox, M. and Nias, A. H. W., 1970, The influence of recovery from sublethal damage on the response of cells to protracted irradiation at low dose rate. *Curr. Topics Radiat. Res. Quarterly*, **7**, 71-103.

Fox, M. H., Arndt-Jovin, D. J., Jovin, T. M., Baumann, P. H. and Robert-Nicoud, M., 1991, Spatial and temporal distribution of DNA replication sites localised by immunofluorescence and confocal microscopy in mouse fibroblasts. *J. Cell Sci.*, **99**, 247-253.

Franke, W. W., 1974, Structure, biochemistry and functions of the nuclear envelope. *Int. Rev. Cytol.*, **4**, 72-236.

Franke, W. W., 1987, Nuclear lamins and cytoplasmic intermediate filament proteins: A growing multigene family. *Cell*, **48**, 3-4.

Frankenberg, D., 1969, A ferrous sulphate dosemeter independent of photon energy in the range from 25 KeV to 59 MeV. *Phys. Med. Biol.*, **14**, 597-605.

Frankenberg, D., Frankenber-Schwager, M. and Harbich, R., 1984a, Interpretation of the shape of survival curves in terms induction and repair/misrepair of DNA double strand breaks. *Br. J. Cancer*, **49**, 233-238.

Frankenberg, D., Frankenberg-Schwager, M., Blöcher, D. and Harbich, R., 1981, Evidence for DNA double strand breaks as the critical lesions in yeast cells irradiated with sparsely or densely ionising radiation under oxic or anoxic conditions. *Radiat. Res.*, 88, 524-532.

Frankenberg, D., Frankenberg-Schwager, M. and Harbich, R., 1984b, Split-dose recovery is due to the repair of DNA double strand breaks. *Int. J. Radiat. Biol.*, **46**, 541-553.

Gao, S., Drouin, R. and Holmquist, G. P., 1994, DNA repair rates mapped along the human *PGK 1* gene at nucleotide resolution. *Science*, **263**, 1438-1440.

Gasser, S. M. and Laemmli, U. K., 1986, The organisation of chromatin loops: Characterisation of a scaffold attachment site. *EMBO J.*, **5**, 511-518.

Gasser, S. M., Laroche, T., Falquet, J., Boy de la Tour, E. and Laemmli, U. K., 1986, Metaphase chromosome structure involvment of topoisomerase II. *J. Mol. Biol.*, **188**, 613-629.

Gavin, A. C., Tsukitani, Y. and Schoderet-Slatkine, S., 1991, Induction of M-Phase entry of prophase-blocked mouse oocytes through microinjection of okadaic acid, a specific phosphatase inhibitor. *Exp. Cell. Res.*, **192**, 75-81.

Gaziez, A. I. and Kutsyi, M. P., 1992, Gamma-irradiated DNA activates histone H1-specific proteinase of rat liver nuclei. *Int. J. Radiat. Biol.*, **61**, 169-174.

Ghosh, S., Paweletz, N. and Schroeter, D., 1992, Effects of okadaic acid on mitotic HeLa cells. *J. Cell Sci.*, **103**, 117-124.

Glass, J. R. and Gerace, L., 1990, Lamins A and C bind and assemble at the surface of mitotic chromosomes. *J. Cell Biol.*, **111**, 1047-1057.

Glisson, B., Gupta, R., Hodges, P. and Ross, W., 1986b, Cross-resistence to intercalating agents in epipodophyllotoxin-resistent Chinese hamster ovary cell line: evidence for a common intracellular target. *Cancer Res.*, **46**, 1939-1942.

Glisson, B., Gupta, R., Smallwood-Kentro, S. and Ross, W., 1986a, Characterisation of aquired epipodophyllotoxin resistance in a Chinese hamster ovary cell line: loss of drug-stimulated DNA cleavage. *Cancer Res.*, **46**, 1934-1938.

Goodhead, D. T., 1989, The initial physical damage produced by ionising radiations. *Int. J. Radiat. Biol.*, **56**, 623-634.

Goodhead, D. T., 1994, Initial events in the cellular effects of ionising radiations: clustered damage in DNA. *Int. J. Radiat. Biol.*, **65**, 7-17.

Graziano, V., Gerchman, S. E., Schneider, D. K. and Ramakrishnan, V., 1994, Histone H1 is located in the interior of the chromatin 30-nm filament. *Nature*, 368, 351-354.

Guilly, M. N., Kob, J. P., Gosti, F., Godeau, F. and Courvalin, J. C., 1990, Lamins A and C are not expressed at early stages of human lymphocyte differentiation. *Exp. Cell Res.*, 189, 145-147.

Hafezparast, M., Kaur, G. P., Zdzienicka, M., Athwal, R. S., Lehmann, A. R. and Jeggo, P. A., 1993, Sub-chromosomal localisation of a gene (*XRCC5*) involved in double strand break repair to the region 2q34-36. *Somat. Cell Molec. Genet.*, 19, 211-217.

Hakes, D. J. and Berezney, R., 1991, DNA binding properties of the nuclear matrix and individual nuclear matrix proteins. *J. Biol. Chem.*, 266, 11130-11140.

Hamilton, A. A. and Thacker, J., 1987, Gene recombination in X-ray-sensitive hamster cells. *Mol. Cell. Biol.*, 7, 1409-1414.

Hanawalt, P. C., 1990, Selective DNA repair in expressed genes in mammalian cells. In: *Mutation and the environment. Part A. Basic mechanisms.* Edited by: M. L. Mendelsohn and R. J. Albertini, (Wiley-Liss Inc., New York), pp. 213-222.

Hartwig, M., 1978, Organisation of mammalian chromosomal DNA: supercoiled and folded circular DNA subunits from interphase cell nuclei. *Acta Biol. Med. Germ.*, 37, 421-432.

Haystead, T. A. J., Sim, A. T. R., Carling, D., Honnor, R. C., Tsukitani, Y., Cohen, P. and Hardie, D. G., 1989, Effects of the tumour promotor okadaic acid on intracellular protein phosphorylation and metabolism. *Nature*, 337, 78-81.

Hecht, S. M., 1986, DNA strand scission by activated bleomycin group antibiotics. *Fed. Procs.*, 45, 2784-2791.

Hinton, D. M. and Bode, V. C., 1975, Ethidium affinity of circular λ deoxyribonucleic acid determined fluorometrically. *J. Biol. Chem.*, 250, 1061-1070.

Hinton, D. M. and Bode, V. C., 1975, Purification of closed circular λ deoxyribonucleic acid and its sedimentation properties as a function of sodium chloride concentration and ethidium binding. *J. Biol. Chem.*, 250, 1071-1079.

Hirano, T. and Mitchison, T. J., 1993, Topoisomerase II does not play a scaffolding role in the organisation of mitotic chromosomes assembled in *Xenopus* Egg Extracts. *J. Cell Biol.*, 120, 601-612.

Holliday, R., 1985, The significance of epimutations in somatic cell genetics. *Heredity*, 55, 280.

Homberger, H. P., 1989, Bent DNA is a structural feature of scaffold-attached regions in *Drosophila melanogaster* interphase nuclei. *Chromosoma*, 98, 99-104.

Horowitz, R. A., Agard, D. A., Sedat, J. W. and Woodcock, C. L., 1994, The three-dimensional architecture of chromatin in situ: Electron tomography reveals fibres composed of a continuously variable zig-zag nucleosomal ribbon. *J. Cell Biol.*, 125, 1-10.

Hozák, P., Hassan, A. B., Jackson, D. A. and Cook, P. R., 1993, Visualisation of replication factories attached to a nucleoskeleton. *Cell*, 73, 361-373.

Hubbard, M. J. and Cohen, P., 1993, On target with a new mechanism for the regulation of protein phosphorylation. *TIBS*, **18**, 172-.

Ide, T., Nakane, M., Anzai, K. and Andoh, T., 1975, Supercoiled DNA folded by non-histone proteins in cultured mammalian cells. *Nature*, **258**, 445-447.

Iliakis, G., Blöcher, D., Metzger, L. and Pantelias, G., 1991a, Comparison of DNA double-strand break rejoining as measured by pulsed field gel electrophoresis, neutral sucrose gradient centrifugation and non-unwinding filter elution in irradiated plateau-phase CHO cells. *Int. J. Radiat. Biol.*, **59**, 927-939.

Iliakis, G., Mehta, R. and Jackson, M., 1992, Level of DNA double-strand break rejoining in Chinese hamster xrs-5 cells is dose dependent: implications for the mechanism of radiosensitivity. *Int. J. Radiat. Biol.*, **61**, 315-321.

Iliakis, G. E., Cicilioni, O. and Metzeger, L., 1991b, Measurement of DNA double strand breaks in CHO cells at various stages of the cell cycle using pulsed field gel electrophoresis by means of ^{125}I decay. *Int. J. Radiat. Biol.*, **59**, 343-357.

Iliakis, G. E. and Pantelias, G. E., 1990, Production and repair of chromosome damage in an X-ray sensitive CHO mutant visualised and analysed in interphase using the technique of premature chromosome condensation. *Int. J. Radiat. Biol.*, **54**, 1213-1223.

Izaurralde, E., Mirkovitch, J. and Laemmli, U. K., 1988, Interaction of DNA with nuclear scaffolds *in vitro*. *J, Mol. Biol.*, **200**, 111-125.

Jackson, D. A. and Cook, P. R., 1985, Transcription occurs at a nucleoskeleton. *EMBO J.*, **4**, 919-925.

Jaffe, D. R., Haraf, D., Schwartze, J. L., Weichselbaum, R. R. and Diamond, A. M., 1990, Radioresistant derivatives of an X-ray-sensitive CHO cell line exhibit distinct patterns of sensitivity to DNA damaging agents. *Carcinogenesis*, **11**, 1265-1269.

Jarvis, W. D., Turner, A. J., Povirk, L. F., Traylor, R. S. and Grant, S., 1994, Induction of apoptotic DNA fragmentation and cell death in HL-60 human promyelocytic leukaemia cells by pharacological inhibitors of protein kinase C. *Cancer Res.*, **54**, 1707-1714.

Jaxel, C., Kohn, K. W., Wani, M. C., Wall, M. E. and Pommier, Y., 1989, Structure-activity study of the actions of camptothecin derivatives on mammalian topoisomerase I: Evidence for a specific receptor site and a relation to antitumour activity. *Cancer Res.*, **49**, 1465-1469.

Jeggo, P. A., 1985, Genetic analysis of X-ray-sensitive mutants of the CHO cell line. *Mutation Res.*, **146**, 265-270.

Jeggo, P. A., 1985, X-ray sensitive mutants of Chinese hamster ovary cell line: radio-sensitivity of DNA synthesis. *Mutation Res. (DNA Repair)*, **145**, 171-176.

Jeggo, P. A., 1990, Studies on mammalian mutants defective in rejoining double-strand breaks in DNA. *Mutation Res.*, **239**, 1-6.

Jeggo, P. A., Caldecott, K., Pidsley, S. and Banks, G. R., 1989, Sensitivity of Chinese hamster ovary mutants defective in DNA double strand break repair to topoisomerase II inhibitors. *Cancer Res.*, **49**, 7057-7063.

Jeggo, P. A., Hafezparast, M., Thompson, A. F., Broughton, B. C., Kaur, G. P., Zdziencka, M. Z. and Athwal, R. S., 1992, Localisation of a DNA repair gene (XRCC5) involved in double-strand-break rejoining to human chromosome 2. *Proc. Natl. Acad. Sci. USA*, **89**, 6423-6427.

Jeggo, P. A. and Holliday, R., 1986, Azacytidine-induced reactivation of a repair gene in Chinese hamster ovary cells. *Mol. Cell. Biol.*, **6**, 2944-2949.

Jeggo, P. A. and Kemp, L. M., 1983, X-ray sensitive mutants of Chinese hamster ovary cell line. Isolation and cross-sensitivity to other DNA damaging agents. *Mutation Res.*, **112**, 313-327.

Jeggo, P. A. and Smith-Ravin, J., 1989, Decreased stable transfection frequencies of six X-ray-sensitive CHO strains, all members of the xrs complementation group. *Mutation Res.*, **218**, 75-86.

Jeggo, P. A., Tesmer, J. and Chen, D. J., 1991, Genetic analysis of ionising radiation sensitive mutants of cultured mammalian cell lines. *Mutation Res.*, **254**, 125-133.

Johnson, R. T. and Rao, R. N., 1970, Mammalian cell fusion: Induction of premature chromosome condensation in interphase nuclei. *Nature*, **226**, 717-722.

Johnston, P. J. and Bryant, P. E., 1991, Lack of interference of DNA single-strand breaks with the measurement of double-strand breaks in mammalian cells using the neutral filter elution assay. *Nucleic Acids Res.*, **19**, 2735-2738.

Joshi, G. P., Nelson, W. J., Revell, S. H. and Shaw, C. A., 1982, X-ray chromosomal damage in live mammalian cells, and improved measurements of its effects on their colony forming ability. *Int. J. Radiat. Biol.*, **41**, 161-181.

Jost, E. and Johnson, R. T., 1981, Nuclear lamina assembly, synthesis and disaggregation during the cell cycle in synchronised HeLa cells. *J. Cell Sci.*, **47**, 25-53.

Jung, T. H. and Streffer, C., 1992, Effects of caffeine on protein phosphorylation and cell cycle progression in X-irradiated two-cell mouse embryos. *Int. J. Radiat. Biol.*, **62**, 161-168.

Kadhim, M. A., MacDonald, D. A., Goodhead, D. T., Lorimore, S. A., Marsden, S. J. and Wright, E. G., 1992, Transmission of chromosomal instability after plutonium α-particle irradiation. *Nature*, **355**, 738-739.

Käs, E., Izaurralde, E. and Laemmli, U. K., 1989, Specific inhibition of DNA binding to nuclear scaffolds and histone H1 by distamycin. The role of oliga(dA).oligo(dT) tracts. *J. Mol. Biol.*, **210**, 587-599.

Käs, E., Poljak, L., Adachi, Y. and Laemmli, U. K., 1993, A model for chromatin opening: stimulation of topoisomerase II and restriction enzyme cleavage of chromatin by distamycin. *EMBO J.*, **12**, 115-126.

Kemp, L. M. and Jeggo, P. A., 1986, Radiation-induced chromosome damage in X-ray-sensitve mutants (xrs) of the Chinese hamster ovary cell line. *Mutation Res.*, **166**, 255-263.

Kemp, L. M., Sedgwick, S. G. and Jeggo, P. A., 1984, X-ray sensitive mutants of Chinese hamster ovary cells deficient in double-strand break rejoining. *Mutation Res.*, **132**, 189-196.

Kim, C. Y., Giaccia, A. J., Strulovici, B. and Brown, J. M., 1992, Differential expression of protein kinase C ε protein in lung cancer cell lines by ionising radiation. *Br. J. Cancer*, 66, 844-849.

Koudelka, G. B., Harbury, P., Harrison, S. C. and Ptashne, M., 1988, DNA twisting and the affinity of bacteriophage 434 operator for bacteriophage 434 repressor. *Proc. Natl. Acad. Sci. USA*, **85**, 4633-4637.

Kovacs, M. S., Evans, J. W., Johnstone, I. M. and Brown, J. M., 1994, Radiation-induced damage, repair and exchange formation in different chromosomes of human fibroblasts determined by fluoescence *in situ* hybridisation. *Radiat. Res.*, **137**, 34-43.

Krohne, G., Waizenegger, I. and Höger, T. H., 1989, The conserved carboxy-terminal cysteine of nuclear lamins is essential for lamin association with the nuclear envelope. *J. Cell Biol.*, **109**, 2003-2011.

Kysela, B. P., Michael, B. D. and Arrand, J. E., 1993, Relative contributions of levels of initial DNA damage and repair of double strand breaks to the ionising radiation-sensitive phenotype of the Chinese hamster mutant, XR-V15B. Part I. X-rays. *Int. J. Radiat. Biol.*, 63, 609-616.

Laemmli, U. K., Cheng, S. M., Adolph, K. W., Paulson, J. R., Brown, J. A. and Baumbach, W. R., 1978, Metaphase chromosome structure: the role of non-histone proteins. *Cold Spring Harbour Symp. Quant. Biol.*, **42**, 109-118.

Larramendy, M. L., López-Larraza, D., Vidal-Rioja, L. and Bianchi, N. O., 1989, Effect of the metal chelating agent *0*-phenanthroline on the DNA and chromosome damage induced by bleomycin in Chinese hamster ovary cells. *Cancer Res.*, **49**, 6583-6586.

Lee, T. H., Solomon, M. J., Mumby, M. C. and Kirschner, M. W., 1991, INH, a negative regulator of MPF, is a form of protein phosphatase 2A. *Cell*, **64**, 415-423.

Lehman, A. R., Jeggo, P. A. and Carr, A. M., 1994, in press, Cloning human DNA repair genes. *Int. J. Radiat. Biol.*,

Levin, J. L. and Cook, P. R., 1981, Reconstruction of complexes of histone and superhelical nuclear DNA. *J. Cell Sci.*, **50**, 209-224.

Levin, J. M. and Cook, P. R., 1981, Conformational changes induced by salt in complexes of histones and superhelical nuclear DNA. *J. Cell. Sci.*, **50**, 199-208.

Levin, J. M., Jost, E. and Cook, P. R., 1978, The dissociation of nuclear proteins from superhelical DNA. *J. Cell Sci.*, **29**, 103-116.

Levy, M. J. and Hecht, S. M., 1988, Copper(II) facilitates bleomycin-mediated unwinding of plasmid DNA. *Biochem. (Wash.)*, **27**, 2647-2650.

Lewin, B., 1990, *Genes IV*. (Oxford University Press, Oxford).

Lewis, C. D. and Laemmli, U. K., 1982, Higher order metaphase chromosome structure: Evidence for metalloprotein interactions. *Cell*, **29**, 171-181.

Liu, L. F., 1989, DNA topoisomerase poisons as antitumor drugs. *Annu. Rev. Biochem.*, 58, 351-375.

Liu, S. Y., Hwang, B. D., Liu, Z. C. and Cheng, Y. C., 1989, Interaction of several nucleoside triphosphate analogues and 10-hydroxy-camptothecin with DNA topoisomerases. *Cancer Res.*, **49**, 1366-1370.

Ljungman, M., 1990, *The role of chromatin in the induction and repair of DNA damage.* (Stockholm University., Ph.D. thesis.)

Lock, R. B. and Ross, W. E., 1990, Inhibition of $p34^{cdc2}$ kinase activity by etoposide or irradiation as a mechanism of G_2 arrest in Chinese hamster ovary cells. *Cancer Res.*, **50**, 3761-3766.

Loeb, L. A., 1989, Endogenous carcinogenesis:Molecular oncology into the twenty-first century. Presidential address. *Cancer Res.*, **49**, 5489-5496.

Lorca, T., Labbé, J. C., Devault, A., Fesquet, D., Capony, J. P., Cavadore, J. C., le Bouffant, F. and Dorée, M., 1992, Dephosphorylation of cdc2 on threonine 161 is required for cdc2 kinase inactivation and normal anaphase. *EMBO J.*, **11**, 2381-2390.

Ludlow, J. W., Glendening, C. L., Livingston, D. M. and DeCaprio, J. A., 1993, Specific enzymatic dephosphorylation of the retinoblastoma protein. *Mol. Cell. Biol.*, **13**, 367-372.

MacLeod, R. A. F. and Bryant, P. E., 1990, Similar kinetics of chromatid aberrations in X-irradiated xrs 5 and wild type Chinese hamster ovary cells. *Mutagenesis*, 5, 407-410.

MacLeod, R. A. F., Christie, A. F., Costa, N. D. and Bryant, P. E., 1990, Repair kinetics in CHO cells of X-ray induced damage and chromatid aberrations during a cell cycle extended by transient hypothermia. *Mutagenesis*, **5**, 279-283.

Mah, D. C. W., Dijkwel, P. A., Todd, A., Klein, V., Price, G. B. and Zannis-Hadjopoulos, M., 1993, *ors*12, a mammalian autonomously replicating DNA sequence, associates with the nuclear matrix in a cell cycle-dependent manner. *J. Cell Sci.*, **105**, 807-818.

Mateos, S., Slijepcevic, P., MacLeod, R. A. F. and Bryant, P. E., 1994, DNA double-strand break rejoining in *xrs5* cells is more rapid in the G2 than in the G1 phase of the cell cycle. *Mutation Res.*, In press,

Matsuoka, A., Yamazaki, N., Suzuki, T., Hayashi, M. and Sofuni, T., 1993, Evaluation of the micronucleus test using a Chinese hamster cell line as an alternative to the conventional *in vitro* chromosomal aberation test. *Mutation Res.*, **272**, 223-236.

Mattern, M. R., Mong, S. M., Bartus, H. F., Mirabelli, C. K., Crooke, S. T. and Johnson, R. K., 1987, Relationship between the intracellular effects of camptothecin and the inhibition of DNA topoisomerase I in cultured L1210 cells. *Cancer Res.*, **47**, 1793-1798.

Mazan, A., Ménissier-de Murcier, J., Molinete, M., Gradwohl, G., Simonin, F. and de Murcia, G., 1989, Poly(ADP-ribose)polymerase: a novel finger protein. *Nucleic Acids. Res.*, **17**, 4689-4698.

McCready, J. J. and Cook, P. R., 1984, Lesions induced in DNA by ultraviolet light are repaired at the nuclear cage. *J. Cell Sci.*, **70**, 189-196.

McCready, S., J., Jackson, D. A. and Cook, P. R., 1982, Attachment of intact superhelical DNA to the nuclear cage during replication and transcription. **4**, 113-130.

McCready, S. J., Godwin, J., Mason, D. W., Brazell, I. A. and Cook, P. R., 1980, DNA is replicated at the nuclear cage. *J. Cell Sci.*, **46**, 365-386.

McKeon, F. D., 1987, Nuclear lamin proteins and the structure of the nuclear envelope: Where is the function? *BioEssays*, **7**, 169-173.

McKeon, F. D., Tuffanelli, D. L., Fukuyama, K. and Kirschner, M. W., 1983, Autoimmune response directed against conserved determinants of nuclear envelope proteins in a patient with linear scleroderma. *Proc. Natl. Acad. Sci. USA*, **80**, 4374-4378.

McManus, J., Perry, P., Sumner, A. T., Wright, D. M., Thomson, E. J., Allshire, R. C., Hastie, N. D. and Bickmore, W. A., 1994, Unusual chromosome structure of fission yeast DNA in mouse cells. *J. Cell Sci.*, **107**, 469-486.

Meek, D. W. and Street, A. J., 1992, Nuclear protein phosphorylation and growth control. *Biochem. J.*, **287**, 1-15.

Meersseman, G., pennings, S. and Bradbury, E. M., 1992, Mobile nucleosomes-a general behavior. *EMBO J.*, **11**, 2951-2959.

Mellgren, G., Vintermeyer, O. K., Bøe, R. and Døskeland, S. O., 1993, Hepatocyte DNA replication is abolished by inhibitors selecting protein phosphatase 2A rather than phosphatase 1. *Exp. Cell Res.*, **205**, 293-301.

Mikkelsen, R. B. and Gentry, C., 1992, A radiation -induced inhibitor of chromosome condensation and nuclear envelope breakdown in HeLa cells. *Radiat. Res.*, **132**, 158-161.

Mills, A. D., Blow, J. J., White, J. G., Amos, W. B., Wilcock, D. and Laskey, R. A., 1989, Replication occurs at discrete foci spaced throughout nuclei replicating in vitro. *J. Cell Sci.*, **94**, 471-477.

Mirkovitch, J., Gasser, S. M. and Laemmli, U. K., 1987, Relation of chromosome structure and gene expression. *Phil. Trans. R. Soc. Lond. B.*, **317**, 563-574.

Mirkovitch, J., Gasser, S. M. and Laemmli, U. K., 1988, Scaffold attachment of DNA loops in metaphase chromosomes. *J. Mol. Biol.*, **200**, 101-109.

Mohamed, R. and Lavin, M. F., 1989, Abnormality in DNA-protein binding in ataxia-telangiectasia nuclear extracts. *Biochem. Biophys. Res. Commun.*, **158**, 749-754.

Moir, R. D. and Goldman, R. D., 1993, Lamin Dynamics. *Curr. Opin. Cell Biol.*, **5**, 408-411.

Montecucco, A., Lestingi, M., Rossignol, J. M., Elder, R. H. and Ciarrocchi, G., 1993, Lack of discrimination between DNA ligases I and II by two classes of inhibitors, anthracyclins and distamycins. *Biochem. Pharm.*, **45**, 1536-1539.

Moore, P. D., Song, K., Chekuri, L., Wallace, L. and Kucherlapati, R. S., 1986, Homologous recombination in a Chinese hamster X-ray sensitive mutant. *Mutation Res.*, **160**, 149-155.

Mullenders, L. H. F., van Kesteren van Leeuwen, A. C., van Zeeland, A. A. and Natarajan, A. T., 1988, Nuclear matrix associated DNA is preferentially repaired in normal human fibroblasts, exposed to a low dose of ultraviolet light but not in Cockayn's syndrome fibroblasts. *Nucleic Acids Res.*, **16**, 10607-10622.

Mullenders, L. H. F., Venema, J., van Hoffen, A., Mayne, L. V., Natarajan, A. T. and van Zeeland, A. A., 1990, The role of the nuclear matrix in DNA repair. In: *Mutation and the environment. Part A. Basic mechanisms.* Edited by: M. L. Mendelsohn and R. J. Albertini, (Wiley-Liss Inc., New York), pp. 223-232.

Müller, W. E. G. and Zahn, R. K., 1977, Bleomycin, an antibiotic that removes thymine from double stranded DNA. *Prog. Nucl. Acid Res.*, **20**, 21-57.

Müller, W. U. and Streffer, C., 1991, Biological indicators for radiation damage. *Int. J. Radiat. Biol.*, **59**, 863-873.

Murray, A. W., 1992, Creative blocks: Cell-cycle checkpoints and feedback controls. *Nature*, 359, 599-604.

Mussa, T. A. K., Singh, B. and Bryant, P. A., 1990, Enhanced mutability at the tk locus in the radiosensitive double-strand break repair mutant xrs5. *Mutation Res.*, **231**, 187-193.

Nagasawa, H., Chen, D. J. C. and Strniste, G. F., 1989, Response of X-ray-sensitive CHO mutant cells to γ radiation. *Radiat. Res.*, **118**, 559-567.

Natarajan, A. T., Obe, G., van Zeeland, A. A., Palitti, F., Meijers, M. and Verdegaal-Immerzeel, E. A. M., 1980, Molecular mechanisms involved in the production of chromosomal aberrations, II. Utilisation of Neurospora endonuclease for the study of aberration production by X-rays in the G1 and G2 stages of the cell cycle. *Mutation Res.*, 69, 293-305.

Neuhoff, V., Arold, N., Taube, D. and Ehrhardt, W., 1988, Improved staining of proteins in polyacrylamide gels including isoelectric focusing gels with clear background at nanogram sensitivity using Coomassie Brilliant Blue G-250 and R-250. *Electrophoresis*, 9, 255-262.

Newport, J. W., Wilson, K. L. and Dunphy, W. G., 1990, A lamin-independent pathway for nuclear envelope assembly. *J. Cell Biol.*, **111**, 2247-2259.

Nicolini, C., Belmont, A. and Zietz, S., 1983, Physico-chemical model for DNA alkaline elution: New experimental evidence and differential role of DNA length, chain flexibility and superpacking. *J. Theor. Biol.*, **100**, 341-357.

North, P., Ganesh, A. and Thacker, J., 1990, The rejoining of double-strand breaks in DNA by human cell extracts. *Nucleic Acids Res.*, **18**, 6205-6210.

Obe, G., Hude, W. v. d., Scheutwinkel-Reich, M. and Baseler, A., 1986, The restiction endonuclease Alu I induces chromosomal aberrations and mutations in the hypoxanthine phosphoribosyl transferase locus but not in the Na^+/K^+ ATPase locus in V79 hamster cells. *Mutation Res.*, **174**, 71-74.

Okayasu, R. and Iliakis, G., 1989, Linear DNA elution dose response curves obtained in CHO cells with non-unwinding filter elution after appropriate selection of the lysis conditions. *Int. J. Radiat. Biol.*, **55**, 569-581.

Olive, P. L., 1992, DNA organisation affects cellular radiosensitivity and detection of initial DNA strand breaks. *Int. J. Radiat. Biol.*, **62**, 389-396.

Olive, P. L. and Banáth, J. P., 1992, Growth fraction measured using the comet assay. *Cell Prolif.*, **25**, 447-457.

Olive, P. L., Wlodek, D., Durand, R. E. and Banáth, J. P., 1992, Factors affecting DNA migration from individual cells subjected to gel electrophoresis. *Exp. Cell Res.*, **198**, 259-267.

Östling, O., Johanson, K. J., Blomquist, E. and Hagelqvist, E., 1987, DNA damage in clinical radiation therapy studied by micro-electrophoresis in single tumour cells. A preliminary report. *Acta Oncologica*, **26**, 45-48.

Pallen, C. J., Tan, Y. H. and Guy, G. R., 1992, Protein phosphatases in cell signalling. *Curr. Opin. Cell Biol.*, **4**, 1000-1007.

Panzeter, P. L., Zweifel, B., Malanga, M., Waser, S. H., Richard, M. C. and Althaus, F. R., 1993, Targeting of histone tails by poly(ADP-ribose). *J. Biol. Chem.*, **268**, 17662-17664.

Pardee, A. B. and Keyomarsi, K., 1992, Modification of cell proliferation with inhibitors. *Curr. Opin. Cell Biol.*, **4**, 186-191.

Paulin-Levasseur, M., Giese, G., Scherbarth, A. and Traub, P., 1989, Expression of vimentin and nuclear lamins during the in vitro differentiation of human promyelocytic leukaemia cells HL-60. *Eur. J. Cell Biol.*, **50**, 453-461.

Paulson, J. R. and Laemmli, U. K., 1977, The structure of histone depleted metaphase chromosomes. *Cell*, **12**, 817-827.

Pedraza-Reyes, M. and Alvarez-Gonzalez, R., 1990, Oligo(3'-deoxyADP-ribosyl)ation of the nuclear matrix lamins from rat liver utilising 3'-deoxyNAD as a substrate. *FEBS Lett.*, **277**, 88-92.

Pergola, F., Zdzienicka, M. Z. and Lieber, M. R., 1993, V(D)J recombinationin mammalian cell mutants defective in DNA double-strand break repair. *Mol. Cell. Biol.*, **13**, 3464-3471.

Perry, P. and Evans, H. J., 1975, Cytological detection of mutagen-carcinogen exposure by sister-chromatid exchange. *Nature*, **258**, 121-125.

Peter, M., Nakagawa, L., Dorée, M., Labbé, J. C. and Nigg, E. A., 1990, In vitro disassembly of the nuclear lamina and M phase-specific phosphorylation of lamins by cdc2 kinase. *Cell*, **61**, 591-602.

Pfeiffer, P., Thode, S., Hancke, J. and Vielmetter, W., 1994, Mechanisms of overlap formation in non-homologous DNA end joining. *Mol. Cell. Biol.*, **14**, 888-895.

Pienta, K. J. and Coffey, D. S., 1984, A structural analysis of the role of the nuclear matrix and DNA loops in the organisation of the nucleus and chromosome. *J. Cell Sci. Suppl.*, **1**, 123-135.

Pines, J. and Hunter, T., 1991, Cyclin-dependent kinases: A new cell cycle motif. *Trends Cell Biol.*, **1**, 117-121.

Poddevin, B., Orlowski, S., Belehradek, J. and Mir, L. M., 1991, Very high cytotoxicity of bleomycin introduced into the cytosol of cells in culture. *Biochem. Pharm.*, **42**, s67-s75.

Povirk, L. F. and Goldberg, I. H., 1987, A role for oxidative DNA sugar damage in mutagenesis by neocarzinostatin and bleomycin. *Biochimie*, **69**, 815-823.

Prise, K. M., 1994, Use of radiation quality as a probe for DNA lesion complexity. *Int. J. Radiat. Biol.*, **65**, 43-48.

Radford, I. R., 1985, The level of induced DNA double-strand breakage correlates with cell killing after X-irradiation. *Int. J. Radiat. Biol.*, **48**, 45-54.

Radford, I. R., 1988, The dose-response for low-LET radiation-induced DNA double-strand breakage: Methods of measurement and implications for radiation action models. *Int. J. Radiat. Biol.*, **54**, 1-11.

Ramakrishnan, V., 1994, Histone structure. *Curr. Opinion Struct. Biol.*, **4**, 44-50.

Reddy, N. M. S. and Lange, C. S., 1989, Similarities in the repair kinetics of sublethal and potentiallly lethal X-ray damage in log phase chinese hamster V79 cells. *Int. J. Radiat. Biol.*, **56**, 239-251.

Resnick, M. A., 1976, The repair of double strand breaks in DNA: A model involving recombination. *J. Theor. Biol.*, **59**, 97-106.

Resnick, M. A. and Moore, P. D., 1979, Molecular recombination and the repair of DNA double-strand breaks in CHO cells. *Nucleic Acids Res.*, **6**, 3145-3160.

Riedel, W. and Werner, D., 1989, Nucleotide sequence of the full-length mouse lamin C cDNA and its deduced amino-acid sequence. *Biochim. Biophys. Acta*, **1008**, 119-122.

Röber, R. A., Sauter, H., Weber, K. and Osborn, M., 1990, Cells of the cellular immune and hemopoietic system of the mouse lack lamins A/C: distinction *versus* other somatic cells. *J. Cell Sci.*, **95**, 587-598.

Roberge, M., Dahmus, M. E. and Bradbury, E. M., 1988, Chromosomal loop/nuclear matrix organisation of transcriptionally active and inactive RNA polymerases in HeLa nuclei. *J. Mol. Biol.*, **201**, 545-555.

Roberge, M., Th'ng, J., Hamaguchi, J. and Bradbury, E. M., 1990, The topoisomerase II inhibitor VM-26 induces marked changes in histone H1 kinase activity, histone H1 and H3 phosphorylation, and chromosome condensation in G_2 phase and mitotic BHK cells. *J. Cell Biol.*, **111**, 173-1762.

Romig, H., Fackelmayer, F. O., Renz, A., Ramsperger, U. and Richter, A., 1992, Characterisation of SAF-A, a novel nuclear DNA binding protein from HeLa cells

with a high affinity for nuclear matrix/scaffold attachment DNA elements. *EMBO J.*, **11**, 3431-3440.

Rowley, R. and Kort, L., 1988, The effect of modulators of radiation-induced G2 arrest on the repair of radiation-induced DNA damage detectable by neutral filter elution. *Int. J. Radiat. Biol.*, **54**, 749-759.

Roy, S. N. and Horwitz, S. B., 1984, Characterisation of the association of radiolabelled Bleomycin A2 with HeLa cells. *Cancer Res.*, **44**, 1541-1546.

Ryan, A. J., Squires, S., Strutt, H. L. and Johnson, R. T., 1991, Camptothecin cytotoxicity in mammalian cells is associated with the induction of persistent double strand breaks in replicating DNA. *Nucleic Acids Res.*, **19**, 3295-3300.

Saitoh, Y. and Laemmli, U. K., 1994, Metaphase chromosome structure: bands arise from a differential folding path of the highly AT-rich scaffold. *Cell*, **76**, 609-622.

Savage, J. R. K., 1975, Annotation: Classification and relationships of induced chromosomal structural changes. *J. Med. Genetics*, **12**, 103-122.

Schägger, H. and von Jagow, G., 1987, Tricine-sodium dodecyl sulphate polyacrylamide gel electrophoresis for the separation of proteins in the range from 1-100 kDa. *Anal. Biochem.*, **166**, 368-379.

Schatz, D. G., Oettinger, M. A. and Baltimore, D., 1990, The V(D)J recombination activating gene (RAG-1). *Cell*, **248**, 1035-1048.

Scheidtmann, K. H., Mumby, M. C., Rundell, K. and Walter, G., 1991, Dephosphorylation of simian virus 40 large-T antigen and p53 protein by protein phospatase 2A: Inhibition by small-t antigen. *Mol. Cell. Biol.*, **11**, 1996-2003.

Scheidtmann, K. H., Virshup, D. M. and Kelly, T. J., 1991, Protein phosphatase 2A dephosphorylates simian virus 40 large T antigen specifically at residues involved in regulation of DNA-binding activity. *J. Virol.*, **65**, 2098-2101.

Schönthal, A., Tsukitani, Y. and Feramisco, J. R., 1991, Transcriptional and post-transcriptional regulation of *c-fos* expression by the tumor promotor okadaic acid. *Oncogene*, **6**, 423-430.

Schwartz, J. L., Cowen, J. M., Moan, E., Sedita, B. A., Stephens, J. and Vaughan, A. T. M., 1993, Metaphase chromosome and nucleoid differences between CHO-K1 and its radiosensitive derivative xrs-5. *Mutagenesis.*, **8**, 105-108.

Schwartz, J. L., Rotmensch, J., Beckett, M. A., Jaffe, D. R., Toohill, M., Giovanazzi, S. M., McIntosh, I. and Weichselbaum, R. R., 1988, X-ray and cis-diammine dichloro-platinum(II) cross-resistance in human tumour cell lines. *Cancer Res.*, **48**, 5133-5135.

Schwartz, J. L., Shadley, J., Jaffe, D. R., Whitlock, J., Rotmensch, J., Cowan, J. M., Gordon, D. J. and Vaughan, A. T. M., 1990, Association between radiation sensitivity, DNA repair, and chromosome organisation in the Chinese hamster ovary cell line xrs 5. In: *Mutation and the Environment. Part A: Basic mechanisms.* Edited by: M. L. Mendelsohn and R. J. Albertini, (Wiley-Liss, New York), pp. 255-264.

Scott, D., Danford, N., Dean, B., Kirkland, D. and Richardson, C., 1983, *In vitro* chromosome aberration assays. In: *Report of the UKEMS sub-committee on guidlines for mutagenicity testing. Part 1: Basic test battery; minimal criteria; professional standards; interpretation; selection of supplememtary assays.* Edited by: B. J. Dean, (The United Kingdom Environmental Mutagen Society., pp. 41-64.

Seki, S. and Oda, T., 1988, An exonuclease possibly involved in the initiation of repair of bleomycin-damaged DNA in mouse ascites sarcoma cells. *Carcinogenesis*, **9**, 2239-2244.

Shadley, J. D., Whitlock, J. L., Rotmensch, J., Atcher, R. W., Tang, J. and Schwartz, J. L., 1991, The effects of radon daughter alpha-particle irradiation in K1 and xrs-5 CHO cell lines. *Mutation Res.*, **248**, 73-83.

Shoeman, R. L. and Traub, P., 1990, The *in vitro* DNA-binding properties of purified nuclear lamin proteins and vimentin. *J. Biol. Chem.*, **265**, 9055-9061.

Sidik, K. and Smerdon, M. J., 1990a, Bleomycin-induced DNA damage and repair in human cells permeabilised with lysophosphatidylcholine. *Cancer Res.*, **50**, 1613-1619.

Sidik, K. and Smerdon, M. J., 1990b, Nucleosome rearrangement in human cells following short patch repair of DNA damaged by bleomycin. *Biochem.*, **29**, 7501-7511.

Simos, G. and Georgatos, S. D., 1992, The inner nuclear membrane protein p58 associates *in vivo* with a p58 kinase and the nuclear lamins. *EMBO J.*, **11**, 4027-4036.

Singh, B. and Bryant, P. E., 1991, Induction of mutations at the thymidine kinase locus in CHO cells by restriction endonucleases. *Mutagenesis*, **6**, 219-223.

Singh, S. P., Mohamed, R., Salmond, C. and Lavin, M. F., 1988, Reduced DNA topoisomerase II activity in ataxia telangiectasia cells. *Nucleic Acids Res.*, **16**, 3919-3929.

Smit, J. A. and Stark, J. H., 1994, Inhibiting the repair of DNA damage induced by gamma irradiation in rat thymocytes. *Radiat. Res.*, **137**, 84-88.

Smith, P. J., 1990a, DNA topoisomerase dysfunction: A new goal for antitumour chemotherapy. *BioEssays*, **12**, 167-172.

Smith, P. J., 1990b, DNA topoisomerases and radiation responses. *Int. J. Radiat. Biol.*, 58, 553-559.

Smith, P. J. and Makinson, T. A., 1989, Cellular consequences of overproduction of DNA topoisomerase II in an ataxia-telangiectasia cell line. *Cancer Res.*, **49**, 1118-1124.

Smith, P. J. and Sykes, H. R., 1992, Simultaneous measurement of cell cycle phase position and ionising radiation-induced DNA strand breakage in single human tumour cells using laser scanning confocal imaging. *Int. J. Radiat. Biol.*, **61**, 553-560.

Smith-Ravin, J. and Jeggo, P. A., 1989, Use of damaged plasmid to study DNA repair in X-ray sensitive (xrs) strains of Chinese hamster ovary (CHO) cells. *Int. J. Radiat. Biol.*, **56**, 951-961.

Sperry, A. O., Blasquez, V. C. and Garrard, W. T., 1989, Dysfunction of chromosomal loop attachment sites: Illegitimate recombination linked to matrix association regions and topoisomerase II. *Proc. Natl. Acad. Sci. USA*, **86**, 5497-5501.

Spivak, I. M., Kostetsky, I. E., Shpielevaya, S. P., Kordyum, V. A. and Zhestyanikov, V. D., 1991, Caffeine-induced reduction of the survival of gamma-irradiated heLa cells and the reversal of the caffeine effect by Escerichia coli RecA protein. *Mutation Res.*, 246, 103-107.

Spotheim-Maurizot, M., Charlier, M. and Sabattier, R., 1990, DNA radiolysis by fast neutrons. *Int. J. Radiat. Biol.*, 57, 301-313.

Stewart, A. F. and Schütz, G., 1987, Camptothecin-induced in vivo topoisomerase I cleavages in the transcriptionally active tyrosine aminotransferase gene. *Cell*, 50, 1109-1117.

Stewart, A. F. and Schütz, G., 1987, Camptothecin-induced in vivo topoisomerase I cleavages in the transcriptionally active tyrosine aminotransferase gene. *Cell*, 50, 1109-1117.

Sumner, A. T., 1992, Inhibitors of topoisomerases do not block the passage of human lymphocyte chromosomes through mitosis. *J. Cell Sci.*, 103, 105-115.

Swedlow, J. R., Agard, D. A. and Sedat, J. W., 1993, Chromosome structure inside the nucleus. *Curr. Opin. Cell Biol.*, 5, 412-416.

Taccioli, G. E., Cheng, H. L., Varghese, A. J., Whitmore, G. and Alt, F. W., 1994a, A DNA repair defect in Chinese hamster Ovary cells affects V(D)J recombination similarly to the murine *scid* mutation. *J. Biol. Chem.*, 269, 7439-7442.

Taccioli, G. E., Rathbun, G., Oltz, E., Stamato, T., Jeggo, P. A. and Alt, F. W., 1993, Impairment of V(D)J recombination in double-strand repair mutants. *Science*, 260, 207-210.

Taccioli, J. E., Gottlieb, T. M., Blunt, T., Priestly, A., Demengeot, J., Mizuta, R., Lehman, A., Alt, F. W., Jackson, S. and Jeggo, P., 1994b; in press, Ku 80 is the product of the *XRCC5* gene. A link with DNA repair and V(D)J recombination.

Tamaoki, T., Nomoto, H., Takahashi, I., Kato, Y., Morimoto, M. and Tomita, F., 1986, Staurosporine, a potent inhibitor of phospholipid/Ca^{++} dependent protein kinase. *Biochem. Biophys. Res. Commun.*, 135, 397-402.

Tanaka, T., Yamagami, T., Oka, Y., Nomura, T. and Sugiyama, H., 1993, The scid mutation in mice causes defects in the repair system for both double-strand DNA breaks and DNA cross-links. *Mutation Res.*, 288, 277-280.

Tate, P. H. and Bird, A. P., 1993, Effects of DNA methylation on DNA binding proteins and gene expression. *Curr. Opinion Gene. Dev.*, 3, 226-231.

Tauchi, H., Enomoto, T. and Sawada, S., 1992, Effect of TPA, okadaic acid, and 1α,25-dihydroxyvitamin D_3 on neoplastic transformation induced by ^{60}Co gamma-rays or ^{252}Cf fission neutrons in Balb/c 3T3 cells. *Int. J. Radiat. Biol.*, 61, 253-262.

Teale, B., Singh, S., Khanna, K. K., Findik, D. and Lavin, M. F., 1992, Purification and characterisation of a DNA-binding protein activated by ionising radiation. *J. Biol. Chem.*, 267, 10295-10301.

Terzaghi, M. M. and Little, J. B., 1976, X-radiation-induced transformation in a C3H mouse embryo-derived cell line. *Mutation Res.*, **36**, 1367-1374.

Th'ng, J. P. H., Guo, X. W., Swank, R. A., Crissman, H. A. and Bradbury, E. M., 1994, Inhibition of histone phosphorylation by staurosporine leads to chromosome decondensation. *J. Biol. Chem.*, **269**, 9568-9573.

Thacker, J. and Stretch, A., 1985, Responses of 4 X-ray sensitive CHO cell mutants to different radiations and to irradiation conditions promoting cellular recovery. *Mutation Res.*, **146**, 99-108.

Tornaletti, S. and Pfeifer, G. P., 1994, Slow repair of pyrimidine dimers at *p53* mutation hotspots in skin cancer. *Science*, **263**, 1436-1438.

Tsao, Y. P., Wu, H. Y. and Liu, L. F., 1989, Transcription driven supercoiling of DNA: Direct biochemical evidence from in vitro studies. *Cell*, **56**, 111-118.

Tsutsui, K., Tsutsui, K. and Muller, M. T., 1988, The nuclear scaffold exhibits DNA-binding sites selective for supercoiled DNA. *J. Biol. Chem.*, **263**, 7235-7241.

Tsutsui, K., Tsutsui, K. and Oda, T., 1989, Incorporation of exogenous circular DNA into large catenated networks in isolated nuclei. Evidence for involvement of the nuclear scaffold. *J. Biol. Chem.*, **264**, 7644-7652.

Ulitzur, N., Harel, A., Feinstein, N. and Gruenbaum, Y., 1992, Lamin activity is essential for nuclear envelope assembly in a *Drosophila* embryo cell-free extract. *J. Cell Biol.*, **119**, 17-25.

Umezawa, H., Hori, S., Sawa, T., Yoshioka, T. and Taccheuchi, T., 1974, A bleomycin inactivating enzyme in mouse liver. *J. Antibiotic (Tokyo)*, **27**, 73-76.

Utsumi, H. and Elkind, M. M., 1991, Caffeine and D_2O medium interact in affecting the expression of radiation-induced potentially lethal damage. *Int. J. Radiat. Biol.*, **90**, 647-655.

van der Schans, G. P., Centen, H. B. and Lohman, P. H. M., 1982, DNA lesions induced by ionising radiation. In: *Progress in mutation research.* Edited by: Natarajan et al., (Elsevier Biomedical Press, pp. 285-229.

van Holde, K. and Zlatanova, J., 1994, Unusual DNA structures, chromatin and transcription. *BioEssays*, **16**, 59-74.

van Holde, K. E., 1989, *Chromatin.* (Springer-Verlag, Inc., New York).

van Rensburg, E., Louw, W. K. A., Izatt, H. and van der Watt, J. J., 1985, DNA supercoiled domains and radiosensitivity of subpopulations of human peripheral blood lymphocytes. *Int. J. Radiat. Biol.*, **47**, 673-679.

van Rensburg, E., Louw, W. K. A. and van der Merwe, K. J., 1987, Changes in DNA supercoiling during repair of gamma-radiation -induced damage. *Int. J. Radiat. Biol.*, **52**, 693-703.

Vassetzky, Y. S., 1989, DNA fragments which specifically bind to isolated nuclear matrix *in vitro* interact with matrix associated DNA topoisomerase II. *Biochem. Biophys. Res. Commun.*, **159**, 3.

Vaughan, A. T. M. and Gordon, D. J., 1992, Hydrogen peroxide lethality is associated with a decreased ability to maintain positive DNA supercoiling. *Exp. Cell Res.*, 202, 376-380.

Vaughn, J. P., Dijkwel, J. P., Mullenders, L. H. F. and Hamlin, J. L., 1990, Replication forks are associated with the nuclear matrix. *Nucleic Acids Res.*, 18, 1965-1969.

Vogelstein, B., Nelkin, B., Pardoll, D. and Hunt, B. F., 1982, The further evidence for physiological association of newly replicated DNA with the nuclear matrix. In: *The nuclear envelope and the nuclear matrix.* Edited by: (Alan R. Liss Inc., New York), pp. 169-181.

von Sonntag, C., 1987, *The chemical basis of radiation biology.* (Taylor and Francis, London).

Walicka, M. and Godlewska, E., 1989, Radiation sensitivities are not related to the sizes of supercoiled domains in L5178Y-R and L5178Y-S cells. *Int. J. Radiat. Biol.*, 55, 953-961.

Wandle, E. O., Ono, K., Kain, R., Herbsthofer, T., Heinert, G. and Höbarth, K., 1989, Linear correlation between surviving fraction and the micronucleus frequency. *Int. J. Radiat. Biol.*, 56, 771-775.

Wang, J. C., 1987, Recent studies of DNA topoisomerases. *Biochim. Biophys. Acta.*, 909, 1-9.

Wardlaw, A. C., 1985, *Practical statistics for experimental biologists.* (John Wiley and Sons Ltd., Chichester).

Warters, R. L. and Lyons, B. W., 1990, Detection of ionising radiation-induced DNA double strand breaks by filter elution is affected by nuclear chromatin structure. *Radiat. Res.*, 124, 309-316.

Warters, R. L., Lyons, B. W., Kennedy, K. and Li, T. M., 1989, Topoisomerase activity in irradiated mammalian cells. *Mutation Res.*, 216, 43-55.

Warters, R. L., Lyons, B. W., Mua Li, T. and Chen, D. J., 1991, Topoisomerase II activity in a DNA double-strand break repair deficient Chinese hamster ovary cell line. *Mutation Res., DNA Repair.*, 254, 167-174.

Weber, K., Plessman, U. and Traub, P., 1990, Protein chemical analysis of purified murine lamin B identifies two distinct polypeptides B1 and B2. *FEBS Lett.*, 261, 361-364.

Weibezahn, K. F. and Coquerelle, T., 1981, Radiation induced double strand breaks are rejoined by ligation and recombination processes. *Nucleic Acids Res.*, 9, 3139-3150.

Weinstein, I. B., 1988, The origins of human cancer: Molecular mechanisms of carcinogenesis and their implications for cancer prevention and treatment. Twenty-seventh G. H. A. Clowes memorial award lecture. *Cancer Res.*, 48, 4135-4143.

Winegar, R. A., Phillips, J. W., Youngblom, J. K. and Morgan, W. F., 1989, Cell electroporation is a highly efficient method of introducing restriction endonucleases into cells. *Mutation Res.*, 225, 49-53.

Wlodek, D. and Olive, P. L., 1992, Neutral filter elution detects differences in chromatin organisation which can influence cellular radiosensitivity. *Radiat. Res.*, 132, 242-247.

Wolffe, A. P., 1991, Developmental regulation of chromatin structure and function. *Trends. Cell Biol.*, **1**, 61-66.

Wood, R. D., Robins, P. and Lindahl, T., 1988, Complementation of the Xeroderma Pigmentosum DNA repair defect in cell free extracts. *Cell*, **53**, 97-106.

Worman, H. J., Yuan, J., Blobel, G. and Georgatos, S. D., 1988, A lamin B receptor in the nuclear envelope. *Proc. Natl. Acad. Sci. USA*, **85**, 8531-8534.

Woynarowski, J. M., Sigmund, R. D. and Beerman, T. A., 1988, Topoisomerase-II-mediated lesions in nascent DNA: Comparison of the effects of epipodophyllotoxin derivatives, VM-26 and VP-16, and 9-anilinoacridine derivatives, *m*-AMSA and *o*-AMSA,. *Biochim. Biophys. Acta*, **950**, 21-29.

Wun, K. L. W. and Shafer, R. H., 1982, Structural changes in mammmalian cell DNA induced by low-dose X-ray damage and subsequent postirradiation incubation in the presence and absence of caffeine. *Radiat. Res.*, **90**, 310-320.

Yamashita, K., Yasuda, H., Pines, J., Yasumoto, K., Nishitani, H., Ohtsubo, M., Hunter, T., Sugimura, T. and Nishimoto, T., 1990, Okadaic acid, a potent inhibitor of type 1 and type 2A protein phosphatases, activates cdc2/H1 kinase and transiently induces a premature mitosis-like state in BHK21 cells. *EMBO. J.*, **9**, 4331-4338.

Yasuda, H., Mueller, R. D. and Bradbury, E. M., 1987, Chromatin structure and histone modifications through mitosis in plasmodia of *Physarum polycephalum*. In: *Molecular regulation of nuclear events in mitosis and meiosis*. Edited by: R. A. Schlegel, M. S. Halleck and P. N. Rao, (Academic press. Inc., Orlando.), pp. 319-361.

Yasui, L. S., Fink, T. J. and Enrique, A. M., 1994, Nuclear scaffold orgaanisation in the X-ray sensitive Chinese hamster mutant cell line, *xrs-5*. *Int. J. Radiat. Biol*, **65**, 185-192.

Yasui, L. S., Ling-Indeck, L., Johnson-Wint, B., Fink, T. J. and Molsen, D., 1991, Changes in the nuclear structure in the radiation-sensitive CHO mutant , xrs-5. *Radiat. Res.*, **127**, 269-277.

Yuan, J., Simos, G., Blobel, G. and Georgatos, S. D., 1991, Binding of lamin A to polynucleosomes. *J. Biol. Chem.*, **266**, 9211-9215.

Zdzienicka, M. Z., Tran, Q., Schans, G. P. v. d. and Simons, J. W. I. M., 1988, Characterisation of an X-ray hypersensitive mutant of V79 Chinese hamster cells. *Mutation Res.*, **194**, 239-249.

Zdzienicka, M. Z., Wessel, N. v. and Schans, G. P. v. d., 1992, A fourth complementation group among ionising radiation-sensitive Chinese hamster cell mutants defective in DNA double strand break repair. *Radiation Res.*, **131**, 309-314.

Zhang, H., Wang, J. C. and Liu, L. F., 1988, Involvement of DNA topoisomerase I in transcription of human ribosomal RNA genes. *Proc. Natl. Acad. Sci. USA*, **85**, 1060-1064.

Zheng, B., Woo, C. F. and Kuo, J. F., 1991, Mitotic arrest and enhanced nuclear protein phosphorylation in human leukaemia K562 cells by okadaic acid, a potent protein phosphatase inhibitor and tumour promotor. *pp2A, pp1, mitosis, cell cycle, mitotic arrest,*

Zhivotovsky, B. D., Perlaky, L., Fónagy, A. and Hanson, K. P., 1988, Nuclear protein synthesis in thymocytes of X-irradiated rats. *Int. J. Radiat. Biol.*, **54**, 999-1006.

Zhu, W., Keng, P. C. and Chou, W.-G., 1992, Differential gene expression in wild-type and X-ray-sensitive mutants of Chinese hamster ovary cell lines. *Mutation Res.*, **274**, 237-245.

Zhu, W., Kriajevskaia, M., Keng, P. C. and Chou, W.-G., 1993, A "trans-acting" factor for activation of transcription is defective in the xrs-5 mutant of the Chinese hamster ovary cell line. *Mutation Res., DNA repair.*, **294**, 101-108.

Zini, N., Santi, S., Ognibene, A., Bavelloni, A., Neri, L. M., Valmori, A., Mariani, E., Negri, **C., Astaldi-Ricotti, G. C. B. and Maraldi, N. M.**, 1994, Discrete localisation of different DNA topoisomerases in HeLa and K562 cell nuclei and subnuclear fractions. *Exp. Cell Res.*, **210**, 336-348.

Appendix

Published papers

Johnston, P. J., and Bryant, P. E. (1991) Lack of interference of DNA single strand breaks with the measurement of double-breaks in mammalian cells using the neutral filter elution assay. Nucleic Acids Res., **19**, 2735-2738.

Bryant, P. E., and Johnston, P. J. (1993) Restriction-endonuclease-induced DNA double strand breaks and chromosomal aberrations in mammalian cells. Mutation Res., **299**, 289-296.

Johnston, P. J., and Bryant, P. E., (1993) Chromosome damage induced by nanomolar concentrations of bleomycin in porated mammalian cells., Biochemi. Pharm., **45**, 569-572.

Johnston, P. J., and Bryant, P. E., (1994) A component of DNA double strand break repair is dependent on the spatial orientation of the lesions within the higher order structures of chromatin. In press; Int. J. Radiat. Biol.

Biochemical Pharmacology, Vol. 45, No. 3, pp. 569–572, 1993.
Printed in Great Britain.

0006-2952/93 $6.00 + 0.00

CHROMOSOME DAMAGE INDUCED BY NANOMOLAR CONCENTRATIONS OF BLEOMYCIN IN PORATED MAMMALIAN CELLS

P. J. JOHNSTON* and P. E. BRYANT

School of Biological and Medical Sciences, University of St Andrews, St Andrews, Fife KY16 9TS, U.K.

(*Received* 4 *September* 1992; *accepted* 17 *November* 1992)

Abstract—We have examined chromosome damage caused by a wide range of bleomycin (BLM) concentrations in Chinese hamster ovary (CHO-K1) cells reversibly porated by the bacterial cytotoxin streptolysin-O (SLO). Chromosome damage was measured using the micronucleus cytokinesis block technique (employing cytochalasin-B). Treatment of exponentially growing cells with 0.045 IU/mL SLO for 5 min resulted in up to a thousand-fold and a million-fold increase in biological effectiveness, compared to treatment in the absence of SLO for 24 hr and 5 min, respectively. Increases in micronuclei of 4–5 times background level were observed after only 5 min exposure to the drug in the presence of SLO at doses as low as 100 pg/mL (≈70 pmol/L). These results indicate that the use of SLO may facilitate the treatment of cells with BLM for periods of time resembling acute exposure to ionizing radiations.

Permeabilization or poration of cell membranes allows the increased uptake of otherwise excluded agents and several poration methods have been used in the study of agents causing cytogenetic damage [1–6]. Of these, one of the most widely used, and successful, techniques is electroporation. However, this technique can suffer from lysis of a significant fraction of the electroporated cells under physiological conditions [7, 8]. A technique for the poration of mammalian cells to facilitate uptake of clastogenic agents has recently been developed in our laboratories using the bacterial toxin streptolysin-O (SLO†) [8]. SLO produces pores in cell membranes with pore sizes, increasing with dose, to diameters in excess of 12 nm which allows the release of proteins up to a relative mass of 483 kDa [9] permitting the poration into cells of a wide range of agents. The technique developed by Bryant [8] uses low doses of SLO to permit entry of macromolecules into cells while maintaining cell viability. This has permitted the introduction of restriction endonucleases e.g. *Pvu II*, into Chinese hamster ovary-K1 cells (CHO) in order to mimic ionizing radiation in causing cytogenetic damage such as micronuclei or chromosomal and chromatid aberrations. Treatment of CHO-K1 cells with 0.045 IU/mL SLO (an optimal concentration for CHO cells) for 5 min results in high cell recovery compared with electroporation of cells under the same physiological conditions.

As a result of this work, and our interest in the DNA damaging properties of bleomycin (BLM), we investigated the effect of BLM in inducing lesions in the absence of a continuous membrane barrier.

BLM [10] is a radiomimetic glycopeptide with chemotherapeutic antitumour properties. It is widely used clinically, particularly in the treatment of malignant lymphomas, Hodgkins' disease and squamous cell carcinoma [11]. The action of BLM is believed to be mediated by the oxidative production of single and double stranded DNA breaks in the presence of Fe(II) [12]. In addition, BLM causes membrane peroxidation [13] and aggregation of DNA [14] with the latter being preferential in newly replicated DNA. BLM-induced damage results in chromosome aberrations and growth inhibition [15, 16]. Generally, the lesions induced by BLM are similar in nature and repair pathways to damage produced by ionizing radiations [17].

However, entry of BLM into cells is known to be strongly hindered by the cell membrane with only approximately 0.1% of available BLM being taken up by HeLa cells and only 20% of this amount entering the nucleus [18]. As a result of this, in order to induce damage in cells comparable to that produced by X-rays, high concentrations of BLM and long exposure times are required. In addition, BLM action is not uniform across the cell population treated [19]. The permeabilization of the cell membrane by lysophosphatidylcholine (LPC) has been shown to facilitate both increased uptake of BLM (as measured by repair synthesis and DNA cleavage), and an increase in the proportion of cells damaged [1]. A drawback of this method is that it only facilitates entry of relatively small molecules (<2 kDa), limiting the range of agents that can be examined [20]. Electroporation has also been shown to enhance uptake of BLM *in vitro* [21] and *in vivo*, electric pulses applied directly to tumour sites have successfully increased the antitumour activity of

* Corresponding author. Tel. (0334) 76161 ext. 7227; FAX (0334) 74004.

† Abbreviations: BLM, bleomycin; SLO, streptolysin-O; EMEMS, supplemented Eagles' minimal essential medium; HBSSM, Hanks' balanced salts solution + $MgCl_2$; CHO, Chinese hamster ovary K1 cells; LPC, lysophosphatidylcholine.

BLM in spontaneous mammary tumours in mice [22]. Other factors which undoubtedly play a part in the clastogenicity of BLM and other radiomimetics are accessibility of the drug to chromatin and the cellular half life of the agent in question since experiments have shown that DNA specifically binds 1 mol of BLM per 10^8 bp for cellular treatments, whereas *in vitro*, DNA binds at an average of 1 mol BLM per 3.1 bp [18]. Cells are known to break down BLM using the BLM-inactivating enzyme, bleomycin hydrolase [23] with varying activities occurring in different cell types [24].

In order to quantify BLM damage to chromosomes in SLO porated mammalian cells we examined the production of micronuclei by BLM, using the cytokinesis block technique [25]. We have examined the frequencies of micronuclei produced by a logarithmic range of BLM concentrations in both untreated cells or cells porated by SLO. CHO-K1 cells were exposed to either chronic (24 hr) treatment in the absence of SLO or acute (5 min) treatment in the presence or absence 0.045 IU/mL SLO.

MATERIALS AND METHODS

Cell culture. CHO cells were grown as monolayers in Eagles' minimal essential medium supplemented with 10% (v/v) calf serum (Gibco BRL, Uxbridge, U.K.), 100 μmol/L $FeCl_3$, 50 U/mL, penicillin and 50 mg/mL streptomycin (EMEMS). All incubations were carried out at 37° in an atmosphere of 5% CO_2, unless otherwise stated. Exponentially growing cells were obtained by seeding 1×10^6 cells per 75 cm^2 tissue culture flasks (Sterilin) and incubating for 24 hr.

Cell poration and bleomycin treatment. Bleomycin sulphate (Lundbeck) and SLO (Wellcome Diagnostics, Beckenham, U.K.) were made up as stock solutions (BLM = 1 mg/mL in H_2O, SLO was made up as per manufacturers instruction to 1.9 IU/mL) and these were stored in aliquots at −20°. Cytochalasin-B (Sigma Chemical Co., Poole, U.K.) was made up as 3 mg/mL stock in dimethyl sulphoxide (Sigma) and stored at −20°. All solutions, except cytochalasin B, were filter sterilized.

Poration was carried out by the method of Bryant [8]. Cells were collected by briefly washing the monolayers twice with 5 mL 0.05% trypsin (Difco Laboratories, Detroit, MI, U.S.A.), 0.02% EDTA followed by 6 min incubation at 37° and resuspension in 10 mL EMEMS. Cells were washed twice by centrifugation with Hanks' balanced salt solution supplemented with 6 mmol/L $MgCl_2$ (HBSSM) at room temperature. For acute BLM treatments (5 min exposure) cells were resuspended at 2×10^6 cells/mL in HBSSM and 100 μL aliquoted into 1.5 mL eppendorf tubes (Treff). HBSSM (100 μL) containing dilutions of BLM ± 0.090 IU/mL SLO was added to give a final cell concentration of 1×10^6 cells/mL and SLO 0.045 IU/mL. The cells were incubated for 5 min at room temperature before addition of 1 mL ice-cold EMEMS. They were then immediately centrifuged (6500 rpm) for 1 min in a microfuge (MSE Micro-centaur) and the supernatant aspirated. The cell pellet was resuspended in 1 mL EMEMS + 3 μg/mL cytochalasin-B before plating out in tissue culture grade multi-well plates (Sterilin). For chronic BLM treatments (24 hr exposure) 2×10^5 cells were plated out in 1 mL EMEMS containing 3 μg/mL cytochalasin-B plus various dilutions of BLM. All cells were incubated for 24 hr in a humidified incubator at 37°.

Cell fixation and scoring. Cells were collected by trypsinization and approximately 5×10^4 cells cytospun (Shandon Cytospin II) onto glass slides (BDH, Poole, U.K.) and air dried. The cells were fixed for 10 min in methanol and again air dried before staining in 10% filtered aqueous Giemsa solution for 20 min. Slides (without coverslips) were examined under high magnification (oil immersion × 1800) and the number of micronuclei per 100 binucleate cells were scored. These frequencies were normalized by subtracting the background level of micronuclei per 100 binucleate cells in the untreated control for each experimental group.

RESULTS AND DISCUSSION

The number of micronuclei induced per 100 binucleate cells by BLM in the presence or absence of 0.045 IU/mL SLO are shown in Fig. 1. It can be seen that SLO markedly increases the frequency of micronuclei from chronic treatments in the absence of SLO especially in the low dose range where concentrations to give the same effect are approximately 10^{-4} times that required in the absence of SLO. Acute treatment (5 min) without SLO gave very low levels of micronuclei even at 100 μg/mL. The dose–response relationship for both acute plus SLO and chronic treatments minus SLO gave maximal micronucleus induction at 10 ng/mL and 10 μg/mL, respectively. At higher concentrations a reduction in frequency occurred especially in the case of BLM plus SLO. The absolute frequencies of micronuclei achieved in the two cases were also different with maximum frequencies of 70.2 (±16.3) and 108.7 (±15.4) micronuclei per 100 binucleate cells scored for chronic and acute treatments, respectively. Background levels of micronuclei for the three experimental groups were: 24 hr, 3.33 (±1.09); 5 min −SLO, 5.0 (±2.04); 5 min +SLO, 4.14 (±0.63). This would indicate that SLO treatment does not increase the numbers of micronuclei by itself, however the possibility of synergism between BLM and the effects of poration cannot be ruled out. The reason for a downturn in numbers of micronuclei at high doses of BLM in porated and non-porated (24 hr) cells is at present uncertain but it may be the result of different forms of damage occurring which cause cell death prior to mitosis.

In order to examine whether SLO treatment increases either the number of binucleates containing damage or the amount of damage within individual damaged binucleate cell, Fig. 2 shows the mean number of micronuclei per damaged binucleate cell versus the percentage of binucleate cells containing micronuclei. This shows the total number of micronuclei is a linear function of both the number of binucleates containing damage and the number of micronuclei per damaged binucleate. Poration would appear to increase the total number of

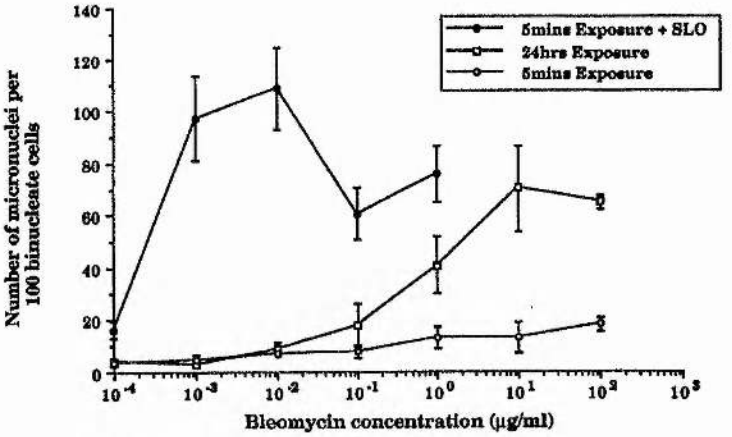

Fig. 1. Number of micronuclei per 100 binucleate cells as a function of BLM concentration, in the presence (filled circles) or absence (squares and open circles) of 0.045 IU/mL SLO. Treatment with BLM was for 5 min (circles) or 24 hr (squares). SLO treatment was concurrent with BLM. Vertical bars represent values of the SEM micronucleus frequency per 100 binucleate cells (normalized with respect to the control). Results are from 2–5 independent experiments.

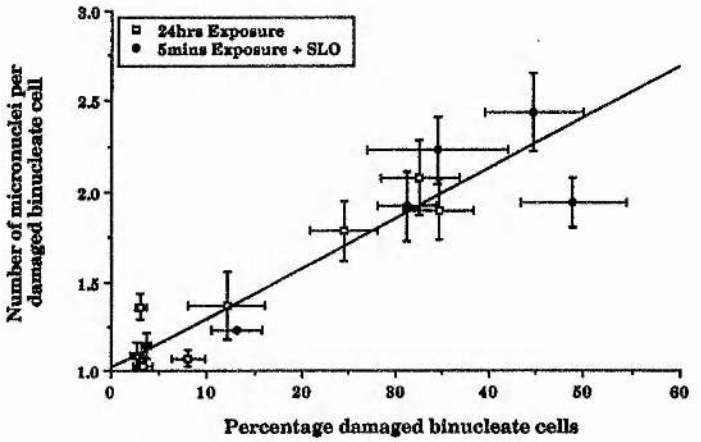

Fig. 2. Correlation between the number of BLM-induced micronuclei per damaged binucleate cell and the percentage of damaged binucleate cells for CHO cells treated in the presence (filled circles) or absence (squares) of 0.045 IU/mL SLO. Treatment with BLM was for 5 min (circles) or 24 hr (squares). SLO treatment was concurrent with BLM. Vertical and horizontal bars represent the SEM for 2–5 independent experiments.

micronuclei by increasing both of these parameters to the same extent, indicating that damage in porated cells is a function of increased amounts of BLM entering all cells of the population rather than either an increased proportion of cells damaged or an increase in numbers of micronuclei within the same fraction of cells susceptible to damage.

From the results presented above it is clear that poration with a low concentration of SLO produces a very large increase in chromosome damage caused by BLM as measured by the production of micronuclei. On a concentration basis, this increase is approximately a thousand-fold and a million-fold compared to treatment in the absence of SLO for 24 hr and 5 min, respectively. The damage caused by BLM in the presence of SLO would appear to be similar since there is no significant variation in the number of micronuclei induced per damaged cell. The cell membrane is thus a very effective barrier to uptake of BLM as also shown by Sidik and Smerdon [1] who have found that the early end-points of DNA breakage and repair are enhanced in LPC-permeabilized human fibroblast cells and also by Poddevin *et al.* [21] who introduced BLM by electropermeabilization and who measured uptake of BLM and relative cloning efficiencies of

transformed Chinese hamster lung fibroblast cells. LPC (80 μg/mL) and electropermeabilization (1500 V/cm) were found to increase the uptake by 50- and 100-fold as measured by repair synthesis levels and relative cloning efficiencies, respectively.

From these results, with BLM, we conclude that SLO can be effectively used to introduce cytotoxic molecules into cells at concentrations much lower than would otherwise be required for non-porated cells. SLO may also permit treatment of cells with other chemical agents on a short timescale that more closely mimics acute treatment with ionizing radiations; although the actual exposure of the cellular target to the introduced drug will still be dependent on the half life of the agent introduced.

Acknowledgements—We thank John Macintyre for valuable technical assistance. This work was supported by funds from the Commission of European Communities and the Cancer Research Campaign.

REFERENCES

1. Sidik K and Smerdon MJ, Bleomycin induced DNA damage and repair in human cells permeabilised with lysophospatidyl-choline. *Cancer Res* **50**: 1613–1619, 1990.
2. Bryant PE, Enzymatic restriction of mammalian cell DNA using *Pvu II* and *Bam H1*: evidence for the double strand break origin of chromosomal aberrations. *Int J Radiat Biol* **46**: 57–65, 1984.
3. Natarjan AT and Obe G, Molecular mechanisms involved in the production of chromosomal aberration, III. Restriction endonucleases. *Chromosoma* **90**: 120–127, 1984.
4. Obe G and Winkel E, The chromosome breaking activity of the restriction endonuclease *Alu I* in CHO cells is independent of the S-phase of the cell cycle. *Mutat Res* **152**: 25–29, 1985.
5. Winegar RA and Preston RJ, The induction of chromosomal aberrations by restriction endonucleases that produce blunt-ended or cohesive ended double strand breaks. *Mutat Res* **197**: 141–149, 1988.
6. Winegar RA, Phillips JW, Youngblom JH and Morgan WF, Cell electroporation is highly efficient method for introducing restriction endonucleases into cells. *Mutat Res* **225**: 49–53, 1989.
7. Costa ND and Bryant PE, The induction of DNA double strand breaks in CHO cells by *Pvu II*: kinetics using neutral filter elution (pH 9.6). *Int J Radiat Biol* **57**: 933–938, 1990.
8. Bryant PE, Induction of chromosomal damage by restriction endonuclease in CHO cells porated with streptolysin-O. *Mutat Res* **268**: 27–34, 1992.
9. Buckingham L and Duncan JL, Approximate dimension of membrane lesions produced by streptolysin S and streptolysin O. *Biochim Biophys Acta* **729**: 115–122, 1983.
10. Umezawa H, Maeda K, Takeuchi T and Okami Y, New antibiotics, bleomycin A and B. *J Antibiot (Tokyo)* **19**: 200–209, 1966.
11. Hecht SM, DNA strand scission by activated bleomycin group antibiotics. *Fed Proc* **45**: 2784–2791, 1986.
12. Byrnes RW, Templin J, Sem D, Lyman S and Petering DH, Intracellular DNA strand scission and growth inhibition of Ehrlich ascites tumour cells by bleomycins. *Cancer Res* **50**: 5275–5286, 1990.
13. Ciriolo MR, Peisach J and Magliozzo RS, A comparative study of the interactions of bleomycin with nuclei and purified DNA. *J Biol Chem* **264**: 1443–1449, 1989.
14. Woynarowski JM and Beerman TA, Preferential effect of bleomycin on newly replicated chromatin in nuclei from L1210 cells. *Biochim Biophys Acta* **1007**: 116–119, 1989.
15. Vig BK and Lewin R, Genetic toxicology of bleomycin. *Mutat Res* **55**: 121–145, 1978.
16. Larramendy ML, Lopez-Larraza D, Vidal-Rioja L and Bianchi NO, Effect of the metal chelating agent *o*-phenanthroline on the DNA and chromosome damage caused by bleomycin in Chinese hamster ovary cells. *Cancer Res* **49**: 6583–6586, 1989.
17. Byfield JE, Lee YC, Tu L and Kulhanian F, Molecular interaction of the combined effects of bleomycin and X-rays on mammalian cell survival. *Cancer Res* **36**: 1138–1143, 1976.
18. Roy SM and Horwitz SB, Characterisation of the association of radiolabelled bleomycin A_2 with HeLa cells. *Cancer Res* **44**: 1541–1546, 1984.
19. Östling O and Johanson KJ, Bleomycin, in contrast to gamma irradiation, induces extreme variation of DNA strand breakage from cell to cell. *Int J Radiat Biol* **52**: 683–691, 1987.
20. Miller MR, Castellot JJ Jr and Pardee AB, A permeable animal cell preparation of studying macromolecular synthesis. DNA synthesis and the role of deoxyribonucleotides in S-phase initiation. *Biochemistry* **17**: 1073–1080, 1978.
21. Poddevin B, Orlowski S, Belehradek J Jr and Mir LM, Very high cytotoxicity of bleomycin introduced into the cytosol of cells in culture. *Biochem Pharmacol* **42**: S67–S75, 1991.
22. Belehradek J Jr, Orlowski S, Poddevin B, Paoletti C and Mir LM, Electrochemotherapy of spontaneous mammary tumours in mice. *Eur J Cancer* **27**: 73–76, 1991.
23. Umezawa H, Hori S, Sawa T, Yoshioka T and Tacheuchi T, A bleomycin inactivating enzyme in mouse liver. *J Antibiot (Tokyo)* **27**: 419–424, 1974.
24. Müller WEG and Zahn RK, Bleomycin, an antibiotic that removes thymine from double-stranded DNA. *Prog Nucl Acid Res* **20**: 21–57, 1977.
25. Fennech M and Morley AA, Measurement of micronuclei in lymphocytes. *Mutat Res* **147**: 29–36, 1985.

Mutation Research, 299 (1993) 289–296

MUTGEN 0003

Restriction-endonuclease-induced DNA double-strand breaks and chromosomal aberrations in mammalian cells

Peter E. Bryant and Peter J. Johnston

School of Biological and Medical sciences, University of St. Andrews, St. Andrews, Fife KY16 9TS, Scotland, UK

(Received 24 June 1992)
(Accepted 21 October 1992)

Keywords: Restriction endonuclease; Endonuclease, restriction; DNA dsb; Double-strand breaks, DNA; Chromosomal aberrations; Mammalian cells

Summary

Restriction endonucleases (RE) can be used to mimic and model the clastogenic effects of ionising radiation. With the development of improved techniques for cell poration: electroporation and recently streptolysin O (SLO), it has become possible more confidently to study the relationships between DNA double-strand breaks (dsb) of various types (e.g. blunt or cohesive-ended) and the frequencies of induced metaphase chromosomal aberrations or micronuclei in cytokinesis-blocked cells. Although RE-induced dsb do not mimic the chemical end-structure of radiation-induced dsb (i.e. the 'dirty' ends of radiation-induced dsb), it has become clear that cohesive-ended dsb, which are thought to be the major type of dsb induced by radiation, are much less clastogenic than blunt-ended dsb. It has also been possible, with the aid of electroporation or SLO to measure the kinetics of dsb in cells as a function of time after treatment. These experiments have shown that some RE (e.g. Pvu II) are extremely stable inside CHO cells and at high concentrations persist and induce dsb over a period of many hours following treatment. Cutting of DNA by RE is thought to be at specific recognition sequences (as in free DNA) although the frequencies of sites in native chromatin available to RE is not yet known. DNA condensation and methylation are both factors limiting the numbers of available cutting sites. Relatively little is known about the kinetics of incision or repair of RE-induced dsb in cells. Direct ligation may be a method used by cells to rejoin the bulk of RE-induced dsb, since inhibitors such as araA, araC and aphidicolin appear not prevent rejoining, although these inhibitors have been found to lead to enhanced frequencies of chromosomal aberrations. 3-Aminobenzimide, the poly-ADP ribose polymerase inhibitor is the only agent that has so far been shown to inhibit rejoining of RE-induced dsb. Data from the radiosensitive xrs5 cell line, where chromosomal aberration frequencies are higher after RE treatments than in their normal parental CHO line, indicates that the xrs dsb repair pathway is involved in the repair of these dsb. We found that cells treated simultaneous with Pvu II and T4 ligase yielded lower levels of chromosomal damage than in the WT parental line indicating that Pvu II induced dsb retain their ability to be blunt-end ligated inside the cell.

Correspondence: Dr. P.E. Bryant, School of Biological and Medical Sciences, University of St. Andrews, St. Andrews, Fife KY16 9TS, Scotland, UK.

Restriction endonucleases (RE) can be used to mimic and model the effects of ionizing radiation and in particular the clastogenic effect of radia-

tion. The major advantage of this approach is that RE induce only DNA double-strand breaks (dsb) with characteristic end-structures, whereas radiation is known to induce several types of DNA lesions such as: single- and double-strand breaks, base-damage, interstrand cross-links and DNA–protein cross-links. Thus, treatment with RE produces dsb of specific types at specific base recognition sequencies in DNA, in the absence of these other complicating lesions.

There are a number of lines of evidence that point to the dsb as the causative lesion in radiation-induced chromosomal aberrations as well as in cell killing, mutations, and oncogenic transformation, for example the dependence on LET of these end-points; the correlation between the biological responses of radiosensitive mutant cell lines (e.g. xrs Chinese hamster cells and rad 52 yeast) and defective dsb repair. In the case of chromosomal aberrations the experiments of Natarajan et al. (1980) indicated that dsb are the clastogenic lesion. In these studies X-irradiated cells were permeabilized by Sendai virus and exposed to the DNA single-strand cutting endonuclease from Neurospora. This converts single-strand breaks in DNA into dsb, increasing these by a factor of 2. A corresponding increase in chromosomal aberrations was observed, providing evidence for the notion that dsb are a major lesion giving rise to chromosomal aberrations. As described in this review, RE were first used in a similar way in permeabilized cells to demonstrate the link between dsb and chromosomal aberrations (Bryant 1984; Natarajan and Obe, 1984).

Restriction-endonuclease-induced dsb as a model for radiation damage

Radiation induces about 40 dsb/Gy/diploid genome in mammalian cells. The induction of dsb has been shown to be a linear function of radiation dose (e.g. Blöcher, 1982). The end-structure of dsb induced by radiation are thought to be highly variable. Firstly, the dsb may have blunt or cohesive termini, the latter type with varying degrees of base-overlap in either a 3′ or 5′ direction. Secondly, the ends may be of either the clean or of the 'dirty' type, that is, with termini other than 3′-hydroxyl and 5′-phosphoryl groups. We can presume that the frequency of blunt-ended dsb is much lower than that of cohesive-ended dsb, simply because the chance of ionizations or radical attack occurring in the close neighbourhood of bonds exactly opposite one another in the DNA would be very low.

RE can be used in cells to mimic these types of (blunt and cohesive) dsb, although the termini of RE-induced dsb are always of the 'clean' type. In addition, various different RE can be used that cause cohesive-ended dsb with varying degrees of base overlap; some RE produce overlap in the 5′ direction (e.g. Bam H1 or Eco R1) while others produce an overlap in the 3′ direction (e.g. Msp 1). Thus, RE in one sense mimic the precise molecular end-structure, i.e. the overlapping or blunt ends that are produced by radiation. However, at present, since we do not understand the mechanisms of repair of radiation-induced dsb, the effect of a 'dirty' end-structure on the clastogenicity of a dsb is unknown. However, it seems likely that cleaning of the ends of radiation-induced dsb would be necessary before ligation can be observed. The other area where RE cannot precisely mimic radiation-induced dsb is where a cluster of ionizations may produce one or more dsb close together along the chromosomal DNA. These multiple dsb sites may be more clastogenic than those 'single' dsb that are induced at random and in isolation.

Specificity of restriction endonucleases cutting in chromosomal DNA

Little is known about the frequencies of sites available to RE in live chromatin. It seems plausible that, like radiation (e.g. Patil et al., 1985) RE would cut DNA preferentially at sites in expressed DNA, since this DNA would have a reduced level of condensation. In addition, methylated sites may be protected from cutting by some RE which are sensitive to the presence of methylated sites. For example, Winegar et al. (1990) showed that Msp 1, which is insensitive to methylation, yielded a 90-fold higher frequency of chromosomal aberrations than its isoschizomer

Hpa II which is sensitive to methylation. This experiment also indicates the specificity of these enzymes in incising DNA.

In another type of experiment indicating that RE retain their specificity towards recognition sites in the DNA when inside the cell, Obe et al. (1987) and Cortes and Ortiz (1992) demonstrated a dramatic decrease in yields of chromosomal aberrations occurred in cells in which thymine had been substituted with BrdU, when the cells were treated with RE which recognize thymine-rich DNA sequencies (e.g. Eco R1 and Dra I).

Methods of introducing restriction endonucleases into cells

There are several methods for permeabilizing or 'porating' cells so that large molecules such as RE can penetrate the outer cell membrane (for review of these see Bryant, 1988). As explained above, early experiments (Bryant, 1984; Natarajan and Obe, 1984) were performed with Sendai virus as a permeabilizing agent. Sendai virus is known to generate approximately 1-nm pores but leads to a relatively low percentage of cells permeabilized. More recently, electroporation has been shown to be an efficient method for introducing RE into cells (Wingar et al., 1989). Electroporation generates pores of 2–4 nm in cell membranes. However, the problem with this method is that it leads to lysis of a large proportion of cells and a voltage-dependent decrease in plating efficiency (Bryant, 1992; West, 1992). It has also been reported that electroporation increases the radiosensitivity of cells for up to 6 h following treatment (West, 1992).

A new method of cell poration involving treatment with the bacterial cytotoxin streptolysin O (SLO) has been reported recently (Bryant, 1992). This method overcomes most of the problems encountered with electroporation. SLO, a 69-kdal protein that is thought to target cholesterol in the membrane (Duncan and Schlegel, 1975; Bhakdi et al., 1985), generates pores greater than 12 nm in size (Gomperts et al., 1987) and thereby allows the entry of RE and other large molecules. SLO does not lead to a large cell kill during treatment; the cell recovery after treatment is about 95%. This method also allows the use of very low concentrations of RE with resultant absence of heavily-damaged cells. The method is also flexible with regard to the volume of cell suspension that can be treated, allowing a volume from as small as 0.1 ml upwards to be used. Cells are simply exposed to a low concentration of the toxin in the presence of RE for 5 min and then transferred back to growth medium. Both metaphase chromosomal aberrations and micronuclei are induced as linear functions of RE dose (Figs. 1 and 2).

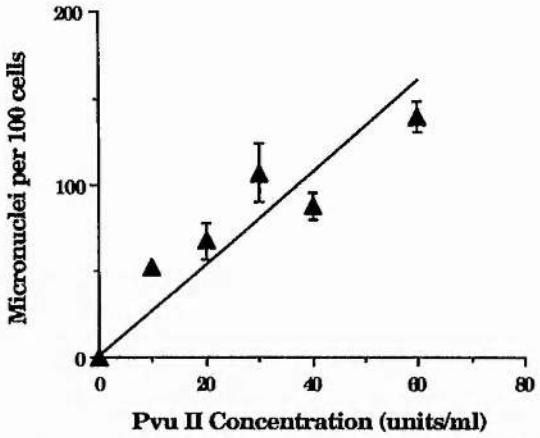

Fig. 1. Frequencies of induced micronuclei in cytokinesis-blocked CHO cells porated with streptolysin O and treated with purified Pvu II. Cells were harvested at 30 h. Background values have been subtracted. Errors are SEM values. (Redrawn from Bryant, 1992)

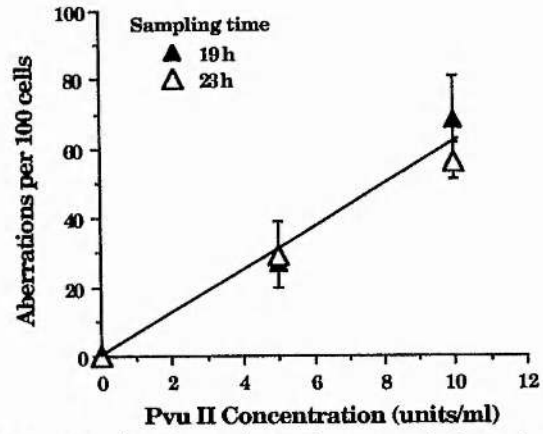

Fig. 2. Frequencies of metaphase chromosomal aberrations in CHO cells porated with SLO and treated with purified Pvu II and sampled at 19 or 23 h including a 1.5 h colcemid block, Background values have been subtracted. Errors are SEM values. (Redrawn from Bryant, 1992)

It was found that the frequencies of micronuclei in cytokinesis-blocked cells varied as a function of time after treatment (Fig. 3). This may reflect variable sensitivity of cells to RE-induced dsb at certain stages of the cell cycle, but could equally well reflect sub-populations of cells that receive different amounts of RE (e.g. because of cell size or different membrane properties). These results are similar to those we have reported previously using electroporation (Moses et al., 1990). The data emphasises the *kinetic* nature of the 'cytochalasin-block' technique. That is, cells are both entering and leaving the binucleate cell 'pool', since quadrinucleate cells are not scored so that the binucleate cells scored at any fixed time represents a 'window'. The frequency of micronuclei in this window therefore can shift up or down with time.

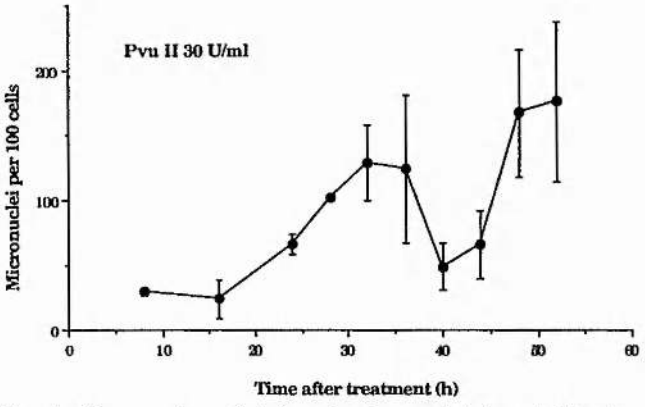

Fig. 3. Frequencies of induced micronuclei in cytokinesis-blocked CHO cells porated with streptolysin O and treated with 30 Units/ml of Pvu II and sampled at various times after treatment. Error bars represent SEM values. (Redrawn from Bryant, 1992)

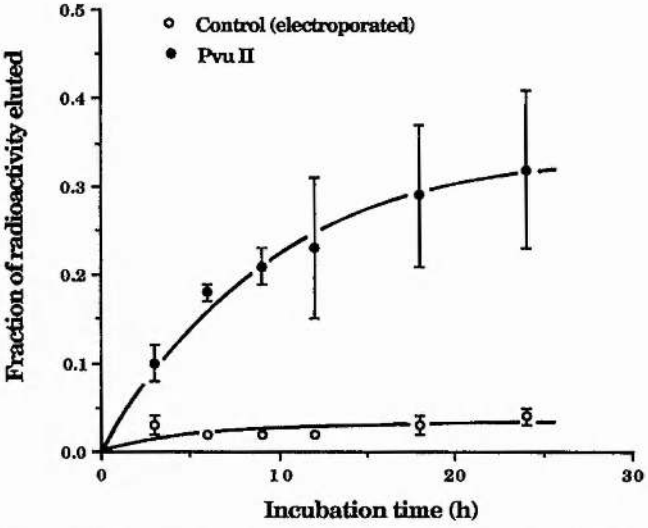

Fig. 4. Fraction of radioactivity eluted (representing dsb) in CHO cells as a function of incubation time after electroporation with or without (control) Pvu II. Error bars represent SEM values. (Graph reproduced from Costa and Bryant, 1990)

Kinetics and mechanisms of dsb induction in restriction-endonuclease-treated cells

It is obviously desirable and important to understand the kinetics of induction of dsb by RE. Early reports (Bryant, 1984; Stoilov et al., 1986) using unwinding and nucleoid sedimentation techniques demonstrated the induction of damage in Sendai virus permeabilized V79 and CHO cells after a fixed time interval. These studies essentially showed an equal induction of breaks by Pvu II and Bam H1 (Bryant, 1984). Clearly the dsb resulting from RE treatment of porated cells cannot all be induced during or immediately following poration since the enzymes require time to seek out their specific base-recognition sites before they incise the DNA. This notion is born out by experiment, for example, extensive studies have been made using the neutral filter elution and pulse-field gel electrophoresis techniques in electroporated cells to measure the dsb induced (Costa and Bryant, 1990; Giaccia et al., 1990; Chung et al., 1991). One of these reports (Costa and Bryant, 1990) showed that at high concentrations of RE, blunt-ended dsb accumulate over a period of many hours following treatment (Fig. 4). This could not be attributed to DNA degradation resulting from premature cell death. However at lower concentrations of RE, dsb transiently accumulate and then disappear again. This was evident from our own experiments (Bryant, 1992) using SLO as a porating agent (Fig. 5).

Taken together these data, on the accumulation of dsb caused by RE indicate that the appearance and frequency of dsb in RE-treated cells may reflect a competition between cutting by the enzyme and rejoining by cellular repair systems. Where high concentrations of RE are used, this competition tips in favour of cutting

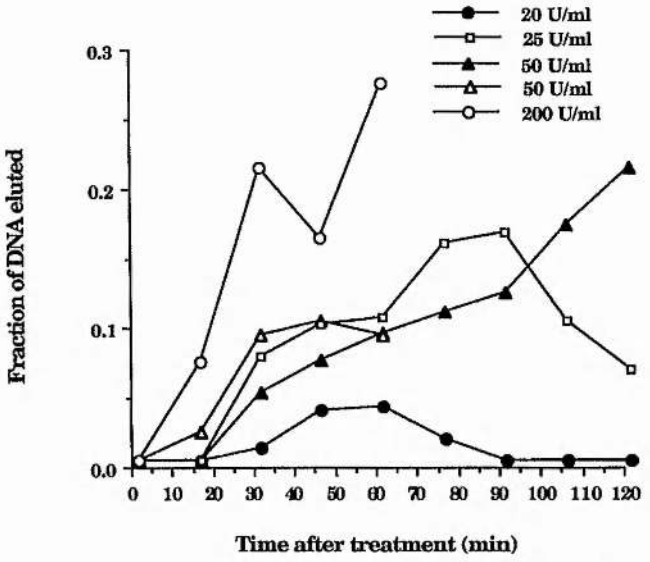

Fig. 5. Fraction of DNA eluted (representing dsb) in CHO cells as a function of incubation time after poration with streptolysin O and treatment with various concentrations of purified Pvu II. (Redrawn from Bryant, 1992)

and dsb accumulate. Where low concentrations of RE are used, repair predominates and dsb disappear.

This 'competition' model (Costa and Bryant, 1990) is supported by the finding that dsb resulting from treatment with either Pvu II or Eco R1 accumulate to a greater extent in the X-ray-sensitive xrs 5 dsb repair defective cell line than in the parental CHO line (Costa and Bryant, 1991a; see Fig. 6). However, the *same* levels of induced dsb

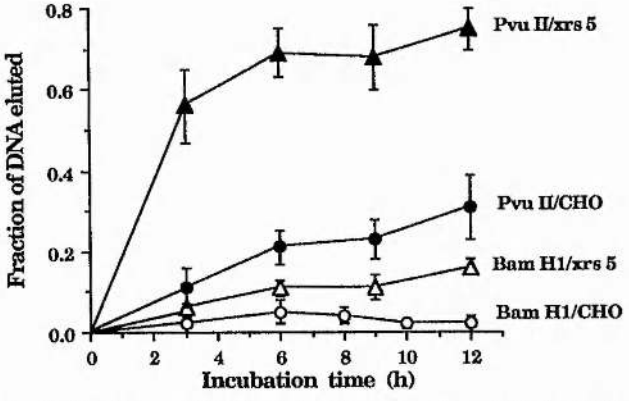

Fig. 6. Fraction of DNA eluted (representing dsb) in CHO and xrs 5 cells as a function of incubation time after electroporation and treatment with purified Pvu II or Bam H1. Error bars represent SEM values.

were reported (Giaccia et al., 1990) for the dsb repair defective XR-1 line treated with Alu I (blunt ends) although in these experiments a very high enzyme dose (500 Units/ml) was used and only a short (20 min) incubation. Dsb induced by Sau 3A (cohesive-ends) in either line were not above background (zero-time incubation).

Little is known about the mechanisms of repair of RE-induced dsb. Some authors have tried the approach of inhibiting the repair of dsb by DNA-repair-blocking agents, in order to accumulate dsb with time. However, the radiation-induced dsb repair inhibitor araA (9-β-D-arabinofuranosyladenine) failed to increase the number of dsb induced in CHO cells by treatment with 200 U/ml of Pvu II, and thus was presumably not effective in blocking the repair of this type of RE induced dsb (Costa and Bryant, 1991b). Chung et

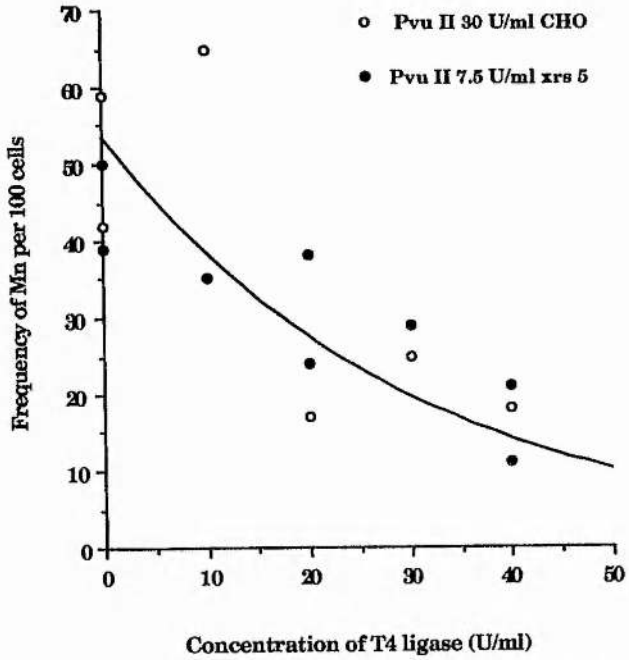

Fig. 7. Frequency of micronuclei induced by Pvu II using the cytokinesis-block technique. Purified Pvu II and T4 ligase were introduced into exponentially growing CHO and xrs-5 cells porated by streptolysin O (0.045 U/ml). Cells were plated in Eagles' minimal essential medium containing 3 μg/ml cytochalasin B. Cells were sampled after 24 h incubation at 37°C, cells were cytospun, fixed in methanol, dried and stained in Giemsa. The frequency of micronuclei per 100 binucleate cells measured. Results are pooled from two independent experiments.

al. (1991) reported that none of the repair inhibitors: araC (1-β-D-arabinofuranosylcytosine), aphidicolin, or caffeine were effective in increasing the yields of dsb induced by Alu I and Sau 3AI (concentrations not reported), although 3AB (3-aminobenzimide), the poly-ADP ribose polymerase inhibitor led to a marginal increase in Alu I-induced dsb at 30 min, that apparently disappeared again at 45 min after treatment. However, both 3AB, araC and aphidicolin led to enhanced yields of chromosomal aberrations generated by Alu I or Sau 3AI.

Durante et al. (1991) showed that introduction of T4 ligase into Pvu II treated cells increased the survival of cells over that seen after Pvu II alone. This work indicates that RE-induced dsb can be repaired by simple ligation.

We have carried out cytogenetic experiments, in which CHO and xrs 5 cells were porated by SLO and treated with purified Pvu II with or without T4 ligase. The results (Fig. 7) showed that frequencies of micronuclei (measured using the cytokinesis block technique) decreased as the concentration of T4 ligase increased. The frequencies of Mn decreased to near background levels in both cell lines indicating that Pvu II-induced dsb in cellular DNA can be rejoined by blunt-end ligation. The fact that both xrs 5 and CHO cells show a reduction in Mn when treated with Pvu II and T4 ligase, indicates that in CHO cells there is not normally sufficient ligase in the cell to cope with all the lesions induced.

Chromosomal aberrations induced by restriction endonucleases

We showed some years ago (Bryant, 1984) that chromosomal aberrations were induced in Sendai virus permeabilized V79 cells by Pvu II. Bam H1, which induces cohesive-ended dsb were found not to induce significant numbers of chromosomal aberrations. This result was confirmed by Natarajan and Obe (1984) in CHO cells and a mouse (PG 19) cell line. We have since demonstrated this difference in clastogenic effectiveness of blunt- and cohesive-ended dsb (Bryant et al., 1987) using Eco RV (blunt-ended) and Eco R1 (cohesive-ended) in Sendai virus permeabilized V79 cells, and by electroporation to introduce purified Pvu II and Eco R1 into CHO cells (Moses et al., 1990).

More recently, using the SLO poration technique referred to above, we have demonstrated the induction of chromosomal aberrations by very low doses of Pvu II, and using these conditions eliminated the problem of heavily-damaged cells which we found occured after treatment with higher enzyme doses in combination with either electroporation or Sendai virus.

Types of chromosomal aberrations induced by restriction endonucleases and radiation

The types of chromosomal aberrations induced by RE are essentially the same as those induced by radiation, i.e. both deletion and exchange types (Bryant, 1984; Natarajan and Obe, 1984). RE appear to truly mimic radiation in the sense that they cause chromosome aberrations in cells treated while in the G1 phase, and chromatid aberrations when in S or G2 phases (Obe and Winkel, 1985).

Furthermore, like radiation, RE were found to produce few chromosomal aberrations in cells treated whilst in mitosis, although there was some disruption of chromosomal morphology (Morgan et al., 1991). However this may be partly due to the general lack of accessibility of RE to the DNA during this phase. When cells were allowed to complete a division cycle following treatment, large numbers of chromosomal aberrations were induced and the most abundant type of aberration was the interstitial deletion.

As with radiation, sister-chromatid exchanges (SCE) are also induced by RE (Natarajan et al., 1985), and RE that recognize sequences rich in GC were found to be most effective. This was presumed to be a result of BrdU incorporation reducing the effectiveness of RE recognising sequences containing T. There was a higher induction in cells which were in early to mid S-phase at the time of treatment, a stage where there were very few chromosomal aberrations evident. In contrast to this work Morgan et al. (1989) reported that they were unable to induce SCEs by RE treatment. The reasons for these conflicting reports are at present not understood.

Interaction between restriction endonucleases and X-rays

It is clear from experiments performed by Tanzarella et al. (1990) and by Morgan et al. (1991) that RE-induced dsb interact synergistically with those induced by X-rays to produce higher levels of chromosomal exchanges and isochromatid breaks. They also showed that blunt-ended dsb (induced by Alu I) produced more interaction than did cohesive-ended dsb (Bam H1). This synergistic interaction between X-rays and RE appeared to be transitory, only occurring when cells were X-irradiated over the first hour after RE treatment (5 U/ml Alu I and 24 U of Sau 3A1), but producing high levels of both exchanges and deletions (Morgan et al., 1991). This may reflect the transitory induction of dsb by low doses of RE referred to above. The synergistic induction of deletions by X-rays and RE indicate that a significant number of deletions are two 'hit' events.

Responses of radiosensitive mutant cell lines to restriction endonucleases

In order to probe the molecular mechanisms underlying the genetic defect involved in the radiosensitivity of mutant cell lines, frequencies of chromosomal aberrations have been examined in radiosensitive and dsb-repair defective cell lines treated with RE. For example, Bryant et al (1987) showed that xrs 5 cells yielded higher levels of chromosomal aberrations than the wild-type parental CHO line in response to treatment by Pvu II and Eco RV (causing blunt-ended dsb), and Bam H1 and Eco R1 (causing cohesive-ended dsb). These results implicate the xrs gene product in the pathway of repair of both blunt- and cohesive-ended dsb, a result confirmed by neutral elution measurements of RE-induced dsb kinetics in xrs 5 and CHO lines (Costa and Bryant, 1991a). Similar enhanced levels of chromosomal aberrations were observed in Eco R1-treated Chinese hamster EM9 cells which are hypersensitive to X-rays and deficient in DNA strand-break repair (Cortes and Ortiz, 1991). However, in these experiments the wild-type (AA8) cells had to be electroporated in order to introduce the RE, whereas the derived mutant EM9 cell line were (because of sensitivity to electroporation resulting in cell death) merely incubated with Eco R1 in storage buffer which appears to facilitate entry of RE into the cells, as found in cultured human lymphocytes by Obe and Winkel (1985).

Conclusions

At the present time it appears that restriction endonuclease treatment is able to truly mimic the clastogenic effects of ionising radiation (in addition to the other biological effects). Although clearly not all aspects of dsb end-structure are mimicked by RE. We do not know the effects the chemical end-structure of a dsb may have on its clastogenicity. This will be an active area of research in the future. With a new method of cell poration (streptolysin O), offering advantages over previous methods, further advances in the field should be possible.

Acknowledgements

This work is supported by the Cancer Research Campaign.

References

Bhakdi, S., J. Tranum-Jensen and A. Szeilgoleit (1985) Infection and Immunity, 47, 52–60.

Blöcher, D. (1982) DNA double-strand breaks in Ehrlich ascites tumour cells at low doses of X-rays, I. Determination of induced breaks by centrifugation at low speed, Int. J. Radiat. Biol., 42, 317–328.

Bryant, P.E. (1984) Enzymatic restriction of in situ mammalian cell DNA using *Pvu* II and *Bam* H1: Evidence for the double-strand break origin of chromosomal aberrations, Int. J. Radiat. Biol., 46, 57–65.

Bryant, P.E. (1988) Review article: Use of restriction endonucleases to study relationships between DNA double-strand breaks, chromosomal aberrations and other end-points in mammalian cells, Int. J. Radiat. Biol., 54, 869–890.

Bryant, P.E. (1992) Induction of chromosomal damage by restriction endonuclease in CHO cells porated with streptolysin O, Mutation Res., 268, 27–34.

Bryant, P.E., D. Birch and P. Jeggo (1987) High chromosomal sensitivity of Chinese hamster xrs 5 cells to restriction-endonuclease-induced DNA double-strand breaks, Int. J. Radiat. Biol., 52, 537–554.

Chung, H.W., J.W. Phillips, R.A. Winegar, R.J. Preston and W.F. Morgan (1991) Modulation of restriction enzyme-induced damage by chemicals that interfere with cellular

responses to DNA damage: A cytogenetic and pulsed-field gel analysis, Rad. Res., 125, 107–113.

Cortes, F., and T. Ortiz (1991) Induction of chromosomal aberrations in the CHO mutant EM9 and its parental line AA8 by Eco Ri restriction enconuclease: electroporation experiments, Mutation Res., 246, 221–226.

Cortes, F., and T. Ortiz (1992) Chromosome damage induced by restriction endonucleases recognizing thymine-rich DNA sequences in electroporated CHO cells, Int. J. Radiat. Biol., 61, 323–328.

Costa, N.D., and P.E. Bryant (1990) The induction of DNA double-strand breaks in CHO cells by Pvu II: kinetics using neutral filter elution (pH 9.6), Int. J. Radiat. Biol., 57, 933–938.

Costa, N.D., and P.E. Bryant (1991a) Elevated levels of DNA double-strand breaks (dsb) in restriction endonuclease-treated xrs 5 cells correlate with the reduced capacity to repair dsb, Mutation Res., 255, 219–226.

Costa, N.D., and P.E. Bryant (1991b) Differences in accumulation of blunt and cohesive-ended double-strand breaks generated by restriction endonucleases in electroporated CHO cells, Mutation Res., 254, 239–246.

Duncan, J.L., and R. Schlegel (1975) Effect of Streptolysin O on erythrocyte membranes, liposomes, and lipid dispersions, J. Cell Biol., 67, 160–173.

Durante, M., G.F. Grossi, D.M. Napolitano and G. Gialanella (1991) Repair of potentially lethal damage by introduction of T4 DNA ligase in eucaryotic cells, Int. J. Radiat. Biol., 59, 963–971.

Giaccia, A.J., R.A. MacLaren, N. Denko, D. Nicolaou and T.D. Stamato (1990) Increased sensitivity to killing by restriction enzymes in the XR-1 DNA double-strand break repair-deficient mutant, Mutation Res., 236, 67–76.

Gomperts, B.D., S. Cockroft, T.W. Howell, O. Nüsse and P.E.R. Tatham (1987) The dual effector system for exocytosis in mast cells: obligatory requirement for both Ca^{2+} and GTP, Biosci. Rep., 7, 369–381.

Morgan, W.F., H.W. Chung, J.W. Phillips and R.A. Winegar (1989) Restriction endonucleases do not induce sister-chromatid exchanges in Chinese hamster ovary cells, Mutation Res., 226, 203–209.

Morgan, W.F., E.R. Valcarcel, E.A. Columna, R.A. Winegar and B. Yates (1991a) Induction of chromosome damage by restriction enzymes during mitosis, Rad. Res., 127, 101–106.

Morgan, W.F., B.L. Yates, J.T. Rufer, E.A. Columna, E.R. Valcarcel and J.W. Phillips (1991b) Chromosomal aberration induction in CHO cells by combined exposure to restriction enzymes and X-rays, Int. J. Radiat. Biol., 60, 627–634.

Moses, S.A.M., A.F. Christie and P.E. Bryant (1990) Clastogenicity of Pvu II and Eco RI in electroporated CHO cells assayed by metaphase chromosomal aberrations and by micronuclei using the cytokinesis-block technique, Mutagenesis, 5, 599–603.

Natarajan, A.T., and G. Obe (1984) Molecular mechanism involved in the production of chromosomal aberration, III. Restriction endonucleases, Chromosoma, 90, 120–127.

Natarajan, A.T., L.H.F. Mullenders, M. Meijers and U. Mukherjee (1985) Induction of sister-chromatid exchanges by restriction endonucleases, Mutation Res., 144, 33–39.

Natarajan, A.T., G. Obe, A.A. van Zeeland, F. Palitti, M. Meijers and E.A.M. Verdegaal-Immerzeel (1980) Molecular mechanisms involved in the production of chromosomal aberrations, II. Utilization of Neurospora endonuclease for the study of aberration production by X-rays in the G1 and G2 stages of the cell cycle, Mutation Res., 69, 293–305.

Obe, G., and E. Winkel (1985) The chromosome breaking activity of the restriction endonuclease Alu I in CHO cells is independent of the S-phase of the cell cycle, Mutation Res., 152, 25–29.

Obe, G., C. Johannes, V. Vasudev, P. Kasper and I. Lamprecht (1987) Induction of cbromosomal aberrations in Chinese hamster ovary cells by the restriction endonucleases Dra I: dose–effect relationships and effect of substitution of chromosomal DNA with bromodeoxyuridine, Mutation Res., 192, 263–269.

Patil, M.S., S.E. Locher and P.V. Harihan (1985) Radiation-induced thymine base damage and its excision repair in active and inactive chromatin of HeLa cells, Int. J. Radiat. Biol., 48, 691–700.

Stoilov, L., L.H.F. Mullenders and A.T. Natarajan (1986) Influence of bromodeoxyuridine substitution of thymidine on sister-chromatid exchanges and chromosomal aberrations induced by restriction endonucleases, Mutation Res., 174, 295–301.

Tanzarella, C., R. De Salvia, F. Degrassi, M. Fiore and F. Palitti (1990) Interaction between X-ray and restriction-induced lesions in tc formation of chromosomal aberrations, Mutation Res., 244, 197–200.

West, C.M.L. (1992) A potential pitfall in the use of electroporation: cellular radiosensitization by pulsed high-voltage electric fields, Int. J. Radiat. Biol., 61, 329–334.

Winegar, R.A., J.W. Phillips, J.H. Youngblom and W.F. Morgan (1989) Cell electroporation is a highly efficient method for introducing restriction endonucleases into cells, Mutation Res., 225, 49–53.

Winegar, R.A., J.W. Phillips, L.H. Lutze and W.F. Morgan (1990) Chromosome aberration induction in Chinese hamster cells by restriction enzymes that have different methylation sensitivity, Som. Cell Mol. Genet., 16, 251–256.

A component of DNA double strand break repair is dependent on the spatial orientation of the lesions within the higher order structures of chromatin.

Running title: A structural requirement for DSB repair in CHO and *xrs-5* cells.

Indexing phrases: nuclear matrix, chromatin structure, ionising radiation sensitivity, neutral filter elution, nucleoid

P. J. Johnston and P. E. Bryant*.
School of Biological and Medical Sciences
Bute Medical Buildings
University of St Andrews
St Andrews
Fife KY16 9TS
Scotland, U. K.

Tel. 0334 63512
Fax. 0334 63600

* To whom reprint requests should be addressed.

Pages: 16
Figures: 3

Abstract.

By the use of a modified neutral filter elution procedure variations in the repair of DNA DSB have been observed between the ionising radiation sensitive mutant *xrs-5* and the parent cell line CHO-K1. Conventional neutral filter elution requires harsh lysis conditions to remove higher order chromatin structures which interfere with elution of DNA containing DSB. By lysing cells with non-ionic detergent in the presence of 2M salt, histone depleted structures which retain the higher order nuclear matrix organisation, including chromatin loops, can be produced (Cook and Brazell, 1975; Cook et al., 1976). Elution from these structures will only occur if two or more DSB lie within a single looped domain delineated by points of attachment to the nuclear matrix. Repair experiments indicate that in CHO cells repair of DSB in loops containing multiple DSB are repaired with slow kinetics whilst DSB occurring in loops containing single DSB are repaired with fast kinetics. *Xrs-5* cells are defective in the repair of multiply damaged loops. This work indicates that the spatial orientation of DSB in the higher order structures of chromatin are a possible factor in the repair of these lesions.

1. Introduction.

The *xrs* mutants are radiosensitive cell lines derived from Chinese hamster ovary (CHO) cells which express a defect in DNA double strand break (DSB) repair (Jeggo and Kemp, 1983; Kemp et al., 1984). *Xrs* cells are capable of repairing a considerable fraction of DSBs induced by ionising radiation, with similar kinetics to wild type for the DSB which are actually repaired (Dahm-Daphi et al., 1993; Kemp et al., 1984; Costa and Bryant, 1988)

The nuclear organisation of *xrs* cells also differs from the wild type. Metaphase chromosomes appear hyper-condensed (Schwartz et al., 1990; 1993) and transmission electron microscopy reveals increased dispersion of heterochromatin and an increase in the perinuclear space of interphase cells (Yasui et al., 1991). Increased digestion of nuclear DNA by DNase I has been given as evidence of reduced attachment of DNA to the nuclear matrix (Yasui et al., 1994). These results imply a component of nuclear structure may be involved in the radiation sensitivity of *xrs-5*. However, there is no direct evidence of this at present and the possibility exists of pleiotropic phenotypes occurring in the mutant cells which are unrelated to sensitivity to ionising radiation.

The purpose of this paper was to examine the relationship of higher order nuclear structures on DSB repair in CHO and *xrs-5*. This was performed by a modification of the neutral filter elution technique (Bradley and Kohn, 1979). Lysis of cells with non-ionic detergent and 2 M NaCl results in protein depleted structures which retain elements of higher order nuclear organisation, including chromatin loops and supporting scaffold (Cook and Brazell, 1975; Cook et al., 1976). The nuclear scaffold constrains chromatin into a number of topologically independent looped domains which are fixed to the nuclear matrix via DNA sequences termed matrix attachment regions (MARs) (Gasser and Laemmli, 1986; Mirkovitch et al., 1984; 1987; 1988). These looped domains can be subsequently grouped into clusters containing 50-60 loops

(Hartwig, 1978). These clusters can, under certain conditions, also act as topologically independent regions and may be involved in the temporal control of DNA replication (Hozák et al., 1993, Fox et al., 1991). The clusters have also been implicated in sensitivity to ionising radiation for some cell lines (Filipovitch et al., 1982; van Rensburg et al., 1985; 1987).

This paper describes experiments involving the elution of DNA from nucleoids extracted from irradiated cells using non-ionic detergent (triton X-100) and high salt concentrations. Elution should only occur from loops containing two or more DSB. This method allows an examination of the influence of the spatial orientation of DSB within higher order structures on the repair of these DSB. This technique was termed non-ionic neutral filter elution (NINFE). In addition to NINFE experiments were performed using slight modifications to "conventional" neutral filter elution with lysis and elution performed in the presence of an ionic detergent (n-lauryl-sarcosine). This allowed an estimation of the relative numbers of DSB in the two cell lines. This method was termed ionic neutral filter elution (INFE).

2. Materials and Methods.

2.1. Cell culture and irradiation.

Chinese hamster ovary (CHO-K1) and *xrs-5* cells were maintained in exponential growth as mono-layers in Eagle's minimal essential medium (supplemented with 10% calf serum containing 100 μM $FeCl_3$, 50 IU ml^{-1} penicillin and 50 mg ml^{-1} streptomycin). All incubations were performed at 37°C in an atmosphere of 5% CO_2 except where stated.

Cells were labelled for 24 hours by the addition of 3.7 kbq ml^{-1} [methyl-^{3}H]-thymidine (1.59 tbq $mmol^{-1}$, Amersham) with 1 μM unlabelled thymidine present to produce even labelling of DNA. The cells were then washed twice with fresh medium and medium containing 1μM unlabelled thymidine added. The cells were incubated for 16 hours to chase any unincorporated [methyl-^{3}H]-thymidine. For dose response

experiments cells were trypsinised and washed twice in Hank's balanced salt solution (HBSS) at 4°C. They were then resuspended in HBSS at 10^6 cells ml^{-1} and irradiated on ice. In repair experiments, cells were irradiated on ice followed by incubation at 37°C for the repair period prior to trypsinisation. Irradiation was performed in a ^{137}Cs IBL437C γ-irradiator (CIS UK Bio International) at a dose rate of 4.6 Gy min^{-1}.

2.2. *Filter elution.*

Filter elution was essentially based on the techniques of Bradley and Kohn (1979) and the modifications made by Okayasu et al. (1988) except that protease was excluded from all treatments. Further modifications were made which are briefly described below.

2.3. *Ionic neutral filter elution (INFE).*

The filter units were disconnected from the apparatus and 1 ml of INFE buffer (40 mM tris; pH 7.5; 10 mM Na-EDTA; 2.5 % N-lauryl-sarcosine), pre-warmed to 60°C, added to the units. The units were then incubated at 60°C for 1 hour. Elution was then performed in the dark at a rate of 2.6 ml hr^{-1} at room temperature using 40 ml of INFE buffer.

2.4. *Non-ionic neutral filter elution (NINFE).*

1 ml of NINFE buffer (40 mM tris-HCl; pH 7.5; 10 mM Na-EDTA; 0.25 % Triton X-100), pre-chilled to 4°C, was added to the filtration units. These were unclamped and 40 ml of NINFE buffer (4°C) added to the reservoirs. Elution was then performed at a rate of 2.6 ml hr^{-1} in a refrigerator at 4°C.

2.5. *Sequential elution.*

NINFE was performed as above. The filter units were then disconnected from the apparatus and 1 ml of INFE buffer pre-warmed to 60°C added. INFE lysis and elution was then performed as above except that elution was performed at 4°C. The eluates from NINFE and INFE were collected separately.

2.6. Calculation of DNA damage.

The radioactivity remaining on the filters and the activity per ml of eluate was calculated by scintillation counting.

The fraction DNA eluted (FE) was calculated using the equation

$$(FE) = \frac{DPM_{eluted}}{DPM_{eluted} + DPM_{filter}} \qquad \text{(equation 1)}$$

Where DPM_{eluate} is total activity eluted and DPM_{filter} is the activity remaining on the filter.

To correct for background levels of elution, which would include background damage and unincorporated [methyl-^{3}H]-thymidine, the relative fraction of DNA eluted (RFE) was calculated by;

$$RFE = \frac{FE_n - FE_{control}}{1 - FE_{control}} \qquad \text{(equation 2)}$$

Where FE_n is the test fraction of DNA eluted and $FE_{control}$ is the fraction of DNA eluted from unirradiated controls.

3. Results and Discussion.

Initial experiments were performed to determine whether elution of DNA occurred from nucleoids under a variety of salt concentrations (data not shown) and there was no significant difference between irradiated CHO and *xrs-5* cells. 2 M NaCl was included in both INFE and NINFE buffers since this salt concentration produced measurable levels of elution compared to lower salt concentrations.

The dose response curves for CHO and *xrs-5* using both INFE and NINFE are shown in figure 1. INFE produced a similar response in both cell lines with an initial linear increase in the relative fraction of DNA eluted followed by saturation of elution at doses > 100 Gy. No significant difference was detected between the two cell lines indicating that equal numbers of DSB were induced (two-way ANOVA; p=0.891,

F=0.33, df=5). The elution of DNA from nucleoids using NINFE was much reduced compared to INFE. The response was approximately linear within the doses used with 50 % elution produced by doses of approximately 200-250 Gy (compared to INFE where 50 % elution occurred at ~ 50 Gy). That no significant difference existed between CHO and *xrs-5* NINFE dose response curves (two-way ANOVA; p=0.891, F=0.33, df=5) indicates that the looped domains involved in elution from nucleoids are relatively similar in size. This is in support of flow cytometric analysis of the size of unstained nucleoids in CHO and *xrs-5* observed by Schwartz et al. (1993).

To examine repair, cells were irradiated with 200 Gy γ-rays and incubated for repair intervals of up to 16 hours. The relative fractions of DNA eluted are expressed as dose equivalent values using the above dose response curves. Repair curves for CHO and *xrs-5* cells are shown in figure 2.

INFE revealed differences in the repair of DSB in *xrs-5* cells, primarily in the slow component, as previously observed (Dahm-Daphi et al., 1993) (two-way ANOVA, p<0.001, F=4.45, df=10).

When the repair of lesions which are measured by NINFE were examined there were significant differences between CHO and *xrs-5* (two-way ANOVA, p<.001, F=4.68, df=10). No fast component to repair was apparent in either cell line. CHO expressed only a slow exponential component to repair with a $t_{1/2}$ of approximately 5 hours. There was no significant decrease in the level of damage remaining after up to 16 hours in *xrs-5* (one-way ANOVA; p= 0.061, F=1.94, df=10) although relatively few time points exist at long repair intervals to discount the possibility of some repair occurring.

The ability of *xrs* cells to repair damage has been shown to be dose dependent, with greater fractions of the initial damage remaining at high doses compared to low doses (Iliakis et al., 1992; Dahm-Daphi et al., 1993). To examine whether this could be the case for the lesions measured by NINFE, the level of residual damage remaining after 16 hours for different doses was examined. The results are shown in figure 3. For

INFE the level of damage remaining increases as a function of dose for *xrs-5* (~ 20 % remaining after 50 Gy and ~ 40 % after 200 Gy). This supports the findings of Iliakis et al. (1992) and Dahm-Daphi et al. (1993).

With NINFE the difference between the amounts of damage repaired by CHO and by *xrs-5* was increased compared to INFE. This may be attributed to the lack of a measurable fast component with the NINFE technique. For *xrs-5*, although there is some dose dependency for the levels of residual damage at low doses, after ~ 150 Gy there is virtually no measurable repair. For CHO the fraction of residual damage is similar whether measured by INFE or NINFE and irrespective of dose with approximately 11% of the initial lesions remaining after 16 hours.

The repair curves indicated that NINFE only measured a slow component to repair. However, a distinction must be drawn between INFE which measures the relative size of DNA fragments which is proportional to the total numbers of DSB, and NINFE which measures the amount of DNA released from a nucleoid. As stated previously this will depend on both the frequency of DSB occurring within the same looped domain and on the size of the domains. There exists the possibility that the defect observed in *xrs-5* is the result of DSB mis-repair: the release of DNA fragments could be caused by two adjacent DSB joined at the nuclear matrix with the loss of the intervening segment. This form of repair would be exhibited as a reduction in the total numbers of DSB, as estimated by INFE, but would not be measured by NINFE which would still measure the release of the fragment.

A sequential elution protocol was performed on cells irradiated with 200 Gy and permitted to repair for 16 hours. This involved NINFE lysis and elution of cells followed by exposure of the residual nucleoids to INFE lysis and elution. The latter INFE stage should measure the levels of DSB remaining within the DNA attached directly to the nuclear matrix. These experiments (data not shown) indicated that in addition to CHO rejoining NINFE elutable fragments these cells can also repair DSB remaining within the nucleoid. *Xrs-5* exhibited an elevated level of residual damage,

as compared with CHO, contained within the residual nucleoid after NINFE removes elutable fragments. This indicates that a significant proportion of damage remains within the nucleoids and that misrepair involving joining of matrix attached DSB ends was not occurring.

Therefore, the technique of elution of DNA from nucleoids would appear to provide evidence of a structural component to the repair of ionising radiation induced damage, in particular DNA double strand breaks. The role of looped domains in the repair of these lesions would appear to be important. The presence of multiple DSB within a single looped domain would appear to necessitate different repair mechanisms to the repair of DSB which exist singly. It is the multiple lesion repair mechanism that would appear to be defective in *xrs-5*, although additional repair mechanisms and lesions may also be affected.

The production of multiple lesions could be the result of the interaction of DSB produced by independent radiation tracks. This may be the cause of the quadratic component to the dose dependent increase in the fraction of non-repaired damage observed with INFE. Alternatively, it is possible that a single track may interact at two sites along a looped domain either by traversing the two 30 nm strands or by production of clustered damage with multiple DSB occurring within a relatively short distance (Goodhead, 1994). The probability of these latter two mechanisms producing multiple lesions would be a linear function of dose. That the dose response curve for induction is predominantly linear (figure 1b) whilst for damage remaining (figure 3b) an quadratic function is present may indicate that repair mechanisms are dose dependent.

The identity of the looped domain involved in the above repair processes remains unknown. As mentioned above, two major looped structures exist within the chromatin of higher eukaryotes. The 60 kbp loops are already implicated in many nuclear processes including DNA replication, transcription and the control of gene expression (van Holde, 1989). The clusters of the 60 kbp loops which, under certain

conditions, act as independent looped domains 2-7 Mbp in length (Hartwig, 1978; Cook and Brazell, 1975; van Rensburg, 1975, 1987) have been implicated in the radiation sensitivity of cells. Several studies have correlated increased size of these domains with sensitivity to ionising radiation (Filipovitch et al., 1982; van Rensburg et al., 1985, 1987) although this correlation does not exist for all radiosensitive cell lines (Walicka and Godlewska, 1989). That approximately 50 % elution occurs after 200-250 Gy would indicate that it is possibly the clusters rather than the component 60 kbp loops that NINFE detects the presence of multiple DSB.

Further work is required to produce a definite identification of the looped domain involved in the repair of DSB.

4. Conclusions.

Using a modified neutral filter elution technique it has been possible to provide evidence of a structural component to DNA double strand break repair. The position of DSB in relation to other DSB and higher order structures of chromatin would appear to affect the rate of repair of DSB. In the ionising radiation sensitive mutant *xrs-5* the repair defect observed may be attributed to an inability to repair lesions which occur in multiples within an unidentified looped structure.

Acknowledgements.

We thank John Macintyre for valuable technical assistance.
This work was supported by the Commission of European Communities Radiation Protection Programme.

References.

BRADLEY, M. O. and Kohn, K. W., 1979, X-ray induced DNA double strand break production and repair in mammalian cells as measured by neutral filter elution. *Nucleic Acids Res.*, **7**, 793-804.

COOK, P. R. and Brazell, I. A., 1975, Supercoils in human DNA. *J. Cell Sci.*, **19**, 261-279.

COOK, P. R., Brazell, I. A. and Jost, E., 1976, Characterisation of nuclear structures containing superhelical DNA. *J. Cell Sci.*, **22**, 303-324.

COSTA, N. D. and Bryant, P. E., 1988, Repair of DNA single-strand and double-strand breaks in the Chinese hamster *xrs 5* mutant cell line as determined by DNA unwinding. *Mutation Res.*, **194**, 93-99.

DAHM-DAPHI, J., Dikomey, E., Pyttlik, C. and Jeggo, P. A., 1993, Reparable and non-reparable DNA strand breaks induced by X-irradiation in CHO K1 cells and the radiosensitive mutants *xrs1* and *xrs5*. *Int. J. Radiat. Biol.*, **64**, 19-26.

FILIPOVITCH, J. V., Sorokina, N. J., Soldatenkov, V. A. and Romantzev, E. F., 1982, Supercoiled DNA repair in thymocyte fractions differing in radiosensitivity. *Int. J. Radiat. Biol.*, **42**, 31-44.

FOX, M. H., Arndt-Jovin, D. J., Jovin, T. M., Baumann, P. H. and Robert-Nicoud, M., 1991, Spatial and temporal distribution of DNA replication sites localised by immunofluorescence and confocal microscopy in mouse fibroblasts. *J. Cell Sci.*, **99**, 247-253.

GASSER, S. M. and Laemmli, U. K., 1986, The organisation of chromatin loops: Characterisation of a scaffold attachment site. *EMBO J.*, **5**, 511-518.

GOODHEAD, D. T., 1994, Initial events in the cellular effects of ionising radiations: clustered damage in DNA. *Int. J. Radiat. Biol.*, **65**, 7-17.

HARTWIG, M., 1978, Organisation of mammalian chromosomal DNA: supercoiled and folded circular DNA subunits from interphase cell nuclei. *Acta Biol. Med. Germ.*, **37**, 421-432.

HOZÁK, P., Hassan, A. B., Jackson, D. A. and Cook, P. R., 1993, Visualisation of replication factories attached to a nucleoskeleton. *Cell*, **73**, 361-373.

ILIAKIS, G., Mehta, R. and Jackson, M., 1992, Level of DNA double-strand break rejoining in Chinese hamster *xrs-5* cells is dose dependent: implications for the mechanism of radiosensitivity. *Int. J. Radiat. Biol.*, **61**, 315-321.

JEGGO, P. A. and Kemp, L. M., 1983, X-ray sensitive mutants of Chinese hamster ovary cell line. Isolation and cross-sensitivity to other DNA damaging agents. *Mutation Res.*, **112**, 313-327.

KEMP, L. M., Sedgwick, S. G. and Jeggo, P. A., 1984, X-ray sensitive mutants of Chinese hamster ovary cells deficient in double-strand break rejoining. *Mutation Res.*, **132**, 189-196.

MIRKOVITCH, J., Gasser S. M. and Laemmli, U. K., 1987, Relation of chromosome structure and gene expression. *Phil. Trans. R. Soc. Lond. B.*, **317**, 563-574.

MIRKOVITCH, J., Gasser, S. M. and Laemmli, U. K., 1988, Scaffold attachment of DNA loops in metaphase chromosomes. *J. Mol. Biol.*, **200**, 101-109.

MIRKOVITCH, J., Mirault, M. E. and Laemmli, U. K., 1984, Organisation of the higher order chromatin loop: Specific DNA attachment sites on nuclear scaffold. *Cell*, **39**, 223-232.

OKAYASU, R., Blöcher, D. and Iliakis, G., 1988, Variation through the cell cycle of DNA neutral filter elution dose response in X-irradiated synchronous CHO-cells. *Int. J. Radiat. Biol.*, **53**, 729-747.

SCHWARTZ, J. L., Cowen, J. M., Moan, E., Sedita, B. A., Stephens, J. and Vaughan, A. T. M., 1993, Metaphase chromosome and nucleoid differences between CHO-K1 and its radiosensitive derivative *xrs-5. Mutagenesis.*, **8**, 105-108.

SCHWARTZ, J. L., Shadley, J., Jaffe, D. R., Whitlock, J., Rotmensch, J., Cowan, J. M., Gordon, D. J. and Vaughan, A. T. M., 1990, Association between radiation sensitivity, DNA repair, and chromosome organisation in the Chinese hamster ovary cell line *xrs-5*. In: *Mutation and the Environment. Part A: Basic mechanisms*. . Edited by: M. L. Mendelsohn and R. J. Albertini (Wiley-Liss, New York), pp. 255-264.

VAN HOLDE, K. E., 1989, *Chromatin* (Springer-Verlag, Inc., New York).

VAN RENSBURG, E., Louw, W. K. A., Izatt, H. and van der Watt, J. J., 1985, DNA supercoiled domains and radiosensitivity of subpopulations of human peripheral blood lymphocytes. *Int. J. Radiat. Biol.*, **47**, 673-679.

VAN RENSBURG, E. J., Louw, W. K. A. and van der Merwe, K. J., 1987, Changes in DNA supercoiling during repair of gamma-radiation -induced damage. *Int. J. Radiat. Biol.*, **52**, 693-703.

WALICKA, M. and Godlewska, E., 1989, Radiation sensitivities are not related to the sizes of supercoiled domains in L5178Y-R and L5178Y-S cells. *Int. J. Radiat. Biol.*, **55**, 953-961.

YASUI, L. S., Fink, T. J. and Enrique, A. M., 1994, Nuclear scaffold organisation in the X-ray sensitive Chinese hamster mutant cell line, *xrs-5. Int. J. Radiat. Biol*, **65**, 185-192.

YASUI, L. S., Ling-Indeck, L., Johnson-Wint, B., Fink, T. J. and Molsen, D., 1991, Changes in the nuclear structure in the radiation-sensitive CHO mutant, *xrs-5*. *Radiat. Res.*, **127**, 269-277.

Figure Legends.

Figure 1. Gamma ray dose response. CHO and *xrs-5* cells were irradiated on ice and a) INFE or b) NINFE lysis and elution performed. The graph shows the relative fraction of DNA eluted from the filter versus dose of γ-rays. Error bars show the SEM of a minimum of 3 independent experiments. Curves fitted by eye.

Figure 2. Repair of damage. Graph shows the dose equivalent amount of damage remaining at various repair intervals as measured by a) INFE and b) NINFE for CHO and xrs-5. Error bars show the SEM of a minimum of 3 independent experiments. Curves fitted by eye.

Figure 3. Residual damage. CHO and xrs-5 were irradiated on ice and subsequently incubated at 37°C for 16 hours. Cells were then subjected to either a) INFE or b) NINFE. Graph shows the level of damage remaining in dose equivalents versus the initial dose. Error bars show the SEM from a minimum of 3 independent experiments. Curves fitted by eye. Also shown are lines of parity (····).

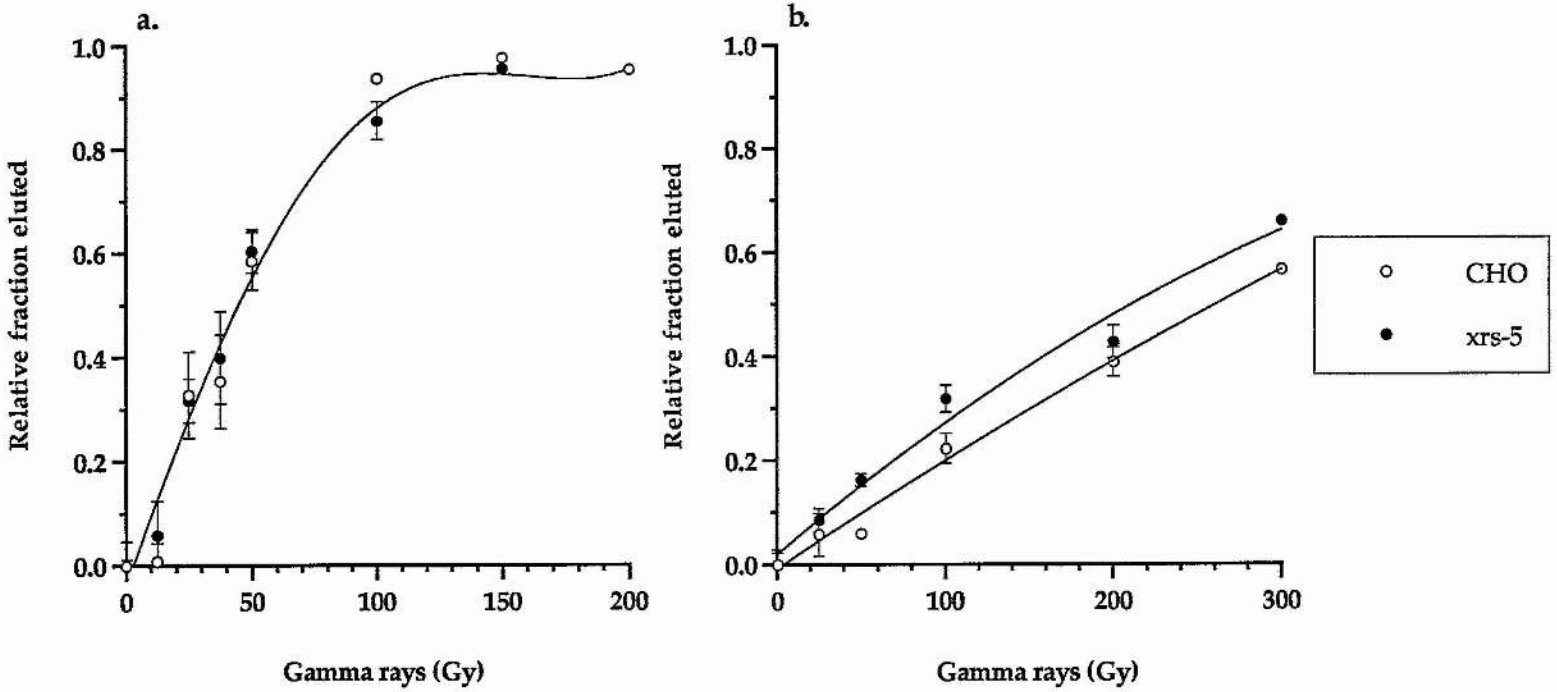
a.
b.
Relative fraction eluted
Gamma rays (Gy)
1.0
0.8
0.6
0.4
0.2
0.0
0
50
100
150
200
300
CHO
xrs-5

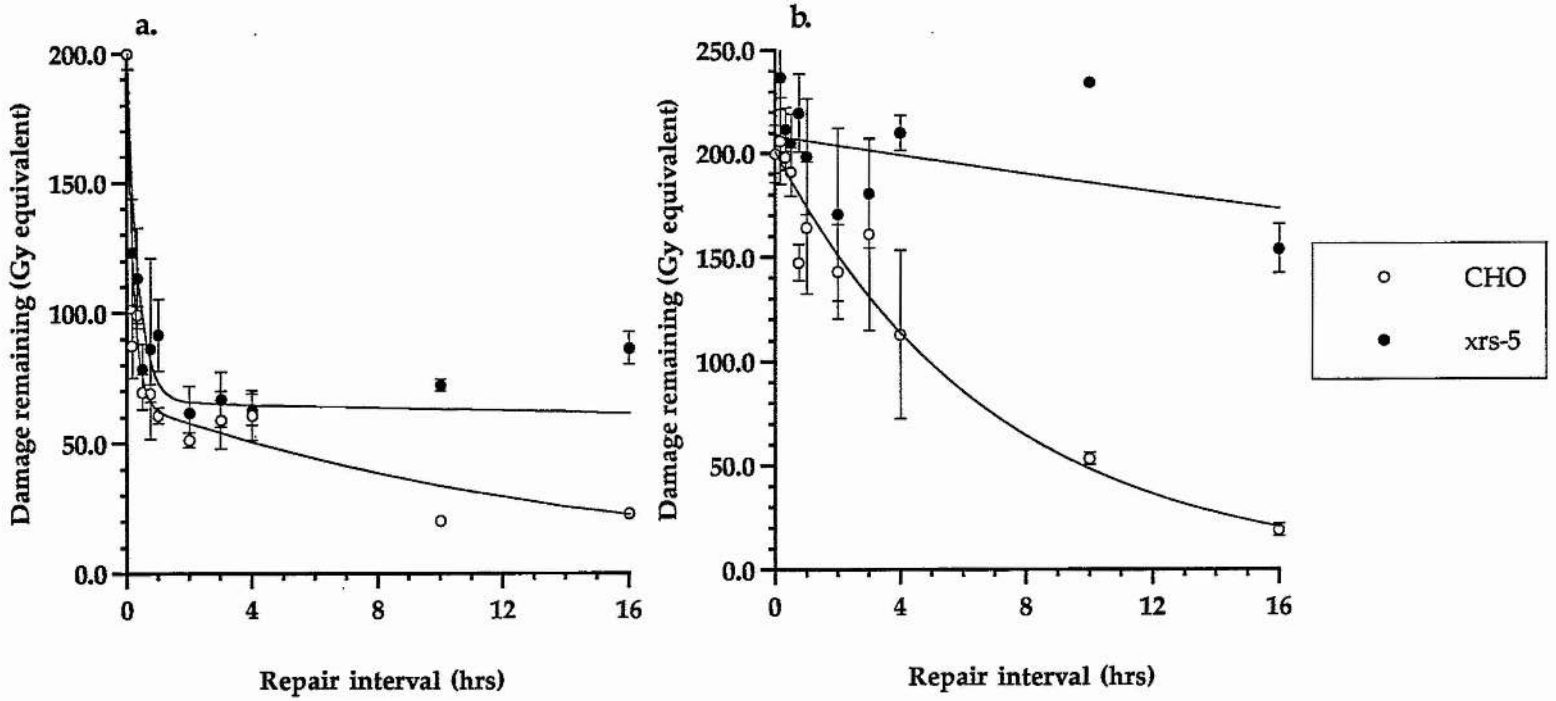
a.
b.
Damage remaining (Gy equivalent)
Repair interval (hrs)
200.0
150.0
100.0
50.0
0.0
250.0
0
4
8
12
16
CHO
xrs-5

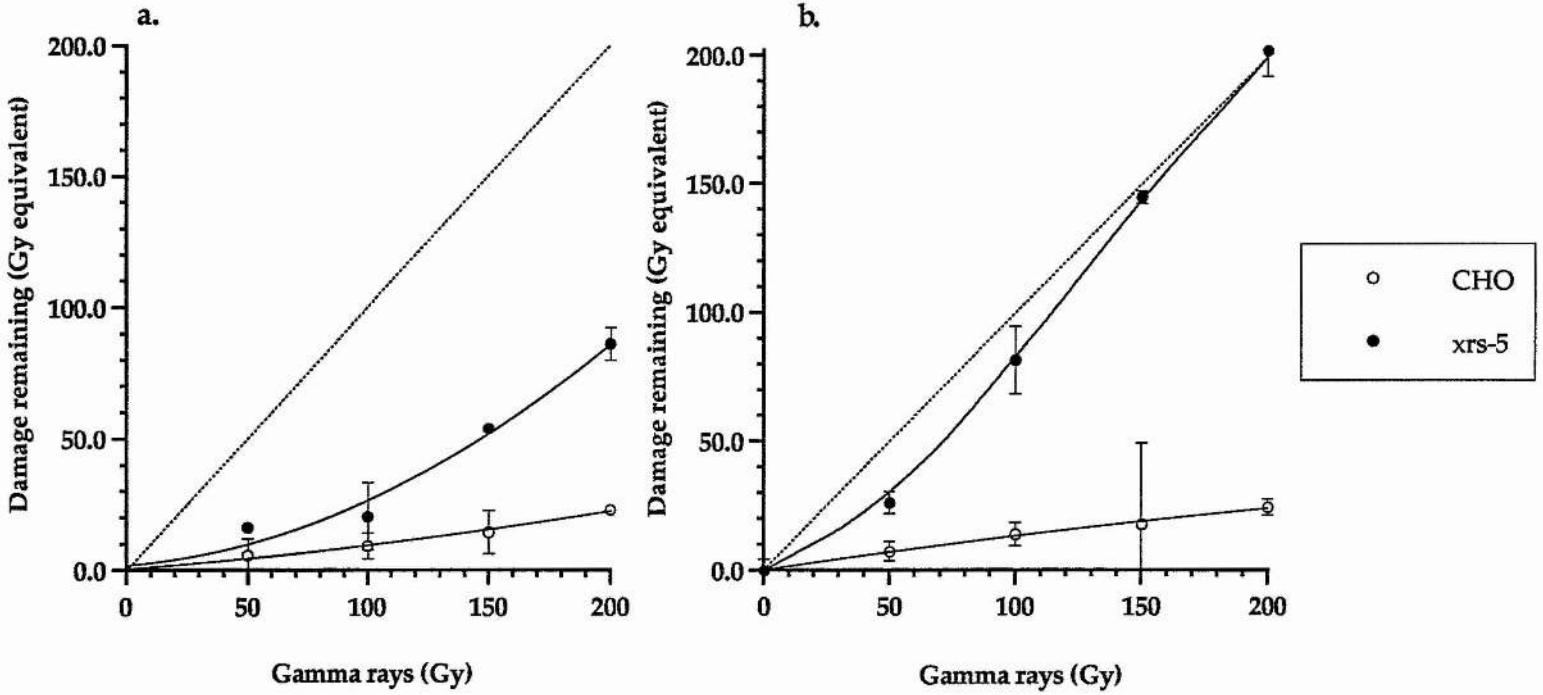
a.
b.
Damage remaining (Gy equivalent)
200.0
150.0
100.0
50.0
0.0
0
50
100
150
200
Gamma rays (Gy)
CHO
xrs-5